Dissertation

submitted to the

Combined Faculties for the Natural Sciences and for Mathematics

of the Ruperto-Carola University of Heidelberg, Germany

for the degree of

Doctor of Natural Sciences

presented by

Dipl.-Biol. Sonja Blasche

born in Oberkirch (Baden), Germany

Oral-examination: December 19, 2012

Escherichia coli as Host and Pathogen

Referees: PD Dr. Stefan Wiemann
Prof. Dr. Victor Sourjik

Zusammenfassung

Enterohämorrhagische *Escherichia coli* (EHEC) sind durch kontaminierte Speisen oder Wasser übertragene, hochinfektiöse Pathogene, die weltweit vorkommen und immer wieder lokale Krankheitsausbrüche verursachen. Ihre Pathogenitätsfaktoren beinhalten Shigatoxine und ein Typ III Sekretionssystem mit Effektorproteinen, die in die menschliche Wirtszelle injiziert werden, um diese zu manipulieren. Die Pathogenitätsfaktoren liegen auf dem bakteriellen Chromosom in so genannten Pathogenitätsinseln, die von Sequenzen lambdoider Phagen flankiert werden. Manche dieser Phagen sind noch in der Lage nach UV-Induktion infektiöse Partikel zu bilden.
Im Rahmen dieser Arbeit habe ich zwei Protein-Protein Interaktome generiert, nämlich das EHEC-Mensch und das Phage Lambda-*E. coli* Interaktom.
Für das EHEC-Mensch Interaktom wurden 34 Effektorproteine kloniert und im Hefe-Zwei-Hybrid-System gegen menschliche ORF Kollektionen und cDNA-basierte Gensammlungen gescreent. Insgesamt konnten 35 reproduzierbare Interaktionen von 15 EHEC Effektoren mit 34 menschlichen Proteinen identifiziert werden, von denen bisher lediglich vier in der Literatur bekannt sind. Das EHEC-Mensch Interaktom wurde durch die in BioGRID befindlichen Interaktionen der 34 menschlichen Proteine erweitert. Dadurch konnte festgestellt werden, dass die EHEC Effektorproteine in der Wirtszelle untereinander über primäre und sekundäre Interaktionen mit menschlichen Proteinen vernetzt sind.
Für den 'translocated intimin receptor' (TIR) wurden acht Interaktionen (darunter zwei bereits bekannte) identifiziert. Die menschlichen Interaktoren wurden dann zu Vergleichszwecken in binären Hefe-Zwei-Hybrid Tests auf Interaktionen mit dem homologen TIR von enteropathogenen *E. coli* (EPEC) untersucht. Fünf der acht EHEC-TIR Interaktoren interagierten auch mit EPEC-TIR.
Eine weitere Interaktion zwischen dem Effektorprotein NleF und der menschlichen Caspase-9 wurde im Rahmen dieser Arbeit entdeckt. Durch LUMIER Tests gegen weitere menschliche Caspasen wurden auch die Caspasen 4 und 8 als Interaktionspartner identifiziert. *In vitro* Versuche mit aufgereinigtem Protein ergaben, dass NleF ein potenter Inhibitor der Proteaseaktivität aller drei Caspasen ist. Weiterhin ist es in der Lage die Caspaseaktivität in Zelllysaten zu mindern und die Apoptoseinduktion in HeLa und Caco-2 Zellen signifikant zu hemmen. Einem Kollaborationspartner gelang es die Kristallstruktur des Caspase-9/NleF Komplexes aufzulösen, welche eine dominante Rolle der carboxyterminalen vier Aminosäuren von NleF bei der Caspase-9 Bindung und Hemmung vermuten ließ. Durch die Generierung von NleF Mutanten mit verändertem Carboxyterminus gelang es mir, dies zu bestätigen. Die Verhinderung oder Verzögerung der Apoptoseinduktion in Wirtszellen ist eine gängige Strategie vieler Pathogene. Obwohl NleF längst nicht das einzige Effektorprotein ist, das in die Apoptoseinduktion eingreift, so ist es doch der einzige bekannte Effektor, der direkt an Caspasen bindet, um diese zu inhibieren.
Das Phage Lambda-*E. coli* Interaktom wurde von mir während eines Forschungsaufenthaltes am J. Craig Venter Institut in Rockville USA realisiert. Dazu habe ich 68 Phage Lambda Proteine im Hefe-Zwei-Hybrid-System gegen eine *E. coli* W3110 ORF Sammlung gescreent, wodurch 144 reproduzierbare Proteininteraktionen zwischen Lambda und *E. coli* identifiziert wurden. Die in Interaktionen involvierten Phage Lambda und *E. coli* Proteine wurden in funktionelle Gruppen unterteilt und auf Interaktionen zwischen den Virus- und Wirtsgruppen untersucht.

Summary

Enterohemorrhagic *E. coli* (EHEC) are highly infectious food-borne pathogens that cause severe diarrhoea in both, industrialised and developing countries all over the world. Their pathogenicity factors involve shiga-like toxins and a type III secretion system along with so-called effector proteins, which are translocated directly into the cytoplasm of their host cells, usually enterocytes. Most of these proteins are encoded in pathogenicity islands within the bacterial genome that are framed by sequences of lambdoid phages. Some of these phages are still able to produce infectious particles after UV induction.

In this study I generated two protein-protein interactomes, namely EHEC-host and phage lambda-*E. coli*. For the EHEC-host interactome, 34 effector proteins that had been previously shown to be secreted into human host cells were cloned and screened against pooled human cDNA and ORF libraries via yeast two-hybrid screening. This resulted in 35 reproducible interactions of 15 EHEC effectors with 34 human proteins, of which only four had been published previously. Inclusion of secondary human protein interactors retrieved from the BioGRID database revealed that EHEC effectors are interconnected in the human cell.

The translocated intimin receptor (TIR) that was found to interact with eight human proteins was compared to its homologue in enteropathogenic *E. coli* (EPEC). This revealed that five of the eight EHEC TIR interactors also interact with EPEC TIR.

Another interaction discovered in this study involves the EHEC effector NleF, previously a protein of unknown function, and human caspase-9. LUMIER assays against other human caspases identified caspase-4 and -8 as additional binding partners of NleF. Tests with purified enzymes revealed that NleF can potentially inhibit all three caspases. The effector decreased caspase activity significantly in HeLa cell lysate and impaired apoptosis induction in HeLa and Caco-2 cells. A collaboration partner solved the crystal structure of the NleF/caspase-9 complex, which suggested a dominant role of the carboxy-terminal four amino acids in caspase-9 binding and inhibition. I was able to confirm these findings by constructing NleF versions with mutagenized carboxy-termini. NleF versions that lacked the last four amino acids or comprised an additional carboxy-terminal alanine were unable to bind any of the three caspases or impair apoptosis. Apoptosis inhibition is a strategy often applied by viral and bacterial pathogens. Even though NleF is not the only effector protein capable of inhibiting apoptosis in human cells, direct inhibition of caspases by bacterial effectors has not been reported to date.

The phage lambda-*E. coli*.interactome was generated during my research stay at the J. Craig Venter Institute in Rockville (USA). I screened 68 phage lambda proteins against the *E. coli* W3110 ORF library via yeast two-hybrid screening using two different vector systems. This resulted in 144 reproducible interacting pairs. The phage lambda and *E. coli* proteins involved in interactions were categorized in functional groups and analysed for interactions between phage and host groups.

Acknowledgement

It’s about time to give special thanks to Manfred Koegl, who supervised me from the beginning of my doctoral studies. He gave me not only the opportunity to join his lab and work on an exciting research topic, but also supported me throughout my work, even after he left the DKFZ in 2010. His trust in me helped me through many odds and difficulties. I will always admire his enthusiasm and ‘never give up’ attitude.

For the extraordinary opportunity to work one year in his laboratory at the J. Craig Venter Institute in Rockville (MD, USA) I owe many thanks to Peter Uetz. I appreciate his willingness to share with me his immense experience and expertise in yeast two-hybrid screening. His open and direct way to approach and discuss scientific issues is without equal.

I am grateful to my lab mates Gabriella Siszler, Kerstin Mohr, Nadja Wermke, Sabine Kelkenberg and Sara Burmester, who always supported me as good as they possibly could. Their optimism and good humor made lab work enjoyable even in less pleasant times.

Many thanks also to Frank Schwarz for bioinformatic support and helpful discussions.

I thank Stefan Wiemann for accepting me as his PhD student, for his continuous support and his patience to answer questions and give advice.

Ganz herzlich möchte ich meinen Eltern, meiner Schwester Jutta und meiner Oma Hilde danken, auf deren Freundschaft und Hilfe ich mich selbst in stressigen Zeiten immer verlassen konnte. Herzlichst gedankt sei auch meiner Tante Karin, die mich zu jeder Zeit auf ihre offene und unkomplizierte Art und Weise unterstützt hat.

I would also like to mention Ute Ernst for her support in sequencing and Barbara Leuchs for allowing me to perform BSL-2 work in her laboratory. Thanks also to Monika Langlotz for her kind and uncomplicated support with the FACS devices.

Last but not least there are numerous people who supported me in one way or the other. Without you this work would not have been brought to completion. I would like to thank all of you; you know who you are.

Table of contents

Abbreviations

3-AT	3-Aminotriazole (3-AT)
4-MU	4-methylumbelliferyl-2-D-galactoside
AA	amino acid
AD	activation domain
A/E	attaching and effacing
Amp	ampicillin
BIR	baculovirus IAP repeat
bp	base pairs
BP	attB and attP recombination (Gateway)
BSA	albumin bovine serum
CDC	chaperone binding domain
CFU	colony forming unit
CSM	Complete Supplement Mixture
DBD	DNA-binding domain
DKFZ	Deutsches Krebsforschungszentrum (German Cancer Research Center)
DMSO	dimethyl sulfoxide
DNA	desoxy ribonucleic acid
dNTP	desoxy nucleosid triphosphate
EDTA	ethylenediaminetetraacetic acid
EHEC	Enterohemorrhagic *Escherichia coli*
EPEC	Enteropathogenic *Escherichia coli*
ER	Endoplasmic reticulum
FACS	Fluorescence activated cell sorting
GAL4	yeast transcription factor of the galactose pathway
Gent	gentamicin
GOI	gene of interest
GBD	GTPase-binding domain
GEF	guanine exchange factor
HUS	hemolytic-uremic syndrome
IAP	inhibitor of apoptosis protein
IC50	half maximal inhibitory concentration (IC50)
kDa	kilo Dalton
Kan	kanamycine
kb	kilo base pairs
LEE	locus of enterocyte effacement
LB	Luria Bertani
LEHD-FMK	LEHD-fluoromethylketone
LR	attL and attR recombination (Gateway)
LUMIER	LUminescence-based Mammalian IntERactome mapping
MT	mating type (locus)
µl	microliter
µM	micromolar
M	molar
mM	millimolar

Nle	non-LEE encoded effector protein
NLR	NOD-like receptor
OD	optical density
ORF	open reading frame
PAMP	pathogen-associated molecular patterns
PCD	programmed cell death
PCR	polymerase chain reaction
PEG	polyethylene glycol
POI	protein of interest
PPI	protein-protein interaction
PRD	proline-rich domain
RNA	ribonucleic acid
rpm	rounds per minute
ROS	reactive oxygen species
RT	room temperature
SD	synthetic defined media
Spec	spectinomycin
STEC	shiga-like toxin-producing *E. coli*
Stx	shiga toxin, shiga-like toxin
T3SS	type III secretion system
TAE	tris acetate EDTA buffer
Tm	melting temperature
TRAIL	Tumor Necrosis Factor Related Apoptosis Inducing Ligand
U	units
UTR	untranslated region
v/v	volume per volume
w/v	weight per volume
TRIS	tris-(hydoxymethyl)-aminomethane
WT	wild type
YFP	yellow fluorescent protein
YNB	yeast nitrogen base
YPD	yeast peptone dextrose
YPDA	yeast peptone dextrose plus adeneine
Y2H	yeast two-hybrid
Zeo	zeocin
Z-VAD-FMK	Z-VAD-fluoromethylketone

1 Introduction

1.1 Pathogenic Escherichia coli

Pathogenic bacteria that cause infectious diarrhoea are a major health problem worldwide. Among them are enterohemorrhagic *Escherichia coli* (EHEC), which cause severe foodborne diarrhoea and hemolytic-uremic syndrome (HUS). As highly infectious pathogens requiring less than 100 CFU to cause disease in humans, susceptible food, such as ground beef can be easily contaminated during industrial food processing in developed countries, especially since EHEC is a natural inhabitant of the intestine of ruminants (BfR, 2012). Due to these facts and EHECs ability to also contaminate vegetables (Berger et al., 2010; Wendel et al., 2009) more than 900 EHEC/STEC (shiga-like toxin-producing *E. coli*) cases occur annually in Germany (data obtained from the website of the Robert Koch Institute; http://www3.rki.de/SurvStat/), which is comparable to its occurrence in the United States. Although the number of EHEC/STEC cases is usually low, it can rise to up to several thousand affected people during outbreaks, as happened 2011 in Germany.

1.1.1 Type III secretion

E. coli are common inhabitants of the intestinal tract of several mammals and humans. Even though mainly beneficial for their carrier, some strains, such as EHEC O157:H7, acquired pathogenicity islands via horizontal gene transfer (Berger et al., 2010). These genomic islands are framed by sequences originating from lambdoid phages out of which some are still capable of producing functional virions after induction by e.g. UV light or some antibiotics (Datz et al., 1996; Gamage et al., 2003; Herold et al., 2005; Miyamoto et al., 1999; Yokoyama et al., 2000). The best known pathogenicity island is probably the so-called locus of enterocyte effacement (LEE). It encodes the type III secretion system, the adhesin intimin, chaperones, several effector proteins and the LEE encoded regulator (Ler) that is involved in the regulation of the LEE2-4 promoters (Elliott et al., 2000). The type III secretion system (T3SS) is a syringe like apparatus composed of more than 20 proteins and highly similar to the flagellum of gram negative bacteria (Erhardt et al., 2010). It is shared by and conserved among many gram negative pathogens such as *Salmonella* sp., *Yersinia* sp., enteropathogenic and enterohemorrhagic *Escherichia coli* (EPEC and EHEC), *Shigella* sp., *Chlamydia* sp. and even plant pathogens like *Erwinia carotovora* (Blocker et al., 2003; Galan and Wolf-Watz, 2006). Its main function lies in the injection of bacterial effector proteins into host cells. Even though the number of these virulence-effectors is variable between bacterial strains, they act in concert aiming at the subversion of cellular antagonistic responses and the establishment of an environment suitable for pathogen proliferation. Effector protein secretion is a complex process, on effector site commonly involving an amino-terminal export signal and a downstream chaperone binding domain that recognizes a class I chaperone. Class I chaperones are dedicated chaperones that bind their cognate effectors (some chaperones can bind to more than one effector), targeting them to the T3S machinery (Cornelis, 2006; Ghosh, 2004; Parsot et al., 2003). The chaperons prevent premature interactions between effectors and facilitate rapid unfolding of to be translocated proteins (Galan and Wolf-Watz, 2006; Stebbins and Galan, 2003), which is required due to the small channel of the T3SS (~25 Å inner diameter) (Cornelis, 2006). The process of T3S is schematized in figure 1.

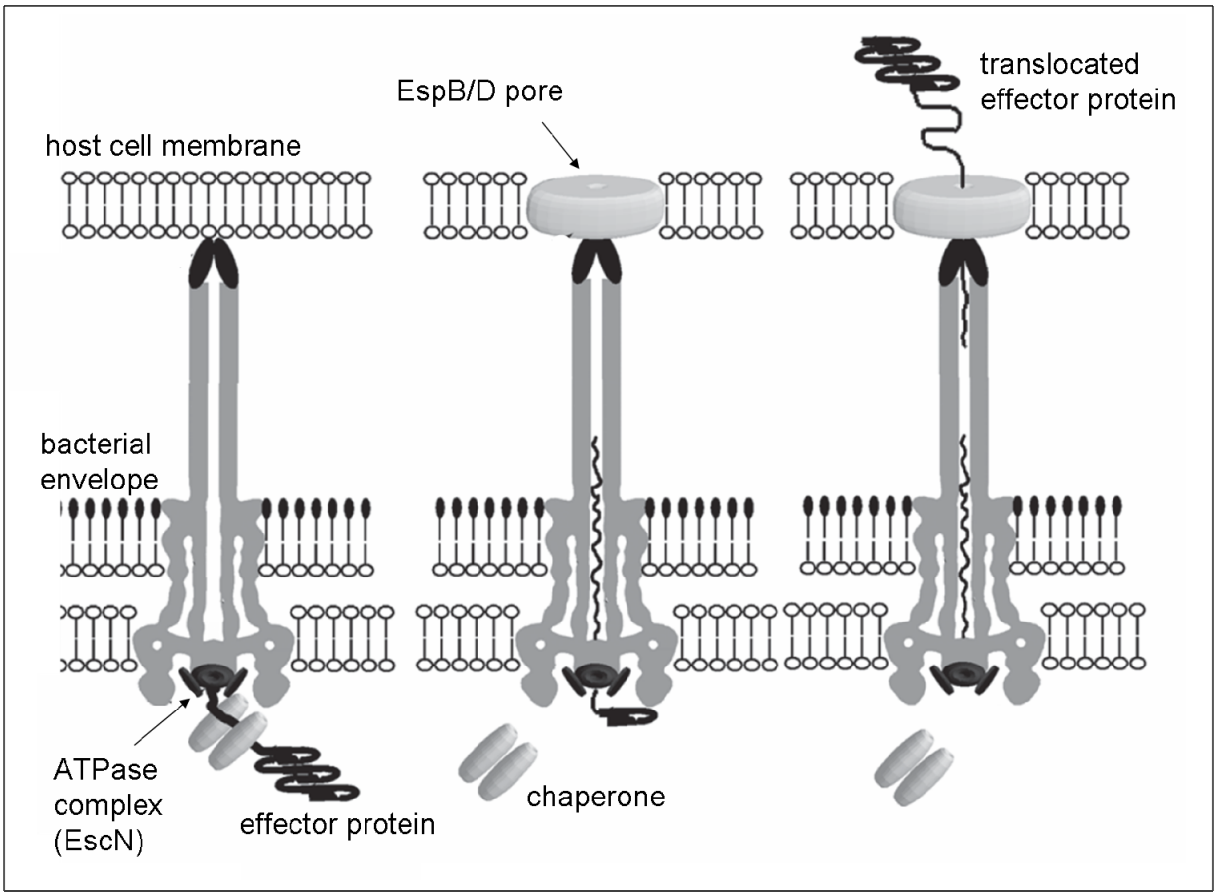

Figure 1. Type III secretion. Effector proteins bind to their cognate chaperons and the complex is targeted to the T3SS, where it is recognized by the ATPase complex. The latter strips the effector from the chaperone and mediates translocation of the unfolded protein through the central channel of the secretion system and the translocon pore formed by EspB and EspD. The figure is taken from (Galan and Wolf-Watz, 2006).

After translocon formation by EspA, EspB and EspD, involving membrane insertion of the latter two, the T3SS is ready for injection of subsequent effectors (Hartland et al., 2000; Ide et al., 2001; Knutton et al., 1998; Wachter et al., 1999), including those responsible for the characteristic attaching and effacing (A/E) lesions. These lesions occur as a consequence of intimate attachment of the pathogens to the plasma membrane of enterocytes and involve the destruction of microvilli and rearrangements of the cytoskeleton underneath adherent bacteria (reviewed in Frankel et al., 1998). EHEC and EPEC mutants deficient in lesion formation can neither colonize their host nor cause disease, marking the process as critical for pathogenicity (Kaper et al., 2004; Spears et al., 2006).

1.1.2 TIR signalling and pedestal formation

(Shaw et al., 2005) demonstrated that the A/E phenotype is mainly caused by the interaction of the effector protein TIR, the translocated intimin receptor, with the intimate adhesin intimin. After the translocon forming proteins EspB and EspD, TIR is the first effector protein translocated into the host cell. It integrates into the plasma membrane with both, the amino- and the carboxy-terminus exposed to the host cell cytoplasm. A 55 amino acid extracellular loop on the host cell surface mediates intimin binding (Hamaguchi et al., 2008; Hartland et al., 1999), which further leads to TIR clustering and the formation of actin-rich pedestals (Campellone et al., 2004). These structures are highly flexible and even able to promote

bacterial motility on top of cultured cells (Campellone, 2010). Despite the homology of EPEC and EHEC TIR, these bacteria employ different ways to achieve actin polymerization. After clustering, EPEC TIR is phosphorylated at the tyrosine residue Y474 and sometimes also at Y454. Phosphorylation can be performed by different host kinases like c-Fyn, Abl, Ark and Etk (Bommarius et al., 2007; Phillips et al., 2004; Swimm et al., 2004) and is essential for pedestal formation by EPEC (Kenny, 1999). A 12 amino acid (AA) sequence around phosphorylated Y474 binds the host cell adaptor proteins Nck1 and Nck2 through their phosphotyrosine-binding SH2 regions (Campellone et al., 2002; Gruenheid et al., 2001). The adaptors then recruit and activate the cellular N-WASP protein either by direct binding of the Nck SH3 domain to the proline-rich domain (PRD) of N-WASP or indirectly through a WIP-like protein (Campellone, 2010). So activated N-WASP is in turn able to stimulate Arp2/3-triggered actin polymerization that finally results in pedestal formation (figure 2 A). Aside from previously described mechanism, EPEC has additional Nck independent pathways that influence pedestal formation.

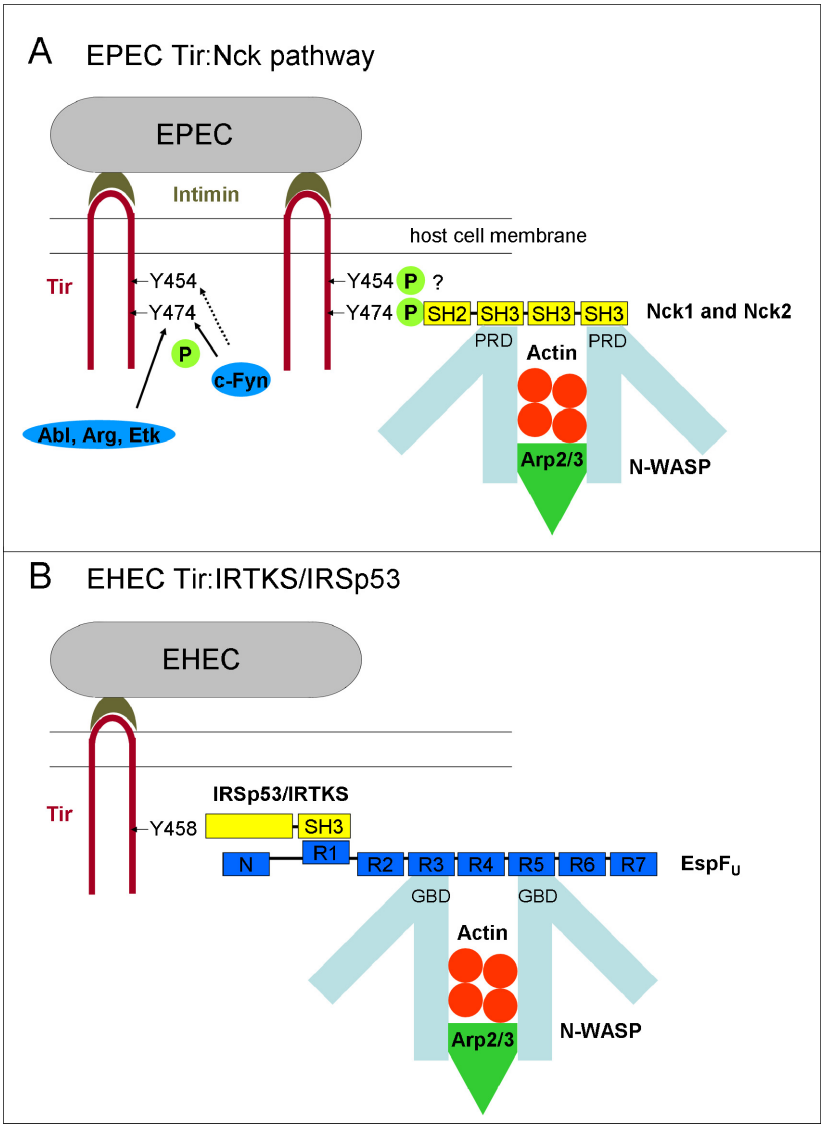

Figure 2. EPEC (A) and EHEC (B) Tir signalling.
P – phosphate; PRD – proline-rich domain; N – amino-terminal secretion signal; R1-7 – proline-rich repeats of $EspF_U$; GBD - GTPase-binding domain. Figure modified after (Campellone, 2010; Wong et al., 2011).
(A) EPEC mediates pedestal formation employing the phosphorylated Y474 Tir residue, which is crucial for Nck recruitment, in turn resulting in N-WASP activation and Arp2/3 mediated actin polymerization. (B) EHEC uses the non-phosphorylated NPY458 motif for IRSp53/IRTKS recruitment. These host cellular proteins bind to the EHEC effector $EspF_U$ which is able to activate N-WASP and trigger Arp2/3 – mediated actin assembly.

EHEC TIR has no equivalent to EPEC TIR Y474 and does not bind Nck1 or Nck2. As a consequence EHEC TIR is unable to form pedestals when expressed in EPEC (Kenny, 2001). Instead, pedestal formation by EHEC TIR requires the conserved Asn-Pro-Tyr (NPY458) motif, which is homologous to NPY454 in EPEC TIR. This motif is able to recruit

IRSp53 and IRTKS (Vingadassalom et al., 2009; Weiss et al., 2009) which in turn bind to another EHEC effector not present in EPEC, namely TccP/EspF$_U$. This second effector consists almost entirely of proline-rich repeats capable of binding to the GTPase-binding domain (GBD) of N-WASP and as a consequence activating the protein to stimulate Arp2/3-mediated actin assembly. The two ways of pedestal formation used by EPEC and EHEC are schematized in figure 2 (previous page).

1.1.3 EHEC effector proteins

The EHEC strain O157:H7 Sakai, known from severe outbreaks in Sakai (Japan) in 1982 and 1996, encodes for 62 effector genes including duplicates (Tobe et al., 2006). The known cellular functions of these virulence proteins include cytoskeleton remodelling, guanine exchange factor (GEF) mimicry, inhibition of apoptosis, manipulation of inflammatory signalling pathways and interference with phagocytosis (reviewed in (Wong et al., 2011). A list of EHEC effectors along with their (putative and known) host interaction partners and cellular function(s) is shown in table 1.

Table 1. EHEC O157:H7 effector proteins along with their host cellular localization and function. The table is obtained from (Wong et al., 2011). TJ – tight junction; PM – plasma membrane; ER – endoplasmic reticulum; AJ – adherens junction. Aside from EspK, EspM, EspN, EspR, EspV, EspW, EspX, EspY and EspF$_U$ these effectors are shared by EPEC O127:H6 E2348/69.

EHEC effector	Localization	Host binding partners	Cellular function
EspB	Cytosol, PM	Alpha 1-antitrypsin, alpha-catenin, myosin-1c	Translocation pore component, AJ disruption, binds myosins to inhibit phagocytosis
TIR	PM	14-3-3tau, alpha-actinin, cortactin, CK18, IQGAP1, IRTKS, IRSp53, Nck, PI3K, talin, vinculin	Receptor for the adhesion intimin, actin pedestal formation, downregulates Map-dependent filopodia formation, SGLT-1 inactivation
EspF	Mitochondria, cytosol, nucleus, TJ, apical membrane, lateral membrane	14-3-3zeta, ABCF2, actin, Arp2, CK18, N-WASP, profilin, SNX9, ZO-1/ZO-2	Mitochondrial disruption, NHE3 inactivation, SGLT-1 inactivation, TJ disruption, disrupts nucleolus, disrupts intermediate filaments, activates SNX9 to induce membrane remodelling, binds and activates N-WASP, inhibits PI3K-dependent phagocytosis
Map	Mitochondria	EBP50 (NHERF1), NHERF2, Cdc42	Cdc42 GEF that induces transient filopodia formation, mitochondrial disruption, SGLT-1 inactivation, TJ disruption
EspG	Cytosol, golgi	Tubulin, Arf1/6, PAK1/2/3	Disrupts microtubules, blocks ARF GTPase signalling and stimulates PAKs to inhibit endomembrane trafficking
EspH	PM, pedestal	DH-PH RhoGEFs	Blocks Rho GTPase signalling and FCgR-mediated phagocytosis, promotes actin pedestal length
EspZ	PM	CD98	Enhances b1-integrin and FAK signalling to inhibit apoptosis and cellular cytotoxicity

EspI/NleA	Golgi, PM	Syntrophin, Sec23/24, MALS3, PDZK11, SNX27, TCOF1, EBP50 (NHERF1), NHERF2, MAGI-3, SAP97, SAP102, PSD-95	Inhibits COPII-dependent protein export from ER, TJ disruption
EspJ	Cytosol, mitochondria	Unknown	Inhibits FCgR-mediated and CR3-mediated trans-phagocytosis
EspK	Unknown	Unknown	Unknown
EspL	Pedestal	Annexin 2	Enhances F-actin bundling activity of Annexin 2
EspM	Cytosol	RhoA	RhoA GEF that induces stress fibre formation
EspN	Unknown	Unknown	Unknown
EspO	Unknown	Integrin-linked kinase (ILK)	Unknown
EspR	Unknown	Unknown	Unknown
EspV	Cytosol	Unknown	Modulates cytoskeleton
EspW	Unknown	Unknown	Unknown
EspX	Unknown	Unknown	Unknown
EspY	Unknown	Unknown	Unknown
NleB	Cytosol	Unknown	Inhibits TNF-induced NF-kB activation
NleC	Cytosol, nucleus	p65 (RelA), p50, c-Rel, IkB	Metalloprotease that cleaves p65 (RelA), c-Rel, p50 and IkB to inhibit NF-kB activation
NleD	Cytosol	JNK	Metalloprotease that cleaves JNK to inhibit AP-1 activation
NleE	Cytosol	Unknown	Blocks IkB degradation to inhibit NF-kB activation
NleF	Unknown	Unknown	Unknown
NleG/NleI	Cytosol	UBE2D2	U-box E3 ubiquitin ligase
NleH	ER, PM, cytosol	Bax-inhibitor 1, NHERF2, RPS3	Binds Bax-inhibitor 1 to block apoptosis, sequesters RPS3 to inhibit NF-kB signalling
$EspF_U$	Cytosol	N-WASP, IRTKS, IRSp53, cortactin	Relieves N-WASP autoinhibition to trigger actin pedestal formation

An interesting group of effector proteins present not only in EHEC and EPEC, but also in *Shigella* sp. and *Salmonella* sp. as well as other pathogens harbouring a T3SS are the so-called WxxxE effectors. This group comprises a number of non-homologous proteins that share a characteristic Trp-X-X-X-Glu signature motif (Alto et al., 2006) and the ability to bind and activate cellular GTPases by mimicking guanine exchange factors (GEFs). The EHEC WxxxE effectors Map and EspM target the GTPases Cdc42 and RhoA (Arbeloa et al., 2010; Huang et al., 2009), respectively, which further leads to their activation and the formation of filopodia and stress fibres within the host cell (Orchard and Alto, 2012) (figure 3).
Aside from GEF mimicry, Map is also involved in the disruption of tight junctions and mitochondria as well as in the inactivation of the sodium-dependent glucose co-transporter SGLT-1, which leads to decreased fluid uptake by the host cells (Dean and Kenny, 2004; Dean et al., 2006; Kenny and Jepson, 2000; Ma et al., 2006).
Actions like those of Map and EspF (degenerates anti-apoptotic proteins; see table 1 for other functions), along with the bundle-forming pili and the surface properties of EHEC and EPEC provide sufficient stimuli to trigger intrinsic and extrinsic apoptosis pathways in host cells (Abul-Milh et al., 2001; Barnett Foster et al., 2000; Nougayrede and Donnenberg, 2004; Nougayrede et al., 2007; Papatheodorou et al., 2006).

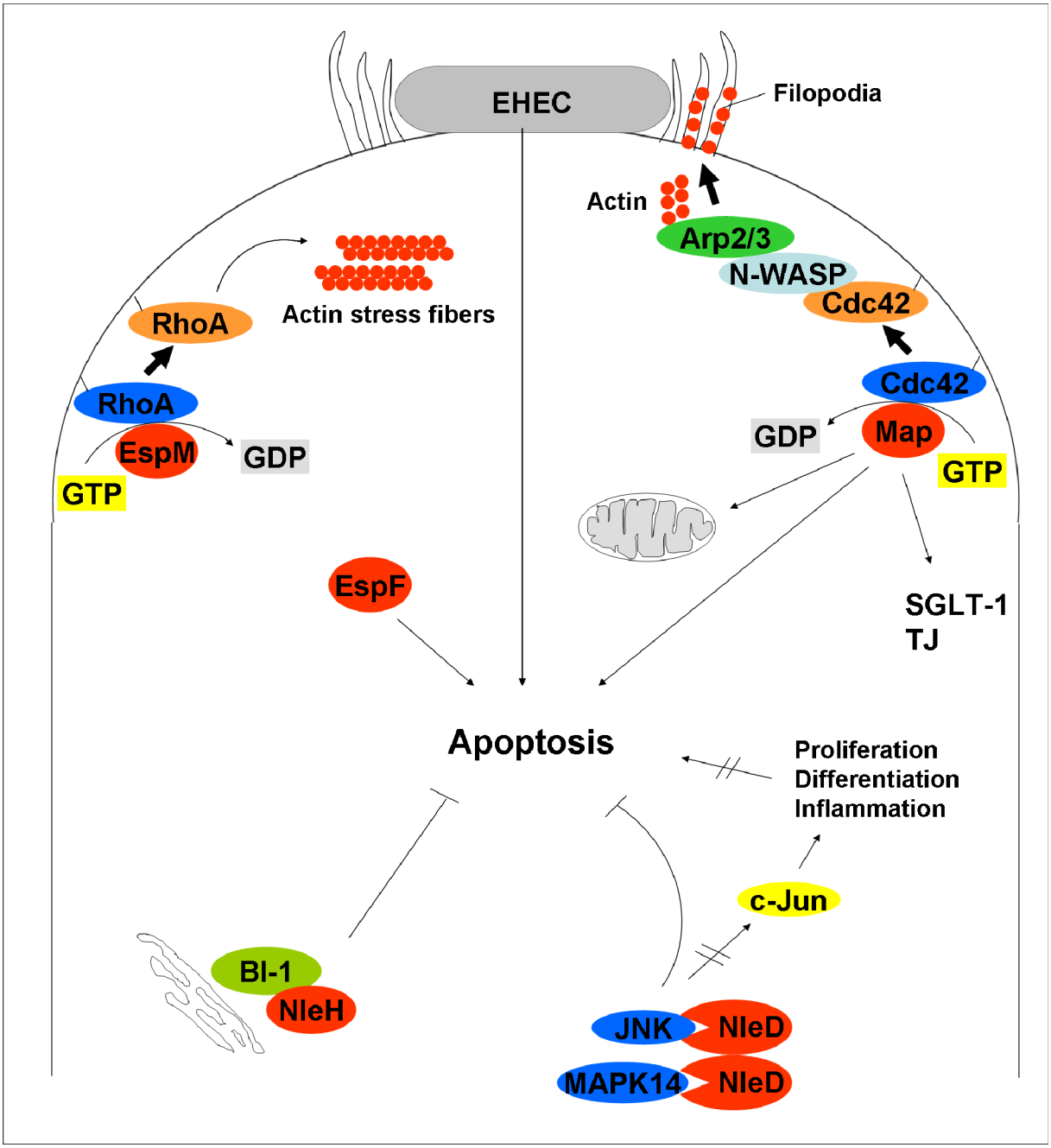

Figure 3. Actions of selected EHEC effectors in enterocytes. The two WxxxE effectors Map and EspM mimic Cdc42 and RhoA GEFs, respectively, and thus trigger formation of filopodia and stress fibers. The actions of Map and EspF as well as of attached bacteria stimulate apoptosis induction, which is counteracted by NleD and NleH. NleH binds Bax inhibitor-1 (BI-1) and blocks different intrinsic apoptotic pathways. NleD cleaves MAPK14 and JNK, which prevents c-Jun dependent transcription and thus associated pathways (cell proliferation, differentiation and inflammation) which can normally lead to apoptosis induction. Figure modified after (Orchard and Alto, 2012; Wong et al., 2011)

But despite the presence of these pro-apoptotic factors, a decrease in apoptotic rates was observed upon infection of rabbits with a related REPEC O103 strain (Heczko et al., 2001). This successful subversion of pro-apoptotic effects is mediated by effectors interfering directly or indirectly with apoptosis pathways, such as NleD and NleH. NleD is a zinc metalloprotease that cleaves MAPK14 and JNK, the c-Jun N-terminal kinase also known as MAPK8, which is required for TNF-alpha and UV radiation induced apoptosis (Tournier et al.,

2000) and thus prevents previously mentioned apoptotic pathways (Baruch et al., 2011). The two NleH effectors NleH1 and NleH2 bind the anti-apoptotic protein, Bax inhibitor-1 (BI-1) and as a consequence are able to block several intrinsic apoptotic pathways (Hemrajani et al., 2010). Aside from NleD and NleH, another effector, namely EspZ, is able to reduce cytotoxicity of EPEC infections probably by stabilization of the host epithelium (Shames et al., 2010). However regarding the importance that subversion of apoptosis has for many viral and bacterial pathogens, it is likely that more than just the three previously described effectors are involved in this process. The roles of WxxxE and anti-apoptotic effectors are schematized in figure 3.

1.1.4 EPEC versus EHEC

Although EHEC and EPEC share many pathogenicity factors such as the T3SS and most effector proteins, they differ in the expression of shiga-like toxins, which are harboured by EHEC only. Shiga-like toxins belong to the group of AB_5 toxins and as such harbour one toxic A and five receptor-binding B subunits. The five B subunits bind to the ganglioside globotriaosylceramide, which results in the uptake of the A subunit through a macropinosome (Lukyanenko et al., 2011) and thus to A-dependent arrest of protein synthesis through cleavage of the 28S RNA of the 60S ribosomal subunit (Kaper et al., 2004; Sandvig et al., 2010). This usually results in cell death. Shiga-like toxins (Stx) are the causing agents of hemolytic-uremic syndrome, which can only be caused by EHEC and STEC. However, their function and contribution to EHEC pathogenesis is not subject of this work.

1.2 Infection, cell death and pathogen interference

Bacterial and viral pathogens can cause cell death through different ways, namely necrosis, pyroptosis and apoptosis (Ashida et al., 2011).

1.2.1 Necrosis

Necrosis is a rather broad term describing a caspase-independent cell death, which can be induced among others by reactive oxigen species production, lysosomal destabilization, calpain activation, cathepsin release and depletion of ATP (Ashida et al., 2011; Lamkanfi and Dixit, 2010; Vanlangenakker et al., 2008). Aforementioned conditions can occur as a result of trauma, intoxication or infection.

1.2.2 Pyroptosis

Pyroptosis is defined as caspase-1 dependent cell death and shares features with necrosis as well as with apoptosis. It is usually a result of pathogen invasion of dendritic cells or macrophages, which leads to the assembly of inflammasomes and subsequent caspase-1 activation (Lamkanfi and Dixit, 2009). Studies in mice revealed that at least four different inflammasomes can be assembled, depending on which pathogen is involved. They comprise receptors (usually members of the NOD-like receptor (NLR) family (Kanneganti et al., 2007)) that are able to recognize pathogen-associated molecular patterns (PAMPs) in intracellular compartments using variable leucine rich repeat (LRR) motifs (Kawai and Akira, 2006; Lamkanfi and Dixit, 2010). The four inflammasomes are named after aforementioned receptors as the Ipaf inflammasome (Franchi et al., 2006; Mariathasan et al., 2004; Miao et al., 2006), the Nlrp1b inflammasome (Boyden and Dietrich, 2006), the Nlrp3 inflammasome (Barnett Foster et al., 2000; Kanneganti et al., 2006; Mariathasan et al., 2006; Sutterwala et

al., 2006) and the AIM2 inflammasome (Fernandes-Alnemri et al., 2010; Jones et al., 2010; Rathinam et al., 2010; Sauer et al., 2010).

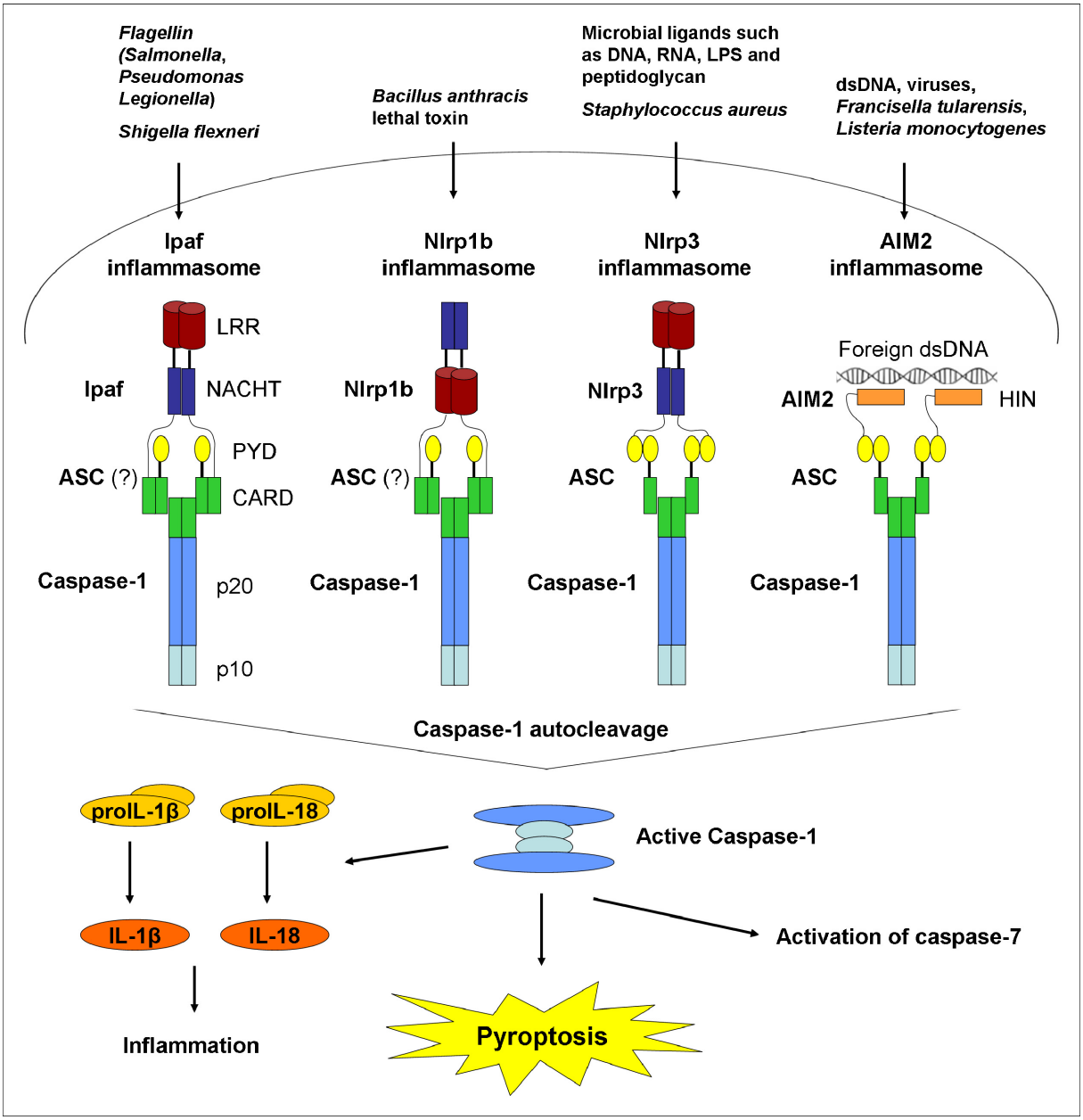

Figure 4. Pathogen stimuli and resulting formation of inflammasomes in mammalien cells. The figure is modified after (Lamkanfi and Dixit, 2010). As a result of different pathogen stimuli, four different inflammasomes can assemble in mammalian cells, namely the Ipaf, the Nlrp1b, the Nlrp3 and the AIM2 inflammasomes, which are named after their corresponding NOD-like receptors (NLR). Aside from AIM2 that harbours a HIN-200 and a PYD domain, the NLRs have LRR and NACHT domains for the sensing of PAMPs and self-oligomerization, respectively, as well as PYD or CARD domains for the interaction with the adaptor protein ASC. Procaspase-1 interacts with ASC and is activated upon pathogen attack. In its active form it cleaves proIL-1β and proIL-18, activates caspase-7 and yet unknown other substrates and as a consequence induces pyroptosis and inflammation processes.

The adaptor protein 'apoptosis-associated speck-like protein containing a caspase recruitment domain' (ASC; also known as 'PYD and CARD domain containing' = PYCARD) is believed to bridge the interaction between the receptors and caspase-1 (direct proof exists only for AIM2 and Nlrp3 inflammasomes) (Burckstummer et al., 2009; Fernandes-Alnemri et

al., 2009; Hornung et al., 2009), which as a consequence undergoes autoactivation (Lamesch et al., 2007). Active caspase-1 then processes proIL-1β and proIL-18 into the active proinflammatory forms interleukin (IL)-1β and IL-18 and activates caspase-7 as well as other to be identified substrates resulting in membrane permeabilization and DNA fragmentation (Lamkanfi and Dixit, 2010). Pyroptosis finally results in cell death and inflammation (see figure 4).

1.2.3 Apoptosis

Apoptosis is the most common form of programmed cell death. It critically contributes to the maintenance of cellular homeostasis in multicellular organisms by deletion of damaged, aged and excess cells and also by removal of infected cells along with associated pathogens (Elliott and Ravichandran, 2010; Johnstone et al., 2008; Strasser et al., 2000). In contrast to pyroptosis, it is a non-inflammatory process after whose completion dead cells are cleared through engulfment by professional phagocytes or neighbouring cells (Elliott and Ravichandran, 2010). Apoptotic cells are characterized by typical morphological and biochemical features such as membrane blebbing, cell shrinkage, chromosomal DNA fragmentation, nuclear condensation, the formation of so-called apoptotic bodies and presentation of ‘eat-me’ signals on the cell surface (e.g. phosphatidylserine).
Apoptosis can be induced through different pathways in response to extrinsic or intrinsic stimuli and is executed by a family of cysteinyl aspartate-specific proteases called caspases. Caspases can be categorized in initiator and executioner caspases. Initiator caspases like caspase-2, -8, -9 and -10 are the first to be recruited and activated (by autoprocessing) upon apoptotic stimulation. Executioner caspases such as caspase-3, -6, and -7 are activated through proteolytic processing by active initiator caspases and, once active, cleave numerous cellular substrates, which finally leads to the typical morphological hallmarks of apoptosis (Fischer et al., 2003; Taylor et al., 2008; Timmer and Salvesen, 2007).
Depending on the stimulus cells execute either of two major apoptosis pathways, namely the extrinsic receptor-mediated one or the intrinsic mitochondria-mediated way. The extrinsic pathway is activated by extracellular factors such as the ‘tumor necrosis factor related apoptosis inducing ligand’ (TRAIL), the tumor necrosis factor (TNF) and the Fas ligand (FasL) that bind death receptors like DR4, DR5 (TRAIL receptors) (Song and Lee, 2008), Fas and the TNF receptor. As a consequence of ligand binding the receptors trimerize and form together with the adaptor protein ‘Fas-associated death domain’ (FADD) the characteristic death-inducing signalling complex (DISC) (Johnstone et al., 2008). Through FADD-binding, the caspases 8 and 10 are recruited to the DISC and activated by proximity-induced autoprocessing. Active caspase-8 activates caspase-3 and cleaves the Bcl-2 homology domain 3 (BH3)-only protein Bid. Cleaved Bid (tBid = truncated Bid) activates the proapoptotic Bcl-2 family proteins Bax and Bak and inhibits antiapoptotic Bcl-2, which leads to the permeabilization of the mitochondrial membrane and thus to the release of cytochrome-c, Smac/DIABLO and HtrA2/Omi (Johnstone et al., 2008; Lamkanfi and Dixit, 2010). The release of cytochrome c from the mitochondria instigates the intrinsic apoptotic pathway, which is also activated in response to intracellular apoptotic stimuli such as DNA damaging agents, chemotherapeutic drugs, UV irradiation, growth factor depletion and infection (Saelens et al., 2004). After cytochrome c release, a 700-1400 kDa protein complex called apoptosome is assembled. It consists of the released cytochrome c bound to the carboxy-terminal WD-40 repeats of the ‘apoptotic protease-activating factor-1’ (Apaf-1) and procaspase-9, associated with the amino-terminal CARD domain of the same protein. Caspase-9 is activated by autoprocessing within the apoptosome and activates recruited

caspase-3 by proteolytic cleavage, which in turn executes apoptosis together with other effector caspases (Cain et al., 2002; Lamkanfi and Dixit, 2010). Intrinsic and extrinsic apoptosis pathways are schematized in figure 5.
Extrinsic and intrinsic apoptosis pathways are connected by Bid, which can be cleaved by caspase-8 as well as by other cellular proteases like granzyme B and cathepsin B (Saelens et al., 2004). This interconnection is of special interest for the distinction between so-called type I and type II cells that differ in their way to execute Fas-induced apoptosis. In type I cells, typically lymphocytes, activated initiator caspase-8 directly cleaves a sufficient amount of effector caspases to execute apoptosis, whereas in type II cells (most somatic cells are type II) caspase-8 dependent Bid cleavage and thus apoptosome formation and caspase-9 activation are required for apoptosis induction (Jost et al., 2009; Strasser et al., 2009; Wang et al., 1996; Yin et al., 1999). However, the definition was challenged for jurkat cells (type II), which seem to be independent from apoptosome-mediated caspase-9 activation (Shawgo et al., 2009).

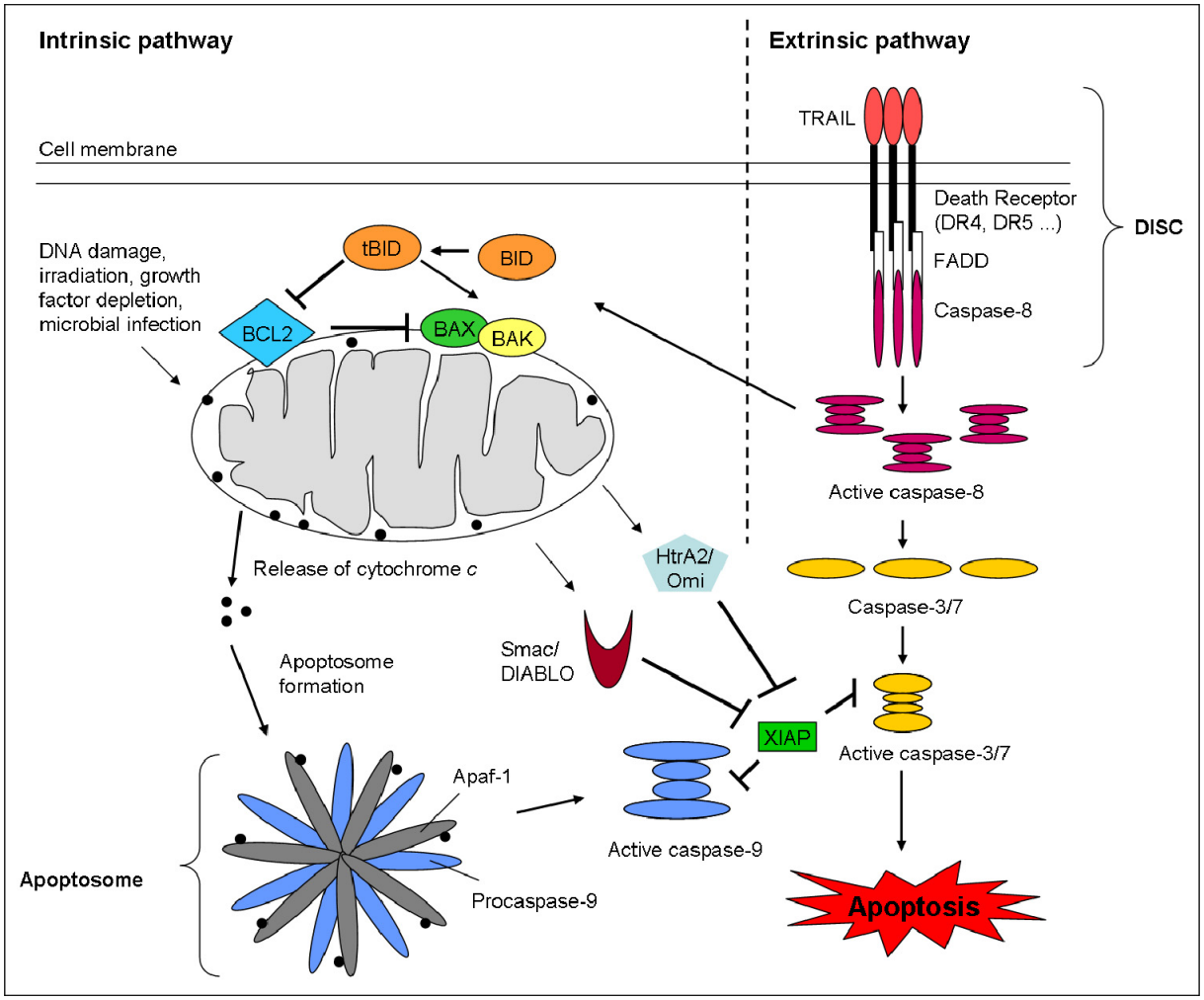

Figure 5. Intrinsic and extrinsic apoptosis pathway. Apoptosis can be induced by different stimuli, such as extracellular ligands that bind death receptors and intrinsic insults. Extrinsic stimuli activate caspase-8, which cleaves Bid and activates effector caspases to execute apoptosis. Intrinsic stimuli like DNA damage or infection stimulate the release of cytochrome c from the mitochondria which leads to apoptosome formation and caspase-9 activation. Active caspase-9 then cleaves the effector caspases.

To keep their suicide a tightly regulated process and prevent accidental induction, the cells employ different pro- and antiapoptotic proteins that are able to promote or stop apoptosis

signalling. Proapoptotic proteins include Smac/DIABLO and HtrA2/Omi, which upon their release from the mitochondria are able to block the X-linked inhibitor of apoptosis (XIAP) (Lamkanfi and Dixit, 2010). XIAP is one of eight presently known human inhibitors of apoptosis proteins (IAPs), which can be recognized by the presence of one or more baculovirus IAP repeats (BIR) and zink finger folds (Altieri, 2010). Aside from XIAP, which is able to directly inhibit caspases 3, 7 and 9, the seven other human IAPs are c-IAP-1, c-IAP-2, ILP2, ML-IAP (LIVIN), survivin, NAIP and BRUCE (Altieri, 2010; Deveraux and Reed, 1999; Shin et al., 2001).

1.2.4 Caspases

Caspases play a crucial role in different cellular processes, such as apoptosis, inflammation and development. These conserved cysteine proteases are synthesized as inactive zymogens and require proteolytic cleavage to become active. They share an amino-terminal prodomain, an intermediate large domain (17 – 21 kDa) and a carboxy-terminal small subunit domain (10 – 13 kDa). All caspases possess an active cysteine residue in the central domain and cleave specifically after an aspartate residue in substrate proteins (Yazdi et al., 2010). Aside from the human apoptosis initiator caspases 2, 8, 9 and 10 and the apoptosis executioner caspases 3, 6 and 7, there is a group of inflammatory caspases consisting of caspase-1, -4, and -5. The best characterized inflammatory caspase is caspase-1, which is involved in pryoptosis (see the chapter on pyroptosis above).
Caspase-5 is a component of the Nlrp (Nalp) inflammasome (Martinon et al., 2002; Martinon and Tschopp, 2007).
Caspase-4 was suggested to play a role in ER stress induced apoptosis (Hitomi et al., 2004; Pelletier et al., 2006), a conclusion that was challenged by other studies (Obeng and Boise, 2005) and remained controversial thus far (Martinon and Tschopp, 2007). A recent study found that caspase-4 is a positive regulator of TNF-α-induced NF-kB signalling (Nickles et al., 2012). However, further work will be necessary to clarify to what extent caspase-4 is involved in apoptosis and inflammation.

1.2.5 Pathogens and apoptosis

Pathogens do both, they induce and inhibit apoptosis (Bannerman and Goldblum, 2003; Grassme et al., 2001; Hay and Kannourakis, 2002). They induce apoptosis accidentally, as a result of exposure by the immune system or on purpose as a defence mechanism as employed by many bacteria that target macrophages or neutophiles to prevent their deletion (Faherty and Maurelli, 2008; Grassme et al., 2001; Kobayashi et al., 2003). Several viral pathogens inhibit apoptosis to keep their host cells alive until the process of replication is completed. Well-timed apoptosis induction can then promote spreading to neighbouring cells that engulf the virus-loaded apoptotic bodies, which leads to the infection of surrounding cells with minimal risk of detection by the immune system due to avoidance of any contact with extracellular fluids (Hay and Kannourakis, 2002; Teodoro and Branton, 1997).
Examples for viral inhibitors of apoptosis are baculovirus p35 and IAP, Epstein-Barr virus (EBV) BHRF1, LMP-1 and BALF1, human papillomavirus E6, SV40 Large T antigen, human immunodeficiency virus (HIV) GPx, Tat, Vpr and p17/p24 and cowpox virus (CPV) CrmA. that interfere with different parts of the intrinsically and extrinsically mediated apoptosis pathway (Hay and Kannourakis, 2002).
The need for bacteria to prevent apoptosis is not as obvious as for viruses, since bacteria are autonomous self-replicating systems that do not depend on the viability of their host cells in

an absolute manner as viruses naturally do. However, not only obligate intracellular pathogens such as *Ehrlichia chaffeensis*, *Rickettsia rickettsii* and *Chlamydia trachomatis*, but also facultative intracellular (*Shigella sp.*, *Salmonella sp.*) and extracellular pathogens (EHEC, EPEC) seem to profit from apoptosis prevention *in vivo*. According to (Faherty and Maurelli, 2008) apoptosis inhibition by pathogenic bacteria can be grouped into three different classes: 1. Protection of mitochondria, 2. Activation of cell survival pathways and 3. Regulation of caspase activity.

Examples for the first group, protection of mitochondria and prohibition of cytochrome c release, are *Neisseria sp.* and *Chlamydia sp*. *Chlamydia sp.* secrete a protein named 'clamydial proteasome-like activity factor' (CPAF), which targets cellular BH3 domain containing proteins like Bik, Puma and Bim for degradation and thus prevents mitochondrial membrane permeabilization and subsequent cytochrome c release (Dong et al., 2005; Fischer et al., 2004; Pirbhai et al., 2006; Xiao et al., 2004; Zhong et al., 2006). *Neisseria sp.* targets its outer membrane protein PorB to the hosts' mitochondria where it is thought to bind and block the mitochondrial permeability transition pore leading to the prevention of cytochrome c release (Massari et al., 2000; Massari et al., 2003) (see figure 6).

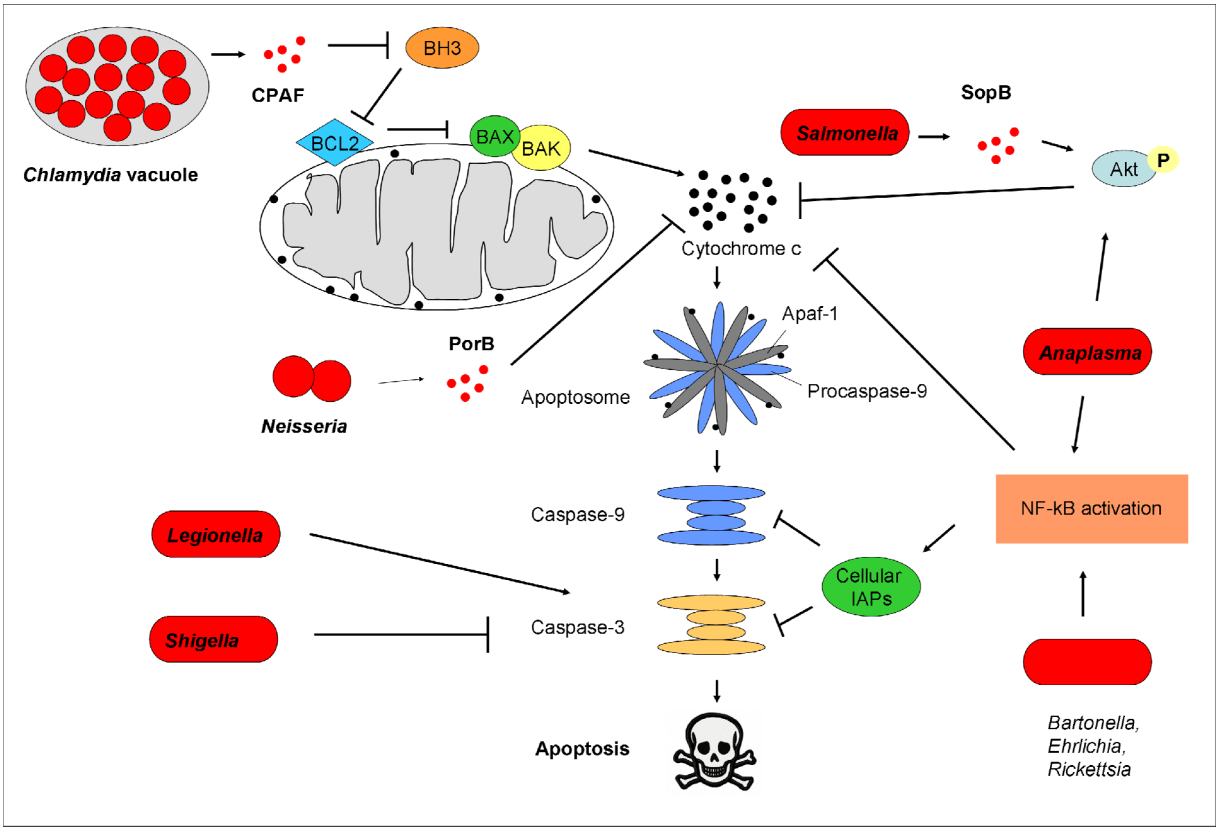

Figure 6. Interference of different pathogens with host cell pathways to prevent apoptosis. The inhibition modes of depicted pathogens are described in the text.

The second strategy, activation of cell survival pathways, is employed by intracellular pathogens like *Bartonella*, *Ehrlichia* and *Rickettsia* that prevent cytochrome c release indirectly through upregulation of NF-kB and pro-survival gens (also cellular IAPs). *Anaplasma phagocytophilum*, the cause of granulocytic anaplasmosis, prevents apoptosis in its host cells, neutrophiles, not only by NF-kB activation, but also by upregulation of the p38 MAPK, the extracellular signalregulated kinase (ERK) and the PI3K/Akt pathways (Choi et al., 2005; Lee and Goodman, 2006; Sarkar et al., 2012). *Salmonella* manipulate PI3K/Akt

signalling through phosphorylation and thus activation of the cellular pro-survival serine/threonine kinase Akt via the bacterial T3SS effector SopB. Akt activation is sufficient to prevent cytochrome c release and thus apoptosis.
The third strategy involves the manipulation of caspase activity and is used by *Legionella pneumophila* and *Shigella flexneri*. *Shigella flexneri* is able to prevent caspase-3 activation with one of its 17 MxiE regulated T3SS effectors; which one is unknown. *Legionella pneumophila* activates caspase-3 to evade the endosomal-lysosomal pathway (Abu-Zant et al., 2005) but keeps the host cell alive until at a late stage of infection, apoptosis is permitted and facilitates the pathogen's escape from the dying cell (figure 6).
Numerous pathogenic bacteria encode for several proteins involved in apoptosis regulation and employ more than one strategy to modify apoptosis pathways. This, and the fact that the majority of pathogens has evolved such mechanisms, suggests the assumption that apoptosis regulation provides an evolutionary advantage in successful host colonization *in vivo*. However, novel bacterial apoptosis regulators are identified constantly, thus further research is required to estimate the range of human cellular pathways manipulated by the large toolbox of bacterial pathogens.

1.3 Phage Lambda

1.3.1 Phages and bacterial pathogenesis

Phages are viruses that target bacteria. With 10^7 particles/ml in coastal seawater and a global population of 10^{31} phages, they are the most abundant species on earth (Hendrix et al., 1999; Wommack and Colwell, 2000) and can be found pretty much everywhere from water and soil through to the intestine of animals. Phage infections do not always follow the common predator-prey mode that ends in bacterial lysis and release of phage progeny. Some pages are able to integrate into the hosts' genome and stay there as prophages in a dormant stage to form so-called lysogenic bacteria or lysogens. During dormancy, prophage protein expression is, though reduced, not completely silent; they still express a small number of proteins that perform actions in the host cell, such as repression of the phages' lytic genes. As horizontally mobile elements phages play a major role in the transfer of new genes into bacterial cells and thus promote bacterial evolution (Tinsley et al., 2006). To support spreading, delivered genes alter the phenotype of infected bacteria and provide evolutionary advantages, such as pathogenicity factors and/or toxins, to the lysogen, a process called lysogenic conversion. Well known examples for toxin encoding prophages are the CTXϕ phage of *Vibrio cholerae* (Waldor and Mekalanos, 1996), the β-phage of *Corynebacterium diphtheriae* and the H-19B phage of *Escherichia coli* that encode the cholera toxin ctxAB, the diphtheria toxin tox and the shiga-like toxins stx1 and stx2, respectively (Brussow et al., 2004). Additionally most EHEC and EPEC effector proteins and the T3SS are linked to a metagenome mainly consisting of lambdoid prophages (Tobe et al., 2006). Thus phage biology is closely linked to bacterial pathogenicity and a closer look at different phages will certainly be worthwile cosidering the impact of phage infection on their host bacteria.

1.3.2 Coliphage lambda

Since its discovery in 1951 by Esther Lederberg, enterobacteria phage lambda is one of the most intensely studied biological organisms (Lederberg, 1951). There are many thousand papers about this phage and various molecular tools were derived from its genetic make-up.

Examples of such tools are phage display, the gateway technology and the recombineering technique, only to mention a few. Taxonomically enterobacteria phage lambda belongs, together with lambda-like viruses such as HK97, HK022 and the Stx-converting phages, to the family of *Siphoviridae*. Characteristics of this bacteriophage family are double stranded genomic DNA and a non-contractile tail.

The lambda virion consists of an icosahedral capsid (the head), a tail and tail fibers. Due to a frame shift, the tail fibers are absent in laboratory strains, but occur in Ur-lambda (Hendrix and Duda, 1992). The head comprises a linear 48.5 kb double stranded DNA genome with 12 bp single-stranded ends, the so-called cohesive ends or cos sites (Gottesman and Weisberg, 2004). In total, the phage lambda DNA comprises 92 open reading frames (ORFs), out of which 73 encode proteins.

To perform infection, phage adsorption on the bacterial surface is required. It is mediated through an interaction between the tip protein of the central tail fiber, gpJ and the *E. coli* receptor lamB, which is a trimeric maltoporine located in the outer membrane (Charbit, 2003; Werts et al., 1994). The binding of gpJ to lamB leads to conformational changes in the tail and as a consequence triggers the injection of the DNA (Roessner et al., 1983) into the cytoplasm of the host, where it circularizes with the help of the terminal cos sites and finally gets fused by the host's DNA ligase. The transition through the plasma membrane is not as well understood as through the outer membrane, but the proteins ManY and ManZ, which serve as a mannose transporter, are involved in lambda DNA transport though the inner membrane (Erni et al., 1987; Huber and Erni, 1996; Wegrzyn et al., 2012; Williams et al., 1986).

Once inside the bacterial cell, phage lambda can 'choose' between the lysogenic and the lytic way of infection. Establishment of either of the two life cycles is mediated through a complex set of regulations involving the presence of bacterial proteases and thus the condition of the host cell. Among the first lambda proteins to be expressed are early lytic genes like N, O and P as well as cII and cIII (Echols, 1986). CIII is a small 54 residue protein comprising a central α-helical domain (AS 14 to 37) sufficient for its function. It directly interacts with the bacterial FtsH (HflB) protease, which in turn is complexed with HflK and HflC at the cytoplasma membrane. Once bound cIII acts as a competitive inhibitor and at the same time as a substrate of HflB, keeping the protease busy, so that cII is unable to bind. The half-life of the so protected cII protein increases and with it its promoting effect on cI expression (Datta et al., 2005a; Herman et al., 1997; Kobiler et al., 2007). In addition cII was shown to interact with HflD, another protein that contributes to cII short half-life in the bacterial cell (Gottesman et al., 1981; Kihara et al., 2001; Parua et al., 2010).

Altogether high levels of cIII correspond negatively with high levels of HflB and/or with an increased protease activity of the latter. Since stability of cII and expression of cI depend on sufficient levels of cIII for stabilization, phage lysogeny is only established when protease (HflB and probably others) activity is low.

Once established lysogeny is a stable state until the lysogens are exposed to UV light or other DNA damaging agents leading to the activation of RecA, which in turn cleaves the lambda repressor cI, subsequently leading to induction of the lytic cycle. Further information on the establishment of lysogeny and the genetic switch can be obtained from (Court et al., 2007; Friedman and Court, 2001; Gottesman and Weisberg, 2004; Ptashne, 2006).

1.3.2.1 Lambda-host protein-protein interactions

Just as for the lysis/lysogeny decisison, phage-host protein-protein interactions are relevant for different parts of the lambda life cycle, such as gpN and gpQ antitermination, replication, virion assembly and even lambda DNA integration into the bacterial genome, an essential

step for lysogeny establishment. In the following, I will discuss interactions of host and phage proteins involved in gpN antitermination and phage DNA replication as examples. A list of known phage lambda-host interactions is shown in table 2.

Table 2. Published phage lambda-*E. coli* protein-protein interactions. Table obtained from (Hauser et al., 2012).

λ	Host	Description	References
Transcription			
cI	RecA	RecA degrades cI*	(Kobiler et al., 2004)
cI	RpoA		(Kedzierska et al., 2007)
cI	RpoD		(Li et al., 1994; Nickels et al., 2002)
cI	σ70	Interaction required for cI dependant gene expression at PRM promoter	(Nickels et al., 2002)
cII	ClpYQ	ClpYQ degrades cII *in vitro*	(Kobiler et al., 2004)
cII	ClpAP	ClpAP degrades cII *in vitro*	(Kobiler et al., 2004)
cII	HflD	HflD makes cII more vulnerable to FtsH (hfl = high frequency lysogenization)	(Kihara et al., 2001)
cII	HflB	HflB (= FtsH) protease degrades cII	(Kobiler et al., 2004; Shotland et al., 2000)
cII	RpoA		(Kedzierska et al., 2004; Marr et al., 2004)
cII	RpoD		(Kedzierska et al., 2004)
cIII	HflB	cIII inhibits HflB; HflB degrades cIII	(Herman et al., 1997; Kornitzer et al., 1991)
gpN	NusA	Transcriptional regulation	(Friedman and Court, 2001)
gpN	Lon	Lon degrades gpN	(Gottesman et al., 1981; Kobiler et al., 2004)
gpQ	σ70	gpQ antitermination	(Marr et al., 2001; Nickels et al., 2002; Roberts and Roberts, 1996; Roberts et al., 1998)
gpQ	rpoB	gpQ interacts with the β subunit of the RNA polymerase during gpQ antiterminaton	(Deighan et al., 2008)
Head			
gpB	GroE	genetic interaction; *E. coli* GroE	(Ang et al., 2000; Georgopoulos et al., 1973; Murialdo, 1979)
gpE	GroE	genetic interaction	(Georgopoulos et al., 1973)
Tail			
gpJ	LamB	LamB is the *E. coli* receptor	(Buchwald and Siminovitch, 1969; Clement et al., 1983; Mount et al., 1968; Wang et al., 2000; Werts et al., 1994)
Stf	OmpC	OmpC is a secondary *E. coli* receptor	(Hendrix and Duda, 1992)
Recombination			
Xis	Lon	Xis is degraded by *E. coli* Lon protease	(Leffers and Gottesman, 1998)
Xis	FtsH	Xis is degraded by *E. coli* FtsH protease	(Leffers and Gottesman, 1998)
Xis	Fis	both required for excIsion	(Ball and Johnson, 1991; Cho et al., 2002; Esposito and Gerard, 2003)
Int	IHF	Both catalyze recombination at attP/attB	(Campbell et al., 2002; Crisona et al., 1999)
Gam	RecB	Gam inhibits RecBCD	(Marsic et al., 1993)
Gam	sbcC		(Kulkarni and Stahl, 1989)
Bet	S1	Ribosomal S1 protein interacts with lambda bet	(Muniyappa and Mythili, 1993)
NinB	SSB	NinB also binds ssDNA	(Maxwell et al., 2005)

λ	Host	Description	References
Replication			
gpO	ClpXP	ClpXP degrades gpO	(Kobiler et al., 2004)
gpO	DnaK		(Liberek et al., 1988)
gpO	rpoB		(Szambowska et al., 2011)
gpP	DnaK		(Liberek et al., 1988)
gpP	DnaA		(Datta et al., 2005b; Datta et al., 2005c)
gpP	DnaB		(Mallory et al., 1990)

1.3.2.2 Antitermination

For the successful completion of the phage lambda lytic cycle, gpN and gpQ antitermination are required. The gpN antitermination complex is among the largest procaryotic transcription complexes; it comprises the phage lambda antitermination protein gpN along with several host proteins like NusA, NusB, NusE (s10) and NusG (Wegrzyn et al., 2012).

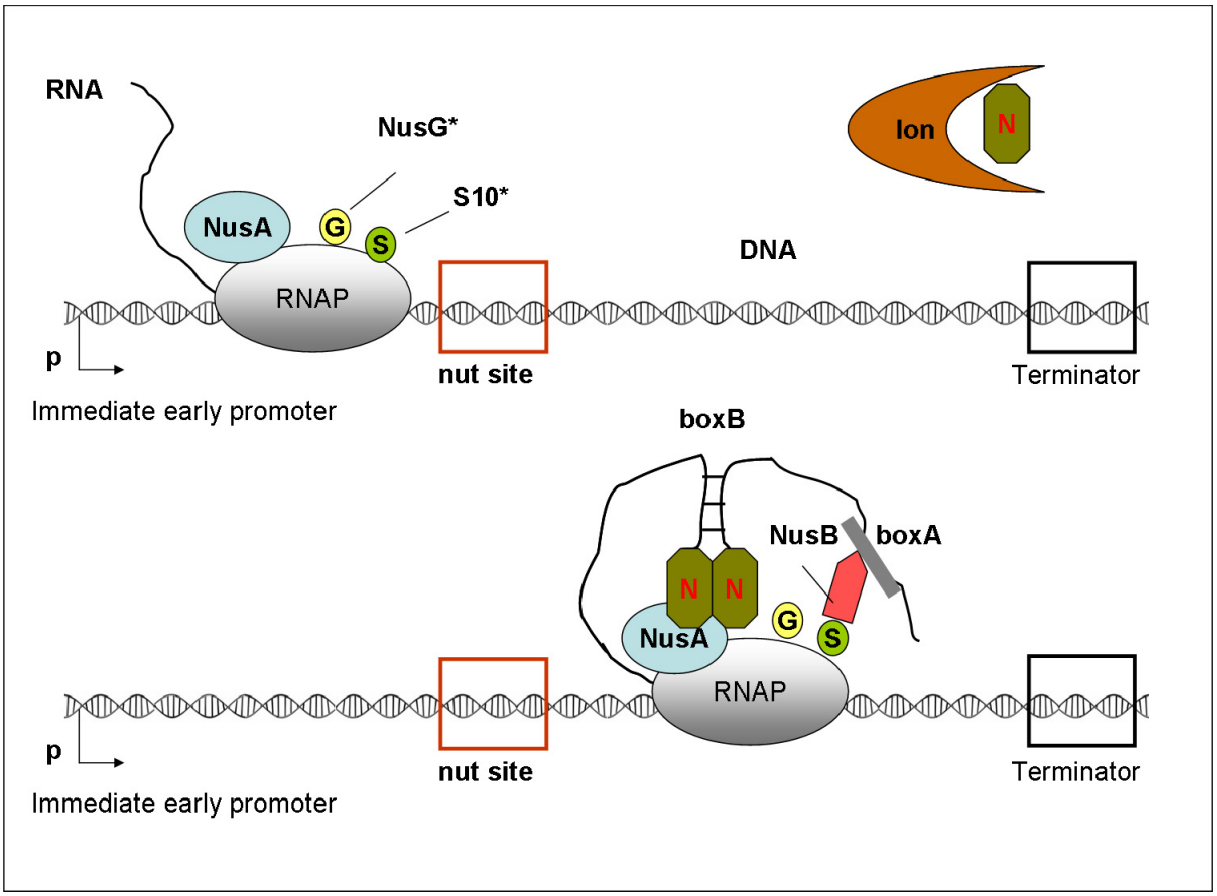

Figure 7. A model of the gpN antitermination complex. RNA polymerase transcribes the phage lambda DNA starting from the immediate early promoter, which leads to the expression of gpN. As soon as gpN is present and the nut sites are transcribed, it modifies the transcription complex by recognizing the nut sites and directly interacting with NusA. Note: lambda gpN interacts with RNA (not DNA) comprising the nut sequence. The modified complex is capable of overreading the normally valid termination signal. Lambda gpN is degraded by the host lon protease, thus ongoing antitermination requires constant transcription of gpN.
* = weekly bound to the RNA polymerase. Modified after (Das, 1992; Mason and Greenblatt, 1991). See also (Hauser et al., 2012).

GpN antitermination can start as soon as the lambda nut sites (N utilization sequence) are transcribed. The N protein captures the bacterial RNA polymerase (RNAP) by directly interacting with the RNAP-bound adaptor protein NusA. In addition gpN recognizes the boxB stem loop within the nut site and modifies the transcription complex such that it is capable of overreading the termination signal normally preventing delayed early transcription. N antitermination depends on the presence of the nut sites and thus affects only terminators located in the early phage lambda operons that reveal these sites (Conant et al., 2005). Since lambda gpN is constantly threatened by degradation through the host lon protease, ongoing antitermination requires constant transcription of gpN. Lambda gpN antitermination is schematized in figure 7.
The other phage lambda antiterminator, gpQ, that controls the expression of the late genes, contacts the RNAP via the σ^{70} factor and competes with it for access to the flap domain of the β-subunit of the RNAP (rpoB). Another difference between gpN and gpQ antitermination is that gpN binds to nut sites on previously transcribed RNA, whereas the gbQ binding element (QBE, olso called qut site) is on DNA level (Deighan et al., 2008; Nickels et al., 2002).

1.3.2.3 Replication initiation

Since lambda does not bring its own DNA polymerase, phage DNA replication critically depends on the hijacking of the host's machinery via the replication proteins gpO and gpP. Lambda gpO, once expressed, forms dimers capable of binding to the four 18 bp direct repeats of the lambda origin, which in turn is located within the sequence of the lambda O gene. Each of the repeats is able to bind a gpO dimer, leading to a total of eight monomers directly bound to the DNA. In addition, non-DNA-bound gpO protein associates with the complex solely by protein-protein interaction (Dodson et al., 1986). The so formed nucleoprotein complex is called the O-some. After O-some assembly, the gpP protein withdraws the host's DnaB helicase from the DnaB-DnaC complex (Zylicz et al., 1989). The DnaB helicase is inactive as long as it is tightly associated with gpP. The protein pair is added to the O-some through the protein-protein interaction between gpP and gpO. The three heat shock proteins DnaK, DnaJ and GrpE recruited in the following (DnaK through direct interaction with gpP and gpO) activate the DnaB helicase by liberating it from its inhibitory interaction with gpP. Then gpP as well as the chaperones are released and replication starts with the help of primase, DNA polymerase III, gyrase and the SSB (single-strand binding) proteins (Dodson et al., 1986; LeBowitz and McMacken, 1986).
In addition to the process described above, there are other factors that support replication *in vivo*, such as transcriptional activity in the lambda O region proceeding downstream of the lambda origin. Systems utilizing solely purified enzymes do not rely on transcriptional activation, whereas it is restored as soon as HU (histone-like) protein is added (Mensa-Wilmot et al., 1989). Recently Szambowska et al. showed that the RNA polymerase β subunit (rpoB) directly interacts with gpO. Even though not yet fully understood, the role of the host RNA polymerase seems to be more complex than simply changing DNA topology as previously believed (Szambowska et al., 2011). Phage lambda DNA replication initiation is depicted in figure 8.

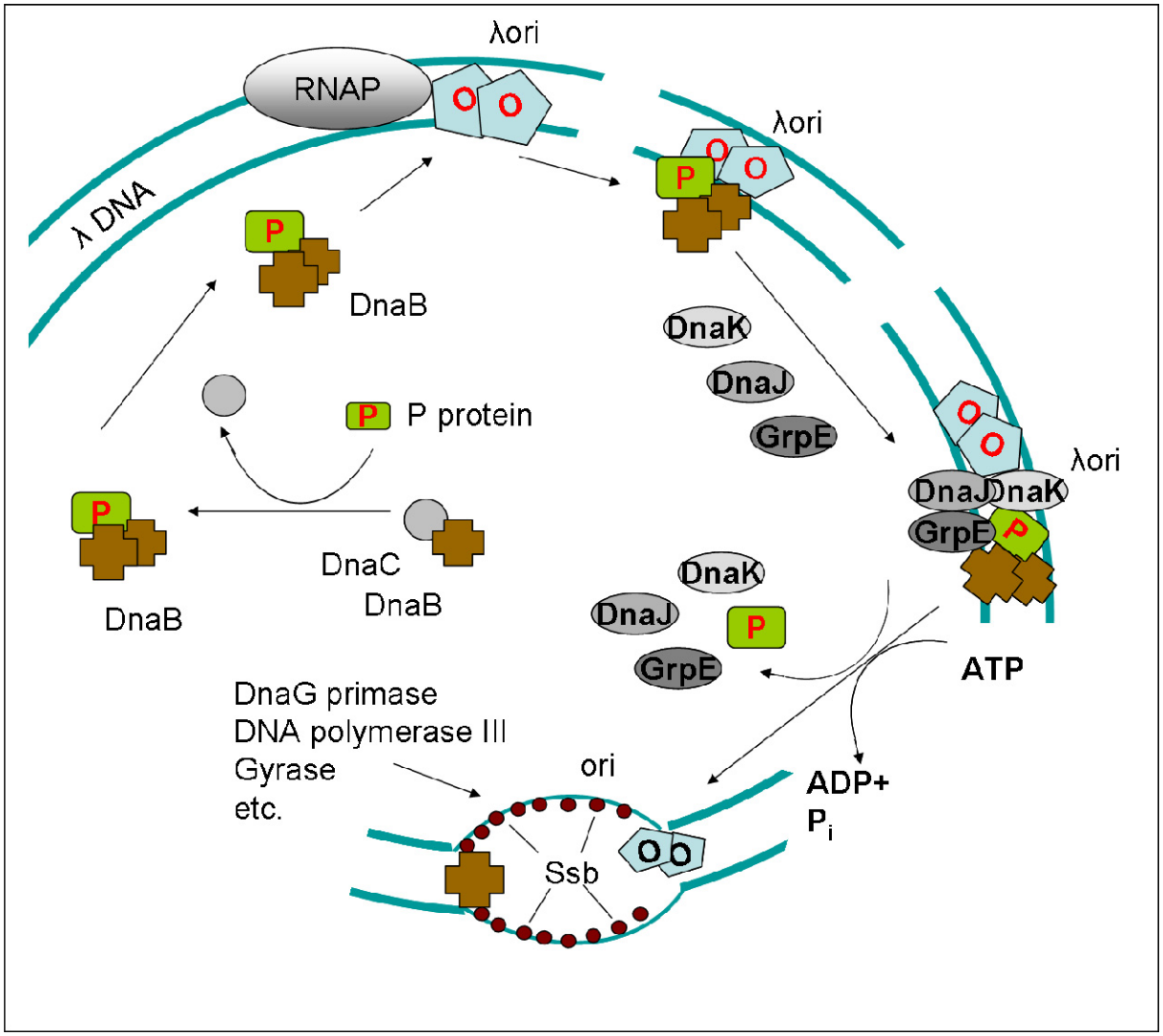

Figure 8. Initiation of phage lambda DNA replication. Four dimers of the replication initiator protein gpO bind to sequences in the phage lambda origin. Subsequent delivery of the DnaB helicase by lambda gpP and its liberation from gpP by the host proteins DnaK, DnaJ and GrpE lead to the assembly of the lambda primosome and the initiation of replication. Figure obtained from (Hauser et al., 2012)

1.3.2.4 Lambda protein-protein interactions

Only recently a study was published in which phage lambda proteins were systematically tested for protein-protein interactions (PPIs) among themselves using yeast two hybrid array screening (Rajagopala et al., 2011). In total 97 lambda-lambda interactions were detected, out of which 16 were previously published ones. This tells that even in a well-investigated organism such as phage lambda not all occurring PPIs are known and suggests the assumption that also many phage-host interactions are yet uncovered. However, a comparable approach for phage lambda-host interactions has not been published to date.

1.4 Yeast two-hybrid

A variety of methods can be used to investigate protein-protein interactions. These involve bimolecular fluorescence complementation (BiFC) (Hu et al., 2002), phage display, yeast two-hybrid (Y2H) and co-immunoprecipitation as well as biophysical methods like surface plasmon resonance and microscale thermophoresis (MST) (Baaske et al., 2010; Wienken et al., 2010). Despite the availability of many different methods, co-immunoprecipitation of endogenous proteins is still seen as gold standard for the isolation of protein complexes and the detection of protein-protein interactions. However, as a labor-intensive method it suffers from several limitations making it unsuitable for high-throughput applications.
A method that can be easily automated is yeast two-hybrid. It is an *in vivo* technique for the detection of binary protein interactions using yeast as a vessel to provide a cellular environment for protein folding. Aside from automatization, its main advantages in comparison to alternate methods include the avoidance of protein purification and the production of specific antibodies, making it a rather fast and cost-effective method and thus the technology of choice for the generation of high-throughput interactome datasets.

1.4.1 The method in general

Yeast two-hybrid (Y2H) was developed by Stanley Fields in 1989 (Fields and Song, 1989) and has thenceforth been a widely used method. In peak times nearly one thousand research articles were published annually using yeast two-hybrid for the detection of protein-protein interactions. In addition, the principle was adapted by many other methods to detect not only protein-protein, but also protein-DNA and protein-RNA interactions. Some protocols use *E. coli* instead of yeast as a vessel (bacterial two-hybrid) (Hurt et al., 2003; Joung et al., 2000).
The basic principle of yeast two-hybrid relies on the binding of a transcription factor, usually GAL4, to DNA sequences resulting in the activation of downstream reporter genes. Transcription factors consist of two domains, namely a DNA-binding domain (DBD) and a transcription activation domain (AD), which do not work independently. The two domains are separately expressed from two different vectors, whereas the one harbouring the DBD is called bait vector and the other one that contains the AD is the prey vector. Two proteins of interest to be tested for binary interactions are then cloned into bait and prey vectors, which leads to gene-fusions with the GAL4-DBD and GAL4-AD, respectively. These clones are transformed either separately or combined into haploid yeast cells. In case of a separate transformation, two yeast strains with complementary mating types are used and bait and prey clones are combined in diploid yeast after mating. For high-throughput applications separate transformations are far more practical, since this allows one bait protein to be easily combined with many preys without the effort of retransformation.
Yeast harbouring both plasmids is grown on selective medium usually lacking three essential amino acids, namely tryptophan, leucine and histidine. Whereas the leucine and tryptophan auxotrophy selection markers are constitutively expressed from the bait and prey vectors, respectively, the *HIS3* gene is only expressed when a functional GAL4 transcription factor is available. Since GAL4-DBD and GAL4-AD are split, a functional GAL4 is only achieved if bait and prey protein interact with each other, leading to a reunification of both domains and thus to a recovery of GAL4 function. If bait and prey do not interact, the yeast remains histidine auxotroph and as such unable to grow on selective media lacking histidine. See figure 9 for an overview.

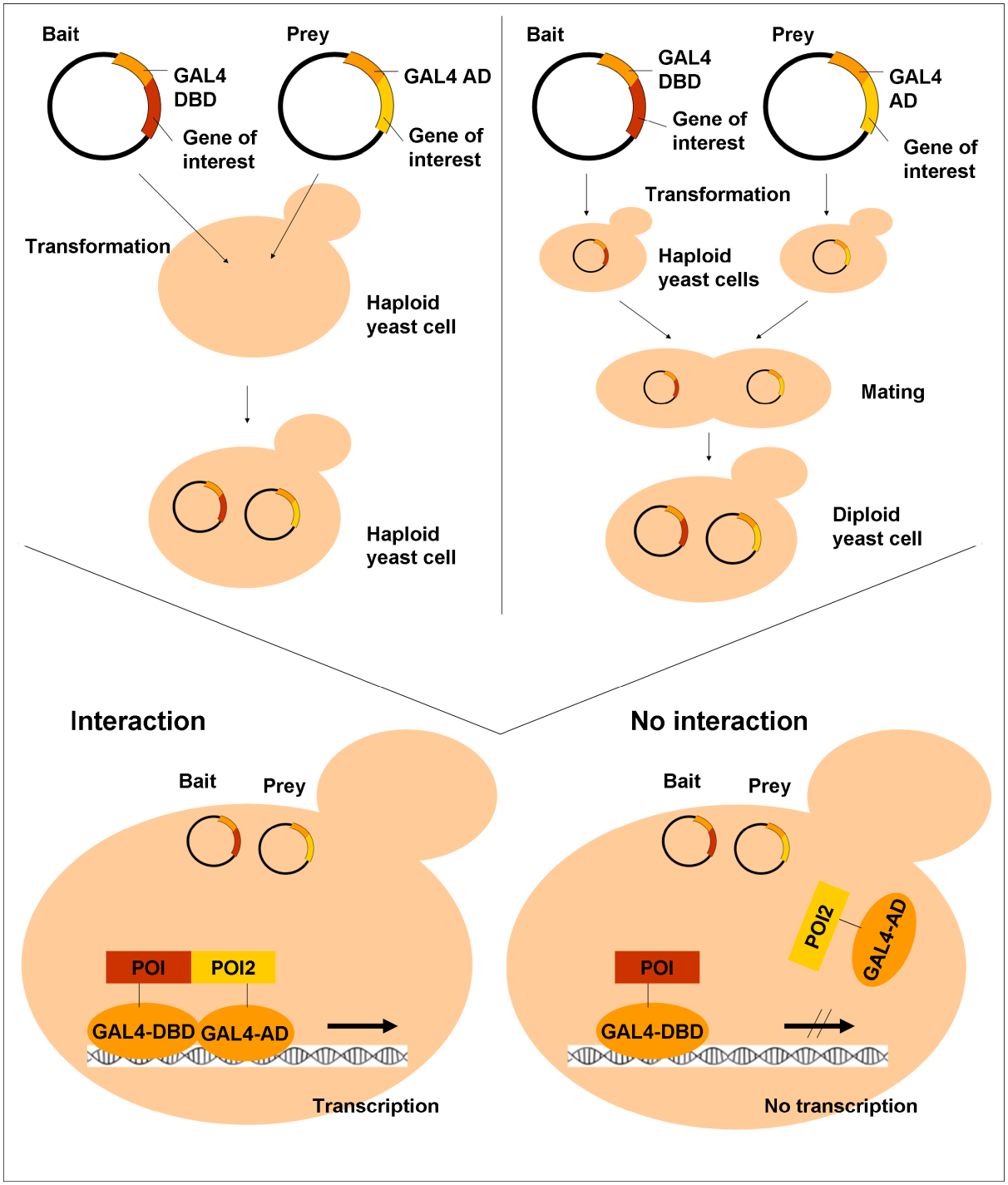

Figure 9. Flow chart visualizing the principle of yeast two-hybrid screening. Two genes of interest are fused to the GAL4 DBD and AD domains in the bait and prey vectors, respectively. Both vectors are transformed in haploid yeast, either as single or as co-transformations. For single transformants, bait and prey plasmids are combined by mating. If bait and prey are expressed as GAL4-DBD and -AD fusions in one yeast cell, the two domains of GAL4 are reunified if both proteins of interest (POI and POI2) interact with each other. This leads to GAL4-dependent transcription of reporter genes such as *HIS3* (imidazoleglycerol-phosphate dehydratase) and *Mel1* (α-galactosidase). If POI and POI2 do not interact, no transcription occurs.

The stringency of Y2H can be varied by adding a competitive inhibitor of the imidazoleglycerol-phosphate dehydratase (the *HIS3* gene product), such as 3-amino-1,2,4-triazole (3-AT), to the medium. This reduces the concentration of functional enzyme and thus

the growth speed and survival rate of yeast on HIS selective medium. Many proteins generate unspecific interaction signals when co-expressed in yeast. These signals are often weaker than those from biologically relevant interactions and can thus be removed by adding variable amounts of 3-AT.

1.4.2 High-throughput application

As previously mentioned, Y2H provides many advantages for automatization and thus for high throughput application. These involve its practicability in any lab with no need for sophisticated equipment, its cost efficiency and scalability as well as its data quality, which is comparable to that of coaffinity purification followed by mass spectrometry (Yu et al., 2008). The method has already been used for the generation of many interactomes, e.g. (Albers et al., 2005; Hauser et al., 2011; Rajagopala et al., 2011; Sabri et al., 2011; Titz et al., 2008; Uetz et al., 2006; Uetz et al., 2000), which as such verified its applicability.

1.4.2.1 Array screens versus pooled library screens

Automatization can be done in different ways: as a series of binary tests arrayed as quadruplicates on agarose plates in a 384 format (array screens) or as pooled library screens. Array screens qualify especially for the generation of rather small interactomes such as those of bacteria, viruses and phages. Their advantage lies in the fact that each protein can be tested for binding separately against all potential interaction partners. However, even for bacteria with an average genome size like *E. coli* (~ 4200 protein coding genes in *Escherichia coli* str. K-12 substr. MG1655) this equals 4200*4200 (~ 18 million) binary tests. As a consequence this can only be afforded with the help of pipetting robots and is impracticable for organisms with larger genomes.

When testing a relatively small number of baits against large proteomes as is the case for pathogen-host interactomes, pooled library screens (Mohr and Koegl, 2012) can be an alternative. The principle relies on the screening of a single bait protein against libraries containing a pool of prey proteins to be tested for interaction with the corresponding bait. Pooled libraries can contain a mixture of sequence-verified full-length ORF clones as well as batch-cloned cDNA or sheared genomic DNA of procaryotes. Both library types have advantages and disadvantages such as the increased quality of ORF clones and the coverage of a complete transcriptome or genome in case of batch-cloned libraries.

Depending on the experimental requirements, both methods, array and pooled library screening, can be combined, leading to an array of small-scale pooled library screens. Therefore the bait protein is tested for binding against a prey pool consisting of up to 50 preys. After the mating of bait and prey pool, the diploids are arrayed instead of spread on agarose plates. The interacting preys are identified by sequencing as done in standard pooled library screens. The combination of both methods reduces the number of binary tests usually required for array screens. However, if the bait interacts with more than one protein in the small prey pool, each prey has to be retested in pairwise tests. See figure 10 for a visualization of the procedures of array and pooled library screening.

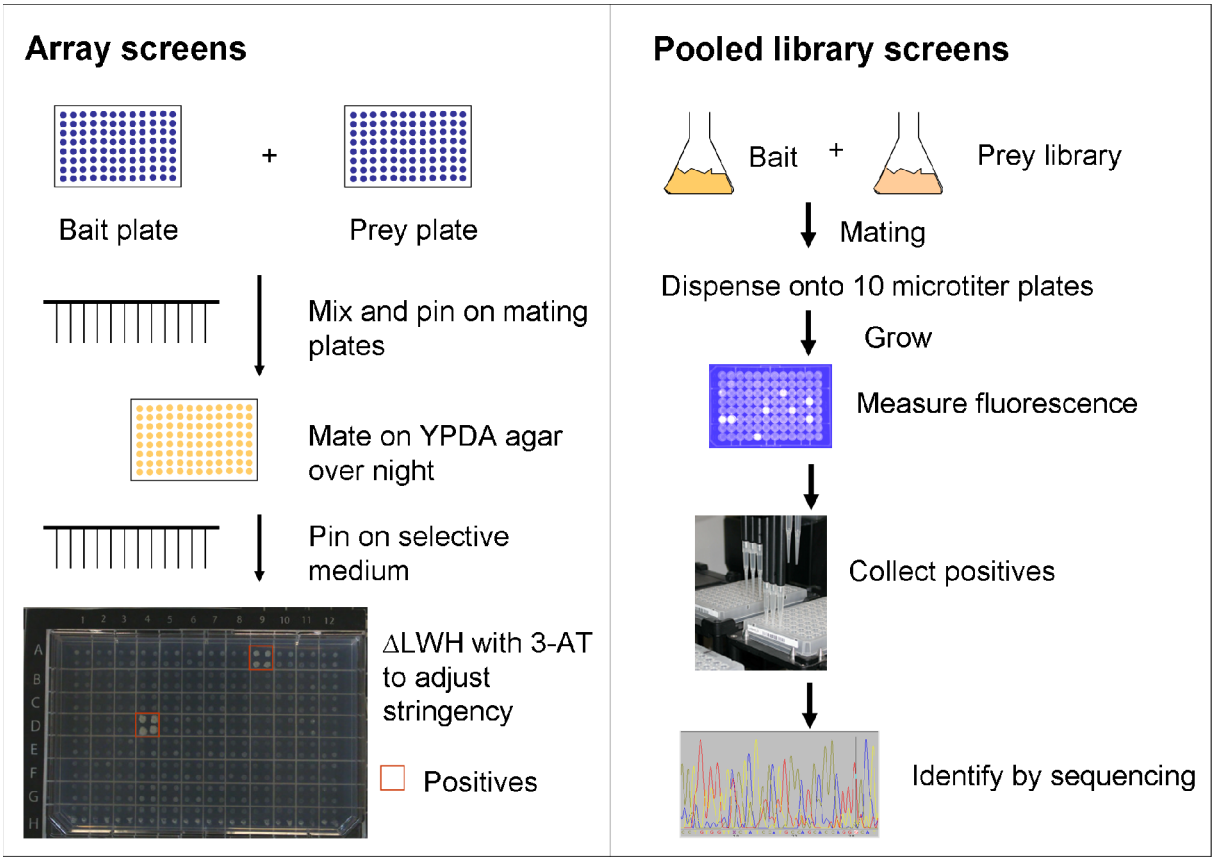

Figure 10. Yeast two-hybrid automatization as array and pooled library screening. Figure 'pooled library screens' modified after (Mohr and Koegl, 2012).

1.4.2.2 False positives versus false negatives

The usually high number of novel protein-protein interactions identified in high-throughput studies constrains the possibilities for verification by alternative methods and thus makes it especially prone to false positive and false negative identifications. To reduce the rather high false-discovery rate of yeast two-hybrid screens (Deane et al., 2002) several efforts have been made in the past (Chen et al., 2010; Koegl and Uetz, 2007; Stellberger et al., 2010). Screening with different vector systems that allow different expression levels of bait and prey proteins as well as the use of amino- and carboxy-terminal fusions of GAL4 domains result in the detection of different proteins of a 'gold standard' reference set of well characterised interactions. Even though the overlap between the vector systems is usually low, they can complement each other such that up to 80 percent of all interactions can be detected when more than one vector system is used for screening (Chen et al., 2010). This reduces the false negative rate to 20 percent, which is even lower than that determined by a comparable study using several different methods for the detection of the same gold standard reference set (Braun et al., 2009).

The problem concerning false positive discoveries is more difficult to address, since there are many different reasons for their occurrence. Examples are proteins that are able to activate reporter gene transcription on their own (transcriptional activation), false-folded proteins aggregating randomly with any other protein or proteins that truly interact but would never get in touch with each other in their native biological systems. Even though useful strategies to address this problem have been introduced previously, such as binary tests of all bait proteins against pure prey vectors or the utilization of multiple reporter genes (Serebriiskii

and Golemis, 2001), more comprehensive approaches are required to identify artefacts and thus clean up high throughput datasets from false positive interactions.

1.5 Aims of this work

E. coli is both, a suitable host for bacteriophages like phage lambda and a severe pathogen for several mammals and humans. With this work I hope to contribute to the clarification of the roles protein-protein interactions (PPIs) play in these cross-species reciprocations. My goal was to identify novel PPIs and thus to generate two representative host-pathogen interactomes, namely that of phage lambda and *E. coli* as well as that of EHEC effector proteins and their human target cells.

Another aim arising in the course of this work was the functional characterization of a particular interesting interacting pair, namely EHEC NleF and human caspase-9, which was discovered in the frame of this study.

2 Material and methods

2.1 Chemicals

Unless otherwise specified, chemicals were ordered from Sigma-Aldrich Chemie GmbH (Steinheim), Carl-Roth GmbH (Karlsruhe), AppliChem GmbH (Darmstadt), MP Biomedicals (Illkirch Cedex, France), Bio-Rad (Munich), NeoLab (Heidelberg) and Biozyme GmbH (Hessisch Oldendorf). All solutions and buffers were prepared with deionised water and autoclaved for 20 min at 121 °C (2 bar) or sterile filtered with filters from Millipore (Schwalbach), 0.22 µM pore size.
All enzymes and buffers for molecular biology were further ordered from Invitrogen GmbH (Karlsruhe), Fermentas (St. Leon-Rot), Promega (Mannheim), Roche (Mannheim) and New England Biolabs (Frankfurt am Main).

2.2 Buffers and solutions

1 M 3-AT	1 M	3-amino-triazole

Dissolved in SD-ΔLWH and stored at 4 °C.

1 M $CaCl_2$	111.1 g	$CaCl_2$ (anhydrous)
	add 1 L	ddH_2O

For 100 mM $CaCl_2$ with 15 % glycerol mix 100 ml 1 M $CaCl_2$ with 300 ml 50 % (v/v) glycerol and 600 ml ddH_2O.

Carrier DNA	10 mg/ml	herring- or salmon sperm DNA in ddH_2O

The carrier DNA solution was denaturized for 5 min at 95 °C and then stored at -20 °C.

Caspase-9 storage buffer	20 mM	Tris-HCl pH 8.0
	130 mM	NaCl

10 mM Coelenterazine	1.0 mg	coelenterazine (PJK GmbH, Kleinblittersdorf) (MW 423.5g)
	236.0 µl	methanol

The stock solution is stable at -20 °C.
Note: Coelenterazine is stable only in methanol, ethanol and basic solutions. Preferentially it is stored in methanol or in an inert gas.

6x DNA loading dye:	10 mM	Tris-HCl (pH 7.6)
	60 mM	EDTA
	0.03 %	bromophenol blue
	0.03 %	xylene cyanol FF
	60 %	glycerol

0.5 M EDTA	186.1 g	EDTA
	17.0 g	NaOH pellets
	add 1 L	H_2O

Note: EDTA is soluble only at pH 8.0. The solution was autoclaved for 20 min at 121 °C (2 bar).

20 % Glucose	20 % (w/v)	glucose in H_2O (autoclaved)
HMFM part I	3.6 g	$MgSO_4$ x 7 H_2O
	18.0 g	trisodium cItrate ($Na_3C_6H_5O_7$ x 2 H_2O)
	36.0 g	$(NH_4)_2SO_4$
	1760.0 g	glycerol
	add 3.2 L	H_2O

The solution was autoclaved for 20 min at 121 °C (2 bar).

HMFM part II	72.0 g	KH_2PO_4
	188.0 g	K_2HPO_4
	add 0.8 L	H_2O

The solution was autoclaved for 20 min at 121 °C (2 bar).

1 L 10x HMFM	800.0 ml	HMFM part I
	200.0 ml	HMFM part II
1 M K_xPO_4	1.0 M	KH_2PO_4
	add 1 L	H_2O

The solution is adjusted to pH 5.1 using KOH.

Lithium acetate solution (100 ml)	10 ml	1 M lithium acetate
	1 ml	1 M Tris-HCl, pH 7.8
	0.2 ml	500 mM EDTA pH 8.0
	89 ml	ddH_2O
LUMIER lysis buffer part I (1.1x)	22.0 mM	Tris-HCl, pH 7.5
	1.1 %	Triton X 100
	275.0 mM	NaCl
	11.0 mM	EDTA (pH 8.0)

After mixing the buffer can be stored at 4 °C for up to one year. Note: The buffer is prepared as a 1.1x concentration.

LUMIER lysis buffer	900.0 µL	LUMIER lysis buffer part I
	100.0 µL	Phosphatase Inhibitor Cocktail (Roche, Mannheim; stock: 1 tablet per 1 ml water)
	40.0 µL	Protease Inhibitor Cocktail (Roche, Mannheim, stock: 1 tablet per 2 ml water)
	10.0 µL	1M DTT
	0.5 µL	Benzonase (Novagen, 25 U/µl)

200 µl Dynabeads M-280 sheep anti-rabbit IgG 6-7x108 beads/ml, approximately 10 mg/ml (Roche) are used for 1 ml lysis buffer. Prior to use their storage liquid is removed and the beads are washed 3 times with 1 x PBS using a magnetic stand and finally resuspended in lysis buffer. The LUMIER lysis buffer is prepared freshly prior to use. The Phosphatase Inhibitor Cocktail, Protease Inhibitor Cocktail, DTT and Benzonase stock solutions are stored at -20 °C and the Dynabeads at 4 °C, respectively.

LUMIER renilla buffer	1.10 M	NaCl
	2.20 mM	EDTA pH 8.0
	0.22 M	KxPO4 pH 5.1
	0.44 g/L	BSA powder (Serva 11930)
	*2.50 µM	coelenterazine (PJK 260350; MW 423.5)
	add 1 L	H_2O

In general 1 L of LUMIER renilla buffer was prepared and stored in 50 ml aliquots at -20 °C for future usage.
*The coelenterazine is added from a 10 mM stock (also stored at -20 °C) freshly prior to use.

60 mM 4-MU	100 mM	4-methylumbelliferyl-alpha-D-galactoside (4Mu-X, Biosynth, Sigma, M-7633)
	5 ml	dimethylformamide

No sterilisation is required; the solution is stored at -20 °C.

NleF storage buffer	25 mM	Hepes-NaOH pH 7.5
	250 mM	NaCl

10x PBS	80.0 g	NaCl
	2.0 g	KCl
	14.6 g	Na_2HPO_4 (anhydrous)
	2.0 g	KH_2PO_4
	add 1 L	H_2O

The solution was adjusted to pH 7.4 (HCl) and autoclaved for 20 min at 121 °C (2 bar).

40 % PEG	40 % (w/v)	PEG_{6000} in H_2O

The solution was autoclaved. For 50 % PEG use 50 % (w/v) PEG_{6000} in H_2O.

40 % PEG solution (100 ml)	80 ml	50 % PEG_{6000}
	10 ml	1 M lithium acetate
	1 ml	1 M Tris-HCl pH 8.0
	0.2 ml	0.5 M EDTA pH 8.0
	9 ml	ddH_2O

0.25 % SDS	2.5 g	sodium dodecyl sulfate (SDS)
	add 1 L	H_2O

The solution was autoclaved.

Solution I (500 ml)	125 ml	2 M sorbitol (autoclaved)
	5 ml	1 M Bicine-NaOH pH 8.35
	15 ml	ethylene glycol
	25 ml	DMSO
	330 ml	ddH_2O

Solution II (50 ml)	40 ml	50 % PEG_{6000}
	10 ml	1 M Bicine-NaOH pH 8.35

Solution III (50 ml)	1.5 ml	5 M NaCl (autoclaved)
	500 µl	1 M Bicine-NaOH pH 8.35
	48 ml	ddH_2O
staurosporine 1 mg/ml	500 µg	staurosporine (Roche Diagnostics, Mannheim, Germany)
	500 µl	DMSO

The solution is stored at 4 °C for 3 months at maximum or at -80 °C for up to 6 months.

50x TAE	242.0 g	Tris base
	57.1 ml	glacial acetic acid
	100 ml	0.5M EDTA pH 8.0
	add 1 L	H_2O

The solution was adjusted to pH 8.0 and autoclaved.

20 % Triton X-100	20 % (v/v)	Triton X-100 in H_2O

The solution is stored at 4 °C.

2.3 Culture media

LB medium	10 g	Bacto Tryptone
	5 g	yeast extract (Becton Dickinson)
	10 g	NaCl
	add 1 L	H_2O

The medium was adjusted to pH 7.0.
For preparation of LB solid medium 12 g/L of agar (GERBU Biotechnik GmbH, Wieblingen) was added prior to autoclaving.

Antibiotic selection	**Stock**	**Final concentration**
LB Kan	30 mg/ml (H2O)	30 µg/ml
LB Amp	100 mg/ml (50%EtOH)	100 µg/ml
LB Chloramphenicol	35 mg/ml (EtOH)	35 µg/ml
LB Zeocin	250 mg/ml (ready to use)	25 µg/ml (low salt medium)
LB Spectionomycin	50 mg/ml (H2O)	50 µg/ml
LB Gentamycin	10 mg/ml (ready to use)	10 µg/ml

Kanamycin, ampicIllin, chloramphenicol, zeocin, spectinomycin and gentamycin were obtained from AGS GmbH (Heidelberg), Sigma-Aldrich Chemie GmbH (Steinheim), Invitrogen GmbH (Karlsruhe), Genaxxon BioScience GmbH (Biberach) and PAA Laboratories GmbH (Pasching, Austria), respectively.

200x Adenine	4.0 g	adenine
	Dissolve in 0.1 M	NaOH (in H_2O)

The solution was sterile filtered.

10x CSM-ΔL	70.0 g	CSM -Leu (MP Biomedicals, Illkirch Cedex, France)
	add 1.0 L	H_2O

The solution was sterile filtered.

10x CSM-ΔLW	67.0 g	CSM -Leu -Trp (MP Biomedicals, Illkirch Cedex, France)
	add 1.0 L	H_2O

The solution was sterile filtered.

10x CSM-ΔLWH	62.0 g	CSM -Leu -Trp -His (MP Biomedicals, Illkirch, Cedex, France)
	add 1.0 L	H_2O

The solution was sterile filtered.

10x CSM-ΔW	74.0 g	CSM -Trp (MP Biomedicals, Illkirch, Cedex, France)
	add 1.0 L	H_2O

The solution was sterile filtered.

SD-Medium	100 ml	10x YNB
	100 ml	20% glucose
	100 ml	10x CSM solution
	700 ml	H_2O (autoclaved)

For SD-ΔL, SD-ΔW, SD-ΔLW and SD-ΔLWH, 10x CSM-ΔL, 10x CSM-ΔW, 10x CSM-ΔLW and 10x CSM-ΔLWH were used, respectively. For agar plates autoclave 700 ml H_2O with 16 g agar in a 1 L bottle and add the YNB, 20 % glucose and CSM solutions to the still liquid H_2O/agar (~60 °C).

10x YNB	67.0 g	YNB (MP Biomedicals, Illkirch Cedex, France)
	add 1.0 L	H_2O

The solution is sterile filtered.

YPDA full medium	22.2 g	Bacto Peptone
	11.1 g	yeast extract
	add 895 ml	H_2O

The medium was autoclaved and the following solutions were added.

	100 ml	20 % glucose
	5 ml	200x Adenine

Alternatively YPD ready to use powder was ordered at MP Biomedicals (Illkirch Cedex, France).

2x YPD	100 g/L	YPD powder

The solution is sterile filtered. For 1x YPDA it is diluted 1:1 with sterile ddH_2O and 5 ml 200x adenine were added per 1 L medium.

YPDA/PEG mating medium	12 ml	2x YPD
	60 µl	200x adenine
	12 ml	40 % PEG_{6000}

The solution requires being prepared freshly prior to usage.

Human cell culture MEM	500 ml	Minimum Essential Medium (MEM)
	50 ml	fetal calf serum (FCS)
	5 ml	nonessential amino acids (NeAA)
	5 ml	sodium pyruvate (100mM)
	5 ml	Pen/Strep

MEM, FCS, NeAA and sodium pyruvate were obtained from Gibco (Invitrogen). Pen/Strep (penicIllin and streptomycin) was ordered from the PAN Biotech GmbH (Aidenbach)

2.4 Human cell culture

2.4.1 HEK-293T, HeLa and Caco-2 cell culture

All three human cell lines were grown in 100 mm tissue-culture dishes (Grainer) with 10 ml of minimum essential medium and 10 % of fetal calf serum at 37 °C and 5 % CO_2 atmosphere. For cell passaging, which was done every third day, the cells were washed with DPBS (Gibco, Invitrogen), trypsinized as needed with 1.5 ml of 0.05 % trypsin-EDTA (PAN Biotech) and resuspended in 5.5 ml culture medium. Generally 0.5 – 1.0 ml of the cell suspension was added to 10 ml culture medium and replated in a fresh culture dish.

2.4.2 Freezing and thawing cells

Two culture dishes with human cells were grown for two days and harvested as described above for cell passaging. After trypsinization the cells were resuspended in 10 ml culture medium, sedimented at 400 rpm for 5 min and resuspended in 8 ml medium supplemented with 12.5 % DMSO. The cell suspension was distributed to four CryoTubes (nunc^{TM}), placed in a freezing container (Nalgene) filled with 2-propanol and stored for 2 days in a -80 °C freezer. Finally the tubes were transferred to a liquid nitrogen container.
If needed, the cells were thawed in a water bath at 37 °C until the medium was defrosted (not longer than 10 min, otherwise the viability of the cells decreases rapidly) and washed with 10 ml of room temperature culture medium. Then the cells were resuspended in 10 ml prewarmed (37 °C) medium and plated in a tissue-culture dish. To remove dead cells the culture medium was changed daily until a cell density was reached that allowed passaging.

2.4.3 Transient transfection of human cell lines

300,000 HeLa or Caco-2 cells per well were plated on 6-well culture plates (Greiner) in 3 ml antibiotic-free culture medium at least 3 h before transfection. The transfection mixture was prepared in two separate tubes with 160 µl OptiMEM (invitrogen) in each. 1.5 µl of Lipofectamine™ 2000 (Invitrogen) were added to the first tube and 1.8 µg plasmid DNA to the other. After 5 min incubation time, the two tubes were combined and incubated for 20 to 30 min at room temperature. Then the mixture was added to the cells (don't remove the culture medium). After 6 hours the transfection media was replaced by 3 ml of antibiotic-free medium. After another 10 h the medium was changed into MEM containing 1 % Pen/Strep (PAN Biotech). Transfected cells were used 48 h after transfection.
Transfection of HEK-293T cells was mostly done in 96-well plates with 10,000 cells and 100 µl culture media per well. The transfection mixtures contained 0.075 µl Lipofectamine™ 2000 and 24 ng plasmid in 12 µl OptiMEM each. For HEK-293T cells no medium changes are required.

2.5 Molecular biology

2.5.1 Primers

If not otherwise specified, all primers used in the context of this work were ordered from Invitrogen GmbH (Karlsruhe), Sigma-Aldrich GmbH and Eurofins MWG GmbH (Ebersberg).
Underlined, bold and red letters indicate restriction sites, start/stop codons and the Kozak sequence (CCACC), respectively.
Y = C or T; Y is illustrated in red and bold.
If Y equals T, there is no *Bam*HI restriction site in the sequence indicating that the primer has a terminal stop codon. In case of Y = C, a *Bam*HI site is available, which reveals that there is no stop codon in the end. This strategy allows the one shot cloning of constructs with and without terminal stop codon. Finally colonies were selected due to the presence or absence of a *Bam*HI restriction site.

List of primers used in this work

ID	Name	Primer sequence (5´-3´)
o0155	ECs0061 forw	AGGCTCCACC**ATG**AAAGTATCAGTTCCAGG
o0156	ECs0061 rev	CTGGGTGGATYCATTCAATAATTGCGTTGTCAGTAATT
o0157	ECs0847 forw	AGGCTCCACC**ATG**AAAATTCCCTCATTACAG
o0158	ECs0847 rev	CTGGGTGGATYCATTGCTGATTGTGTTTGTCCAC
o0159	ECs0848 forw	AGGCTCCACC**ATG**TTATCGCCATATTCTGT
o0160	ECs0848 rev	CTGGGTGGATYCAAATTTTACTTAATACCACACTAATAAGATC
o0161	ECs0850 forw	AGGCTCCACC**ATG**CGCCCTACGTCCCTC
o0162	ECs0850 rev	CTGGGTGGATYCAAAGCAATGGATGCAGTCTTAC
o0163	ECs0876 forw	AGGCTCCACC**ATG**GATTGTTCAAAATGCAATG
o0164	ECs0876 rev	CTGGGTGGATYCACAGCCATGCGTCTGGCG
o0165	ECs1560 forw	AGGCTCCACC**ATG**CTGCCCACTACAAATATC
o0166	ECs1560 rev	CTGGGTGGATYCAACGCCACGCAACAGG
o0167	ECs1561 forw	AGGCTCCACC**ATG**AAAATAACAAACTATATACTGCC
o0168	ECs1561 rev	CTGGGTGGATYCATTTCGATGCATTTACCATTGAG
o0169	ECs1567 forw	AGGCTCCACC**ATG**CCATTTTCAATCAAAAACAG
o0170	ECs1567 rev	CTGGGTGGATYCATTCTTTTGTGTTGTGTATCTCTG
o0171	ECs1568 forw	AGGCTCCACC**ATG**CTTCCTACATCGC
o0172	ECs1568 rev	CTGGGTGGATYCAAGAATATTTATATGTGGAACCAGAGTAT
o0173	ECs1812 forw	AGGCTCCACC**ATG**AACATTCAACCGACC
o0174	ECs1812 rev	CTGGGTGGATYCAGACTCTTGTTTCTTGGATTATATCAAAG
o0175	ECs1814 forw	AGGCTCCACC**ATG**TTATCGCCCTCTTC
o0176	ECs1814 rev	CTGGGTGGATYCATATCTTACTTAATACTACACTAATAAGATCCAG
o0177	ECs1815 forw	AGGCTCCACC**ATG**TTACCAACAAGTGGTTC
o0178	ECs1815 rev	CTGGGTGGATYCATCCACATTGTAAAGATCCTTTGTTG
o0179	ECs1824 forw	AGGCTCCACC**ATG**CCTGTCATATTAAACTTTTC
o0180	ECs1824 rev	CTGGGTGGATYCAAATTCTAGTGCATATATTTTGTGTGG
o0181	ECs1825 forw	AGGCTCCACC**ATG**CCAGTAAATGCGACA
o0182	ECs1825 rev	CTGGGTGGATYCACCCCTGTATAACACGACTCAT
o0183	ECs1994 forw	AGGCTCCACC**ATG**CCATTAACCTCAGATA
o0184	ECs1994 rev	CTGGGTGGATYCAATTACCCTTTATAACGAAGTTTCCTC
o0185	ECs1995 forw	AGGCTCCACC**ATG**CCTGTTACCACC
o0186	ECs1995 rev	CTGGGTGGATYCACTTACAACAAAAAGCTTCTCTTTTTG
o0187	ECs1996 rev	CTGGGTGGATYCAATTTTTTAAAACGAAGTTACCTCTGTCAG
o0188	ECs2154 forw	AGGCTCCACC**ATG**CCTGTAGATTTAACGCC
o0189	ECs2156 rev	CTGGGTGGATYCAATTACCCTTTATAATGAAGTTTCCTCTG
o0190	ECs2714 forw	AGGCTCCACC**ATG**TCAATTATAAAAAACTGCTTATC
o0191	ECs2714 rev	CTGGGTGGATYCATTTTTTGAGAGGATATATGTCAACATCG
o0192	ECs2715 forw	AGGCTCCACC**ATG**ATTAACAATGTTTCTTCACTTTT
o0193	ECs2715 rev	CTGGGTGGATYCACGAGCGCTTAGATGTATTAAT

o0194	ECs3485 forw	AGGCTCCACC**ATG**CCGATGAATACTACAG
o0195	ECs3485 rev	CTGGGTGGATYCATCCCTGTATAGCACGCATC
o0196	ECs3486 forw	AGGCTCCACC**ATG**CCAGTCATATTAAATTTTTCTAA
o0197	ECs3486 rev	CTGGGTGGATYCAAATACTGTTTTGTTGAAGTGGGTATATG
o0198	ECs3487 forw	AGGCTCCACC**ATG**CCCAAAATATCATCAGT
o0199	ECs3487 rev	CTGGGTGGATYCAATTTCTAACCAAGGGGTCCCATG
o0200	ECs3855 forw	AGGCTCCACC**ATG**CCAATAATAAACAAATCGG
o0201	ECs3855 rev	CTGGGTGGATYCAATTGGAATAATAATTATATACATCGAGGAA
o0202	ECs3857 forw	AGGCTCCACC**ATG**TTATCTTCATTAAATGTCCTTC
o0203	ECs3857 rev	CTGGGTGGATYCACCATGAACTGCAGGTATACAT
o0204	ECs3858 forw	AGGCTCCACC**ATG**ATTAATCCTGTTACTAATACTC
o0205	ECs3858 rev	CTGGGTGGATYCACTCAATTTTAGAAAGTTTATTATTTATGTATTTC
o0206	ECs4550 forw	AGGCTCCACC**ATG**CTTAATGGAATTAGTAACG
o0207	ECs4550 rev	CTGGGTGGATYCACCCTTTCTTCGATTGCTCATAGG
o0208	ECs4554 forw	AGGCTCCACC**ATG**AATACTATTGATAATACTCAAG
o0209	ECs4554 rev	CTGGGTGGATYCACCCAGCTAAGCGACCCG
o0210	ECs4561 forw	AGGCTCCACC**ATG**CCTATTGGTAATCTTGG
o0211	ECs4561 rev	CTGGGTGGATYCAGACGAAACGATGGGATCCC
o0212	ECs4562 rev	CTGGGTGGATYCACAATCGGGTATCCTGTACA
o0213	ECs4564 rev	CTGGGTGGATYCATAATACGCTATAAGAGGAAGCTC
o0214	ECs4571 rev	CTGGGTGGATYCAGGCATATTTCATCGCTAATGC
o0215	ECs4590 rev	CTGGGTGGATYCAAGTGTTTTGTAAGTACGTTTCAGATG
o0216	ECs4653 rev	CTGGGTGGATYCAAGCCTGGGTTATATTTTGTACAATATCG
o0217	Second Primer attB2	GGGGACCACTTTGTACAAGAAAGCTGGGTGGATYCA
o0218	Second Primer attB1	GGGGACAAGTTTGTACAAAAAAGCAGGCTCCACC**ATG**
o0219	ECs4562 forw	AGGCTCCACC**ATG**TTTAGTCCAATGACAATG
o0220	ECs4564 forw	AGGCTCCACC**ATG**TCGTTATCAGGAGC
o0221	ECs4571 forw	AGGCTCCACC**ATG**GAAGCAGCAAATTTAAG
o0222	ECs4590 forw	AGGCTCCACC**ATG**ATACTTGTTGCCAAATTG
o0223	ECs4653 forw	AGGCTCCACC**ATG**GTCGCTAAATTAAAACCA
o0243	seq* pDONR221 forw	CGGCCAGTCTTAAGCTCGGGC
o0244	seq* pDONR221 rev	GGGGATATCAGCTGGATGGC
o0245	seq* ECs0061 forw	CAATGAACTCAAAACATGCGC
o0246	seq* ECs0847 forw	GCCGATCACAGACATTTCG
o0247	seq* ECs0848 forw	CGAGTGTGGACTATAACAGGTTG
o0248	seq* ECs0876a forw	GTGATGAGAAAGGGATCACCG
o0249	seq* ECs0876b forw	CGCAATTAACTGATGGCATG
o0250	seq* ECs0876c forw	TGTCAGAGATGATCCAGAAACG
o0251	seq* ECs1560a forw	GCATATGATGTCAGTCAAGGC
o0252	seq* ECs1560b forw	GTAATACCATTAATCTAGGAGGGTG
o0253	seq* ECs1560c forw	TTATCCTGTCACACAGCAGAGTG
o0254	seq* ECs1568a forw	GCATCGAGTGCCTGACGG
o0255	seq* ECs1568b forw	AACGCAGTATGGGACCCC
o0256	seq* ECs1812a forw	CCTAGTTCCGTTTCAGGCATC
o0257	seq* ECs1812b forw	CTCTAGGGCTGGAGTTTGGC
o0258	seq* ECs1814 forw	CTCTGTTCATTCGAACAGACCTG
o0259	seq* ECs2715 forw	CCTCTGCCTGATGTGGCTC
o0260	seq* ECs3487 forw	AACGGTTATAAAACTACAAGGGC
o0261	seq* ECs3855a forw	CGCGACGCATAAACGAG
o0262	seq* ECs3855b forw	CCATACCTGGTTTATATCAGGC
o0263	seq* ECs3857 forw	GAATCATACCCTGCCAGTGAGAG
o0264	seq* ECs4550 forw	CACCGCCGCCACCG
o0265	seq* ECs4554 forw	GCGGCTAAAGGGGCTGG
o0266	seq* ECs4561 forw	CAGAGGAATGGTGTTGAGACC
o0267	seq* ECs4561 forw	GCGATTCCGTCAGGGG
o0268	seq* ECs4590 forw	GTGCTCCTGGAGTCAAACG
o0269	seq* ECs4653a forw	CTACACGGGGGCTACTTCG
o0270	seq* ECs4653b forw	GGAGGATGTTGTCCTGGCTC
o0271	seq* ECs4653c forw	GTGGAGATAGGTGCAAAGACTG
o0272	seq* ECs4653d forw	CCGCCGCCAGATGG

o0273	seq* pGBKCg rev	CATGTCAAGGTCTTCTCGAGG
o0274	ECs4561 rev	CTGGGTGGATYCAGTCGGTCGTGGTTGGGC
o0275	ECs4561 forw	AGGCTCCACC**ATG**GAAAATAATGCTCAGGCGC
o0276	ECs1561 rev	CTGGGTGGATYCAACTTTCCCTCCCGTAAAG
o0277	ECs1561 forw	AGGCTCCACC**ATG**GGGGGGCTGAGTGGTG
o0278	ECs1561 rev	CTGGGTGGATYCACCAAATAAACTGCTGCCCGC
o0279	ECs1561 forw	AGGCTCCACC**ATG**GGCGGGCAGCAGTTTATTTGG
o0280	ECs4653 rev	CTGGGTGGATYCAACAGTCTTTGCACCTATCTCCA
o0281	ECs4653 forw	AGGCTCCACC**ATG**AGTGGAGATAGGTGCAAAGACTG
o0282	ECs0876 rev	CTGGGTGGATYCAGCGCATTACT CGCCCAGA
o0283	ECs0876 forw	AGGCTCCACC**ATG**ACGCAATTAACTGATGGCATG
o0284	ECs1560 rev	CTGGGTGGATYCACCCTCCTAGA TTAATGGTAT TAC
o0285	ECs1560 forw	AGGCTCCACC**ATG**TAATACCATTAATCTAGGAGGGTG
o0304	Casp8 forw	AGGCTCCACCATGGACTTCAGCAGAAATCTT
o0305	Casp8 rev	CTGGGTGGATTCAATCAGAAGGGAATACAAGCTT
o0306	Casp8 rev open	CTGGGTGGATCCAATCAGAAGGGAATACAAGCTT
o136	Y2H PCRI forw	CTACAGGGATGTTTAATACCACTACAATGG
o137	Y2H PCRI rev	GGTTACATGGCCAAGATTGAAACTTAGAGG
o0080	Y2H PCRII forw	TGTTTAATACCACTACAATGGATGATG
o0081	Y2H PCRII rev	CATAAAAGAAGGCAAAACGATG
o0229	pGADCg PCRI forw	CAAGCATACAATCAACTCCAAG
o0230	pGADCg PCRI rev	GAGGAGGCAATTGGTTGTG
o0231	pGADCg PCRII forw	GCAAAGATGGATAAAGCGG
o0232	pGADCg PCRII rev	GAGGTTCGGACCGTTGC
o0303	ECs1815 C188Srev	CTGGGTGGATTCATCCAGATTGTAAAGATCCTTTGTTG
o0313	ECs1815 -1 rev	CTGGGTGGATTCAACATTGTAAAGATCCTTTGTTG
o0314	ECs1815 +1 rev	CTGGGTGGATTCACGCTCCACATTGTAAAGATCCTTTGTTG
o0315	ECs1815 -4 rev	CTGGGTGGATTCAAGATCCTTTGTTGTAAGTAAGATC
o0316	ECs1815 L186A rev	CTGGGTGGATTCATCCACATTGGGCAGATCCTTTGTTG
o0317	ECs1815 Q187A rev	CTGGGTGGATTCATCCACATGCTAAAGATCCTTTGTTG
o0318	ECs1815 C188A rev	CTGGGTGGATTCATCCAGCTTGTAAAGATCCTTTGTTG
o0319	ECs1815 G189A rev	CTGGGTGGATTCATGCACATTGTAAAGATCCTTTGTTG
o0320	EPEC TIR forw	AGGCTCCACC**ATG**CCTATTGGTAACCTTGG
o0321	Nterm rev (stop)	CTGGGTGGATTCAATCGGTGGTTGTAGGATC
o0322	EPEC TIR rev (stop)	CTGGGTGGATTCAAACGAAACGTACTGGTCCC
o0323	Cterm forw	AGGCTCCACC**ATG**GAAAGCAATGCACAGGCGC
o0324	Nterm rev (w/o stop)	CTGGGTGGATCCAATCGGTGGTTGTAGGATC
o0325	EPEC TIR rev (w/o stop)	CTGGGTGGATCCAAACGAAACGTACTGGTCCC

Seq* = sequencing; Primers marked as such were only used for sequence verification purposes.

2.5.2 DNA Vectors

The following vectors were used for cloning, transformation and transfection into *E. coli*, yeast and human cell lines.

Entry vectors

pDONR/zeo	*ZeoR, gateway cassette*
pDONR221	*KanR, gateway cassette*

LUMIER

pTREX-dest30-ntPrA	*AmpR, gateway cassette, SV40 origin of replication, N-terminal Staphylococcus aureus protein A tag.*
pcDNA3-Rluc-GW	*AmpR, gateway cassette, SV40 origin of replication, N-terminal Renilla reniformis luciferase tag.*

Protein expression in HeLa, Caco-2 and HEK-293T cells

pdEYFP-C1amp	*AmpR, gateway cassette, N-terminal eYFP tag, SV40 origin of replication, CMV promotor*

Yeast two-hybrid prey vectors

pDEST22	*AmpR, Trp, gateway cassette, N-terminal GAL4-AD tag, ARS4/CEN6 origin (low copy vector in yeast)*
pGAD424_GW	*AmpR, Leu, gateway cassette, N-terminal GAL4-AD tag, 2 µ origin (high copy vector in yeast)*
pGADT7g	*AmpR, Leu, gateway cassette, N-terminal GAL4-AD tag, 2 µ origin (high copy vector in yeast)*
pGADCg	*AmpR, Leu, gateway cassette, carboxy-terminal GAL4-AD tag (Stellberger et al., 2010), 2 µ origin (high copy vector in yeast)*

Yeast two-hybrid bait vectors

pDEST32	*AmpR, Leu, gateway cassette, N-terminal GAL4-DBD tag, ARS4/CEN6 origin (low copy vector in yeast)*
pGBT9_GW	*AmpR, Trp, gateway cassette, N-terminal GAL4-DBD tag, 2 µ origin (high copy vector in yeast)*
pGBKT7g	*KanR, Trp, gateway cassette, N-terminal GAL4-DBD tag, 2 µ origin (high copy vector in yeast)*
pGBKCg	*KanR, Trp, gateway cassette, carboxy-terminal GAL4-DBD tag (Stellberger et al., 2010), 2 µ origin (high copy vector in yeast)*

2.5.3 PCR

DNA amplification for purposes other than cloning was generally performed with Taq polymerase from *Thermus aquaticus*. A polymerase with proofreading abilities, such as Pfu polymerase from *Pyrococcus furiosus* or Phusion® High Fidelity DNA Polymerase, a synthetic polymerase (New England Biolabs, Frankfurt am Main, Germany), were used if a precise nucleotide sequence was required.

2.5.3.1 Standard PCR

The standard PCR was done in a 50 µl reaction volume using the BIOTAQ™ Red DNA Polymerase and corresponding reaction buffer from Bioline (Luckenwalde, Germany). An exemplary PCR reaction reads as follows:

10x NH_4 Buffer	5.0 µl
50 mM $MgCl_2$	2.0 µl
100 mM dNTP Mix (Bioline)	0.5 µl
Template	1.0 µl
Primer forward	1.0 µl
Primer reverse	1.0 µl
BIOTAQ™ Red	1.0 µl
ddH_2O	38.5 µl

The standard PCR program reads as follows:

	Initial denaturation	95 °C	3 min
25x	Denaturation	94 °C	1 min
	Annealing	55 °C	1 min
	Elongation	72 °C	1 min per 1 kb DNA
	Final elongation step	72 °C	10 min
	Hold	4 °C	

An annealing temperature (T_a) of 55 °C was used as standard. If the optimal temperature differed significantly or if unspecific bands were observed, it was adjusted using the following formula: $T_a = [4 \times (G+C) + 2 \times (A+T)] - 5°C$

For ***E. coli*** **colony PCR** a variety of the standard PCR was used with a prolonged initial denaturation time of 5 min.

2.5.3.2 Yeast colony PCR

The yeast colonies obtained after each yeast two-hybrid library screen were identified using a two-step colony PCR protocol. For efficient lysis, a yeast colony was first resuspended in 50 µl of a 0.25 % SDS (in ddH_2O) and boiled at 95 °C for 5 min. 5 µl of the lysate were used in the first PCR step (see below).

PCR no. 1	10x NH_4 Buffer	5.0 µl
	50 mM $MgCl_2$	2.0 µl
	100 mM dNTP Mix (Bioline)	0.5 µl
	Yeast lysate	5.0 µl
	Primer o136 Y2H PCRI*	0.3 µl
	Primer o137 Y2H PCRI*	0.3 µl
	ddH_2O	35.9 µl

After mixing, 2.5 µl of the reaction mix are removed and replaced by 2.5 µl of 20 % Triton X-100.

	Add BIOTAQ™ Red	1.0 µl

Run the following PCR program:

	Initial denaturation	95 °C	5.0 min
	Denaturation	95 °C	0.5 min
27x	Annealing	55 °C	1.5 min
	Elongation	72 °C	3.5 min
	Final elongation step	72 °C	7.0 min
	Hold	4 °C	

1 µl of PCR no. 1 was used as template for PCR no. 2.

PCR no. 2	10x NH_4 Buffer	5.0 µl
	50 mM $MgCl_2$	2.0 µl
	100 mM dNTP Mix (Bioline)	0.5 µl
	PCR no. 1	1.0 µl
	Primer o0080 Y2H PCRII*	0.3 µl
	Primer o0081 Y2H PCRII*	0.3 µl
	ddH_2O	39.9 µl
	BIOTAQ™ Red	1.0 µl

The program for PCR no. 2 is similar to that of the first PCR step, but with only 20 cycles and an increased annealing temperature of 58 °C.
* The primers mentioned here are for the amplification of prey library inserts in pGADT7 or pGAD424 prey vectors. If a prey library with a carboxy-terminal GAL4 activation domain tag is used (vector: pGADCg), the primer pairs o0229/o0230 and o0231/o0232 have to be used for PCR no.1 and no.2, respectively.

2.5.3.3 PCR mutagenesis

Site-directed mutagenesis of the NleF C-terminus was done using the modified reverse primers o0313 – o0319 along with the ECs1815 forward primer (o0177). Due to the short length of *nle*F, amplification was done using the reaction mixture described for standard PCR (and the enzyme BIOTAQ™ Red, Bioline). The PCR program was slightly modified, since it included the stepwise attachment of the Gateway ® attB sites. The program reads as follows:

	Initial denaturation	95 °C	5 min
9 x	Denaturation	95 °C	1 min
	Annealing	50 °C	1 min
	Elongation	72 °C	1 min
25 x	Denaturation	95 °C	1 min
	Annealing	55 °C	1 min
	Elongation	72 °C	1 min
	Final elongation step	72 °C	10 min
	Hold	4 °C	

This program was run twice, once with EHEC genomic DNA as template and the gene-specific primers (o0313 – o0319 and o0177) and again with 1 µl of the first PCR as template and the Gateway ® attB primers (o0217 and o0218).

2.5.4 Gel electrophoresis and DNA extraction from agarose gels

First all samples were mixed with 6x loading dye, then the electrophoresis of DNA was done using agarose gels containing 1 % agarose in 1x TAE buffer for 1 h at 90 -120 V, depending on the size of the gel. The gels were finally incubated in an ethidium bromide bath (1 L ddH_2O plus 1 ml 1 % ethidium bromide solution from AppliChem, Darmstadt, Germany) for 15 – 20 min and photographed using a LAS-4000 imaging system (Fujifilm Life Sclence, USA).
Purification of DNA from the agarose gel was performed using the QIAquick PCR purification Kit (Qiagen, Hilden, Germany).

2.5.5 Gateway cloning

The gateway cloning system is based on the integration and excision mechanism of bacteriophage λ. A gene of interest (GOI) is amplified in a two-step PCR that includes the stepwise attachment of the attB recombination sites and the PCR product is then inserted in an entry vector containing a so-called gateway cassette. This cassette contains the toxic *ccd*B gene (Bernard and Couturier, 1992) that is exchanged during the recombination reaction with the gene of interest and so allows a selection step aside from the antibiotic resistance marker. In a second recombination reaction, the GOI can be shuttled in different destination vectors for expression in bacteria or eukaryotic cells. Further information on gateway cloning can be obtained from (Hartley et al., 2000) and the Gateway ® Technology Manual provided by Invitrogen. Exemplary BP and LR recombination reactions read as follows:

BP	PCR product with attB sites	6 µl
	5x BP buffer	2 µl
	pDONR vector (entry vector)	1 µl (150 ng/µl)
	BP clonase enzyme mix	1 µl
LR	ddH2O	5 µl
	entry vector with GOI	1 µl
	destination vector	1 µl
	5x LR buffer	2 µl
	LR clonase enzyme mix	1 µl

Usually both reactions are performed at 25 °C over night. After completion 1 µl of 2 µg/µl Proteinase K is added and the reaction is incubated at 37 °C for 10 min to degrade the clonase. Finally 5 µl are transformed in competent *E. coli* cells.

All cloning in the frame of this work was done using the gateway technology. The correctness of the entry clones and expression vectors was assessed by sequencing and BsrGI restriction, respectively.

2.5.6 Restriction of DNA

The restriction enzymes used in the context of this work are listed below. If not stated otherwise, enzymes and corresponding buffers were ordered from (New England Biolabs, Frankfurt am Main, Germany).

Enzyme	**Source**	**Reaction temperature**
*Afl*II	*Anabaena flos-aquae*	37 °C
*Apa*I	*Acetobacter pasteurianus*	25 °C
*Bsr*GI	*Bacillus stearothermophilus GR75*	37 °C
*Bam*H1	*Bacillus amyloliquefaciens*	37 °C
*Not*I	*Nocardia otitidis-caviarum* (ATCC 14630)	37 °C
*Spe*I	*Sphaerotilus* species (ATCC 13923)	37 °C
*Xho*I	*Xanthomonas holcicola*	37 °C

Standard DNA restriction was done in 15 µl total volume for 1 h, an exemplary restriction mix (BsrGI) reads as follows:

BsrGI	Template DNA	200 ng – 1 µg
	10x BSA	1.5 µl
	10x NEBuffer (2 or 4)	1.5 µl
	H_2O	add up to 15 µl

The quality of digestion was assessed using gel electrophoresis.

2.5.7 Cloning and plasmid propagation in *E. coli*

The strains *E. coli* DH5α, *E. coli* DH10B, *E. coli* TOP10 (Invitrogen, Karlsruhe) were used for standard cloning purposes, whereas propagation of Gateway® Vectors harbouring the *ccd*B gene was done in the strain *E. coli* DB3.1 (Invitrogen).

2.5.7.1 Preparation and transformation of chemically competent *E. coli* cells

A single *E. coli* colony was picked and grown in 50 ml LB medium over night at 37 °C and 200 rpm. 500 ml LB were inoculated with this starter culture to an OD_{600} of 0.05 and grown for 2 – 3 h until an OD_{600} of 0.4 was reached. Then the culture was placed on ice for 30 min and harvested at 4000 rpm and 4 °C. Subsequently the medium was discarded and the pellet was washed with 25 ml of ice cold 100 mM $CaCl_2$. Finally, the cells were resuspended in 5 ml ice cold 100 mM $CaCl_2$ with glycerol (15 % v/v), divided in 50 µl aliquots and frozen in liquid nitrogen. The tubes can be stored at –80 °C for up to 1 year, afterwards the transformation efficiency decreases.

For transformation, an aliquot of competent cells was thawed on ice for about 20 min, then 5 µl of gateway recombination reaction or 1 µl of plasmid DNA were added and the cells were incubated for another 30 min on ice. Subsequently a heat shock was done at 42 °C for 60 sec and the cells were cooled down on ice for another 2 min before 750 µl of room temperature LB medium were added followed by an incubation period of 1 h at 37 °C and 700 rpm. Finally 100 µl of the cell suspension was plated on selective agar plates.

2.5.7.2 Electrocompetent *E. coli* cells

For the preparation of electrocompetent *E. coli*, 500 ml bacterial culture were grown to an OD_{600} of 0.5 as previously described for chemically competent *E. coli* and then placed on ice for 20 min. All subsequent steps were performed at 4 °C. The cells were harvested at 4000 rpm for 15 min, washed in 250 ml sterile ice cold ddH_2O and resuspended in 10 ml ice cold ddH_2O with 10 % glycerol. Finally the cells were distributed in 50 µl aliquots into pre-chilled tubes, frozen in liquid nitrogen and stored at -80 °C.

The transformation of pooled libraries that required increased transformation efficiency was done using electrocompetent *E. coli*. An aliquot of the cells was thawn on ice and mixed with 1 µl (0.5 – 1 µg) plasmid DNA. Then the suspension was incubated on ice for 5 min, transferred into a precooled electroporation cuvette (1 mm electrode gap, Peqlab, Erlangen) and pulsed once at 1.8 kV with a MicroPulser™ (Bio-Rad Laboratories GmbH, München). Directly after electroporation, the bacteria were mixed with 750 µl of LB medium and incubated at 37 °C for 1 h at 700 rpm. Finally the cells were plated on selective medium.

2.5.8 Plasmid DNA preparation

Preparation of plasmids from bacteria was done using the Qiagen Mini, Midi and Maxi plasmid kits (Qiagen, Hilden, Germany). The purity and concentration of DNA was determined using the NanoDrop Spectrophotometer (Thermo Scientific, Wilmington, USA).

2.5.9 DNA Precipitation

The DNA was mixed with 0.1 volumes of 3 M sodium acetate (pH 5.2) and 2.7 volumes of ice cold ethanol, then incubated for at least 2 h at -20 °C and further centrifuged at 20,000 rpm and 4°C for 1 h. The pellet was washed with 800 µl of ice cold 70 % ethanol, dried for 15 min under sterile conditions and finally resuspended in an appropriate amount of ddH_2O.

2.6 Proteomics

2.6.1 Yeast two-hybrid

Yeast two-hybrid (Y2H) is a method to detect interactions between two proteins in a living cell. The method is based on a transcription factor (GAL4) split in its two domains that do not work independently. If these two domains, namely GAL4-DNA-binding-domain (GAL4-DBD) and GAL4-activation-domain (GAL4-AD), are expressed as fusion proteins with two proteins of interest (POI) having affinity for each other, the two parts of the split protein are recombined and its function is restored.
Yeast two-hybrid can be used in large-scale to screen whole interactomes as well as in small-scale for the detection of binary protein-protein interactions (PPI). In this work, Y2H was used to identify unknown interaction partners of defined bait proteins by screening against pooled prey libraries and for the verification of identified binary protein-protein interactions.

2.6.1.1 Yeast strains

Bait:

CG1945 *MAT a, ura3-52, his3-200, ade2-101, lys2-801, trp1-901, leu2-3 112, gal4-542, gal80-538, cyh^{r}2, LYS2::GAL1$_{UAS}$-GAL1$_{TATA}$-HIS3, URA3::GAL4$_{17mers(x3)}$-CYC1$_{TATA}$ –lacZ*

AH109 *MAT a, ura3-52, his3-200, trp1-90, leu2-3 112, gal4□ □ gal80□ □, LYS2::GAL1$_{UAS}$-GAL1$_{TATA}$-HIS3, GAL2$_{UAS}$- GAL2$_{TATA}$-ADE2, URA3::MEL1$_{UAS}$-MEL1$_{TATA}$ –lacZ, MEL1*

Prey:

Y187 *MAT alpha, ura3-52, his3-200, ade2-101, trp1-901, leu2-3, 112, gal4□ Δ, met-, gal80□ Δ, URA3::GAL1$_{UAS}$-GAL1$_{TATA}$ -lacZ, MEL1*

2.6.1.2 Competent yeast cells and transformation

This protocol was used to transform bait plasmids for Y2H pool screening and bait and prey plasmids for Y2H binary tests.
An overnight culture of 5 to 10 ml in volume was grown at 30 °C in YPDA at 180 rpm (Infors HT Multitron Cell incubator), inoculated in 500 ml 1x YPDA (start OD_{600} ~0.3) and grown for another 2 to 3 h until an OD_{600} of 0.6 – 0.8 was reached (this equals roughly a cell density of 0.6 – 0.8*10^7 yeast cells per ml). Then the cells were harvested at 2900 rpm (~1000x g) for 2 min, washed with 0.5 volumes (250 ml) of Solution I and resuspended in 0.02 volumes

(10 ml) of Solution I. Finally the yeast cells were divided in 0.2 ml aliquots and slowly frozen at -80 °C. To maximise transformation efficiency, all steps before freezing were done at room temperature.
For competent yeast transformation, salmon or herring sperm carrier DNA (10 mg/ml) was denaturated at 95 °C for 5 min and placed on ice immediately. One 0.2 ml yeast aliquot per plasmid was taken out of the -80 °C freezer and also placed on ice. Then 2 µg plasmid DNA and 5 µl of denaturated carrier DNA were added to the still frozen yeast suspension and the mix was incubated for 10 – 15 seconds at 37 °C. After that it was mixed until the melting was complete, then 1.4 ml Solution II were added and after thorough mixing the suspension was incubated at 30 °C for 1 h at 700 rpm in a Thermomixer comfort (Eppendorf, Hamburg). Finally the cells were spun down (3000 rpm for 10 sec), resuspended in 150 µl Solution III and plated on selective agar plates (SD-ΔW or SD-ΔL, depending on the selective marker of the transformed plasmid).

2.6.1.3 Yeast two-hybrid library transformation

A colony of the yeast prey strain Y187 was precultured in 5 ml YPDA over night at 30 °C and 180 rpm. About 1 ml of the overnight culture was inoculated in 500 ml YPDA (start OD_{600} ~0.1) and grown until an OD_{600} of 0.6 was reached, then the cells were harvested at 2900 rpm (~1000x g) for 2 min at room temperature and washed in 120 ml sterile ddH_2O. A second washing step was performed with 50 ml lithium acetate solution before the pellet was resuspended in 5 ml lithium acetate solution. Subsequently the cell suspension was distributed in 4 aliquots into 50 ml Falcon tubes and the following transformation mixture was prepared for each:

yeast cell suspension	1250 µl
carrier DNA	50 µl
plasmid DNA (prey library)	12.5 µg
40 % PEG solution	7.5 ml

The solution was mixed well and incubated for 30 min at 30 °C, followed by a heat shock at 42 °C for 15 min. After the heat shock, the cells were spun down at 2900 rpm for 2 min at room temperature and resuspended in 1 ml of selective medium per tube. The yeast suspension was then plated on one selective agar plate per tube (Bio-Assay dishes, 245 x 245 x 25 mm, nunc, Thermo scientific, Langenselbold) and grown for 2 -3 days at 30 °C. The number of yeast colonies was determined and the yeast was washed from the agar plates using 15 ml YPDA with 15 % glycerol. The suspension was divided in 50 µl aliquots and slowly frozen at –80 °C. For a pooled ORF library containing 12,000 genes, at least 120,000 yeast colonies should be harvested (equals a 10x coverage), whereas for a human cDNA library at least 5 million colonies are required.
Before usage one 50 µl aliquot was taken from the -80 °C freezer, inoculated in 35 ml selective medium and grown over night at 30 °C and 180 rpm to an OD_{600} between 1.0 and 3.0.

2.6.1.4 Yeast two hybrid pooled libraries

E. coli W3110 libraries	See (Rajagopala et al., 2010) for the origin of the clones. The library in pDEST22 and pGADT7g was provided by Peter Uetz and SV Rajagopala
Universal human cDNA library	ordered ready to use from Clontech

ORF.01/02 and *ORF.03*	collection of 12,000 human genes in gateway compatible pGAD424 (ORF.01/02) and pGADCg (ORF.03) bait vectors with amino- and carboxy-terminal GAL4-DBD, respectively

The ORF libraries ORF.01/02 and ORF.03 both originate from the same human gene collection (Brasch et al., 2004; Lamesch et al., 2007; Temple et al., 2009) in pDONR223 entry vector that was shuttled into amino- and carboxy-terminally tagged prey vectors. The ORF.01/02 was provided ready to use by M. Koegl, whereas the ORF.03 was produced by myself.

2.6.1.5 Library screens

A single yeast colony harbouring the bait plasmid to be tested and an aliquot of the corresponding library were inoculated in 12 ml of selective medium each and grown over night at 30 °C and 180 rpm until an OD_{600} of approximately 1.0 was reached. Note that bait and prey plasmids require distinct selection markers to allow control for successful mating. Then both were mixed in a 50 ml plastic tube (Falcon™) and spun down at 2900 rpm for 2 min at room temperature. The supernatant was discarded, 24 ml of YPDA/PEG mating medium were added and the yeast suspension was mixed thoroughly. Yeast mating was performed at 30 °C and 100 rpm for exactly 3 h before the cells were harvested at 2900 rpm for 2 min at room temperature. Then the pellet was washed with 10 ml of ΔLWH selective medium and resuspended in 200 ml ΔLWH comprising 75 µl of 60 mM 4-Methylumbelliferyl-alpha-D-galactoside (4Mu-X, Biosynth) and 80 µl of 1 M 3-AT (0.4 mM final concentration).
For determination of the mating efficiency (= screening depth), 10 µl of yeast solution were diluted with 990 µl ΔLW and 100 µl of those were plated on an ΔLW agar plate. Colonies were counted after 2 days and the screening depth (in millions) was determined with the following formula:
Screening depth in millions (for 200 ml suspension in total) = number of colonies x 0.2
The number should be above 5 million.
The remaining yeast suspension was distributed to 10 96-well plates (Flat-bottom transparent microtiter plates), 200 µl per well, and grown at 30 °C without shaking for 6 days. Then the fluorescence of the plates was measured at an excitation of 360 nm and an emission of 465 nm using the TECAN Infinite 200 Reader (equipped with stacker, automated loading system, and bar-code reader). All wells harbouring a yeast colony and revealing fluorescence at least two fold above that of the plate mean were seen as positive for an interaction. 10 µl of each positive yeast colony were then collected, re-arrayed on a fresh 96-well microtiter plate harbouring 200 µl ΔLWH per well and grown for another two days. Finally the re-array plates were used as template for the previously described yeast colony PCR steps and the PCR product was sequenced (GATC, Konstanz, Germany) to identify the prey insert. A flow diagram visualizing the principle of Y2H pool screening is shown in figure 11. Further details can be obtained from (Mohr and Koegl, 2012).

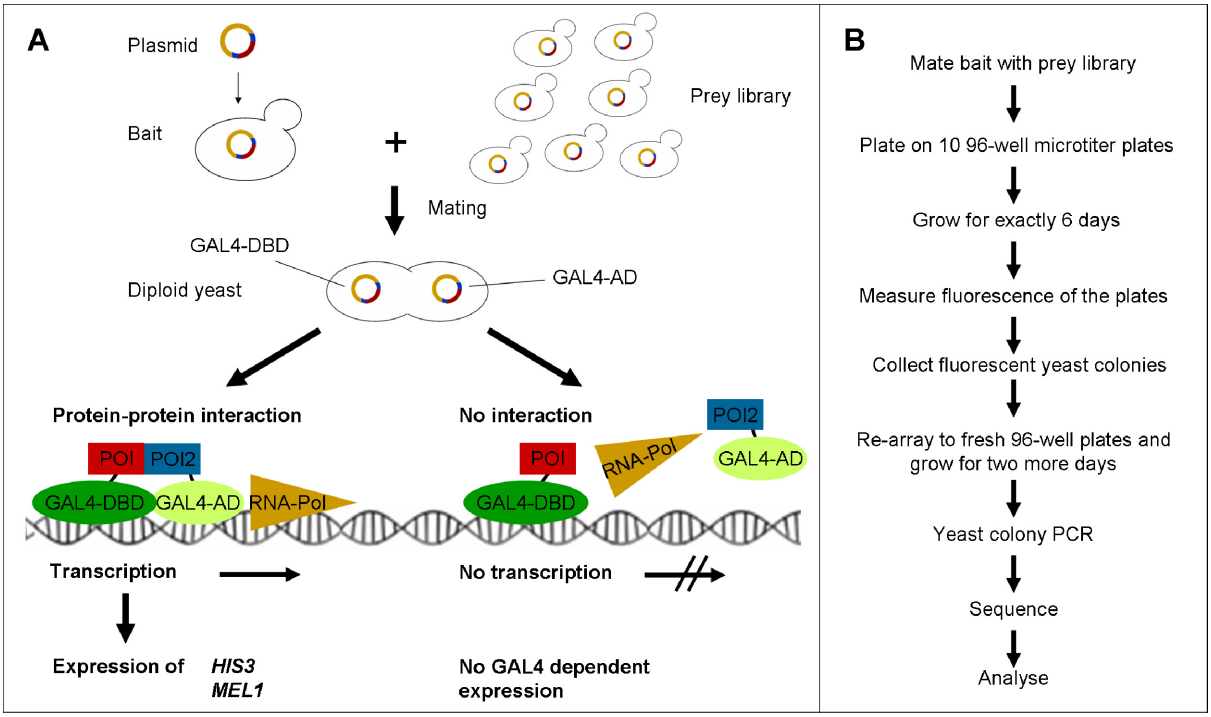

Figure 11. Flowchart visualising the principle (A) and procedure (B) of yeast two-hybrid pool screening. (A) The bait harbours a plasmid encoding a protein (protein of interest, POI) to be tested for interaction against a prey library containing several thousand different plasmids. Bait and prey library are mated to combine the bait protein with the library. If the bait found an interacting protein, the GAL4-DBD and the GAL4-AD fused to bait and prey protein, respectively, are joined leading to GAL4 functioning as transcription factor and thus to GAL4-dependent expression of the selective markers *HIS3* and *MEL1*. *HIS3* encodes the imidazoleglycerol-phosphate dehydratase whose expression leads to histidine prototrophy. *MEL1* encodes an α-galactosidase that cleaves 4-MU and thus generates measurable fluorescence when expressed. (B) Scheme of the different steps of the Y2H pool screening procedure. Further explanation can be obtained from the text.

2.6.1.6 Pairwise tests

To test binary interactions in Y2H, a single bait and a single prey plasmid were transformed in bait and prey yeast strains (as previously described in 'Competent yeast cells and transformation'), respectively. A colony of each was then grown over night in 1 ml selective medium at 30 °C and 180 rpm. Subsequently 500 µl of bait and prey were mixed, spun down at 2900 rpm for 2 min at room temperature and 1.5 ml YPDA/PEG mating medium were added. Cells and mating medium were mixed thoroughly and the mating was performed at 30 °C and 100 rpm for 3 h. Then the cells were harvested at 2900 rpm for 2 min, washed with 2 ml ΔLW medium and resuspended in 1 ml ΔLW. The diploids were grown for 2 days in liquid ΔLW at 30 °C without shaking and then plated on selective agar plates (ΔLWH). If bait and prey protein interact, visible colonies appear after 2 days. If required the stringency was adjusted by adding an appropriate amount of 3-AT to the selective agar plates.

2.6.2 LUMIER assay

Luminescence-based mammalian interactome mapping (LUMIER) was used to test for binary protein-protein interactions in 96-well format (Barrios-Rodiles et al., 2005; Pfefferle et al., 2011; Tahoun et al., 2011). The two proteins of interest, harbouring an N-terminal *Staphylococcus aureus* protein A and *Renilla reniformis* luciferase tag, respectively, were transiently expressed in HEK-293T cells. Roughly 40 h after transfection (see 'Transient

transfection of human cell lines'), the medium was removed and 10 µl ice cold LUMIER lysis buffer, including the sheep anti-rabbit IgG-coated magnetic beads (Dynabeads M280, Invitrogen), were added to each well. The lysis was done for 15 min on ice and 100 µl of 1x PBS were added afterwards. 10 µl of the lysate were then placed in another plate to determine the total luciferase activity of each sample (lysate plate). The remaining 100 µl were washed five times with 1x PBS using a TECAN HydroFlex^{TM} bead washer. The bead washer is set to leave 20 µl of 1x PBS in each well after the washing is completed. Luciferase activity of the washed beads as well as of the lysate plate was determined using a TECAN Infinite 200 Reader. 10 sec before measuring, the TECAN reader injected 70 µl of LUMIER Renilla buffer to each well to start the luciferase reaction.
A vector harbouring a dimer of protein A was used as negative control and tested for binding to the *Renilla reniformis* luciferase tagged second protein. Also for the negative control both the lysate before washing and the washed beads were measured. This adds up to a total of four values measured for each protein pair to be tested for binary interaction. For data analysis, a signal to background ratio was determined as follows:
(Signal of washed beads)/(signal of 10 µl of the lysate, non-washed) for both the interaction test (the two proteins to be tested for binary interaction) and the negative control (protein A dimer and the luciferase-tagged second protein) to obtain "signals normalised for expression levels". The JUN/FOS protein pair was used as positive control.

2.6.3 Detection of Caspase activity

For the detection of caspase-9 activity *in vitro*, the Caspase-9 inhibitor screening kit (KA0763, Abnova, Taiwan) and the Caspase-Glo ® 9 assay (Promega, Madison, USA) were used. Detection of caspase-4 and -8 was done with the Caspase-4 and -8 inhibitor screening kits (KA0747 and KA0758, Abnova, Taiwan), respectively. All three Abnova caspase inhibitor screening kits provide active caspase along with the corresponding kit. Active caspase-9 and NleF (purity of both proteins >90 % per SDS page) were obtained from Proteros (Martinsried, Germany) as part of a cooperation project. Detection of caspase-9 activity in cell lasates was performed using the Apopcyto caspase-9 fluorometric assay kit (MBL, Massachusetts, USA).

2.6.3.1 Caspase-9 activity in cell lysate

3 h after splitting or 48 h after transfection, HeLa cells (6-well plates containing 300,000 cells in 3 ml culture medium) were treated with 25 ng/ml SuperKillerTrail (ENZO Life Sclences) or 5 µM staurosporine (Roche Diagnostics) for 6 h. The medium was collected in 15 ml centrifuge tubes, the cells were washed with PBS and trypsinized with 200 µl of 0.05 % trypsin-EDTA (PAN Biotech). The washing buffer and the trypsinized cells were added to the previously collected medium, the tube was centrifuged at 300 rpm for 5 min and the supernatant was discarded. The cell pellet was placed on ice before 250 µl of ice cold lysis buffer (Apopcyto kit, MBL) were added. Lysis was performed for 10 min on ice. Subsequently the cell lysate was centrifuged at 10,000x g for 5 min at 4 °C and the supernatant was transferred into a new eppendorf tube and diluted with more lysis buffer (the lysate can be stored at -80 °C for up to 6 months). 25 µl of 2x reaction buffer (supplemented with 10 mM DTT) and 22.5 µl of the cell lysate were placed per well in a precooled black 96-well plate. 0.5 µl of the LEHD-FMK caspase-9 inhibitor (1 mM stock, Apopcyto, MBL) were added to the negative control. For the determination of native caspase-9 activity in presence of purified NleF, 2.5 µg NleF were added. The reaction was started by adding 2 µl caspase-9 substrate (Apopcyto, MBL). Then the plate was incubated for 1 – 2 h at 37 °C before the fluorescence was measured at excitation 380 nm and emission 460 nm using a TECAN Infinite 200

Reader. Caspase-9 activity with and without NleF was compared for purified and expressed NleF.

2.6.3.2 Caspase-4, -8 and -9 activity *in vitro*

The activities of caspases 4, 8 and 9 were measured using the Abnova caspase inhibitor screening kits. For determination of the IC_{50} (caspases 4 and 8) 1:2 serial dilutions of NleF were prepared starting at a caspase:NleF ratio of 8:1 and ending at 1:256. Each row was done in triplicate and the whole plate was repeated twice or more. Usually the reaction was performed in a total volume of 50 µl comprising 0.5 units of caspase. Blank reactions were done without active caspase and specificity of measured activity was assessed by comparing wells containing 20 µM Z-VAD-FMK to inhibitor-free caspase reactions. The plate (black nunc, 96-well) was incubated for 1 – 2 h at 37 °C and measured with a TECAN Infinite 200 Reader at 400 nm excitation and 505 nm emission. Further information can be obtained from the manufacturer's instructions.
The IC_{50} of caspase-9 was determined using the Caspase-Glo ® 9 assay (Promega, Madison, USA) and purified caspase-9 from Proteros (Martinsried, Germany). The serial dilutions of NleF were done as described for the Abnova assays, the reaction volumes were either 50 or 100 µl and between 1 and 5 units of active caspase-9 were used per reaction. The experimental procedure was performed following the manufacturers protocol. Luminescence was measured with a TECAN Infinite 200 Reader.
Inactivation of purified NleF was done using 1 µl of Proteinase K (2 µg/µl) per 50 µg purified NleF in 10 µl 25 mM HEPES pH 7.5. The digestion was done for 30 min at 37 °C and the Proteinase K was then inactivated for 45 min at 85 °C.
To determine the concentration of active sites of caspase-4, -8 and -9, the Z-VAD-FMK (Z-VAD-fluoromethylketone, non-omethylated, MP Biomedicals, Eschwege, Germany) inhibitor was used.

2.7 Flow cytometry (FACS)

HeLa or Caco-2 cells were transfected as previously described (6.4.3 Transient transfection of human cell lines) with pdEYFP-C1amp containing YFP-fusions of BCL2, Protein A, XIAP, NleF and different NleF fragments as well as mutagenized versions of NleF. Apoptosis was induced for 6h with 25 ng/ml SuperKillerTrail (ENZO Life Sclences) or 5 µM staurosporine (Roche Diagnostics), 48 hours after transfection. After apoptosis induction, the culture medium was collected in 15 ml plastic tubes, the cells were washed with 1x PBS and trypsinized with 200 µl of 0.05 % trypsin-EDTA (PAN Biotech). Washing buffer and trypsinized cells were collected together with the culture medium. The cells were spun down at 300 rpm for 5 min, the pellet was washed with 1 ml 1x PBS and resuspended in 100 µl 1x Annexin-V binding buffer (BD Pharmingen™). For staining necrotic and apoptotic cells, 5 µl of each, propidium iodide (PI) and Annexin-V-allophycocyanine (APC) (both BD Biosciences Pharmingen), were added. Subsequently the cells were incubated for 20 min in the dark on ice to allow binding of the dye and transferred to FACS tubes. Then 400 µl of 1x Annexin-V binding buffer was added. Flow cytometry was performed using the BD FACS Canto II flow cytometer with a 488 nm laser. PI, Annexin-APC and YFP were measured with a 670 nm long pass filter, a 660/20 nm and a 530/30 nm band pass filter, respectively. Blots were analyzed using the FACSDiva software (BD Biosclences).

2.8 Bioinformatic tools and web interfaces

For the identification of protein domains, InterProScan (Quevillon et al., 2005) (http://www.ebi.ac.uk/Tools/pfa/iprscan/) was used.
Predictions of intrinsic protein disorder and globularity were done with GlobPlot (Linding et al., 2003) (http://globplot.embl.de/).
Interaction maps were generated using Cytoscape (Shannon et al., 2003) and published human interactions were retrieved from the BioGRID database (Stark et al., 2011) (thebiogrid.org).

2.9 Data analysis

Analysis of raw data was usually done using Microsoft Access and Excel (both, the 2003 and the 2010 versions). Significance of the results was assessed using the two-tailed unpaired Student's t-test. * $p<0.05$; ** $p<0.01$; *** $p<0.001$; **** $p<0.0001$.

3 Results

3.1 Part I: The EHEC-host interactome

According to Tobe et al. 2006 enterohemorrhagic *Escherichia coli* (EHEC) O157:H7 strain Sakai harbours more than 60 putative effector proteins out of which 39 were experimentally proven to be injected into human host cells (Tobe et al., 2006). In order to identify novel host interaction partners of these EHEC effector proteins, I cloned 34 out of the 39 effectors to screen them against three human libraries, namely the Universal human (Clontech), the ORF.01/02 and the ORF.03, using Y2H pool screening.

3.1.1 Construction of a C-terminally tagged human prey library

The ORF.03 library (carboxy-terminal GAL4-AD tag) was constructed mainly for this work, since screening a bait protein N- and C-terminally tagged against N- and C-terminally tagged libraries increases the number of detected interactors and thus the coverage of Y2H screening significantly (Stellberger et al., 2010).
The pooled human ORF collection comprising roughly 12,000 human ORFs (Brasch et al., 2004; Lamesch et al., 2007; Temple et al., 2009) was shuttled into the pGADCg prey vector (Stellberger et al., 2010) via six standard gateway LR reactions and transformed into *E. coli*. The transformation was done in six batches resulting in > 1.4 million harvested *E. coli* colonies. The plasmids of the pooled colonies were isolated and retransformed into the haploid yeast strain Y187, which in turn led to 776,759 yeast colonies in total. This exceeds the minimal coverage of pooled Y2H libraries (10x) by more than six times (see 'Yeast two-hybrid library transformation' for details).

3.1.2 Pool screens of EHEC effector proteins against human libraries

The 34 EHEC effectors (see table 3 for a complete list) were cloned into a pDONR221 entry vector using the gateway technology and shuttled into pGBT9 and pGBKCg Y2H bait vectors harbouring an amino- and carboxy-terminal GAL4-DNA-binding domain, respectively.

Table 3. Cloned and screened EHEC effector proteins. The columns 'Hits' and 'Verifiable Hits' state, if positive yeast colonies and verifiable interactors were identified in the Y2H pool screens. Out of the 34 EHEC effector proteins, 21 interacted with host proteins in Y2H screens, whereas for 15 effectors one or more of these host interactors was detected repeatedly. The remaining 12 EHEC effectors did not give any hits, not even when screened at the lowest stringency (0 mM 3-AT). The 6 effectors that only found single hits or promiscuous preys were categorized as putative random interactors and as such excluded from further evaluation.

	EHEC str. Sakai effector protein	ECs ID	Effector family	Hits	Verifyable hits
1	**EspY1**	ECs0061	SopD_Nterm	yes	yes
2	**NleC**	ECs0847	NleC	yes	yes
3	**NleH1-1**	ECs0848	NleH	yes	-
4	**NleD**	ECs0850	NleD	yes	yes
5	**EspX2**	ECs0876	PPR	-	-
6	**EspX7**	ECs1560	PPR; LRR	-	-
7	**EspN**	ECs1561	CNF	-	-
8	**EspO1-1**	ECs1567	OspE	yes	yes
9	**EspK**	ECs1568	LRR	yes	-
10	**NleA**	ECs1812	NleA	yes	yes

	EHEC str. Sakai effector protein	ECs ID	Effector family	Hits	Verifyable hits
11	**NleH1-2**	ECs1814	NleH	yes	yes
12	**NleF**	ECs1815	NleF	yes	yes
13	**NleG**	ECs1824	NleG	yes	-
14	**EspM1**	ECs1825	IpgB	-	-
15	**NleG2-2**	ECs1994	NleG	yes	-
16	**NleG6-1**	ECs1995	NleG	-	-
17	**NleG5-1**	ECs1996	NleG	-	-
18	**NleG2-3**	ECs2156	NleG	-	-
19	**EspJ**	ECs2714	EspJ	yes	yes
20	**TccP**	ECs2715	EspF	yes	yes
21	**EspM2**	ECs3485	IpgB	-	-
22	**NleG8-2**	ECs3486	NleG	-	-
23	**EspW**	ECs3487	HopW	-	-
24	**EspL2**	ECs3855	AR	-	-
25	**NleB1**	ECs3857	NleB	yes	yes
26	**NleE**	ECs3858	NleE	yes	-
27	**EspF1**	ECs4550	EspF	yes	yes
28	**EspB**	ECs4554	EspB	yes	yes
29	**TIR**	ECs4561	TIR	yes	yes
30	**Map**	ECs4562	IpgB	yes	yes
31	**EspH**	ECs4564	EspH	yes	-
32	**EspZ**	ECs4571	EspZ	-	-
33	**EspG**	ECs4590	EspG	yes	yes
34	**EspY4**	ECs4653	SopD_Nterm	-	-

These effector proteins were screened as N- and C-terminally tagged bait proteins against three pooled Y2H prey libraries, namely a human cDNA-based library as well as the C-and N-terminally tagged libraries based on full length open reading frames. This resulted in the identification of 296 different human prey proteins and 328 interacting bait/prey pairs. 273 of the latter were single or unconfirmed hits, meaning these bait/prey pairs were found only once. Single hits may be artefacts, but may as well be real interactors. A final statement cannot be made, since weak or short-term interactions may also come up as single hits.
56 interacting pairs were detected repeatedly, out of which 35 could be classified as high confidence hits. The latter are defined as non-promiscuous prey proteins found to interact repeatedly with the same bait protein. In addition 35 preys were classified as potentially promiscuous. See table 4 and figure 12 for a summary of the resulting screen data and a flowchart visualizing the sequence of the screening procedure, respectively.

Table 4. Y2H data sheet. The total number of prey proteins, promiscuous preys, bait/prey pairs, single hits, repeatedly detected hits and high confidence hits found in the EHEC/host screens.

Total number of identified human prey proteins	296
Promiscuous human prey proteins	35
Unique bait/prey pairs	328
Single Hits	273
Repeatedly detected hits	56
High confidence hits	35

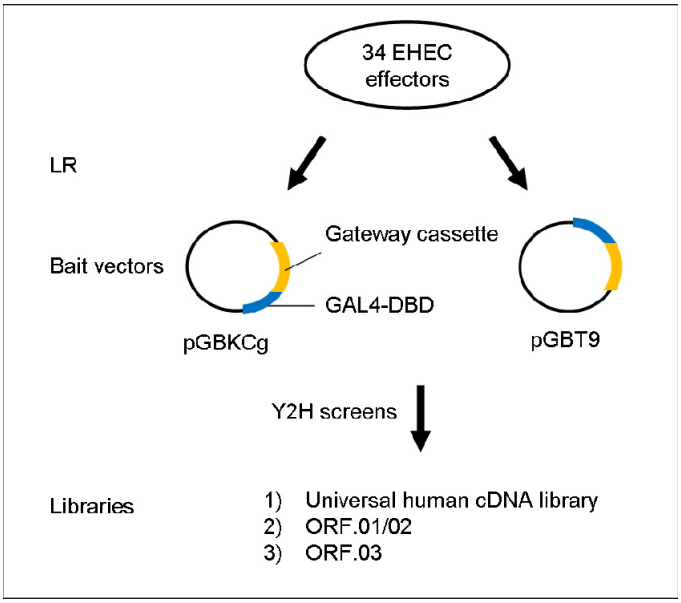

Figure 12. Flowchart visualizing the Y2H pool screening procedure performed in this work. The 34 EHEC effector proteins were shuttled into two gateway compatible bait vectors using a gateway LR reaction. pGBT9 and pGBKCg harbour an amino- and carboxy-terminal GAL4-DBD, respectively. The resulting 68 clones were screened each against the following three libraries, a human cDNA-based library as well as the C-and N-terminally tagged libraries based on full length open reading frames. The human prey proteins detected in all three libraries were summarized and the total occurrence of each unique bait/prey pair was determined.

3.1.2.1 Identification of potentially promiscuous prey proteins

False positive interactions are a long known problem in yeast two-hybrid screening (Serebriiskii and Golemis, 2001). To reduce potential sources of false positives, prey proteins were inspected for their likeliness to interact with different bait proteins. A prey protein was then tagged as potentially promiscuous, if it interacted with more than 1 % of all bait proteins screened via Y2H pool screening at the DKFZ Y2H core facility (Schwarz et al., unpublished). If a prey protein interacted with 1 % of all baits previously screened in the Y2H core facility, a promiscuity factor of 1 was assigned. The higher a preys promiscuity factor, the higher is its probability to be a random interactor and thus to be a false positive hit.

Table 5. Promiscuous prey proteins. 35 human proteins found to interact with EHEC effectors were tagged as potentially promiscuous and thus as putative artefacts. The promiscuity factor equals the relative prey promiscuity in percent.

	Prey gene symbol	Promiscuity factor		Prey gene symbol	Promiscuity factor
1	CRX	23.0	**19**	VEGFB	1.3
2	COPS5	18.3	**20**	ZNF343	1.3
3	MEOX2	14.5	**21**	HBA1	1.2
4	OTX2	9.2	**22**	MTMR9	1.2
5	BEND7	5.3	**23**	PNMA1	1.2
6	TIGD1	2.7	**24**	SEP15	1.2
7	ALX1	2.5	**25**	URM1	1.2
8	CTDSP2	2.5	**26**	CBX4	1.0
9	HBA2	2.2	**27**	MCRS1	1.0
10	PALLD	2.0	**28**	MPV17	1.0
11	SNX3	2.0	**29**	NDUFV3	1.0
12	RING1	1.8	**30**	NEK2	1.0
13	RPL21	1.8	**31**	PTPN6	1.0
14	EIF4B	1.7	**32**	SDHD	1.0
15	CDCA4	1.5	**33**	SFRS3	1.0
16	DNAJC7	1.5	**34**	TIMM8A	1.0
17	XRCC6	1.5	**35**	TTC1	1.0
18	BHMT	1.3			

Preys with a promiscuity factor of ≥ 1 were marked as putative false positives and as a consequence excluded from further data analysis. The 35 human prey proteins found in the EHEC-host screens that were identified as promiscuous and its corresponding promiscuity factors can be obtained from table 5.

3.1.2.2 EHEC-host protein-protein interactions

A complete list of all EHEC-host interactions is provided in supplementary table 1 and a list of the 35 high confidence interactions is shown in table 6.

Table 6. EHEC/host high confidence interactions. The column 'Occurrence' states the number of times a unique bait/prey pair was detected. For high confidence hits, this number is at least 2.

	Bait name	Bait ID	Prey gene symbol	Occurrence	Prey gene ID
1	EspB	ECs4554	RBCK1	78	**10616**
2	EspB	ECs4554	STK16	48	**8576**
3	EspF1	ECs4550	SNX33	16	**257364**
4	EspF1	ECs4550	SNX9	2	**51429**
5	EspG	ECs4590	Hs.658052	3	**100589704**
6	EspJ	ECs2714	IFT20	20	**90410**
7	EspJ	ECs2714	RIC8A	15	**60626**
8	EspJ	ECs2714	CENPH	13	**64946**
9	EspO1-1	ECs1567	FEM1B	2	**10116**
10	EspY1	ECs0061	CDKN2AIPNL	51	**91368**
11	EspY1	ECs0061	PIH1D1	6	**55011**
12	EspY1	ECs0061	PSMC1	5	**5700**
13	EspY1	ECs0061	CAPN3	3	**825**
14	EspY1	ECs0061	PCID2	3	**55795**
15	EspY1	ECs0061	DNAJC14	2	**85406**
16	EspY1	ECs0061	ZNHIT1	2	**10467**
17	Map	ECs4562	SLC9A3R2	13	**9351**
18	Map	ECs4562	RHPN1	3	**114822**
19	NleA	ECs1812	DSCR4	2	**10281**
20	NleB1	ECs3857	LRRC18	7	**474354**
21	NleB1	ECs3857	DRG2	5	**1819**
22	NleB1	ECs3857	POLR2E	3	**5434**
23	NleC	ECs0847	C8orf71	3	**26138**
24	NleC	ECs0847	CTDSPL2	3	**51496**
25	NleD	ECs0850	METTL2A	6	**339175**
26	NleF	ECs1815	CASP9	49	**842**
27	NleF	ECs1815	DHFR	21	**1719**
28	NleH1-2	ECs1814	UFC1	2	**51506**
29	TccP	ECs2715	ZNF626	2	**199777**
30	TIR	ECs4561	HPCAL1	56	**3241**
31	TIR	ECs4561	STK16	11	**8576**
32	TIR	ECs4561	NCALD	7	**83988**
33	TIR	ECs4561	BAIAP2L1	5	**55971**
34	TIR	ECs4561	ARRB1	2	**408**
35	TIR	ECs4561	BAIAP2	2	**10458**

Four out of the 35 high confidence hits were previously published, namely TIR-BAIAP2 (Weiss et al., 2009), TIR-BAIAP2L1 (Vingadassalom et al., 2009), EspF-SNX9 (Marches et al., 2006) and Map-NHERF2 (SLC9A3R2) (Martinez et al., 2010), the remaining 31 are novel interactions. The high confidence EHEC-host interactions are depicted in figure 13.

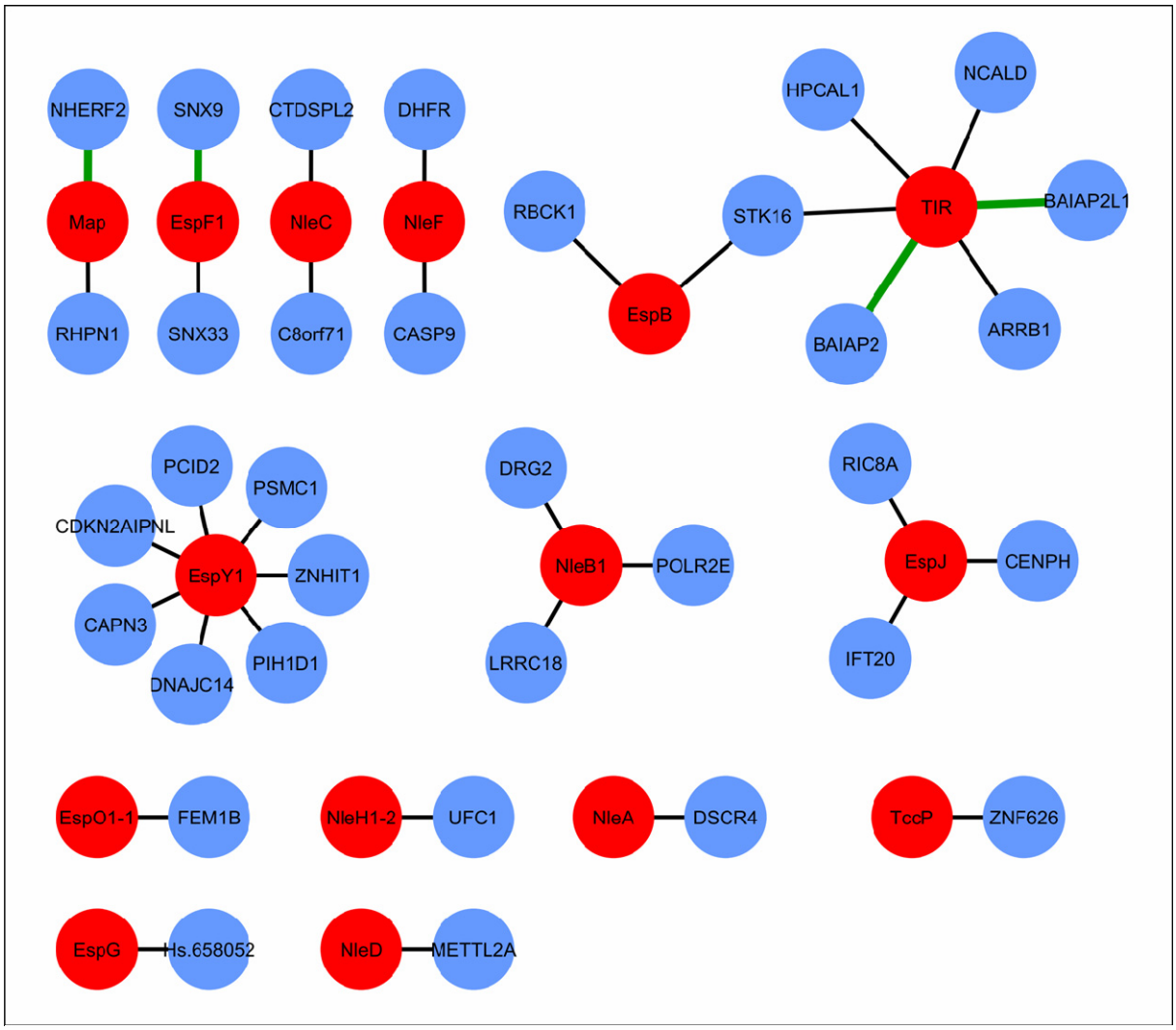

Figure 13. EHEC-host high confidence network. The proteins are depicted as nodes. Edges represent protein-protein interactions. EHEC effectors and human proteins are colored in red and blue, respectively. Previously published interactions are represented as green lines.

Only one human interaction partner revealed high confidence interactions with more than one EHEC effector protein, namely STK16, and there are no primary human interactors that bind to each other.

To test if the EHEC effector proteins are connected to each other by secondary interactions, the published interaction partners of the human EHEC effector binders (direct interactors, blue nodes in figure 13) were retrieved from the BioGRID database and added to the network (figure 15; secondary interaction partners and corresponding annotations are shown in supplementary table 2). The network was then analyzed for the occurrence of connections between the effector proteins. A connection exists if two direct EHEC interaction partners both interact with a third human protein, a so-called secondary interactor. If the two direct interactors also bind the same effector protein, the connection was termed a loop. Examples for connections and loops are depicted in figure 14.

In total 23 connections, including four loops, between 6 EHEC effector proteins were detected and involved 12 different secondarily interacting human proteins. A list of detected connections is shown in table 7.
In addition to observed connections, the 6 effector proteins are interconnected over a varying amount of edges (see figure 15), which suggests that these effectors are part of a common protein complex or pathway

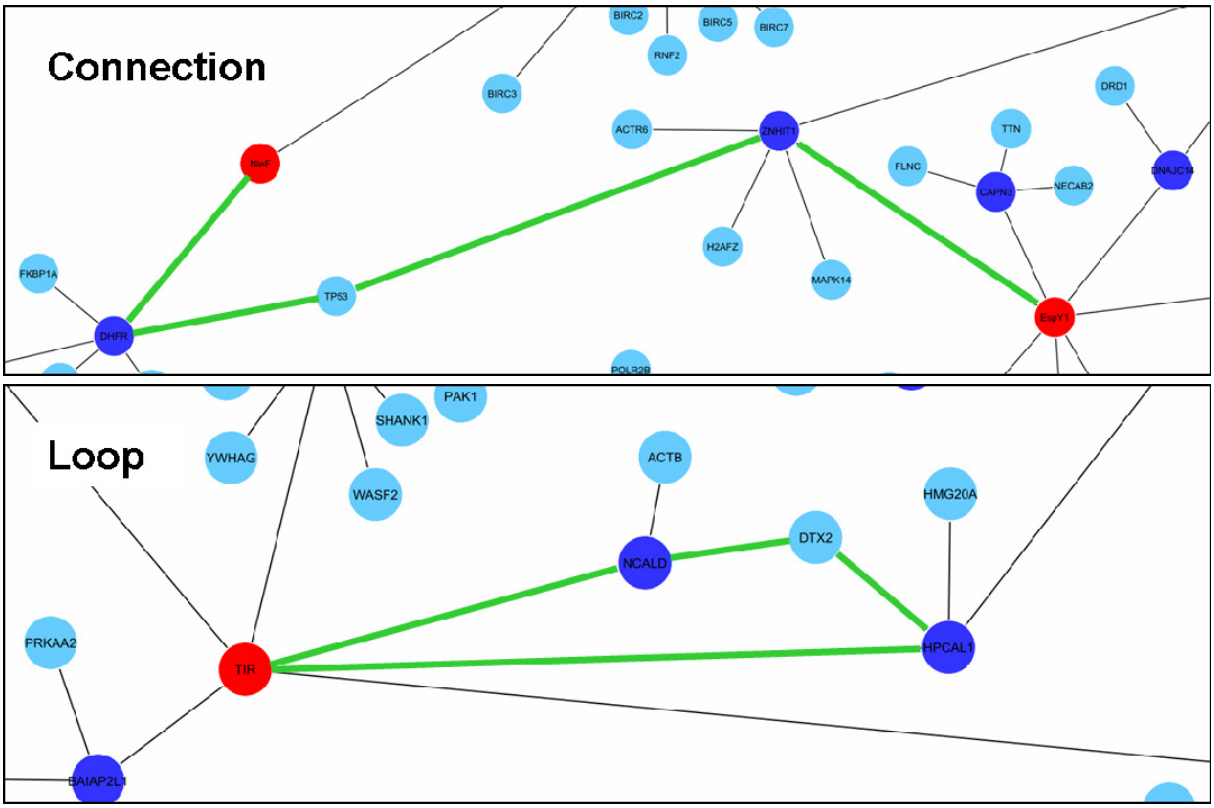

Figure 14. Connections and loops between EHEC effector proteins. A connection takes place between two different EHEC effectors, whereas within a loop, an effector protein is connected with itself. The edges involved in connections and loops are depicted in green. EHEC proteins, human direct interactors and human indirect interactors are shown in red, dark blue and light blue, respectively.

Table 7. Indirect connections between EHEC effector proteins. The columns 'Effector A' and 'Effector B' comprise the two EHEC effectors that are connected by their human interactors ('Human direct A' and 'Human direct B') over a common interaction with a third human protein ('Human indirect').

Effector A	Human direct A	Human indirect	Human direct B	Effector B	Loop?
EspB	RBCK1	IKBKG	HPCAL1	TIR	-
EspB	RBCK1	IKBKG	POLR2E	NleB1	-
EspB	RBCK1	UBC	CASP9	NleF	-
EspB	RBCK1	UBC	PSMC1	EspY1	-
EspB	RBCK1	UBC	ZNHIT1	EspY1	-
EspB	STK16	KCTD17	LRRC18	NleB1	-
EspJ	RIC8A	TERF1	BAIAP2L1	TIR	-
EspY1	PSMC1	UBC	ZNHIT1	EspY1	loop
NleB1	POLR2E	RPAP3	PIH1D1	EspY1	-
NleB1	POLR2E	RUVBL2	PIH1D1	EspY1	-
NleF	CASP9	UBC	PSMC1	EspY1	-
NleF	CASP9	UBC	ZNHIT1	EspY1	-
NleF	DHFR	TP53	ZNHIT1	EspY1	-

Effector A	Human direct A	Human indirect	Human direct B	Effector B	Loop?
NleF	DHFR	UBC	CASP9	NleF	loop
NleF	DHFR	UBC	PSMC1	EspY1	-
NleF	DHFR	UBC	ZNHIT1	EspY1	-
NleF	DHFR	UBC	RBCK1	EspB	-
TIR	ARRB1	CDC42	BAIAP2	TIR	loop
TIR	ARRB1	ITCH	POLR2E	NleB1	-
TIR	ARRB1	MDM2	DHFR	NleF	-
TIR	ARRB1	NEDD4	POLR2E	NleB1	-
TIR	HPCAL1	DTX2	NCALD	TIR	loop
TIR	HPCAL1	IKBKG	POLR2E	NleB1	-

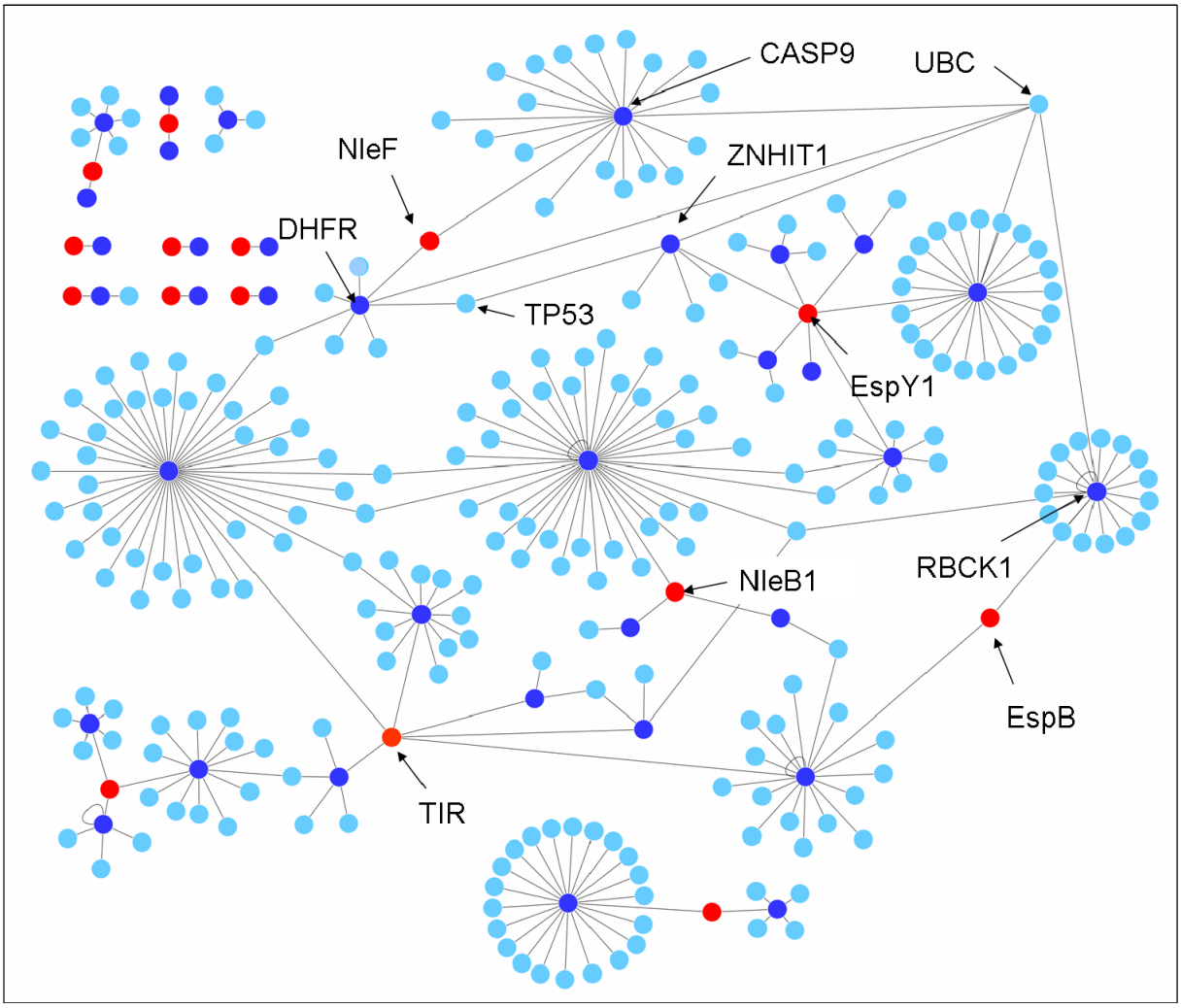

Figure 15. EHEC-host network including indirect interactions. EHEC proteins, human direct interactors and human indirect interactors are shown in red, dark blue and light blue, respectively.

3.1.3 EHEC effector TIR interacts with 8 host proteins

As a part of the yeast two-hybrid EHEC-host interactome, 8 human proteins were detected as binding partners of the EHEC translocated intimin receptor (TIR), namely HPCAL1, STK16, NCALD, BAIAP2L1, ARRB1, BAIAP2, HPCAL4 and PDE6D. Among them, two single hits and six high confidence interactions, whereas two of the latter were published previously.

3.1.3.1 LUMIER assays of EHEC TIR and its host interaction partners

To verify the TIR interactions, LUMIER assays of the human TIR interactors were performed against full-length TIR as well as against its amino-and carboxy-terminal intracellular fragments (see table 8 for details).

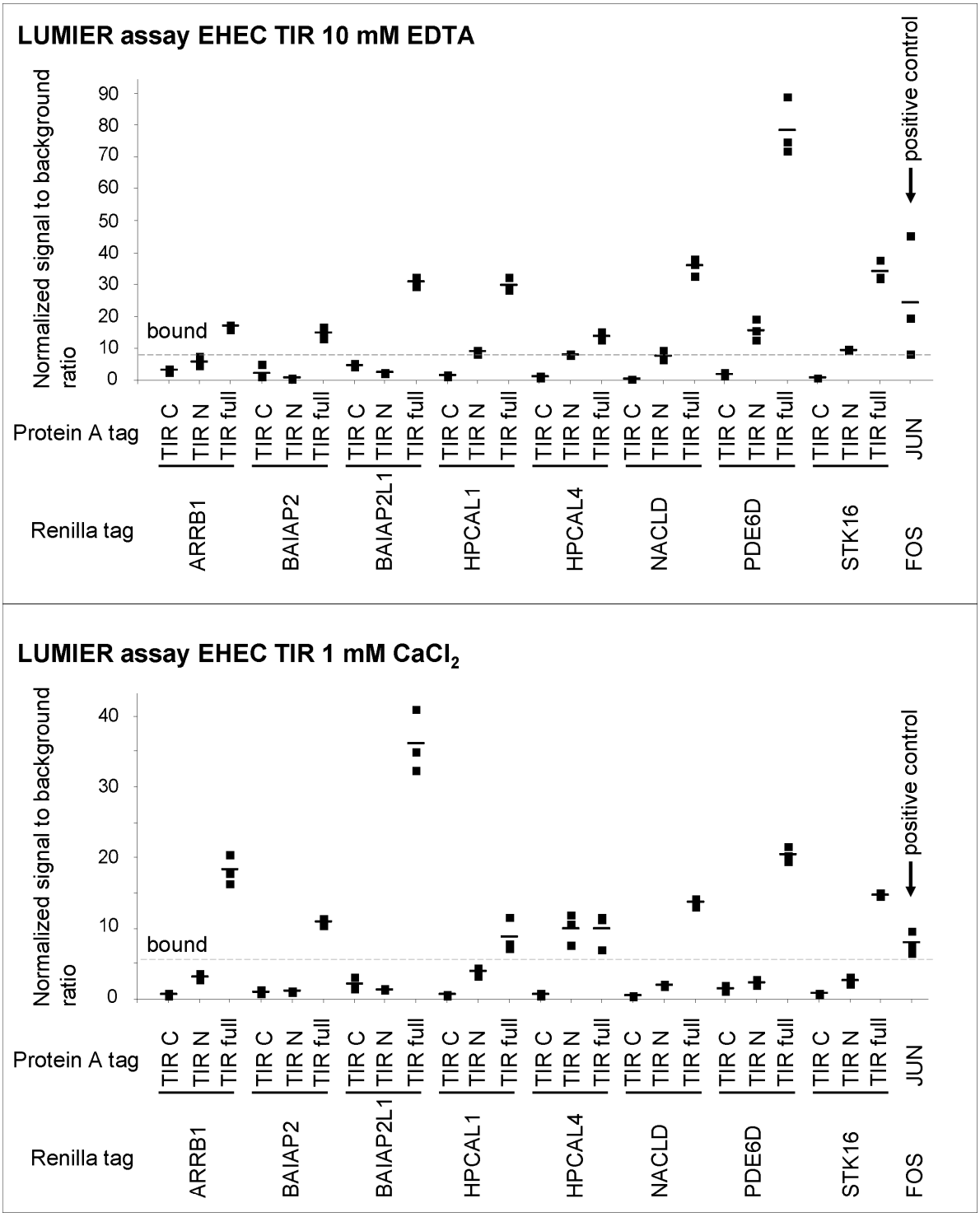

Figure 16. LUMIER assay testing the eight human TIR interaction partners previously identified in yeast two-hybrid pool screens against full-length TIR and its N-and C-terminal intracellular domains. All human proteins tested interact with full-length TIR. To test if calcium affects the binding ability of the three calcium binding proteins, HPCAL1, HPCAL4 and NCALD, an equivalent assay was done with 1 mM $CaCl_2$ (bottom) instead of 10 mM EDTA (top), but the two assays revealed no significant differences in TIR binding. TIR C: TIR C-terminus, amino acids 333-559; TIR N: TIR N-terminus, amino acids 1-267; TIR full: full-length TIR.

These revealed that all eight human proteins interact clearly with full-length TIR. None of the TIR fragments interacted with ARRB1, BAIAP2 and BAIAP2L1, whereas HPCAL1, HPCAL4, NCALD and STK16 exhibited a tendency to interact with the N-terminal TIR fragment. The PDE6D clearly interacted with the TIR N-terminus.
Since three of the eight human interaction partners identified were calcium-binding proteins, namely HPCAL1, HPCAL4 and NCALD, it was determined if calcium would alter their binding abilities. A standard LUMIER assay was performed with the only difference that the 10 mM EDTA, usually removing the Ca^{+2} ions from the HEK-293T cell lysate, were substituted with 1 mM $CaCl_2$. However, a comparison of both LUMIER assays only revealed minor variations in the binding strength, but no significant differences. The results are depicted in figure 16.

3.1.3.2 Comparison of EHEC and EPEC TIR interactions

EPEC harbours a TIR protein homologous to that of EHEC, but despite their similarity, EHEC and EPEC TIR employ different pathways for pedestal formation in host cells (Wong et al., 2011). Both proteins harbour several identical parts, but also some regions with lower similarity in the carboxy-terminus (see figure 17 for a clustal W alignment of EPEC and EHEC TIR).

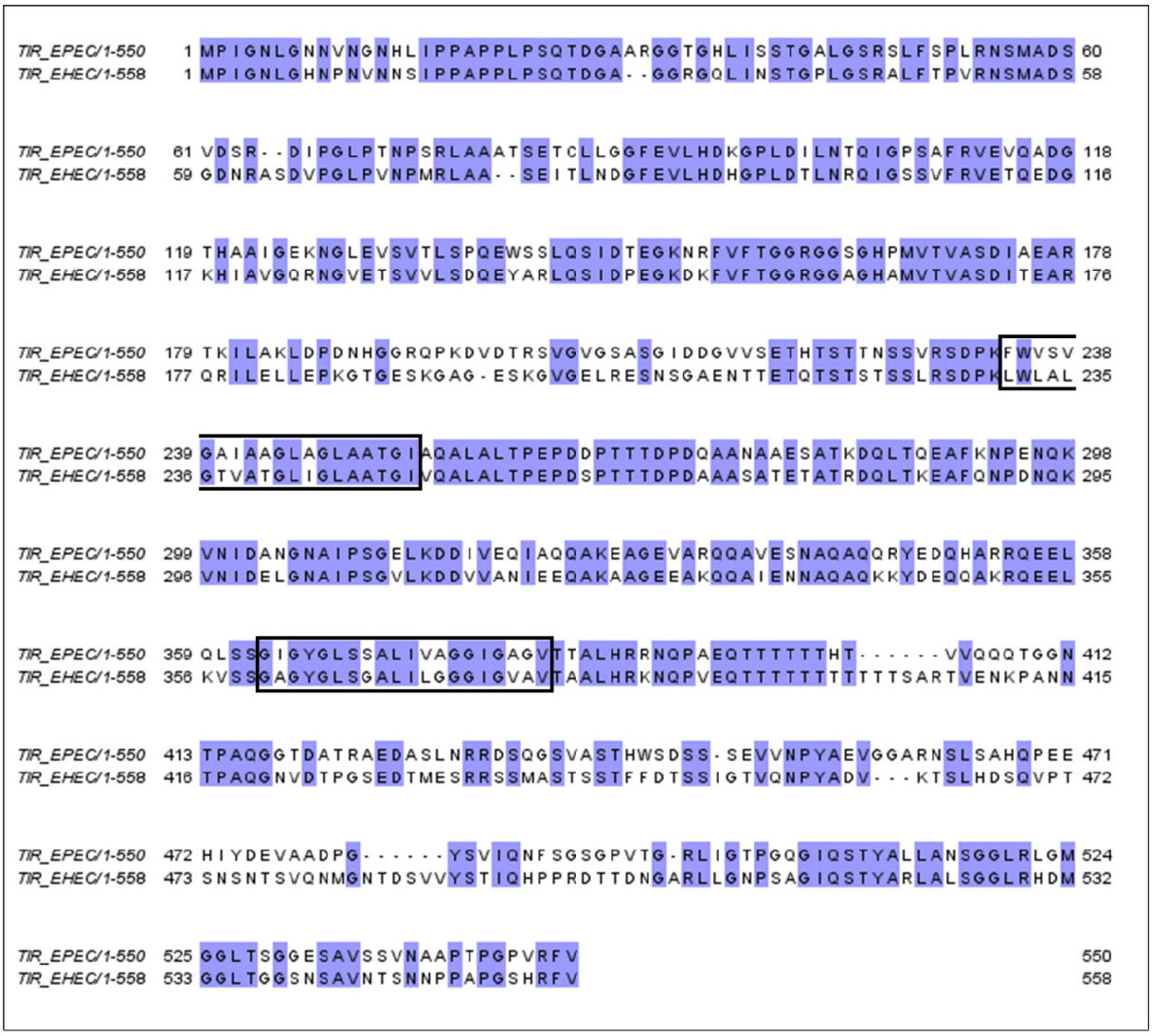

Figure 17. Clustal W alignment of EPEC and EHEC TIR. Identical amino acids are shaded blue. The two transmembrane domains are framed with black boxes.

In order to figure out to what extent EPEC TIR is able to bind the eight human proteins previously detected as EHEC TIR interactors, EPEC TIR was cloned full-length from the EPEC strain O127:H6 E2348/69 and comparable C- and N-terminal fragments were produced. A list of all EHEC and EPEC variations and the bait vectors they were shuttled into is provided in table 8. The eight human prey proteins were obtained with and without native stop codon from the human ORF collection that was also used for the construction of the C-terminally tagged Y2H library.

Table 8. EPEC and EHEC TIR fragments used in this work. AA: amino acids

No.	Taxonomy	Name	Description	AA	Stop codon	Bait vector	Vectot ID
1	EHEC	TIR full	full-length TIR	1-558	yes	pGBT9	v0012
2	EHEC	TIR C	carboxy terminus	333-558	yes	pGBT9	v0012
3	EHEC	TIR N	amino terminus	1-267	yes	pGBT9	v0012
4	EHEC	TIR full	full-length TIR	1-558	no	pGBKCg	v0034
5	EHEC	TIR C	carboxy terminus	333-558	no	pGBKCg	v0034
6	EHEC	TIR N	amino terminus	1-267	no	pGBKCg	v0034
1	EPEC	TIR full	full-length TIR	1-550	yes	pGBT9	v0012
2	EPEC	TIR C	carboxy terminus	338-550	yes	pGBT9	v0012
3	EPEC	TIR N	amino terminus	1-270	yes	pGBT9	v0012
4	EPEC	TIR full	full-length TIR	1-550	no	pGBKCg	v0034
5	EPEC	TIR C	carboxy terminus	338-550	no	pGBKCg	v0034
6	EPEC	TIR N	amino terminus	1-270	no	pGBKCg	v0034

To exclude non-specific interactions, all EHEC and EPEC TIR variants were subjected in one to one Y2H interaction tests against the prey vectors used in this study, namely pGADCg and pGAD424, revealing that none of the TIR variants interacted with plain prey vector. The results are depicted in figure 18, the plate layout is shown in table 9.

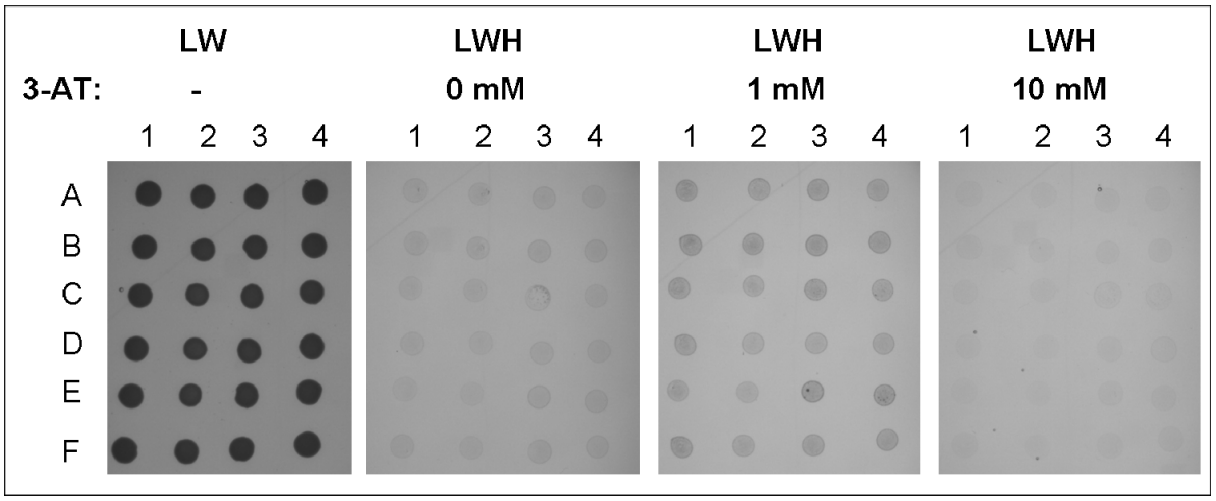

Figure 18. Paiwise tests of EHEC and EPEC baits against pure prey vecor. The columns 1 + 3 and 2 + 4 harbour plain pGAD424 and pGADCg as preys, respectively. The plate layout for the baits can be obtained from table 9. The picture on the left is the mating control on LW selective medium. The other three are the interaction tests done with increasing 3-AT concentrations as indicated.

Table 9. Plate layout of the EHEC and EPEC baits in figure 18.

BAIT	1	2	3	4
A	EHEC TIR full w/o Stop	EHEC TIR full w/o Stop	EPEC TIR full w/o Stop	EPEC TIR full w/o Stop
B	EHEC TIR N w/o Stop	EHEC TIR N w/o Stop	EPEC TIR N w/o Stop	EPEC TIR N w/o Stop
C	EHEC TIR full Stop	EHEC TIR full Stop	EPEC TIR full Stop	EPEC TIR full Stop
D	EHEC TIR N Stop	EHEC TIR N Stop	EPEC TIR N Stop	EPEC TIR N Stop
E	EHEC TIR C Stop	EHEC TIR C Stop	EPEC TIR C Stop	EPEC TIR C Stop
F	EHEC TIR C w/o Stop	EHEC TIR C w/o Stop	EPEC TIR C w/o Stop	EPEC TIR C w/o Stop

For the pairwise tests against the human interactors, full-length EHEC and EPEC TIR as well as the C- and N-terminal intracellular fragments were tested as C- and N-terminal tagged proteins against the human preys. The human prey proteins were also shuttled in C- and N-terminal tagged prey vectors, namely pGADCg and pGAD424. Diploids were selected on ΔLWH agarose plates at varying stringencies. The results obtained for all stringencies were documented photographically. The complete results are depicted in supplementary figure 1. Not all bait and prey vectors or combinations were equally functional. Bait or prey protein fusions that did not find any interactions or seemed to interact randomly were not considered. Figure 19 shows the most informative results of the obtained data.

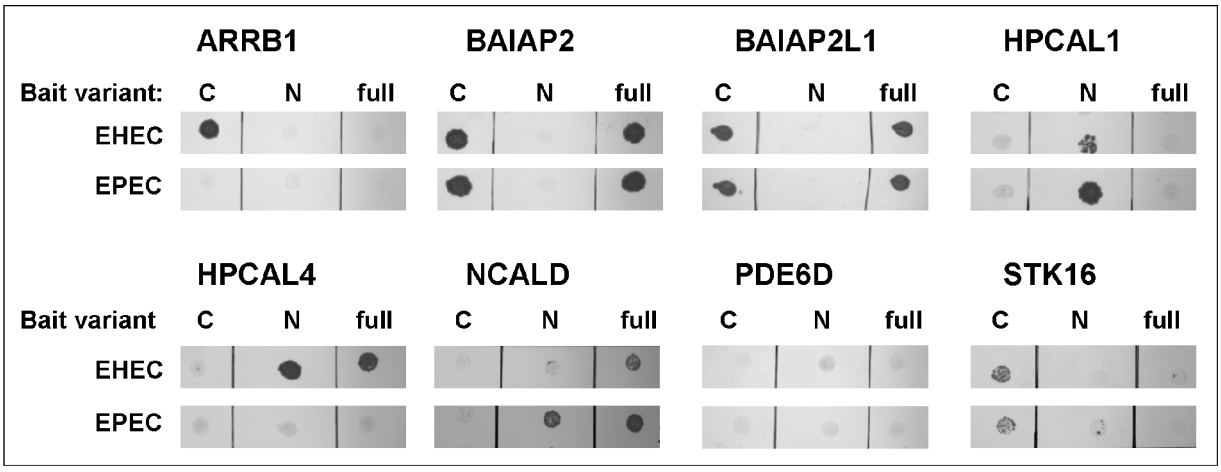

Figure 19. Pairwise Y2H tests of EHEC and EPEC baits against human prey proteins. ARRB1, BAIAP2, BAIAP2L1 and HPCAL4: prey vector pGADCg, bait vector pGBT9, stringency 1 mM 3-AT; HPCAL1: prey vector pGAD424, bait vector pGBKCg, stringency 10 mM 3-AT; NALD: prey vector pGADCg, bait vector pGBT9, stringency 15 mM 3-AT; PDE6D: prey vector pGAD424, bait vector pGBT9, stringency 10 mM 3-AT and STK16: prey vector pGADCg, bait vector pGBKCg, stringency 25 mM 3-AT.

As previously published, BAIAP2 and BAIAP2L1 bound full-length TIR and the carboxy-terminal fragment of both, EHEC and EPEC TIR, proving functionality of both TIR proteins and their C-terminal fragments. Though clearly interacting with full-length EHEC TIR in LUMIER assay, the PDE6D did not reveal any interaction with EPEC or with EHEC TIR in the pairwise Y2H tests. At stringencies lower than 10 mM 3-AT, diploid yeast colonies appeared at random. A possible explanation might be that the protein is instable in yeast or does not function well when fused to GAL4. HPCAL1 and NCALD bound to the amino-terminal fragment of EPEC and EHEC TIR, though the binding to EHEC TIR seems to be slightly weaker than that to EPEC TIR. The STK16 bound to the C-terminal fragment of both TIR proteins. Differences between EPEC and EHEC TIR were only found for ARRB1 and HPCAL4. Both human prey proteins do not bind EPEC TIR. ARRB1 only bound the carboxy-

terminus of TIR EHEC. HPCAL4 clearly interacted with full-length and the N-terminal fragment of the latter.

3.1.4 NleF – host interactions

As previously shown in table 6 and figure 13, the non-LEE (locus of enterocyte effacement) encoded EHEC effector protein F (NleF) interacts with caspase-9. The NleF-CASP9 unique pair was isolated 49 times in two Y2H pool screens indicating that this interaction is highly reproducible. In addition, caspase-9 exhibits a very low promiscuity factor of 0.2, which qualifies it as a reliable prey and thus makes the NleF/caspase-9 interaction favourable for further investigation.

3.1.4.1 NleF interacts with caspases in LUMIER assay

To verify the NleF/CASP9 interaction with an independent method, LUMIER assays in HEK-293T cells were performed. Further interaction tests with NleF against other human caspases, namely caspase-1, -2, -3, -4, -6, -7, -8, -10, and -14, led to the identification of caspase-4 and -8 as additional interaction partners. The LUMIER results are depicted in figure 20.

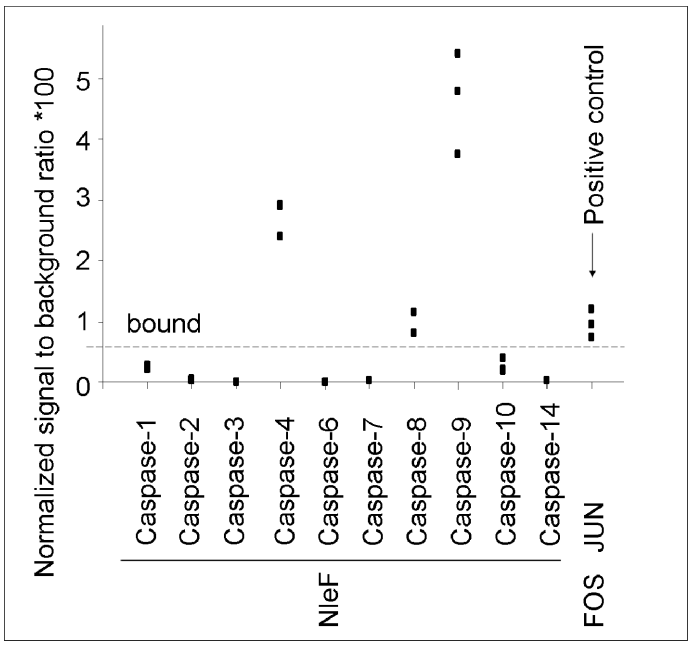

Figure 20. LUMIER assay NleF with human caspases. NleF was tested for interaction with the human caspases -1, -2, -3, -4, -6, -7, -8, -9, -10 and -14 in LUMIER assay. Each NleF/caspase pair was done in triplicate. All signals above the dotted line are positive for interaction. JUN and FOS were used as a positive control.

3.1.4.2 NleF fragments are incapable of caspase binding

NleF is non-functional when fused to a tag at the carboxy-terminus. Prediction of potential globular domains performed with GlobPlot predicts an amino-terminal globular domain and a disordered region at the C-terminus. This suggested a potential role of the NleF carboxy-terminus in caspase binding.

To examine this, I made four different fragments of NleF, namely NleF 1-145, NleF 1-160, NleF 144-189 and NleF 161 189 (numbers referring to amino acids, full length being 189). LUMIER assays of these fragments against caspase 4, -8 and -9 revealed that none of the NleF fragments was capable of caspase binding. The results are depicted in figure 21.

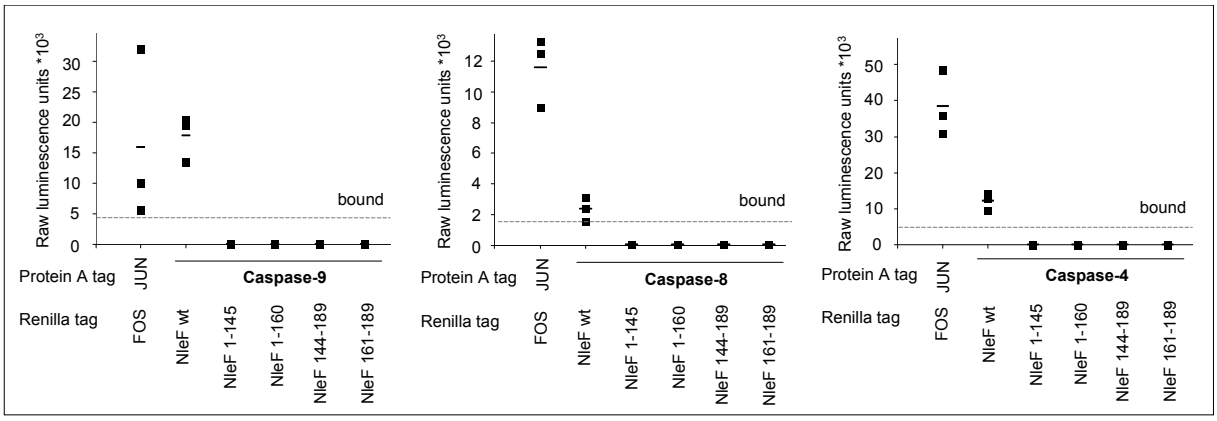

Figure 21. LUMIER assay of the four NleF fragments against the caspases 4, 8 and 9. None of the four fragments, NleF 1-145, 1-160, 144-189 and 161-189 is capable of caspase binding, whereas full-length NleF (189 amino acids, wild type) clearly interacts with all three caspases. JUN and FOS are the positive control.

3.1.4.3 Caspase inhibition by NleF and IC_{50} *in vitro*

Caspases are cysteine proteases that play substantial roles in a number of cellular processes, among them inflammation and apoptosis (Alnemri et al., 1996). As initiator caspases of the extrinsic and intrinsic apoptosis pathway, caspase-8 and -9 are of special importance for the initiation of programmed cell death, which can be induced e.g. as a response to pathogen infestation or cell damage (Munoz-Pinedo, 2012). In the literature two biological roles are discussed for caspase-4, namely as an initiator caspase responding to ER stress (Hitomi et al., 2004) and as an inflammatory caspase (Martinon and Tschopp, 2007). Considering their roles, all three caspases might be relevant targets for EHEC.

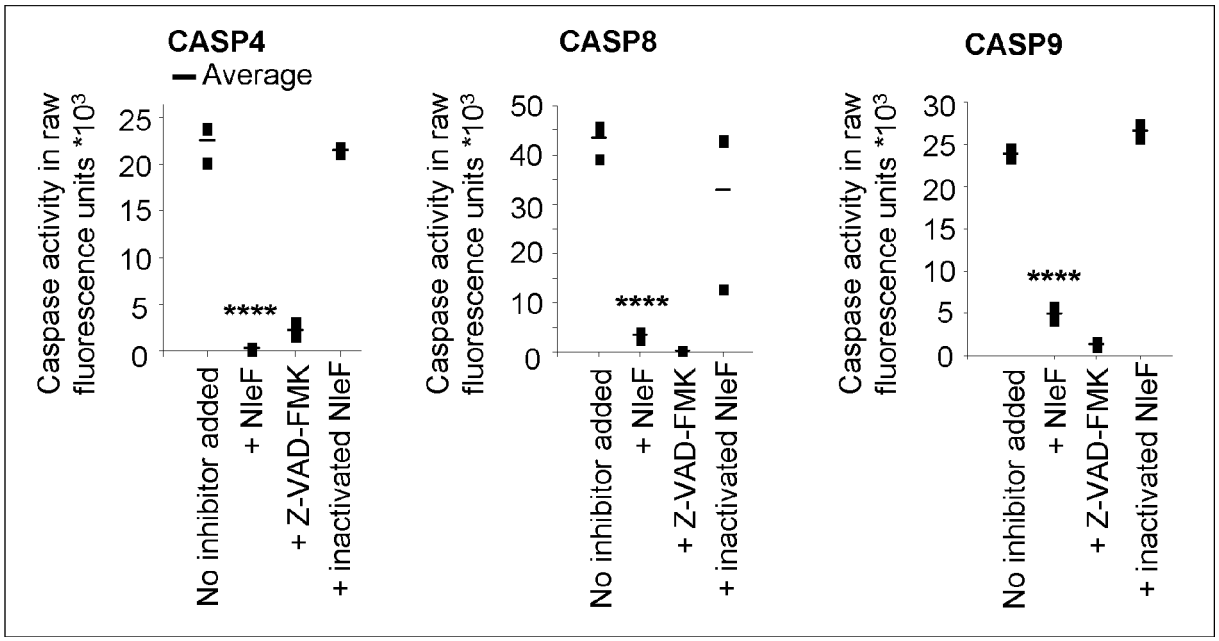

Figure 22. *In vitro* inhibition of caspases -4, -8 and -9 by NleF, the small molecule inhibitor Z-VAD-FMK and inactivated NleF. The significance was determined by two-tailed unpaired Student's t-test. **** p<0.0001

To test if NleF is able to inhibit the caspases 4, 8 and 9, their activity was assessed *in vitro*. 1.5 µg of purified NleF was mixed with one unit of active caspase and its proteolytic activity was measured. The data were compared with NleF-free samples, samples harbouring the

known caspase inhibitor Z-VAD-FMK and samples with an equivalent amount of inactivated NleF (inactivation was done by proteinase K digestion and subsequent heat inactivation of the protease). This resulted in a potent inhibition of all three caspases in presence of NleF, but not inactivated NleF (see figure 22).

To measure the efficiency of caspase inhibition by NleF, the half maximal inhibitory concentration (IC_{50}) of NleF required to inhibit the caspases was determined. For the caspases 4 and 8 the corresponding caspase inhibitor kits and 0.5 units of caspase-4 (~208 nM) and caspase-8 (~72 nM) were used per well, respectively. Caspase-9 was measured with the Caspase-Glo ® 9 luminescence assay and 1100 nM active caspase-9 matching 5 units were used per well. The NleF dilutions were started with an NleF/caspase molar ratio of 8:1, 80:1 and 3:1 for caspase-4, -8 and -9, respectively, and continued as 1:2 dilution rows. These resulted in an IC50 of 14 nM, 40 nM and 83 nM NleF for the caspases 4, 8 and 9, respectively. The results are graphed in figure 23.

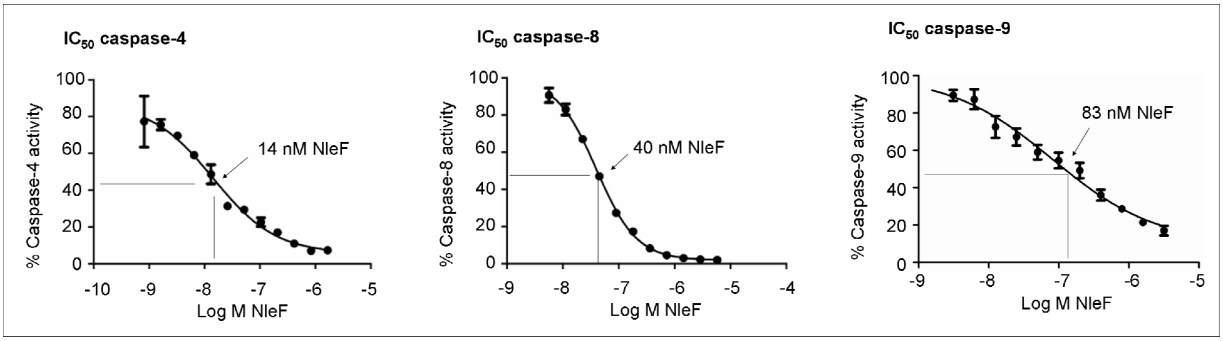

Figure 23. Dose-dependent inhibition of purified caspases by NleF. The Y-axis represents the caspase activity in percent and the X-axis the logarithmic molar concentration of purified NleF. For caspase-4, caspase-8 and caspase-9, an IC50 of 14 nM, 40 nM and 83 nM NleF was observed, respectively.

To determine if the molar concentration of caspases 4, 8 and 9 in the assay correlates with the concentration of caspase active sites, active site titration with the kovalent pan-caspase inhibitor Z-VAD-FMK was performed. FMK inhibitors form covalent adducts with active caspases, whereas one molecule of inhibitor inactivates one active site.
This leads to a linear connection between the applied concentrations of caspase and inhibitor. The concentration of caspase active sites can be obtained from the intercept with the X axis (Stennicke and Salvesen, 1999). As depicted in figure 24, the total concentration of active sites was determined to be 200 nM, 68 nM and 1.1 µM for caspase-4, -8 and -9, respectively. This correlates well with the estimated caspase concentrations of 208 nM, 72 nM and 1.1 µM for caspase-4, -8 and -9, respectively.

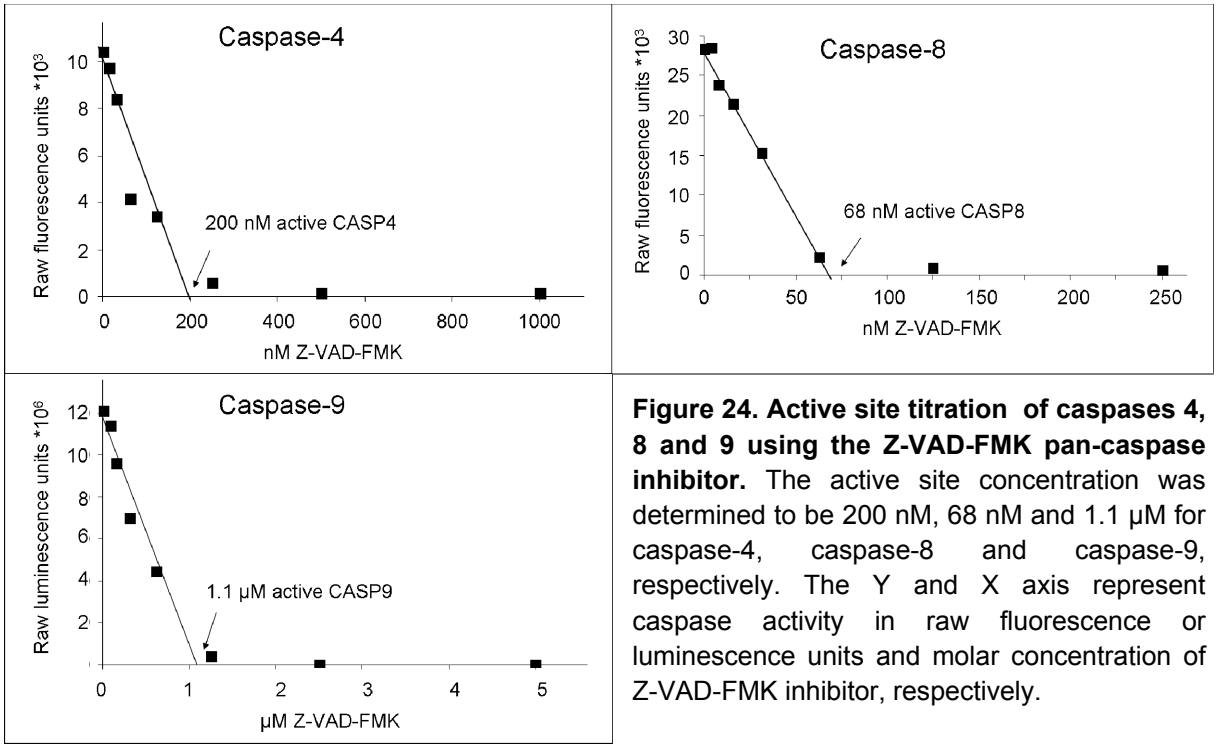

Figure 24. Active site titration of caspases 4, 8 and 9 using the Z-VAD-FMK pan-caspase inhibitor. The active site concentration was determined to be 200 nM, 68 nM and 1.1 µM for caspase-4, caspase-8 and caspase-9, respectively. The Y and X axis represent caspase activity in raw fluorescence or luminescence units and molar concentration of Z-VAD-FMK inhibitor, respectively.

3.1.4.4 *Ex vivo* inhibition of caspase activity

Human enterocytes, the primary host cells of EHEC, are so-called type II cells that rely on the mitochondrial pathway and thus on caspase-9 activation for apoptosis induction (Kantari and Walczak, 2011). To determine if NleF is able to inhibit cellular caspases, caspase activity was determined in HeLa cell lysate. This was done in two different ways: 1. HeLa cells expressing YFP-tagged NleF, an inactive NleF fragment (NleF 1-160) and protein A (*Staphylococcus aureus*), respectively, were treated with TRAIL (Tumor Necrosis Factor Related Apoptosis Inducing Ligand) for apoptosis induction, lysed and caspase-9 activity was assessed in the lysate.

2. TRAIL treated HeLa cells were lysed and purified NleF or an equivalent amount of inactivated NleF was added, respectively. The results are depicted in figure 25.

In both cases caspase-9 activity is significantly increased in TRAIL treated cells that expressed Protein A, the negative control, and NleF 1-160, an inactive NleF fragment, when compared to untreated samples, respectively (figure 25 A). This indicates that TRAIL-treated cells entered apoptosis as expected. In HeLa cells expressing wild type NleF or BCL2, a known inhibitor of apoptosis, caspase-9 activity in TRAIL treated samples was reduced by half. When purified NleF was added to HeLa cell lysate that exhibited native caspase-9 activity after apoptosis induction, caspase-9 activity was decreased by more that two thirds. The addition of an equivalent amount of inactivated NleF had no effect on caspase-9 activity (figure 25 B).

In summary, naturally expressed and purified NleF are both able to decrease caspase-9 activity significantly in cell lysates.

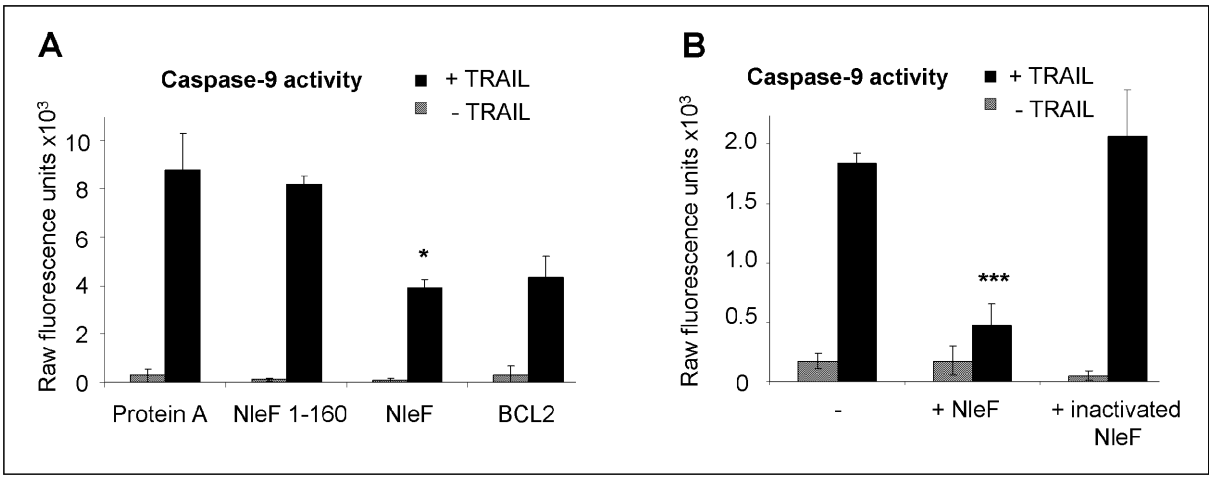

Figure 25. NleF inhibits caspase-9 in HeLa cell lysate. (A) Caspase-9 activity in apoptotic HeLa cell extracts expressing Protein A, an inactive fragment of NleF (amino acids 1-160), wild type NleF or BCL2, respectively. (B) Recombinant NleF inhibits caspase-9 activity in lysates of apoptotic cells. HeLa cells were induced to enter apoptosis by treatment with TRAIL for four hours (black bars) or left untreated (striped bars) before preparation of lysates and measurement of cellular caspase-9 activity in the absence or presence of purified NleF. Significance was determined using the two-tailed unpaired Student's t-test. * $p<0.05$; *** $p<0.001$

3.1.4.5 NleF inhibits apoptosis in HeLa and Caco-2 cells

To test if NleF is not only capable of inhibiting caspase activity, but can also prevent human cells from entering apoptosis, the effect of expressed NleF on HeLa cells that were exposed to apoptotic stimuli was assessed.

NleF, Protein A and NleF 1-160 as well as known inhibitors of apoptosis, namely XIAP and BCL2, were transiently expressed as YFP fusion proteins in HeLa cells. XIAP as an inhibitor of the initiator caspase 9 and the effector caspases 3 and 7 (Deveraux and Reed, 1999) and BCL2 as a known inhibitor of apoptosis were employed for comparison with NleF. The percentage of apoptotic cells was determined using FACS before and after TRAIL treatment revealing a significantly decreased number of apoptotic cells in samples expressing XIAP (6.1 %) , BCL2 (13.4 %) and NleF (6.5 %), but not in the controls expressing Protein A (42.8 %) and NleF 1-160 (37.4 %), respectively (Figure 26 A and C). Thus, NleF is capable of inhibiting TRAIL-induced apoptosis in HeLa cells just as efficient as XIAP and BCL2.

Since HeLa cells are not the native host cells of EHEC, I tested if apoptosis inhibition by NleF is just as efficient in Caco-2 cells. Caco-2 are epithelial colorectal adenocarcinoma cells and as such closer to human enterocytes than HeLa cells. After TRAIL-treatment, NleF and Protein A expressing Caco-2 cells revealed 7.0 % and 25.2 % of apoptotic cells, respectively (see Figure 26 B), confirming, that NleF can prevent apoptosis in Caco-2 cells as well.

TRAIL binds to the death receptors DR4 and DR5 leading to the recruitment and activation of caspase-8 and thus to the induction of apoptosis through the extrinsic pathway (Song and Lee, 2008). As mentioned previously, in case of type II cells (HeLa and Caco-2 are both type II), apoptosis induction through the extrinsic pathway also requires caspase-9. Still it would be interesting to know if NleF prevents apoptosis induced through the intrinsic pathway, with caspase-9 and not caspase-8 being the first caspase activated, just as efficient as TRAIL-induced apoptosis. To test this, apoptosis was induced in HeLa cells with staurosporine, a global protein kinase inhibitor produced by *Streptomyces staurosporeus*, that incuces intrinsic apoptosis as a consequence of cellular damage done by non-specific

kinase inhibition. As depicted in Figure 26 D and E, samples expressing NleF and Protein A revealed 3.7 % and 49.9 % apoptotic cells after staurosporine treatment, respectively.
Thus NleF decreases the number of apoptotic cells in staurosporine treated samples at least as efficiently as in TRAIL treated ones and as a consequence prevents apoptosis entered via the intrinsic as well as via the extrinsic pathway.

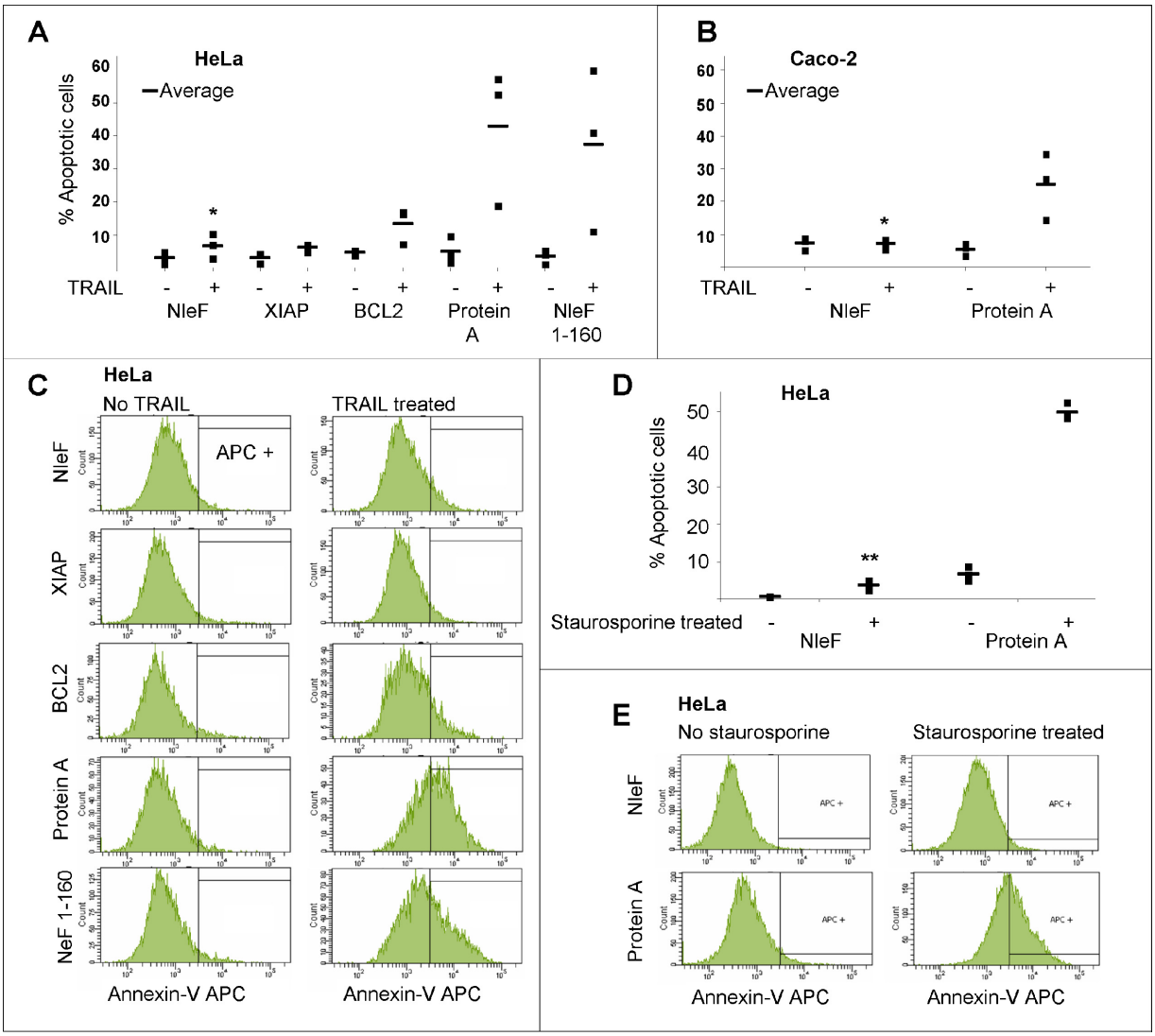

Figure 26. NleF inhibits apoptosis induced by TRAIL and staurosporine. (A) HeLa cells expressing wild type NleF, XIAP and BCL2, respectively, exhibited decreased apoptosis in comparison to cells expressing Protein A or the inactive NleF 1-160 fragment after TRAIL treatment. Squares: percentage of apoptotic cells (three independent experiments); bars: average. (B) Caco-2 cells expressing NleF and Protein A, respectively. Significance (t-test): * $P < 0.05$. (C and E) Representative FACS counts of HeLa cells expressing indicated constructs. Cells that stained positive for annexin V- allophycocyanine (APC+) but negative for propidium iodide were counted as apoptotic cells. (D) Percentage of apoptotic HeLa cells in staurosporine treated (+) and untreated (-) samples expressing NleF and Protein A, respectively.

3.1.4.6 Mutagenesis of the NleF C-terminus

In the frame of a collaboration with Holger Steuber from Proteros (Martinsried, Germany), the structural basis of the caspase-9/NleF complex was solved by co-crystallization. The structure revealed that in addition to other minor contacts, the carboxy-terminal amino acids G189, C188, Q187 and L186 anchor NleF to the S1, S2, S3, and S4 pockets of caspase-9,

respectively. The occupancy of the substrate binding pockets of caspase-9 is a likely explanation for the effective inhibition of caspase-9 activity by NleF.
To test if changes of the last four amino acids of NleF may impair its binding to the caspases 4, 8 and 9, I constructed seven versions of NleF with altered C-termini. These involve NleF +1, NleF -1, NleF -4, NleF L186A, NleF Q187A, NleF C188A and NleF G189A. NleF +1 harbours an extra alanine, NleF -1 and NleF -4 lack 1 and 4 carboxy-terminal amino acids, respectively, and the remaining four are substitutions of L, Q, C and G to alanine (see figure 27 for details).
LUMIER assays of all NleF versions against caspases 4, 8 and 9 revealed different binding profiles. Caspase-9 still bound, though weaker than wild type NleF, four out of the seven NleF versions, namely NleF -1, NleF L186A, C188A and G189A. Caspase-4 was only able to bind NleF C188A, whereas caspase-8 was unable to bind any of the mutagenized NleF versions.

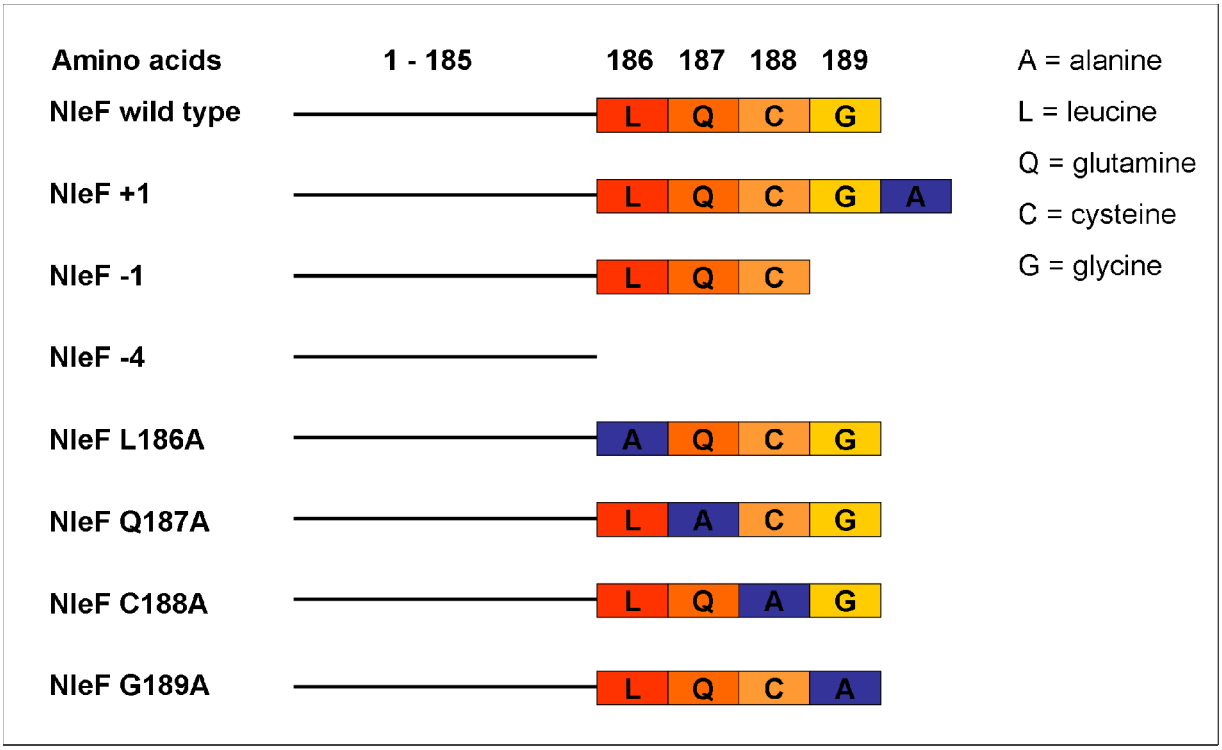

Figure 27. NleF versions with altered carboxy-terminus. Amino acids 1-185 are constant in all NleF versions. NleF +1, NleF -1 and NleF -4 harbour an extra alanine and lack 1 and 4 C-terminal amino acids, respectively. NleF L186A, Q187A, C188A and G189A are substitutions of leucine, glutamine, cysteine and glycine to alanine.

When tested for their ability to prevent apoptosis as transiently expressed YFP-fusions in HeLa cells, NleF +1 and NleF -4 revealed a complete loss of apoptosis inhibition. This indicates that the caspase-9 P1 pocket is unable to tolerate an additional amino acid, which as a consequence leads to a complete loss of NleF +1 function. Since NleF -4 lacks the four carboxy-terminal amino acids predicted to be responsible for caspase-9 inhibition, its inability to prevent apoptosis was expected. NleF -1, NleF L186A, Q187A, C188A and G189A were still able to decrease the number of apoptotic cells significantly, but none did as efficient as wild type NleF. The results are depicted in figure 28.

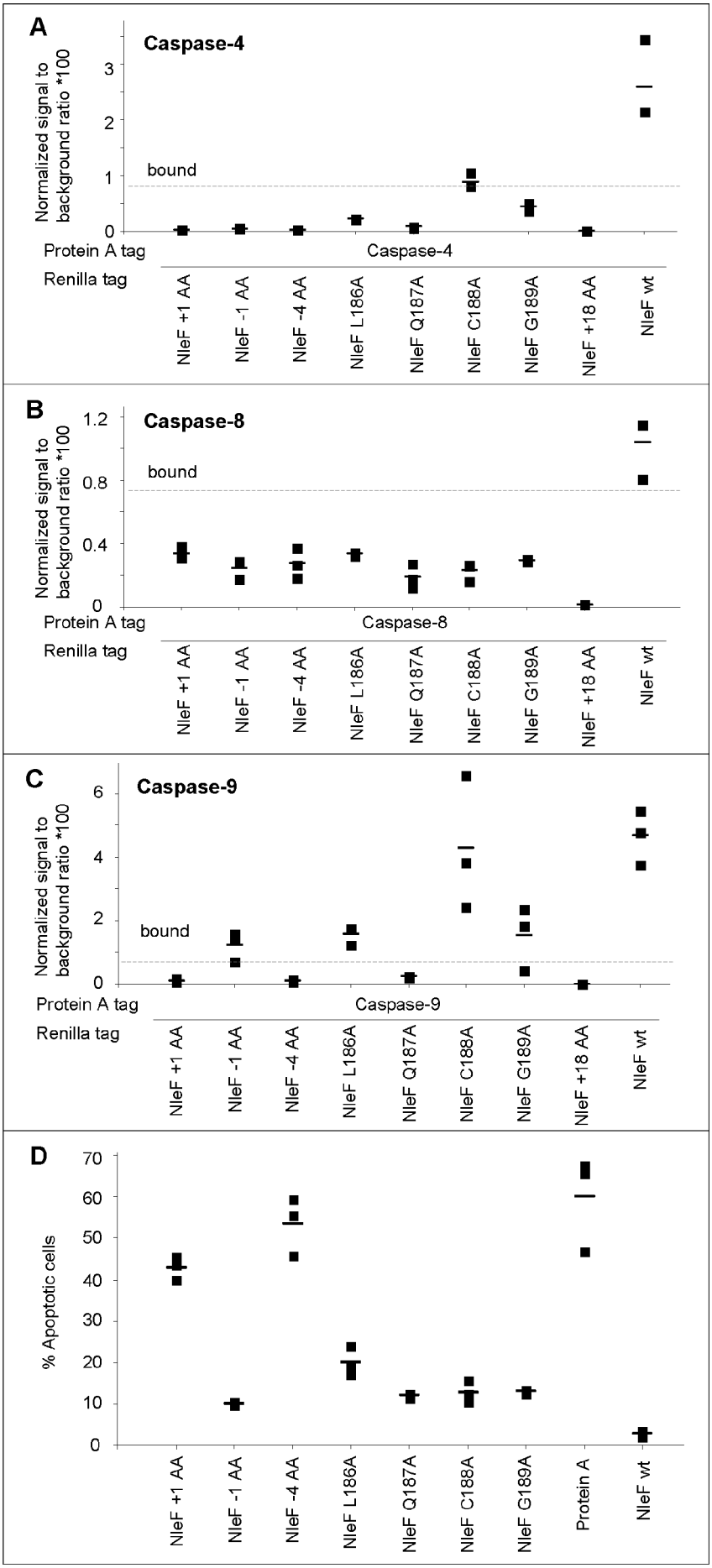

Figure 28. Caspase binding and apoptosis inhibition by modified versions of NleF. (A) Caspase-4, (B) caspase-8 and (C) caspase-9-binding of different versions of NleF assessed by LUMIER assays. (D) Percentage of apoptotic HeLa cells expressing different versions of NleF after induction with staurosporine. NleF +1: NleF with an additional C-terminal alanine; NleF -1 and NleF -4: NleF with the terminal 1 and 4 amino acids removed, respectively; NleF L186A, NleF Q187A, NleF C188A and NleF G189A: NleF versions with indicated amino acids substituted by alanine; NleF +18: NleF with additional 18 amino acids. The last version of NleF lacks its native stop codon. The additional 18 amino acids originate from the LUMIER vector pcDNA3-Rluc-GW.

3.2 Part II: The phage lambda-*E. coli interactome*

As customary for viruses, phage lambda completely relies on its host's cellular machinery for propagation. It can 'choose' out of two ways to propagate, namely to grow lytically by producing a large number of virions and killing its host as a consequence or to insert in chromosomal DNA and duplicate with each cell division performed by the host bacterium. Regardless which way is chosen, protein-protein interactions between phage and host are indispensable either way.

To identify novel interactions between phage lambda and *E. coli*, I analysed 68 phage lambda proteins by Y2H screening against an *E. coli* ORF library. The phage lambda clones and the *E. coli* library originate from (Rajagopala et al., 2011) and (Rajagopala et al., 2010), respectively.

3.2.1 Procedure of the phage lambda/host screens

For the performance of the Y2H pool and arrayed pool screens, the 68 phage lambda clones in the bait vectors pGBKT7g and pDEST32 were screened against the *E. coli* W3110 library in the prey vectors pGADT7g and pDEST22, respectively. The screens were performed in three runs, each including the screening of the phage lambda baits once or more against one library using one screening method (see table 10 for details).

Table 10. Overview summarizing the screening procedures and properties of the lambda baits and the *E. coli* prey libraries.

Baits	Bait vector	Prey libraries	Prey vector	Properties	Screen procedure
Lambda ORFs	pGBKT7g	*E. coli* W3110	pGADT7g	high copy vector	arrayed pool screens
Lambda ORFs	pGBKT7g	*E. coli* W3110	pGADT7g	high copy vector	pool screens
Lambda ORFs	pDEST32	*E. coli* W3110	pDEST22	low copy vector	pool screens

Arrayed pool screens were done using the whole *E. coli* pGADT7g library arranged on two plates, each well containing a separate prey pool. Each bait was mated with each prey pool and the diploids were arrayed on selective agarose plates. A flowchart of the procedure is provided in figure 29.

The pGBKT7g/pGADT7g and pDEST32/22 vector systems differ mainly by copy number and thus in the amount of protein present in the yeast cell. As previously shown by (Rajagopala et al., 2009), the number of obtained screening hits varies clearly between the vector systems and the overlap of unique pairs detected in both systems is usually low. However, the two vector systems complement each other and thus screening with both leads to an increase in identified protein-protein interactions.

The lambda-host screens resulted in the identification of 294 *E. coli* proteins and 631 unique bait/prey pairs in total. 573 pairs were found in the pGBKT7g/pGADT7g vector system and 56 in the pDEST32/22 system. Two were found in both systems, namely lambda G – *E. coli* clpP and lambda A – *E. coli* nohB.

In total 334 pairs were identified as single hits, 103 were found repeatedly in one screen and 54 repeatedly in 2 or more independent screens. 25 potentially promiscuous preys were identified that were involved in 218 lambda/host interactions. The numeric results of the phage lambda-host pool screens are summarized in table 11.

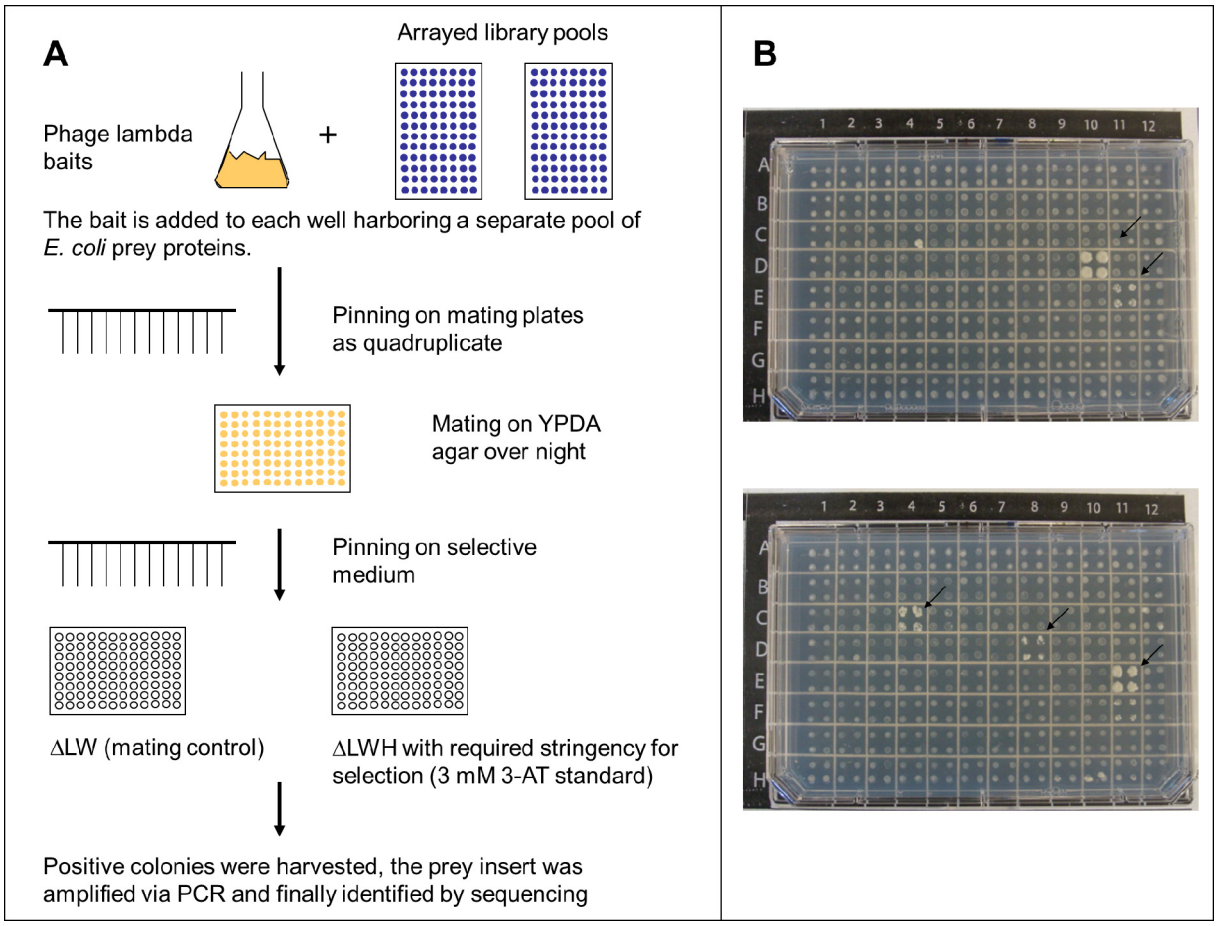

Figure 29. Arrayed pool screens. (A) Flowchart visualizing the procedure of arrayed pool screening and (B) exemplary array plates. The positive yeast colonies are indicated by arrows. The plates are in 384-format and each prey pool is pinned as quadruplicate.

Table 11. Numeric results of the phage lambda/host pool screens.

Identified *E. coli* prey proteins:	Total number	294
	Promiscuous	25
Unique bait/prey pairs:	Total number	631
	Single hits	334
	High-confidence hits	161
	with promiscuous preys	218
Unique bait/prey pairs, pDEST32/22 only:	Total number	56
	Single hits	38
	High-confidence hits	18
Unique bait/prey pairs, pGBKT7g/pGADT7g only:	Total number	573
	Single hits	296
	High-confidence hits	141
Unique bait/prey pairs found in both pDEST32/22 and pGBKT7g/pGADT7g		2

3.2.1.1 Promiscuous preys

A prey protein was considered promiscuous or ‘sticky’ if it interacted with 5 or more different lambda baits and/or if it interacted randomly or excessively in pairwise yeast two-hybrid tests. At the time the phage lambda-host screens were done, the *E. coli* library had not been used extensively, so the main source for the evaluation of preys that behave sticky in this library

were previously described lambda-host screens. A list of potential promiscuous preys and the number of phage lambda baits they interacted with is provided in table 12.

Table 12. List of *E. coli* prey proteins tagged as promiscuous. The column 'Number of baits' states the number of phage lambda baits a prey protein was found to interact with. LeuB was found to interact randomly in the pDEST vector system. PhoB was identified as sticky in the pairwise tests.

	Prey gene symbol	ECK ID	JW ID	b ID	Number of baits
1	ynjB	ECK1752	JW5284	b1754	20
2	yiaF	ECK3541	JW5655	b3554	16
3	flxA	ECK1560	JW1558	b1566	15
4	spr	ECK2169	JW2163	b2175	13
5	mltB	ECK2696	JW2671	b2701	12
6	ydaW	ECK1359	JW5211	b1361	11
7	ynfO	ECK1542	JW5251	b4533	11
8	dicB	ECK1569	JW1566	b1575	10
9	fliA	ECK1921	JW1907	b1922	10
10	metN	ECK0199	JW0195	b0199	10
11	tyrS	ECK1633	JW1629	b1637	8
12	phnG	ECK4094	JW4062	b4101	7
13	ydcE	ECK1455	JW1456	b1461	7
14	ygiT	ECK3012	JW2989	b3021	7
15	yihD	ECK3850	JW3830	b3858	7
16	insN	ECK0257	JW5024	b0255	6
17	tbpA	ECK0069	JW0067	b0068	6
18	yajI	ECK0406	JW5056	b0412	6
19	yjgZ	ECK4267	JW4236	b4277	6
20	yjhV	ECK4276	JW4246	b4286	6
21	fixX	ECK0045	JW0043	b0044	5
22	wza	ECK2056	JW2047	b2062	5
23	ydaL	ECK1337	JW1334	b1340	5
24	phoB	ECK0393	JW0389	b0399	4
25	leuB	ECK0075	JW5807	b0073	1

PhoB was only found to interact with 4 different lambda baits in the pool screens. However, when tested in binary yeast two-hybrid assays it revealed interactions with 27 phage lambda baits. LeuB appeared randomly in screens with the pDEST32/22 vector system. If it was detected, the screens were mostly overgrown and had to be removed. It only came up once in a pool screen.
Most promiscuous preys concerned the pGBKT7g/pGADT7g vector system. The pDEST system revealed only interactions with two sticky proteins, namely leuB and yajI.

3.2.1.2 Promiscuous baits

Potentially promiscuous baits were identified using two different approaches:

1. Binary tests of all baits against the empty prey vector.
2. Identification of baits that revealed non-specific interaction patterns in yeast two-hybrid pool screens and/or binary tests.

In the first approach, the lambda baits in pGBKT7g vector were screened against the empty pGADT7g vector at increasing stringencies. Four baits activated the Y2H reporter when combined with empty vector at stringencies up to 20 mM 3-AT, namely lambdap18, lambdap29, lambdap47 and lambdap67. Even though the signal was lost at 50 mM 3-AT, no usable results were obtained for these baits. Some other baits revealed background signals

at lower stringencies, which did not affect the screening, since the selection of diploid yeast cells was done using a standard stringency of 3 mM 3-AT.

The baits in pDEST32 were only tested at the standard stringency of 3 mM 3-AT, revealing background growth for five baits when tested with pDEST22 vector, namely lambdap05, lambdap06, lambdap29, lambdap47 and lambdap67. The latter three were also identified in the pGBKT7g vector. The plate is depicted in figure 30.

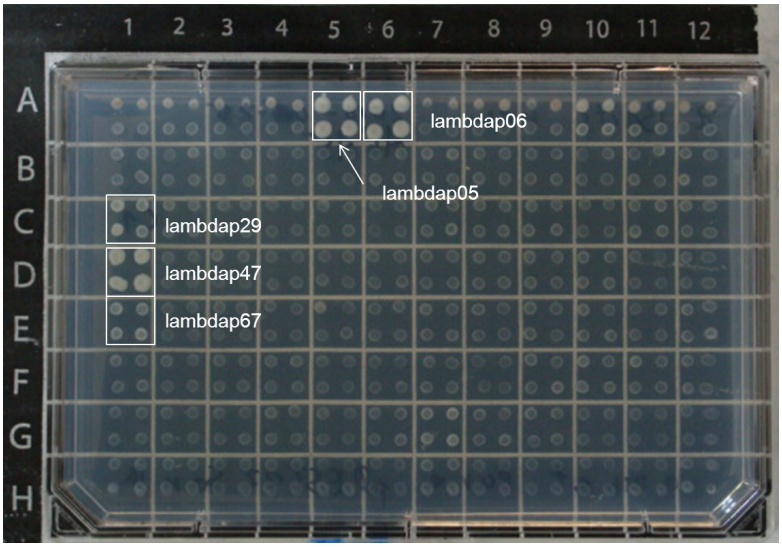

Figure 30. Binary tests of pDEST32 baits against pure pDEST22 vector. The selection was done at ΔLWH at a stringency of 3 mM 3-AT. Five baits revealed interactions with pure prey vector (indicated by white squares).

As a consequence, the six baits interacting with plain vector, lambdap05, 06, 18, 29, 47 and 67 were excluded from further evaluations.

In the second approach, pairwise tests of the phage lambda bait proteins in pGBKT7g against different prey proteins revealed lambdap16 (H), lambdap36 (ea8.5), lambdap45 (ea10), lambdap65 (NinD) and lambda83 (ea22) as putative non-specific interactors. When screened repeatedly, these bait proteins continued to find novel interactors in each screen. Therefore I decided to include only interactors of the concerning baits if they were found at least in three independent screens or binary tests.

3.2.1.3 Verification of single hits by pairwise Y2H assays

334 unique pairs were only found once, as single hits and out of these, 256 involved non-promiscuous prey proteins. To test if these interactions are reproducible, binary tests were performed. Out of 256, 25 were not retested and 139 revealed no interactions with the corresponding prey. However, 92 unique pairs could be confirmed in the pairwise Y2H tests.

3.2.2 The phage lambda-*E. coli* interactome

The procedure of Y2H screening and filtering resulted in 144 validated phage lambda-host interactions in total. See figure 31 for a visualization of the process.
A list of the final 144 phage lambda interactions is provided in table 13. A complete list of all interactions obtained, including the ones involving promiscuous baits and preys as well as single hits, can be obtained from supplementary table 3.

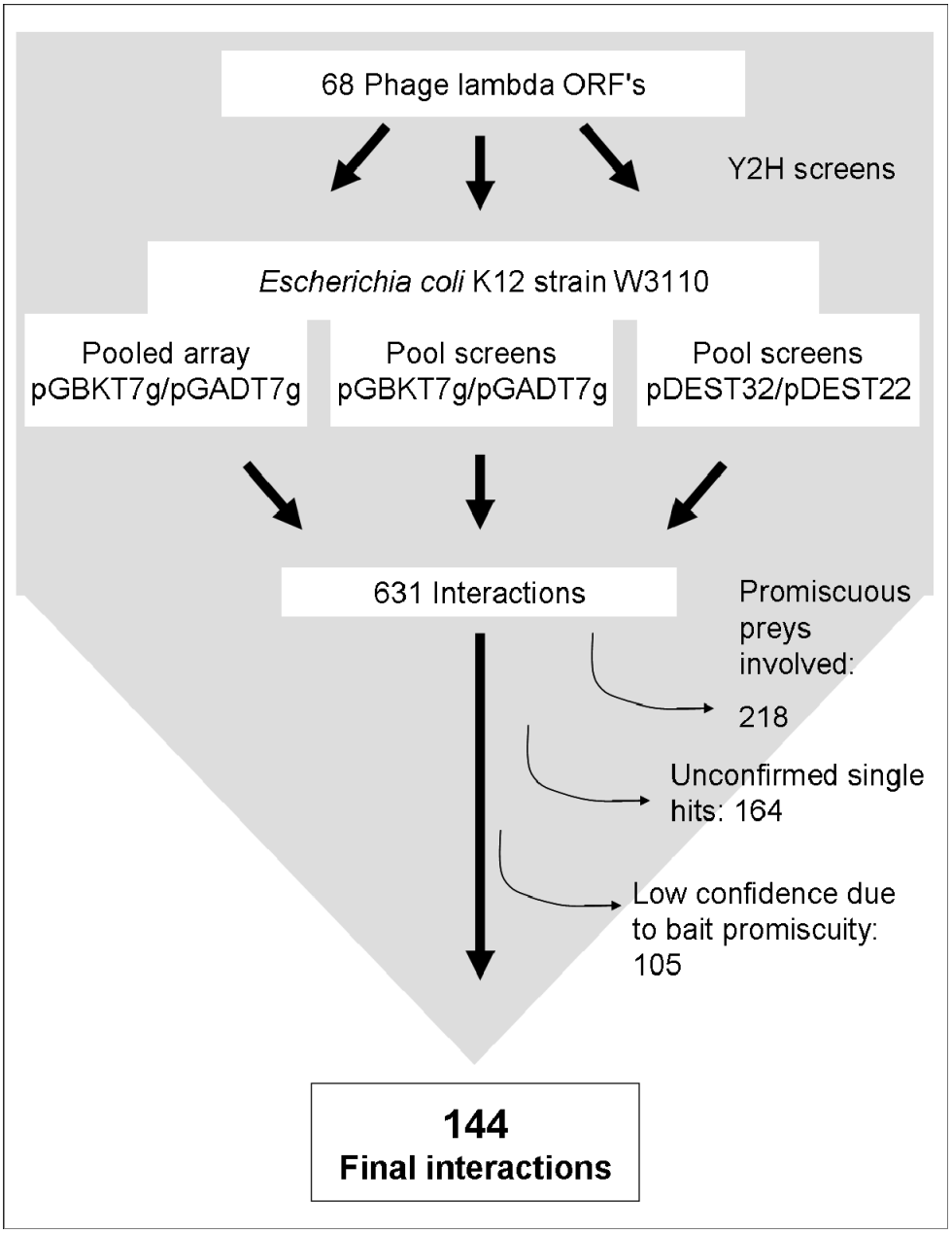

Figure 31. Procedure of phage lambda/host screens and filtering of obtained interactions. From the 631 interactions received in the Y2H pool screens, 218 were removed due to the involvement of promiscuous prey proteins. 164 were unconfirmed single hits and another 105 were removed, since the bait protein exhibited a high bait promiscuity and the corresponding interactions were only found twice or less times in one screen.

Table 13. Phage lambda-*E. coli* interactome. Hits states the number of times a unique pair was detected during the phage-host screens.

Locus tag	Lambda Bait	E. coli prey	Hits	ECK ID	Annotation
lambdap01	nu1	dcrB	2	ECK3456	protein DcrB
lambdap02	A	nohA	9	ECK1541	bacteriophage DNA packaging protein
lambdap02	A	nohB	4	ECK0552	bacteriophage DNA packaging protein
lambdap09	Fi	ydgH	4	ECK1599	protein YdgH
lambdap09	Fi	fixB	3	ECK0043	protein FixB

lambdap09	Fi	smpA	2	ECK2613	small protein A
lambdap09	Fi	cchB	1	ECK2451	ethanolamine utilization protein EutN
lambdap09	Fi	minE	2	ECK1162	cell division topological specificity factor MinE
lambdap14	G	ycbQ	4	ECK0929	fimbrial subunit
lambdap14	G	ycgE	48	ECK1149	HTH-type transcriptional regulator MlrA
lambdap14	G	chaC	4	ECK1212	cation transport protein ChaC
lambdap14	G	yliL	3	ECK0805	b0816 hypothetical protein (yliL)
lambdap14	G	clpP	43	ECK0431	ATP-dependent Clp protease, proteolytic subunit ClpP
lambdap14	G	fdoH	8	ECK3886	formate dehydrogenase, beta subunit
lambdap14	G	proQ	3	ECK1830	ProP effector
lambdap14	G	yceK	2	ECK1036	lipoprotein, putative
lambdap14	G	ykgL	2	ECK0294	hypothetical protein (ykgL)
lambdap14	G	fhuF	21	ECK4357	ferric iron reductase protein FhuF
lambdap14	G	yohN	5	ECK2100	conserved hypothetical protein
lambdap16	H	sfmA	2	ECK0523	type-1 fimbrial protein, A chain
lambdap16	H	sfmF	3	ECK0527	major fimbrial subunit
lambdap16	H	dnaN	3	ECK3693	DNA polymerase III, beta subunit
lambdap16	H	ECK1157	3	ECK1157	putative ATP-binding component of a transport system
lambdap16	H	hyfG	3	ECK2483	hydrogenase-4 component G
lambdap16	H	ynfC	3	ECK1580	lipoprotein YnfC
lambdap16	H	yehD	3	ECK2104	fimbrial protein
lambdap16	H	yraH	3	ECK3130	fimbrial protein
lambdap16	H	ycbQ	4	ECK0929	fimbrial subunit
lambdap16	H	yfcQ	4	ECK2328	conserved hypothetical protein
lambdap16	H	yohH	4	ECK2132	YohH
lambdap16	H	yeiW	4	ECK2164	proteinase inhibitor
lambdap16	H	ybgD	4	ECK0708	fimbrial protein
lambdap16	H	ymjB	4	ECK1314	putative ATP-binding component of a transport system
lambdap16	H	acpS	5	ECK2561	holo-(acyl-carrier-protein) synthase
lambdap16	H	yliL	10	ECK0805	b0816 hypothetical protein (yliL)
lambdap27	orf-401	stfR	89	ECK1367	putative membrane protein
lambdap28	orf-314	tfaR	152	ECK1368	tail fiber assembly protein
lambdap28	orf-314	tfaQ	2	ECK1539	tail fiber assembly protein
lambdap28	orf-314	clpP	7	ECK0431	ATP-dependent Clp protease, proteolytic subunit ClpP
lambdap28	orf-314	ycgE	4	ECK1149	HTH-type transcriptional regulator MlrA
lambdap33	int	nohB	7	ECK0552	bacteriophage DNA packaging protein
lambdap33	int	paaC	6	ECK1387	phenylacetate-CoA oxygenase, PaaI subunit
lambdap33	int	nlpI	6	ECK3151	lipoprotein NlpI
lambdap36	ea8.5	minE	2	ECK1162	cell division topological specificity factor MinE
lambdap36	ea8.5	yeiW	2	ECK2164	proteinase inhibitor
lambdap36	ea8.5	yjdI	3	ECK4119	conserved hypothetical protein

lambdap37	orf61	yqhC	3	ECK3002	putative HTH-type transcriptional regulator YqhC
lambdap37	orf61	yjdI	2	ECK4119	conserved hypothetical protein
lambdap37	orf61	yheL	2	ECK3330	sulfur relay protein TusD/DsrH
lambdap38	orf63	yqhC	4	ECK3002	putative HTH-type transcriptional regulator YqhC
lambdap45	ea10	rpmA	8	ECK3174	ribosomal protein L27
lambdap45	ea10	ycbG	3	ECK0947	protein YcbG
lambdap45	ea10	frvA	43	ECK3893	phosphoenolpyruvate-dependent sugar phosphotransferase system, eiia 2, putative
lambdap45	ea10	rmf	17	ECK0944	b0953 ribosome modulation factor (rmf)
lambdap45	ea10	yliL	8	ECK0805	b0816 hypothetical protein (yliL)
lambdap45	ea10	rpsG	7	ECK3328	ribosomal protein S7
lambdap45	ea10	cedA	5	ECK1729	conserved hypothetical protein
lambdap45	ea10	soxS	3	ECK4054	regulatory protein SoxS
lambdap45	ea10	yqjI	63	ECK3061	transcriptional regulator, PadR family protein
lambdap45	ea10	yjiR	5	ECK4331	aminotransferase, classes I and II superfamily
lambdap45	ea10	priC	4	ECK0461	primosomal replication protein N
lambdap45	ea10	rpsS	4	ECK3303	30S ribosomal protein S19
lambdap45	ea10	ypjJ	4	ECK2641	hypothetical protein (ypjJ)
lambdap45	ea10	cobB	3	ECK1106	NAD-dependent deacetylase
lambdap48	lambdap48	pntA	1	ECK1598	NAD(P) transhydrogenase, alpha subunit
lambdap49	N	nusA	1	ECK3158	transcription elongation protein NusA
lambdap49	N	yicI	4	ECK3646	alpha-glucosidase
lambdap49	N	hcr	3	ECK0863	NADH oxidoreductase hcr
lambdap49	N	ego	2	ECK1506	putative ABC transporter ATP-binding protein ego
lambdap49	N	ppc	2	ECK3947	phosphoenolpyruvate carboxylase
lambdap49	N	secB	3	ECK3599	protein-export chaperone SecB
lambdap49	N	nuoG	2	ECK2277	NADH-quinone oxidoreductase, chain g
lambdap49	N	yebR	2	ECK1831	protein YebR
lambdap49	N	yjeP	2	ECK4155	BspA protein
lambdap49	N	rpoS	1	ECK2736	RNA polymerase sigma factor RpoS
lambdap49	N	envR	1	ECK3251	probable acrEF/envCD operon repressor
lambdap49	N	minC	1	ECK1164	septum site-determining protein MinC
lambdap49	N	ycbG	1	ECK0947	protein YcbG
lambdap49	N	ydiT	1	ECK1698	conserved hypothetical protein
lambdap49	N	yfhL	1	ECK2560	iron-sulfur cluster-binding protein
lambdap49	N	yiiF	1	ECK3883	conserved hypothetical protein
lambdap49	N	nohA	2	ECK1541	bacteriophage DNA packaging protein
lambdap49	N	ybeB	1	ECK0630	iojap-like ribosome-associated protein

lambdap61	P	ycbG	2	ECK0947	protein YcbG
lambdap61	P	eutC	2	ECK2435	ethanolamine ammonia-lyase, light chain
lambdap61	P	atpC	3	ECK3724	ATP synthase F1, epsilon subunit
lambdap61	P	yqhC	2	ECK3002	putative HTH-type transcriptional regulator YqhC
lambdap61	P	ydaG	2	ECK1353	conserved hypothetical protein
lambdap61	P	fliM	2	ECK1943	flagellar motor switch protein FliM
lambdap63	NinB	rpsE	2	ECK3290	ribosomal protein S5
lambdap63	NinB	yqjI	6	ECK3061	transcriptional regulator, PadR family protein
lambdap65	NinD	ydiT	6	ECK1698	conserved hypothetical protein
lambdap65	NinD	minE	4	ECK1162	cell division topological specificity factor MinE
lambdap65	NinD	pyrF	5	ECK1276	orotidine 5'-phosphate decarboxylase
lambdap65	NinD	yfiM	5	ECK2584	conserved hypothetical protein
lambdap65	NinD	yhdW	5	ECK3255	general L-amino acid-binding periplasmic protein AapJ
lambdap65	NinD	slp	4	ECK3490	outer membrane protein slp
lambdap65	NinD	csrA	3	ECK2691	carbon storage regulator
lambdap65	NinD	HycG	3	ECK2714	hydrogenase-4 component I
lambdap65	NinD	sdiA	3	ECK1915	regulatory protein SdiA
lambdap65	NinD	soxS	3	ECK4054	regulatory protein SoxS
lambdap65	NinD	smpA	4	ECK2613	small protein A
lambdap65	NinD	yjdI	4	ECK4119	conserved hypothetical protein
lambdap65	NinD	yebR	3	ECK1831	protein YebR
lambdap66	NinE	nlpI	3	ECK3151	lipoprotein NlpI
lambdap71	Q	nlpI	4	ECK3151	lipoprotein NlpI
lambdap71	Q	yqhC	2	ECK3002	putative HTH-type transcriptional regulator YqhC
lambdap71	Q	glyQ	2	ECK3548	glycyl-tRNA synthetase, alpha subunit
lambdap71	Q	ybeB	1	ECK0630	iojap-like ribosome-associated protein
lambdap71	Q	rfaD	1	ECK3609	ADP-L-glycero-D-manno-heptose-6-epimerase
lambdap71	Q	paaC	1	ECK1387	phenylacetate-CoA oxygenase, PaaI subunit
lambdap71	Q	yibA	2	ECK3583	protein YibA
lambdap75	R	fhuF	10	ECK4357	ferric iron reductase protein FhuF
lambdap75	R	caiF	3	ECK0035	transcriptional activatory protein CaiF
lambdap75	R	ydcK	1	ECK1421	conserved hypothetical protein
lambdap78	orf_78	ispB	4	ECK3176	octaprenyl-diphosphate synthase
lambdap79	orf_79	ybcW	1	ECK0551	conserved hypothetical protein
lambdap80	ea47	yjiT	4	ECK4333	conserved hypothetical protein
lambdap80	ea47	sucC	2	ECK0716	succinyl-CoA synthetase beta chain
lambdap80	ea47	ubiH	2	ECK2902	2-polyprenyl-6-methoxyphenol 4-hydroxylase
lambdap80	ea47	hybO	1	ECK2991	[Ni/Fe] hydrogenase, small subunit

lambdap80	ea47	modC	1	ECK0754	molybdate ABC transporter, ATP-binding protein
lambdap80	ea47	thiF	1	ECK3984	thiazole biosynthesis adenylyltransferase ThiF
lambdap80	ea47	ycdC	1	ECK1004	HTH-type transcriptional regulator RutR
lambdap80	ea47	yqhC	1	ECK3002	putative HTH-type transcriptional regulator YqhC
lambdap83	ea22	ybiS	2	ECK0809	protein YbiS
lambdap83	ea22	soxS	3	ECK4054	regulatory protein SoxS
lambdap83	ea22	yliL	4	ECK0805	b0816 hypothetical protein (yliL)
lambdap83	ea22	norR	26	ECK2704	anaerobic nitric oxide reductase transcription regulator NorR
lambdap88	cI	pldB	3	ECK3819	lysophospholipase L2
lambdap88	cI	mdtE	2	ECK3497	multidrug resistance protein MdtE
lambdap88	cI	smpA	2	ECK2613	small protein A
lambdap88	cI	eutC	2	ECK2435	ethanolamine ammonia-lyase, light chain
lambdap88	cI	fliM	2	ECK1943	flagellar motor switch protein FliM
lambdap88	cI	rseB	2	ECK2569	sigma-E factor regulatory protein RseB
lambdap88	cI	ydiT	2	ECK1698	conserved hypothetical protein
lambdap89	O	clpP	1	ECK0431	ATP-dependent Clp protease, proteolytic subunit ClpP
lambdap89	O	ppk	15	ECK2497	polyphosphate kinase
lambdap89	O	yjhP	15	ECK4296	conserved hypothetical protein
lambdap89	O	tfaQ	3	ECK1539	tail fiber assembly protein
lambdap89	O	mviM	2	ECK1053	putative Virulence factor MviM homolog
lambdap90	orf206b	prfH	3	ECK0237	putative peptide chain release factor H
lambdap90	orf206b	yjbF	2	ECK4019	YmcC
lambdap90	orf206b	ypfJ	2	ECK2471	neutral zinc metallopeptidase family

3.2.2.1 Functional groups

All phage lambda proteins and corresponding *E. coli* interactors were assigned to 9 and 14 different functional groups, respectively. For phage lambda, these were virion head, virion tail, superinfection exclusion, transcription, replication, recombination, lysis, inhibition of host replication and proteins of unknown function. The categories for *E. coli* involve biosynthesis of cofactors prosthetic groups and carriers, cell envelope, phage origin, cellular processes, DNA metabolism, energy metabolism, fimbrial proteins, protein fate, protein synthesis, regulatory functions, transcription, transport and binding proteins, unknown/uncharacterized/hypothetical proteins and others with known function. The phage lambda (L) and host (Eco) proteins along with their assigned functional groups can be obtained from table 14.

Table 14. Functional groups of phage lambda (L) and *E. coli* proteins (Eco). biosynth - biosynthesis of cofactors, prosthetic groups, and carriers; cenv - cell envelope; phage - phage origin; cellProc - cellular processes; DNAmeta - DNA metabolism; enMeta - energy metabolism; fimProt - fimbrial protein; protFate - protein fate; protSynth - protein synthesis; regFunc - regulatory functions; trx - transcription; transBind - transport and binding proteins; unc/unk/hyp - unknown/uncharacterized/hypothetical protein; other - other; tail - virion tail; sep - superinfection exclusion; trx - transcription; repl - replication; unk - unknown; rec - recombination; lysis - lysis; ihr - inhibition of host replication; head - virion head.

Gene	Organism	Function	Gene	Organism	Function
A	L	head	cobB	Eco	other
Fi	L	head	ppk	Eco	other
nu1	L	head	acpS	Eco	other
ea8.5	L	ihr	pldB	Eco	other
R	L	lysis	pyrF	Eco	other
NinB	L	rec	frvA	Eco	other
int	L	rec	tfaQ	Eco	phage
orf63	L	rec	tfaR	Eco	phage
ea10	L	repl	nohA	Eco	phage
O	L	repl	nohB	Eco	phage
P	L	repl	stfR	Eco	phage
SieB (orf48)	L	sep	ybcW	Eco	phage
orf-401	L	tail	ydaG	Eco	phage
orf-314	L	tail	clpP	Eco	protFate
G	L	tail	secB	Eco	protFate
H	L	tail	yeiW	Eco	protFate
cI	L	trx	ypfJ	Eco	protFate
Q	L	trx	glyQ	Eco	protSynth
N	L	trx	prfH	Eco	protSynth
orf_78	L	unk	rmf	Eco	protSynth
NinE	L	unk	rpmA	Eco	protSynth
NinD	L	unk	rpsE	Eco	protSynth
orf206b	L	unk	rpsG	Eco	protSynth
orf_79	L	unk	rpsS	Eco	protSynth
orf61	L	unk	yheL	Eco	protSynth
ea47	L	unk	caiF	Eco	regFunc
ea22	L	unk	envR	Eco	regFunc
ispB	Eco	biosynth	rseB	Eco	regFunc
thiF	Eco	biosynth	sdiA	Eco	regFunc
ubiH	Eco	biosynth	soxS	Eco	regFunc
fliM	Eco	cellProc	ycdC	Eco	regFunc
mdtE	Eco	cellProc	ycgE	Eco	regFunc
minC	Eco	cellProc	yqhC	Eco	regFunc
minE	Eco	cellProc	yqjI	Eco	regFunc
mviM	Eco	cellProc	chaC	Eco	transBind
proQ	Eco	cellProc	ECK1157	Eco	transBind
nlpI	Eco	cenv	ego	Eco	transBind
rfaD	Eco	cenv	fhuF	Eco	transBind
slp	Eco	cenv	modC	Eco	transBind
yceK	Eco	cenv	ydgH	Eco	transBind
yjeP	Eco	cenv	yhdW	Eco	transBind
dnaN	Eco	DNAmeta	ymjB	Eco	transBind
priC	Eco	DNAmeta	nusA	Eco	trx
atpC	Eco	enMeta	rpoS	Eco	trx
cchB	Eco	enMeta	cedA	Eco	unc/unk/hyp
csrA	Eco	enMeta	dcrB	Eco	unc/unk/hyp

Gene	Organism	Function	Gene	Organism	Function
eutC	Eco	enMeta	smpA	Eco	unc/unk/hyp
fdoH	Eco	enMeta	ybeB	Eco	unc/unk/hyp
fixB	Eco	enMeta	ybiS	Eco	unc/unk/hyp
hcr	Eco	enMeta	ycbG	Eco	unc/unk/hyp
hybO	Eco	enMeta	ydcK	Eco	unc/unk/hyp
HycG	Eco	enMeta	ydiT	Eco	unc/unk/hyp
hyfG	Eco	enMeta	yebR	Eco	unc/unk/hyp
norR	Eco	enMeta	yfcQ	Eco	unc/unk/hyp
nuoG	Eco	enMeta	yfiM	Eco	unc/unk/hyp
paaC	Eco	enMeta	yibA	Eco	unc/unk/hyp
pntA	Eco	enMeta	yiiF	Eco	unc/unk/hyp
ppc	Eco	enMeta	yjbF	Eco	unc/unk/hyp
sucC	Eco	enMeta	yjdI	Eco	unc/unk/hyp
yfhL	Eco	enMeta	yjhP	Eco	unc/unk/hyp
yicI	Eco	enMeta	yjiT	Eco	unc/unk/hyp
sfmA	Eco	fimProt	ykgL	Eco	unc/unk/hyp
sfmF	Eco	fimProt	yliL	Eco	unc/unk/hyp
ybgD	Eco	fimProt	ynfC	Eco	unc/unk/hyp
ycbQ	Eco	fimProt	yohH	Eco	unc/unk/hyp
yehD	Eco	fimProt	yohN	Eco	unc/unk/hyp
yraH	Eco	fimProt	ypjJ	Eco	unc/unk/hyp
yjiR	Eco	other			

To observe which functional categories of *E. coli* proteins are targeted most frequently by phage lambda, the interactions occurring between functional groups of phage proteins and functional groups of host proteins were examined.
The results were dissimilar, depending on which functional groups were observed (see figure 32). A highly specific group was the *E. coli* group 'transcription' that was only targeted by phage lambda proteins involved in transcription, whereas the phage lambda transcription category targeted 11 out of 14 host functional groups. However, the most proteins involved in phage transcription interact with host proteins of the functional group energy metabolism.

E. coli / Lambda	Biosynth	CellProc	Cenv	DNAmeta	EnMeta	FimProt	Other	Phage	ProtFate	ProtSynth	RegFunc	TransBind	Trx	Unc/unk/hyp	Total L
Sep					1										1
Head		1			2			2				1		2	8
Ihr		1							1					1	3
Lysis											1	1		1	3
Rec			1		1			1		1	2				6
Repl		2		1	2		4	2	1	4	3			6	25
Tail		1	1	1	2	7	1	3	3		2	4		7	32
Trx		3	3		7		1	1	1	1	3	1	2	9	32
Unk	3	1	2		5		1	1	1	2	6	2		10	34
Total Eco	3	9	7	2	20	7	7	10	7	8	17	9	2	36	144

Figure 32. Interactions between the functional groups of phage lambda and its host *E. coli*.
See text for further explanations.

Interestingly, another group, the *E. coli* fimbrial proteins, interacted exclusively with phage lambda proteins involved in virion tail formation, especially with the lambda protein gpH, the tape measure protein. Even though no similarities between the protein sequences of host fimbrial proteins with phage lambda proteins were detected, it seems as if the tape measure

protein is capable to selectively target host fimbrial proteins. However, if these interactions play a role *in vivo* is still obscure. A similar statement can be made for phage lambda proteins interacting with *E. coli* proteins of prophage origin (functional group: Phage). Altogether seven different *E. coli* proteins of phage origin were involved in 10 phage host interactions, out of which 6 proteins were highly homologous to phage lambda proteins (see table 15). It has been shown previously that lambda gpA interacts with nu1 and orf_79 with itself (Rajagopala et al., 2011), so it is no surprise that these proteins also interact with homologues of nu1 (*E. coli* nohA and nohB) and orf_79 (*E. coli* ybcW), respectively. The nu1 homologue nohA was also found to interact with the phage antiterminator gpN. Even though the biological relevance of this interaction is not fully clear, binding of gpN to lambda nu1 was previously found by (Rajagopala et al., 2011).
Also conceivable are the interactions of the phage lambda defective tail fiber proteins orf-314 and orf-401 with the tail fiber assembly proteins tfaR and tfaQ and the tail fiber protein stfR, respectively. On the other hand the biological relevance of interactions like lambda integrase/*E. coli* nohB, lambda gpO/ *E. coli* tfaQ and lambda gpP/ *E. coli* ydaG is obscure, especially since phage lambda has no homologues of ydaG, which is a protein of Rac prophage origin.

Table 15. Lambda targets *E. coli* proteins of phage origin. The column 'lambda homologue' states the lambda protein which is homologous to the *E. coli* prey.

Lambda bait	*E. coli* preys	Lambda homologue	Description of *E. coli* prey
A	nohA	nu1	bacteriophage DNA packaging protein
N	nohA	nu1	bacteriophage DNA packaging protein
int	nohB	nu1	DLP12 prophage, DNA packaging protein
A	nohB	nu1	DLP12 prophage, DNA packaging protein
orf-401	stfR	orf-314	Rac prophage; predicted tail fiber protein
O	tfaQ	orf-194	Qin prophage; predicted tail fibre assembly protein
orf-314	tfaQ	orf-194	Qin prophage; predicted tail fibre assembly protein
orf-314	tfaR	orf-194	Rac prophage; predicted tail fiber assembly protein
orf_79	ybcW	orf_79	DLP12 prophage; predicted protein
P	ydaG	-	Rac prophage; predicted protein

Eight interactions were found for the *E. coli* group 'protein synthesis' that was targeted mainly by one phage lambda protein involved in replication, namely the putative single strand binding protein ea10. It bound the three ribosomal proteins rpmA, rpsG and rpsS as well as the ribosome modulation factor rmf. The host group 'transport and binding' interacted mainly with virion tail proteins, namely with gpG and gpH.
Remarkably, on both sides, phage and host, proteins of unknown function (or hypothetical proteins) were involved in interactions with several functional categories, but mainly with other proteins of unknown function.

3.2.2.2 Phage lambda – host interaction network

The 144 phage lambda – host interactions were combined in a complete network (see figure 33). Two interactions, namely lambda gpN/*E. coli* nusA (Friedman and Court, 2001) and lambda gpO/ *E. coli* clpP (Kobiler et al., 2004) were published previously (depicted as bold lines in green). The phage lambda-host interactions concerning *E. coli* proteins of phage origin (depicted in light pink in figure 33) were not considered as published interactions, since the interactions published by (Rajagopala et al., 2011) involve homologous proteins.

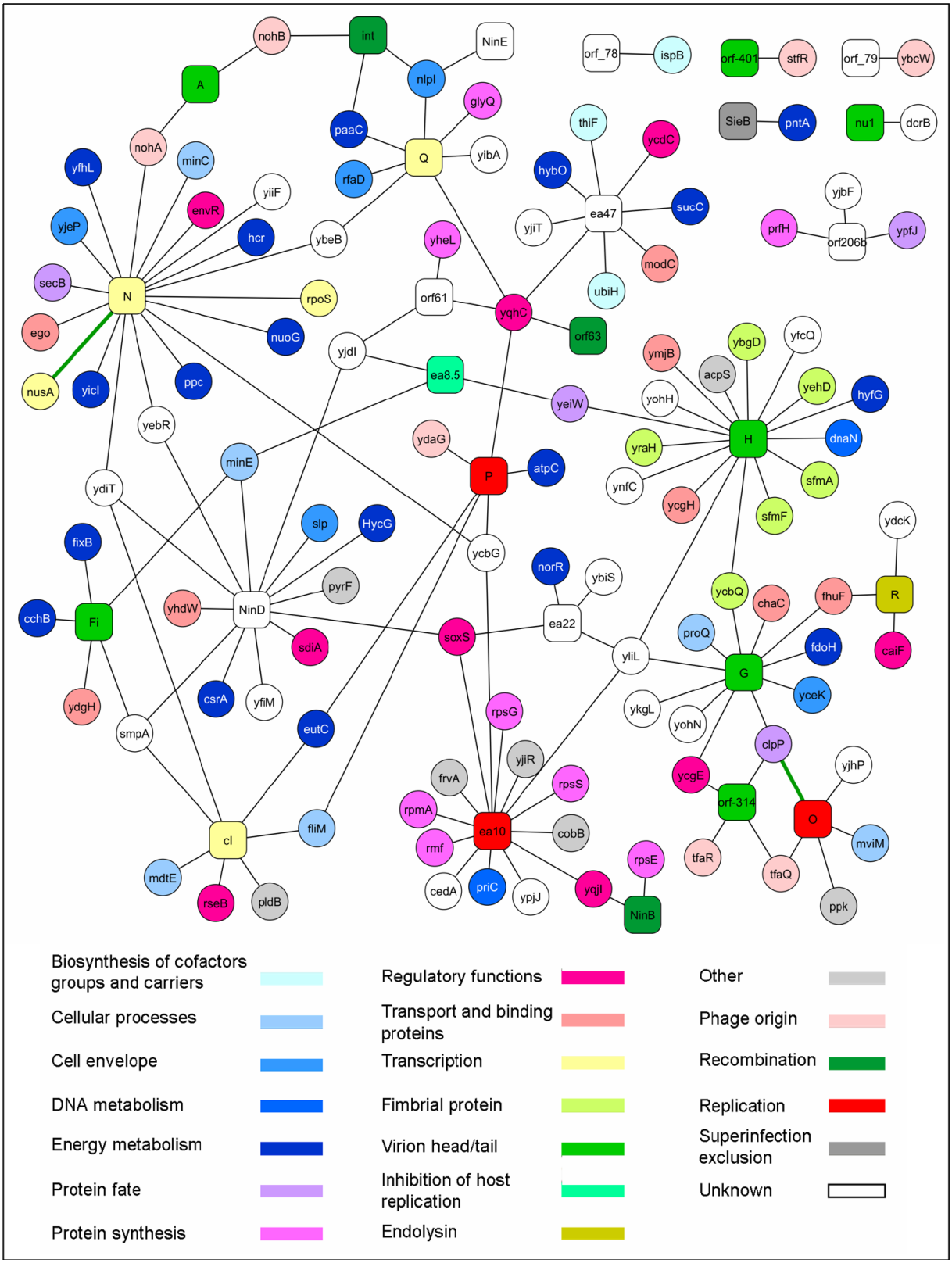

Figure 33. The protein interaction network of phage lambda with its host *E. coli*. The nodes represent proteins and are colored according to their functional class; quadratic and circular shapes stand for phage and host proteins, respectively. Protein-protein interactions are depicted as edges. Published interactions are depicted in green. The network contains the 144 phage/host interactions found in this study.

4 Discussion

4.1 The EHEC-host interactome

The EHEC-host interactome presented in this study was done to discover novel human interactors of both well-studied and lesser-known EHEC effector proteins. I chose the EHEC effector protein – host interactome for the following two reasons:
1. 39 EHEC effectors were experimentally shown to be secreted by the T3SS (Tobe et al., 2006) and were as such likely to reveal interactions with host proteins and
2. in contrast to extracellular and surface proteins that may also reveal interspecies interactions, soluble proteins with an intracellular localization are more likely to be functional in the yeast two-hybrid system.

4.1.1 Data quality and limits of the yeast two-hybrid system

In total 35 non-promiscuous interactions of 15 effectors with 34 human proteins were detected reproducibly. The 273 single hits also found in this study are unconfirmed yeast two-hybrid interacting pairs. They may be real interactions, but it is just as well possible that they arose through different technical artefacts such as more than one prey plasmid per cell, two or more yeast colonies per well or spontaneous mutations, which makes them highly unreliable (Mohr and Koegl, 2012). In addition their frequency of occurrence in pooled library screens is much higher (about 8 times in this study) than that of high-confidence hits, previously published interactions are rarely found among them and most single hits cannot be confirmed with alternate methods (other than yeast two-hybrid). As a consequence I decided to exclude the single hits from further network analysis.
For EHEC effectors, about 60 human putative and known interactors are described in the literature to date (reviewed in (Wong et al., 2011), out of which four were also discovered in this study. These involve TIR-BAIAP2 (Weiss et al., 2009), TIR-BAIAP2L1 (Vingadassalom et al., 2009), EspF-SNX9 (Marches et al., 2006) and Map-NHERF2 (SLC9A3R2) (Martinez et al., 2010). In general, this seems like a low overlap with published data, but since many pathogen-host interactions are rather of regulatory than of structural nature, the interactions may be only temporary and as such less stable. This makes discovery via Y2H screening more difficult. Yeast two-hybrid interactomes focussing on interactions between structural proteins such as (Rajagopala et al., 2011), who mapped the intraviral interactions of bacteriophage lambda, usually reveal a much higher overlap with literature data. Especially the hardwearing interactions of tail and capsid are highly reproducible.
Another limit of yeast two-hybrid is its restriction to direct protein-protein interactions. In the human cell, many proteins are organized into multimeric protein complexes. This allows not only direct, but also indirect protein-protein interactions involving one or more so-called linker proteins as connection(s) between the two indirect interactors. Both, indirect and direct PPIs can be detected with cell based assays such as LUMIER (Luminescence-based mammalian interactome mapping), since in contrast to yeast, mammalian cells can provide missing linker proteins. On the other hand a restriction to direct PPIs can also be advantageous, especially for the generation of interactomes and the distinction between direct and indirect interactors in protein complexes.
Other challenges include that some proteins require the aid of chaperones for efficient folding or only bind when folded into certain spatial conformations, depending on interactions with third proteins or on post translational modifications. Both EHEC effectors and human host

proteins are expressed in a non-natural environment and as such may reveal altered post translational modifications that interfere with their binding capabilities (Koegl and Uetz, 2007). However, despite these odds, most proteins are capable of folding correctly in the environment of the yeast nucleus and these show, as demonstrated by the discovery of previously known interactors, their natural interaction patterns.
Regarding the obtained 35 high confidence hits, it can be estimated, that the majority of these interactions are true interactions. The only exceptions may be NleH-UFC1 and TccP/EspF$_U$-ZNF626, since for both NleH and TccP/EspF$_U$ these interactions are the only high confidence hits among more than 27 single hits. Although these interactions may be less reliable compared to the other 33 high confidence hits, they are nevertheless reproducible PPIs and as such included in the EHEC-host network.
Potential yeast two-hybrid artefacts, also called promiscuous proteins were already removed from the high confidence dataset during the process of data analysis. The identification of putative artefacts relies very much on the threshold set for prey promiscuity. In our system of automated pool screening, which was applied for the generation of the EHEC-host interactome, a conservative specificity cut-off of 1% relative prey promiscuity was chosen. This means, a prey protein that was found to interact with one or more percent of all screened bait proteins was tagged as a potential artefact. Since our human cDNA libraries and ORF collections are also used by the yeast two-hybrid screening service facility of the DKFZ core facilities, a more comprehensive dataset was available for the identification of putative false-positive interactors. This allows an improved distinction between potential artefacts and high-confidence interactions, which corresponds well with the fact that the list of potential promiscuous prey proteins remained widely constant despite the ongoing increase of our dataset (internal data, unpublished). Still not all proteins tagged as promiscuous in our system are indeed artefacts. Some proteins such as TP53 that naturally exhibit a large number of different interactors (465 unique interactors are listed for TP53 in the BioGRID database, state 09/2012) may be sorted out in error. However, the majority of preys tagged erroneously as artefacts cannot be discovered due to the lack of published interaction data.
It is hard to estimate the recall, of our screens, i.e., the percentage of interactions recovered of all the ones that actually occur in nature. Taken the fact that the majority of detected EHEC-host interactions, namely 31, are novel ones, it can be concluded that many interactions between EHEC and its human host cells are not yet discovered.

4.1.2 Connections between effector proteins

The EHEC-host interactome generated within this study revealed several connections between EHEC effectors over indirectly interacting human proteins. These connections include so-called loops, which terms connections between two human interactors of one effector protein and their shared human interaction partner. Connections and loops indicate that the corresponding EHEC effectors are part of the same protein complex or pathway, or at least are in spatial proximity to each other. On the other hand, several of the connections and loops contain ubiquitin (UBC) or ubiquitin ligases (namely DTX2, ITCH, MDM2 and NEDD4) as connecting proteins. This may indicate that the human interactors are tagged (e.g. for degradation) by the same enzyme(s). Other connections seem to be more interesting, for example the one between NleF and EspY1 over their direct interactors DHFR and ZNHIT1 as well as the common indirect interactor TP53, or a trimeric connection between the EHEC effectors TIR, NleB1 and EspB over the common indirect interactor

IKBKG (see figure 34 A). IKBKG (NEMO) is the regulatory subunit of the IKK (inhibitor of kappaB kinase) complex and essential in activation of NF-kB.
A recently published study found that TIR can inhibit NF-kB activation via a direct or indirect interaction of TIR with TRAF2 (Ruchaud-Sparagano et al., 2011).

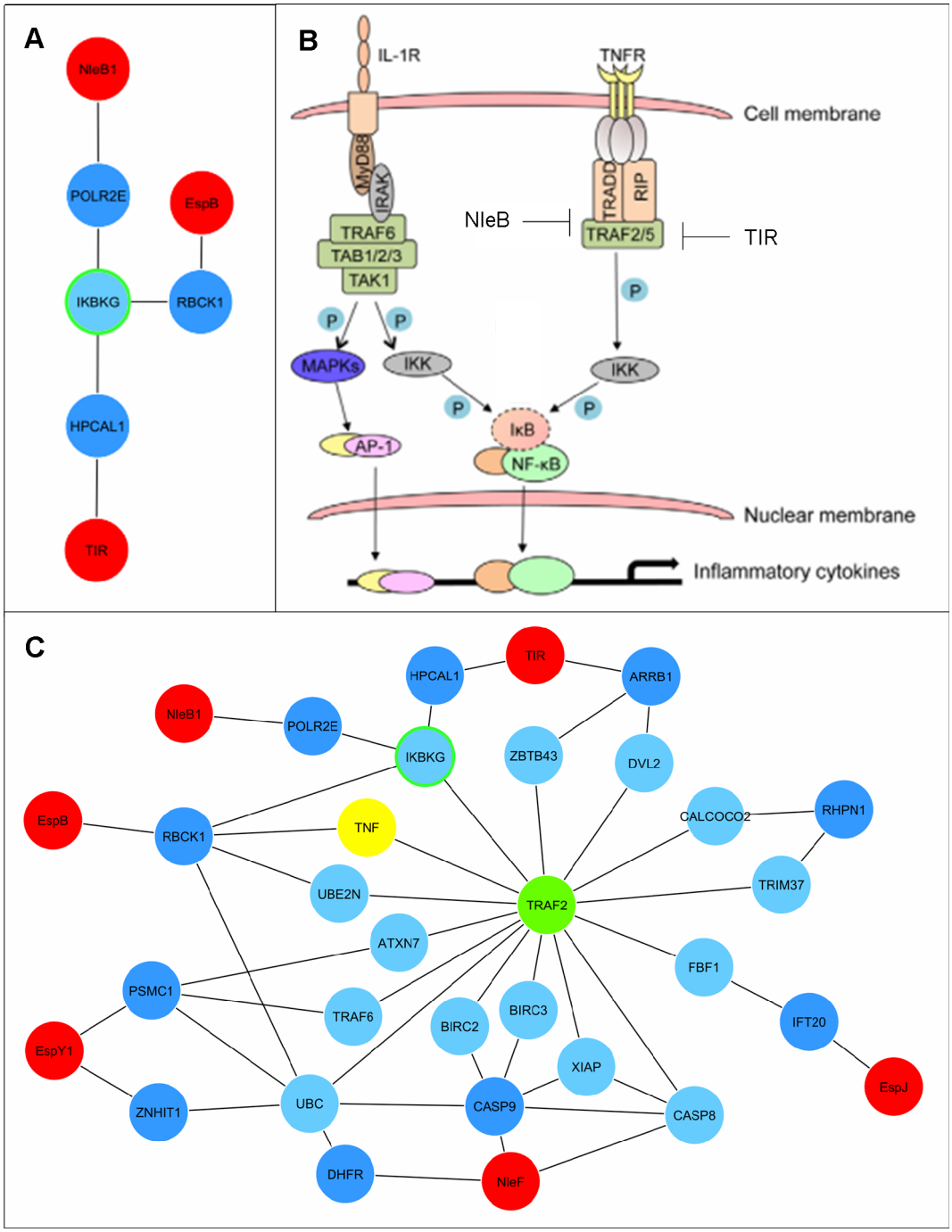

Figure 34. Indirect connections of EHEC effectors. A, EHEC TIR, EspB and NleB1 interact indirectly with IKBKG. B, NleB and TIR putatively inhibit NF-kB signalling at the level of TRAF2, figure modified after (Newton et al., 2010). C, Connections between EHEC effectors and TRAF2 (green node). EHEC effectors, direct and indirect interactors (human) are depicted in red, blue and light blue, respectively. IKBKG is framed in green and TNF is depicted in yellow.

In this study I found no direct interaction of TIR with the adaptor protein TRAF2, only an indirect connection over IKBKG, a direct interactor of TRAF2 (Tang et al., 2003). This connection links not only TIR, but also EspB and NleB1 to IKBKG and thus TRAF2. A finding

that corresponds well with the observation that NleB1 can inhibit TNFα induced NF-kB activation (Newton et al., 2010). However, NleB1 is connected to IKBKG by an interaction with POLR2E, a subunit of the human RNA polymerase II, which is an unusual adaptor protein. It remains to be shown if this connection is of relevance *in vivo*.
TIR- and NleB-dependent inhibition of NF-kB signalling and connections between EHEC effector proteins and human TRAF2 illustrated as network are depicted in figure 34 B and C, respectively.

4.1.3 TIR-host interaction patterns

The EHEC-host network includes two single hits and six high confidence human interactors for EHEC TIR, namely ARRB1, BAIAP2, BAIAP2L1, HPCAL1, HPCAL4, NCALD, PDE6D and STK16. HPCAL4 and PDE6D were found as single hits and BAIAP2 and BAIAP2L1 were published previously (Vingadassalom et al., 2009; Weiss et al., 2009). All eight inteactions could be confirmed by LUMIER assays.
Three out of the eight human interactors, namely HPCAL1, HPCAL4 and NCALD, are homologous calcium binding proteins, which may suggest the assumption that their ability to bind EHEC TIR varies depending on their calcium binding state. Nevertheless, LUMIER assays with 1 mM $CaCl_2$ instead of 10 mM EDTA revealed that TIR binding does not dependent on the availability of calcium. However, it cannot be excluded that the cellular calcium levels regulate binding through translocalization of these proteins from the cytosol to the plasma membrane, an observation previously published for bovine recoverin, a homologous protein (Zozulya and Stryer, 1992).
The eight human interactors found for EHEC TIR were systematically tested for interactions with the homologous EPEC TIR via binary yeast two-hybrid assays. This revealed that five of the eight proteins also interacted with EPEC TIR. Only ARRB1, HPCAL4 and PDE6D did not display interaction signals. However PDE6D was found as single hit in a Y2H pool screen and clearly interacted with EHEC TIR in LUMIER assay. Either it only interacts under certain circumstances or it is an indirect interactor that requires cellular factors for successful binding.
It can be concluded that, despite some differences, the interaction patterns of EHEC and EPEC TIR are similar. However, if ARRB1 and HPCAL4 do indeed only bind to EHEC TIR needs to be validated in functional assays.

4.1.4 NleF, caspase inhibition and apoptosis subversion

NleF was previously shown to be a substrate of the type III secretion system to be injected into human gut cells (Tobe et al., 2006). Within the host cell it localizes to the cytoplasm and experiments in mice and gnotobiotic piglets suggested a contribution of NleF to gut colonization (Echtenkamp et al., 2008). However, no study approaching NleF's role in the host cell has been published to date.
NleF is a 21.4 kDa protein, which is present in many different EHEC and EPEC strains in highly similar versions; often these versions reveal an amino acid identity of 100% (Bugarel et al., 2011; Echtenkamp et al., 2008). Aside from that, there are only few other proteins that reveal similarities with EHEC/EPEC NleF (Echtenkamp et al., 2008), e.g. SDY_P223, an effector protein from *Shigella dysenteriae*, which is 45 amino acids in length and reveals homologies to the EHEC NleF C-terminus
In this study I discovered that human caspases 4, 8 and 9 are direct interaction partners of EHEC NleF. NleF was shown to inhibit caspase activity *in vitro* and in HeLa cell lysate and

further to decrease TRAIL and staurosporine-mediated apoptosis induction in HeLa and Caco-2 cells. This allots NleF a role in apoptosis inhibition, a strategy frequently used by viral and bacterial pathogens to preserve their biological niche (Behar et al., 2011; Brune, 2010). Whereas in viruses apoptosis regulation is a long known phenomenon (Richard and Tulasne, 2012), the first antiapoptotic type III effector of an animal pathogen, namely SopB of *Salmonella*, was discovered in 2005 (Knodler et al., 2005). Soon after, antiapoptotic T3SS secreted effectors were identified in other pathogens, also in EHEC and EPEC. With NleF and the previously published antiapoptotic EHEC effectors NleD and NleH (Baruch et al., 2011; Hemrajani et al., 2010), there are now three known EHEC effectors that inhibit apoptosis by subversion of distinct apoptotic pathways. This suggests the assumption that the need for such countermeasures may be crucial to pathogenic *E. coli*, especially since the bundle-forming pili and some effectors expressed by EPEC and/or EHEC, e.g. EspF and Map, have been demonstrated to induce apoptosis in host cells (Abul-Milh et al., 2001; Barnett Foster et al., 2000; Nougayrede and Donnenberg, 2004; Nougayrede et al., 2007). Despite the presence of these proapoptotic factors, a decrease in normal apoptotic rates was observed upon infection of rabbits with a related REPEC O103 strain, which contains an NleF similar to that of EHEC and EPEC (93 % amino acid identity) (Heczko et al., 2001).

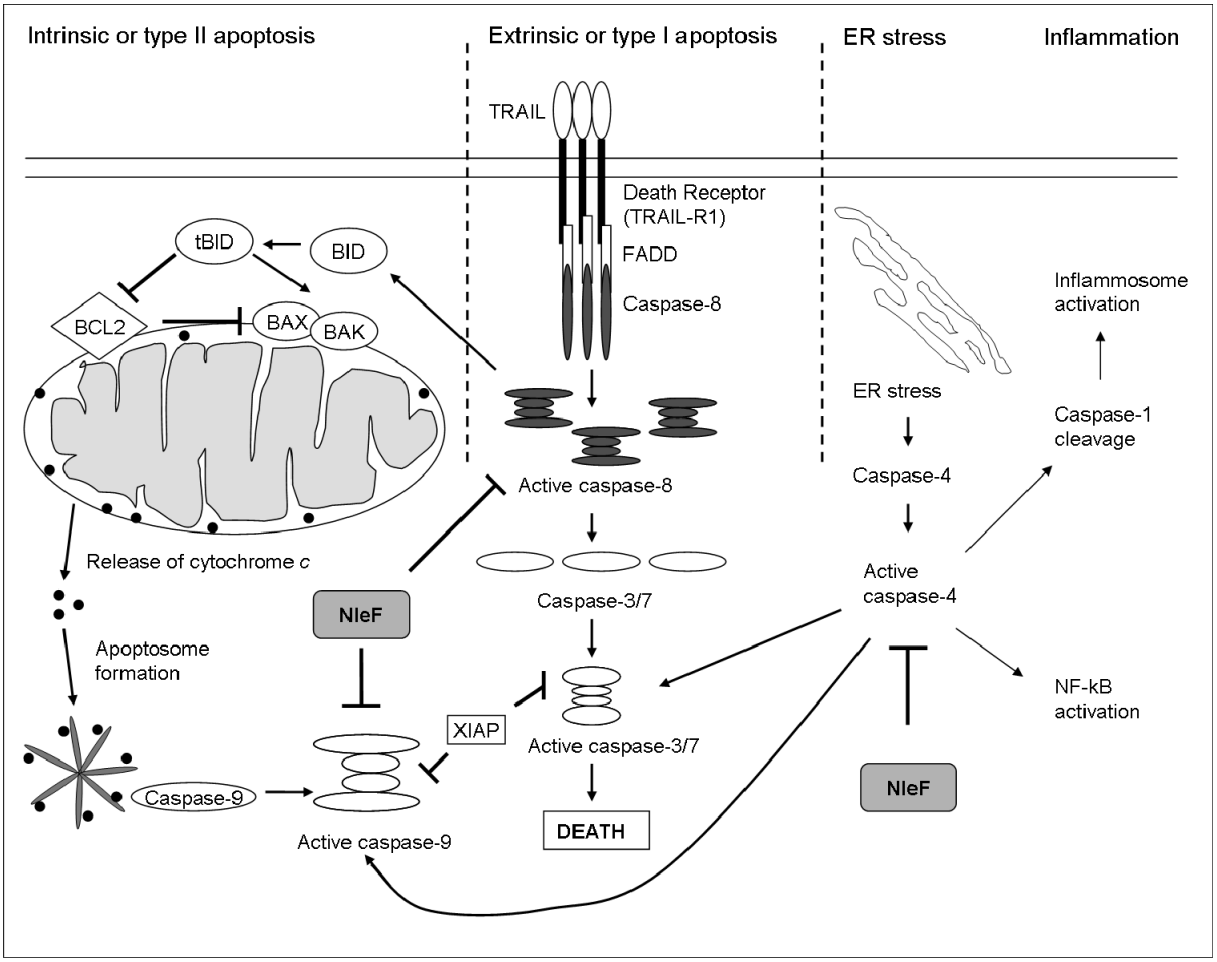

Figure 35. The EHEC effector protein NleF inhibits the caspases 4, 8 and 9. This leads to decreased apoptosis induction through subsequent impairment of the extrinsic and intrinsic (caspases 8 and 9 dependent) apoptosis pathways. The role of NleF dependent caspase-4 inhibition was not clarified. It may either contribute to this phenotype by prevention of ER stress induced apoptosis, or prevent processes involved in inflammation.

By inhibiting the two initiator caspases 8 and 9 of the extrinsic and intrinsic apoptosis pathways, respectively, NleF is likely to add to this phenotype. To what extent caspase-4 inhibition by NleF contributes to apoptosis inhibition is still unclear at present. The role of caspase-4 is controversial; it has been associated with ER stress-induced apoptosis (Hitomi et al., 2004), which was later challenged by (Obeng and Boise, 2005), but could not be disproved to date. A recent publication revealed a novel ER stress-induced apoptotic pathway in which caspase-4 directly activates caspase-9 (Yamamuro et al., 2011).
However, less controversial is an involvement of caspase-4 in inflammation via inflammasome activation and NF-kB regulation (Martinon and Tschopp, 2007; Nickles et al., 2012; Sollberger et al., 2012). Whether NleF is able to inhibit NF-kB activation or prevent caspase-4 dependent caspase-1 activation was not tested in the frame of this study. The suggested role of NleF in apoptosis regulation is schematized in figure 35.

4.1.4.1 NleF binding site and efficiency

A collaboration with Proteros (Martinsried, Germany), led to the co-crystallization of the NleF/CASP9 complex. The structure revealed that in addition to some other contact points between the two proteins, the carboxy-terminal four amino acids Gly189, Cys188, Gln187 and Leu186 of NleF occupy the caspase-9 S1, S2, S3 and S4 pockets, respectively. When the findings of the structure are compared to the results I obtained for the NleF versions with mutagenized carboxy-termini, it can be concluded that the very same amino acids are not only responsible for caspase binding, but also for apoptosis inhibition in host cells. Deletion of the NleF carboxy-terminal 4 amino acids abolishes both, its ability to bind caspase-9 and its ability to prevent apoptosis induction. A similar result was obtained for an NleF version with an extra carboxy-terminal alanine. The results for the NleF substitution mutants were not so clear: Alanine substitutions of Leu186, Gln187, Cys188 and Gly189 tend to show impairment in caspase-9 binding and apoptosis inhibition. However, while caspase-9 binding varies between ‘similar to wild type’ (Cys188Ala) and ‘almost no caspase-9 binding detectable’ (Gln187Ala), the apoptosis inhibition is highly similar between the four substitution mutants. It lies at 10 % apoptotic cells 6 h after apoptosis induction (wild type NleF: ~3-4 %, negative control protein A is over 60 %). Possibly the interactions of the NleF substitutions with caspases are less stable than those of wild type NleF and thus give weaker signals in co-precipitation assays such as LUMIER. This may only have a minor effect on their ability to inhibit apoptosis. A picture of the NleF/CASP9 structure is shown in figure 36.

Regarding both, the results of the NleF versions with altered carboxy-termini and the caspase-9/NleF crystal structure, it can be said that NleF binds and blocks the active center of caspase-9 and probably also of caspase-4 and -8 with its carboxy-terminal four amino acids. However, the efficiency with which NleF inhibits caspase-9 is higher than expected:
According to the NleF/caspase-9 structure, a 1:1 mode of caspase-9 inhibition by NleF has to be expected, since one NleF carboxy-terminus blocks one catalytic site. Nevertheless, the IC_{50} values obtained for NleF-dependent caspase-9 and also caspase-4 inhibition are much lower than expected. The lower limit for an IC_{50} is 1/2 the enzyme concentration (Copeland, 2002), the IC_{50} of NleF in caspase-4 and -9 inhibition are less than 1/10. Thus NleF must be able to inhibit more than one caspase-9 (and -4) catalytic site. Since NleF has no catalytic activity which could contribute to caspase inactivation (data not shown), it either inhibits whole caspase multimers or it decreases caspase activity by reducing the caspase dimers in solution and thus caspase activity.

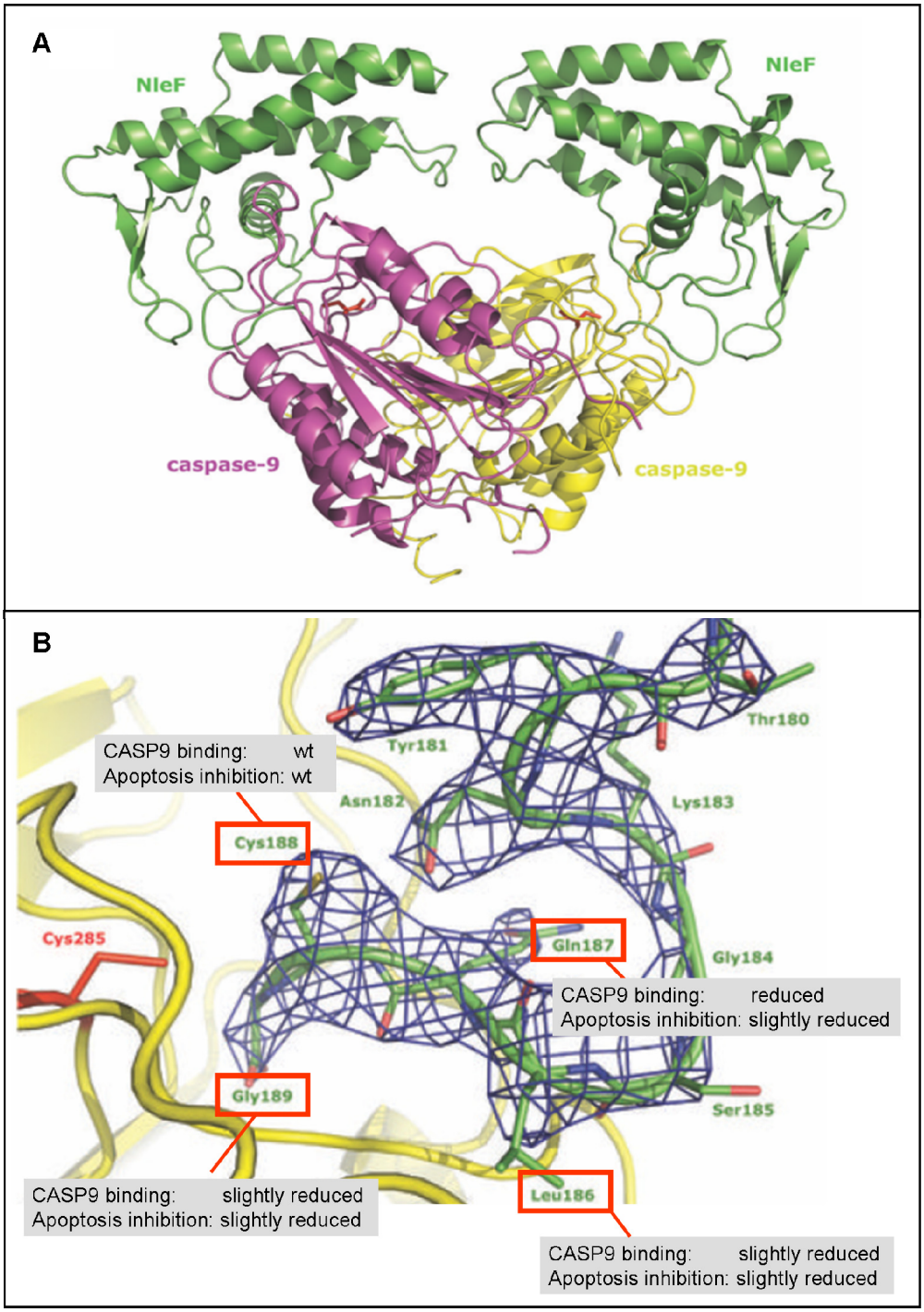

Figure 36. Crystal structure of the caspase-9/NleF complex (Holger Steuber, Proteros). Illustration A depicts the caspase-9/NleF complex consisting of two caspase-9 protease monomers (magenta and yellow) and two NleF effector proteins attached to them (green). The caspase-9 active site cysteins are represented by red sticks. B shows the four NleF C-terminal amino acids Gly189, Cys188, Gln187 and Leu186 in the caspase-9 S1-4 pockets. The grey boxes state the effect on caspase-9 binding and apoptosis inhibition when these residues are substituted by alanine.

4.1.4.2 Role of NleF and occurrence in bacteria

Many EPEC and EHEC strains harbouring a type III secretion system and effector proteins possess a highly similar or identical NleF (Echtenkamp et al., 2008). In other bacteria, the occurrence of proteins homologous to NleF is a rarity. The few exceptions include *Providencia rustigianii*, *Yersinia pseudotuberculosis*, *Shigella dysenteriae* and *S. boydii*. All

are pathogens with a type III secretion system. The NleFs of these bacteria differ significantly from those of EPEC and EHEC. Interestingly the ones from *Shigella* are truncated and contain only the carboxy-terminal 45 amino acids (see figure 37 for an alignment).

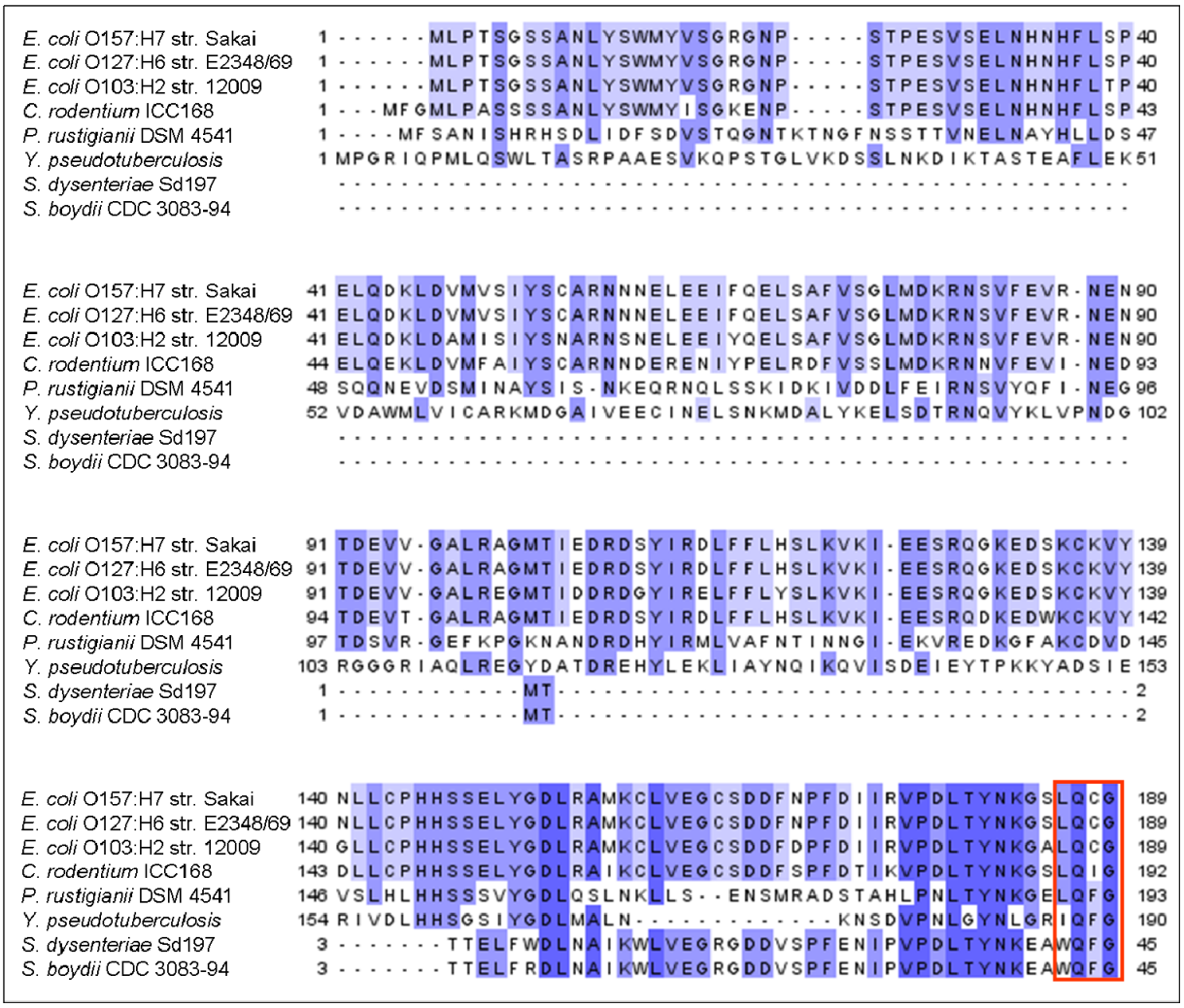

Figure 37. Alignment showing the NleF homologues of different bacteria. The amino acids are colored after conservation. The carboxy-terminal four amino acids involed in caspase binding are framed in red.

Whether these NleF homologues are functional in apoptosis inhibition or caspase-binding was not tested in this study. It is reasonable to expect that at least the NleF versions with similar carboxy-termini are functional. The NleF substitution mutants revealed that a Cys188Ala substitution had only minor effects on caspase-9 binding and apoptosis inhibition, which is in conformance with the rather low degree of conservation found for Cys188 in the NleF homologues of other bacteria. The Gln187 and Gly189 residues are highly conserved in all NleF versions depicted in figure 37 and are involved in NleF functionality.

Another possibility may be that NleF fulfills functions other than apoptosis inhibition in these bacteria. An option supported by the fact that NleF also interacts with human dihydrofolate reductase (DHFR). However, the biological function of this interaction was not examined in this study.

4.2 The phage lambda-host interactome

In the frame of this study, the first systematic interactome between phage lambda and its host *E. coli* was generated. The 631 interactions first discovered in the yeast two-hybrid screens were reduced to 144 interactions after quality filtering. The 144 final pathogen-host intercations include two previously published ones and a number of phage proteins binding to *E. coli* proteins of prophage origin. Many of these interactions are homologous to phage lambda intraspecies interactions (Rajagopala et al., 2011).

4.3 Outlook

The generation of interactomes usually involves the production of large datasets. As a consequence, detailed analysis can only be realised for a small number of interactions. The role of interactomes can be seen as a data-rich resource, which provides the foundation for further research. The EHEC-host network definitely contains, aside from NleF/caspase-9, many more interesting interactions worth to follow up experimentally in future studies.
It is planned to use the phage lambda-*E. coli* dataset for the identification of pathways that play essential roles in phage infection. In addition the comparison of the lambda-host interaction network to other phage-host interactomes may reveal distinct interaction patterns among different phages, e.g. between temperate and lythic phages. Such comparisons of whole interactomes are facilitated by the permanently increasing amount of phage-host interaction data available in the literature (Hauser et al., 2012).

5 References

Abu-Zant, A., Santic, M., Molmeret, M., Jones, S., Helbig, J. and Abu Kwaik, Y. (2005). Incomplete activation of macrophage apoptosis during intracellular replication of Legionella pneumophila. *Infect Immun* **73**, 5339-49.

Abul-Milh, M., Wu, Y., Lau, B., Lingwood, C. A. and Barnett Foster, D. (2001). Induction of epithelial cell death including apoptosis by enteropathogenic *Escherichia coli* expressing bundle-forming pili. *Infect Immun* **69**, 7356-64.

Albers, M., Kranz, H., Kober, I., Kaiser, C., Klink, M., Suckow, J., Kern, R. and Koegl, M. (2005). Automated yeast two-hybrid screening for nuclear receptor-interacting proteins. *Mol Cell Proteomics* **4**, 205-13.

Alnemri, E. S., Livingston, D. J., Nicholson, D. W., Salvesen, G., Thornberry, N. A., Wong, W. W. and Yuan, J. (1996). Human ICE/CED-3 protease nomenclature. *Cell* **87**, 171.

Altieri, D. C. (2010). Survivin and IAP proteins in cell-death mechanisms. *Biochem J* **430**, 199-205.

Alto, N. M., Shao, F., Lazar, C. S., Brost, R. L., Chua, G., Mattoo, S., McMahon, S. A., Ghosh, P., Hughes, T. R., Boone, C. et al. (2006). Identification of a bacterial type III effector family with G protein mimicry functions. *Cell* **124**, 133-45.

Ang, D., Keppel, F., Klein, G., Richardson, A. and Georgopoulos, C. (2000). Genetic analysis of bacteriophage-encoded cochaperonins. *Annu Rev Genet* **34**, 439-456.

Arbeloa, A., Garnett, J., Lillington, J., Bulgin, R. R., Berger, C. N., Lea, S. M., Matthews, S. and Frankel, G. (2010). EspM2 is a RhoA guanine nucleotide exchange factor. *Cell Microbiol* **12**, 654-64.

Ashida, H., Mimuro, H., Ogawa, M., Kobayashi, T., Sanada, T., Kim, M. and Sasakawa, C. (2011). Cell death and infection: a double-edged sword for host and pathogen survival. *J Cell Biol* **195**, 931-42.

Baaske, P., Wienken, C. J., Reineck, P., Duhr, S. and Braun, D. (2010). Optical thermophoresis for quantifying the buffer dependence of aptamer binding. *Angew Chem Int Ed Engl* **49**, 2238-41.

Ball, C. A. and Johnson, R. C. (1991). Efficient excision of phage lambda from the *Escherichia coli* chromosome requires the Fis protein. *J Bacteriol* **173**, 4027-31.

Bannerman, D. D. and Goldblum, S. E. (2003). Mechanisms of bacterial lipopolysaccharide-induced endothelial apoptosis. *Am J Physiol Lung Cell Mol Physiol* **284**, L899-914.

Barnett Foster, D., Abul-Milh, M., Huesca, M. and Lingwood, C. A. (2000). Enterohemorrhagic *Escherichia coli* induces apoptosis which augments bacterial binding and phosphatidylethanolamine exposure on the plasma membrane outer leaflet. *Infect Immun* **68**, 3108-15.

Barrios-Rodiles, M., Brown, K. R., Ozdamar, B., Bose, R., Liu, Z., Donovan, R. S., Shinjo, F., Liu, Y., Dembowy, J., Taylor, I. W. et al. (2005). High-throughput mapping of a dynamic signaling network in mammalian cells. *Science* **307**, 1621-5.

Baruch, K., Gur-Arie, L., Nadler, C., Koby, S., Yerushalmi, G., Ben-Neriah, Y., Yogev, O., Shaulian, E., Guttman, C., Zarivach, R. et al. (2011). Metalloprotease type III effectors that specifically cleave JNK and NF-kappaB. *EMBO J* **30**, 221-31.

Behar, S. M., Martin, C. J., Booty, M. G., Nishimura, T., Zhao, X., Gan, H. X., Divangahi, M. and Remold, H. G. (2011). Apoptosis is an innate defense function of macrophages against Mycobacterium tuberculosis. *Mucosal Immunol* **4**, 279-87.

Berger, C. N., Sodha, S. V., Shaw, R. K., Griffin, P. M., Pink, D., Hand, P. and Frankel, G. (2010). Fresh fruit and vegetables as vehicles for the transmission of human pathogens. *Environ Microbiol* **12**, 2385-97.

Bernard, P. and Couturier, M. (1992). Cell killing by the F plasmid CcdB protein involves poisoning of DNA-topoisomerase II complexes. *J Mol Biol* **226**, 735-45.

BfR, F. I. f. R. A. (2012). Protection from EHEC: careful handling of raw milk, raw meat and sprouts necessary. *Leaflet: Protection against Infections with Enterohaemorrhagic E. coli (EHEC)* **20/2012**.

Bjorgo, E., Moltu, K. and Tasken, K. (2011). Phosphodiesterases as targets for modulating T-cell responses. *Handb Exp Pharmacol*, 345-63.
Blocker, A., Komoriya, K. and Aizawa, S. (2003). Type III secretion systems and bacterial flagella: insights into their function from structural similarities. *Proc Natl Acad Sci U S A* **100**, 3027-30.
Bommarius, B., Maxwell, D., Swimm, A., Leung, S., Corbett, A., Bornmann, W. and Kalman, D. (2007). Enteropathogenic *Escherichia coli* Tir is an SH2/3 ligand that recruits and activates tyrosine kinases required for pedestal formation. *Mol Microbiol* **63**, 1748-68.
Boyden, E. D. and Dietrich, W. F. (2006). Nalp1b controls mouse macrophage susceptibility to anthrax lethal toxin. *Nat Genet* **38**, 240-4.
Brasch, M. A., Hartley, J. L. and Vidal, M. (2004). ORFeome cloning and systems biology: standardized mass production of the parts from the parts-list. *Genome Res* **14**, 2001-9.
Braun, P., Tasan, M., Dreze, M., Barrios-Rodiles, M., Lemmens, I., Yu, H., Sahalie, J. M., Murray, R. R., Roncari, L., de Smet, A. S. et al. (2009). An experimentally derived confidence score for binary protein-protein interactions. *Nat Methods* **6**, 91-7.
Brune, W. (2010). Inhibition of programmed cell death by cytomegaloviruses. *Virus Res* **157**, 144-50.
Brussow, H., Canchaya, C. and Hardt, W. D. (2004). Phages and the evolution of bacterial pathogens: from genomic rearrangements to lysogenic conversion. *Microbiol Mol Biol Rev* **68**, 560-602.
Buchwald, M. and Siminovitch, L. (1969). Production of serum-blocking material by mutants of the left arm of the lambda chromosome. *Virology* **38**, 1-7.
Bugarel, M., Martin, A., Fach, P. and Beutin, L. (2011). Virulence gene profiling of enterohemorrhagic (EHEC) and enteropathogenic (EPEC) *Escherichia coli* strains: a basis for molecular risk assessment of typical and atypical EPEC strains. *BMC Microbiol* **11**, 142.
Burckstummer, T., Baumann, C., Bluml, S., Dixit, E., Durnberger, G., Jahn, H., Planyavsky, M., Bilban, M., Colinge, J., Bennett, K. L. et al. (2009). An orthogonal proteomic-genomic screen identifies AIM2 as a cytoplasmic DNA sensor for the inflammasome. *Nat Immunol* **10**, 266-72.
Cain, K., Bratton, S. B. and Cohen, G. M. (2002). The Apaf-1 apoptosome: a large caspase-activating complex. *Biochimie* **84**, 203-14.
Campbell, A., del-Campillo-Campbell, A. and Ginsberg, M. L. (2002). Specificity in DNA recognition by phage integrases. *Gene* **300**, 13-8.
Campellone, K. G. (2010). Cytoskeleton-modulating effectors of enteropathogenic and enterohaemorrhagic *Escherichia coli*: Tir, EspFU and actin pedestal assembly. *FEBS J* **277**, 2390-402.
Campellone, K. G., Giese, A., Tipper, D. J. and Leong, J. M. (2002). A tyrosine-phosphorylated 12-amino-acid sequence of enteropathogenic *Escherichia coli* Tir binds the host adaptor protein Nck and is required for Nck localization to actin pedestals. *Mol Microbiol* **43**, 1227-41.
Campellone, K. G., Rankin, S., Pawson, T., Kirschner, M. W., Tipper, D. J. and Leong, J. M. (2004). Clustering of Nck by a 12-residue Tir phosphopeptide is sufficient to trigger localized actin assembly. *J Cell Biol* **164**, 407-16.
Charbit, A. (2003). Maltodextrin transport through lamb. *Front Biosci* **8**, s265-74.
Chen, Y. C., Rajagopala, S. V., Stellberger, T. and Uetz, P. (2010). Exhaustive benchmarking of the yeast two-hybrid system. *Nat Methods* **7**, 667-8; author reply 668.
Cho, E. H., Gumport, R. I. and Gardner, J. F. (2002). Interactions between integrase and excisionase in the phage lambda excisive nucleoprotein complex. *J Bacteriol* **184**, 5200-3.
Choi, K. S., Park, J. T. and Dumler, J. S. (2005). Anaplasma phagocytophilum delay of neutrophil apoptosis through the p38 mitogen-activated protein kinase signal pathway. *Infect Immun* **73**, 8209-18.
Clement, J. M., Lepouce, E., Marchal, C. and Hofnung, M. (1983). Genetic study of a membrane protein: DNA sequence alterations due to 17 lamB point mutations affecting adsorption of phage lambda. *EMBO J* **2**, 77-80.

Conant, C. R., Van Gilst, M. R., Weitzel, S. E., Rees, W. A. and von Hippel, P. H. (2005). A quantitative description of the binding states and in vitro function of antitermination protein N of bacteriophage lambda. *J Mol Biol* **348**, 1039-57.
Copeland, R. A. (2002). Enzymes: A Practical Introduction to Structure, Mechanism, and Data Analysis, Second Edition, (ed.: Wiley-Blackwell.
Cornelis, G. R. (2006). The type III secretion injectisome. *Nat Rev Microbiol* **4**, 811-25.
Court, D. L., Oppenheim, A. B. and Adhya, S. L. (2007). A new look at bacteriophage lambda genetic networks. *J Bacteriol* **189**, 298-304.
Crisona, N. J., Weinberg, R. L., Peter, B. J., Sumners, D. W. and Cozzarelli, N. R. (1999). The topological mechanism of phage lambda integrase. *J Mol Biol* **289**, 747-75.
Das, A. (1992). How the phage lambda N gene product suppresses transcription termination: communication of RNA polymerase with regulatory proteins mediated by signals in nascent RNA. *J Bacteriol* **174**, 6711-6.
Datta, A. B., Roy, S. and Parrack, P. (2005a). Role of C-terminal residues in oligomerization and stability of lambda CII: implications for lysis-lysogeny decision of the phage. *J Mol Biol* **345**, 315-24.
Datta, I., Banik-Maiti, S., Adhikari, L., Sau, S., Das, N. and Mandal, N. C. (2005b). The mutation that makes *Escherichia coli* resistant to lambda P gene-mediated host lethality is located within the DNA initiator Gene dnaA of the bacterium. *J Biochem Mol Biol* **38**, 89-96.
Datta, I., Sau, S., Sil, A. K. and Mandal, N. C. (2005c). The bacteriophage lambda DNA replication protein P inhibits the oriC DNA- and ATP-binding functions of the DNA replication initiator protein DnaA of *Escherichia coli*. *J Biochem Mol Biol* **38**, 97-103.
Datz, M., Janetzki-Mittmann, C., Franke, S., Gunzer, F., Schmidt, H. and Karch, H. (1996). Analysis of the enterohemorrhagic *Escherichia coli* O157 DNA region containing lambdoid phage gene p and Shiga-like toxin structural genes. *Appl Environ Microbiol* **62**, 791-7.
Dean, P. and Kenny, B. (2004). Intestinal barrier dysfunction by enteropathogenic *Escherichia coli* is mediated by two effector molecules and a bacterial surface protein. *Mol Microbiol* **54**, 665-75.
Dean, P., Maresca, M., Schuller, S., Phillips, A. D. and Kenny, B. (2006). Potent diarrheagenic mechanism mediated by the cooperative action of three enteropathogenic *Escherichia coli*-injected effector proteins. *Proc Natl Acad Sci U S A* **103**, 1876-81.
Deane, C. M., Salwinski, L., Xenarios, I. and Eisenberg, D. (2002). Protein interactions: two methods for assessment of the reliability of high throughput observations. *Mol Cell Proteomics* **1**, 349-56.
Deighan, P., Diez, C. M., Leibman, M., Hochschild, A. and Nickels, B. E. (2008). The bacteriophage lambda Q antiterminator protein contacts the beta-flap domain of RNA polymerase. *Proc Natl Acad Sci U S A* **105**, 15305-10.
Deveraux, Q. L. and Reed, J. C. (1999). IAP family proteins--suppressors of apoptosis. *Genes Dev* **13**, 239-52.
Dodson, M., Echols, H., Wickner, S., Alfano, C., Mensa-Wilmot, K., Gomes, B., LeBowitz, J., Roberts, J. D. and McMacken, R. (1986). Specialized nucleoprotein structures at the origin of replication of bacteriophage lambda: localized unwinding of duplex DNA by a six-protein reaction. *Proc Natl Acad Sci U S A* **83**, 7638-42.
Dong, F., Pirbhai, M., Xiao, Y., Zhong, Y., Wu, Y. and Zhong, G. (2005). Degradation of the proapoptotic proteins Bik, Puma, and Bim with Bcl-2 domain 3 homology in Chlamydia trachomatis-infected cells. *Infect Immun* **73**, 1861-4.
Echols, H. (1986). Multiple DNA-protein interactions governing high-precision DNA transactions. *Science* **233**, 1050-6.
Echtenkamp, F., Deng, W., Wickham, M. E., Vazquez, A., Puente, J. L., Thanabalasuriar, A., Gruenheid, S., Finlay, B. B. and Hardwidge, P. R. (2008). Characterization of the NleF effector protein from attaching and effacing bacterial pathogens. *FEMS Microbiol Lett* **281**, 98-107.
Elliott, M. R. and Ravichandran, K. S. (2010). Clearance of apoptotic cells: implications in health and disease. *J Cell Biol* **189**, 1059-70.

Elliott, S. J., Sperandio, V., Giron, J. A., Shin, S., Mellies, J. L., Wainwright, L., Hutcheson, S. W., McDaniel, T. K. and Kaper, J. B. (2000). The locus of enterocyte effacement (LEE)-encoded regulator controls expression of both LEE- and non-LEE-encoded virulence factors in enteropathogenic and enterohemorrhagic *Escherichia coli*. *Infect Immun* **68**, 6115-26.

Erhardt, M., Namba, K. and Hughes, K. T. (2010). Bacterial nanomachines: the flagellum and type III injectisome. *Cold Spring Harb Perspect Biol* **2**, a000299.

Erni, B., Zanolari, B. and Kocher, H. P. (1987). The mannose permease of *Escherichia coli* consists of three different proteins. Amino acid sequence and function in sugar transport, sugar phosphorylation, and penetration of phage lambda DNA. *J Biol Chem* **262**, 5238-47.

Esposito, D. and Gerard, G. F. (2003). The *Escherichia coli* Fis protein stimulates bacteriophage lambda integrative recombination in vitro. *J Bacteriol* **185**, 3076-80.

Faherty, C. S. and Maurelli, A. T. (2008). Staying alive: bacterial inhibition of apoptosis during infection. *Trends Microbiol* **16**, 173-80.

Fernandes-Alnemri, T., Yu, J. W., Datta, P., Wu, J. and Alnemri, E. S. (2009). AIM2 activates the inflammasome and cell death in response to cytoplasmic DNA. *Nature* **458**, 509-13.

Fernandes-Alnemri, T., Yu, J. W., Juliana, C., Solorzano, L., Kang, S., Wu, J., Datta, P., McCormick, M., Huang, L., McDermott, E. et al. (2010). The AIM2 inflammasome is critical for innate immunity to Francisella tularensis. *Nat Immunol* **11**, 385-93.

Fields, S. and Song, O. (1989). A novel genetic system to detect protein-protein interactions. *Nature* **340**, 245-6.

Fischer, S. F., Vier, J., Kirschnek, S., Klos, A., Hess, S., Ying, S. and Hacker, G. (2004). Chlamydia inhibit host cell apoptosis by degradation of proapoptotic BH3-only proteins. *J Exp Med* **200**, 905-16.

Fischer, U., Janicke, R. U. and Schulze-Osthoff, K. (2003). Many cuts to ruin: a comprehensive update of caspase substrates. *Cell Death Differ* **10**, 76-100.

Franchi, L., Amer, A., Body-Malapel, M., Kanneganti, T. D., Ozoren, N., Jagirdar, R., Inohara, N., Vandenabeele, P., Bertin, J., Coyle, A. et al. (2006). Cytosolic flagellin requires Ipaf for activation of caspase-1 and interleukin 1beta in salmonella-infected macrophages. *Nat Immunol* **7**, 576-82.

Frankel, G., Phillips, A. D., Rosenshine, I., Dougan, G., Kaper, J. B. and Knutton, S. (1998). Enteropathogenic and enterohaemorrhagic *Escherichia coli*: more subversive elements. *Mol Microbiol* **30**, 911-21.

Friedman, D. I. and Court, D. L. (2001). Bacteriophage lambda: alive and well and still doing its thing. *Curr Opin Microbiol* **4**, 201-7.

Galan, J. E. and Wolf-Watz, H. (2006). Protein delivery into eukaryotic cells by type III secretion machines. *Nature* **444**, 567-73.

Gamage, S. D., Strasser, J. E., Chalk, C. L. and Weiss, A. A. (2003). Nonpathogenic *Escherichia coli* can contribute to the production of Shiga toxin. *Infect Immun* **71**, 3107-15.

Georgopoulos, C. P., Hendrix, R. W., Casjens, S. R. and Kaiser, A. D. (1973). Host participation in bacteriophage lambda head assembly. *J Mol Biol* **76**, 45-60.

Ghosh, P. (2004). Process of protein transport by the type III secretion system. *Microbiol Mol Biol Rev* **68**, 771-95.

Gottesman, M. E. and Weisberg, R. A. (2004). Little lambda, who made thee? *Microbiol Mol Biol Rev* **68**, 796-813.

Gottesman, S., Gottesman, M., Shaw, J. E. and Pearson, M. L. (1981). Protein degradation in *E. coli*: the lon mutation and bacteriophage lambda N and cII protein stability. *Cell* **24**, 225-33.

Grassme, H., Jendrossek, V. and Gulbins, E. (2001). Molecular mechanisms of bacteria induced apoptosis. *Apoptosis* **6**, 441-5.

Gruenheid, S., DeVinney, R., Bladt, F., Goosney, D., Gelkop, S., Gish, G. D., Pawson, T. and Finlay, B. B. (2001). Enteropathogenic *E. coli* Tir binds Nck to initiate actin pedestal formation in host cells. *Nat Cell Biol* **3**, 856-9.

Hamaguchi, M., Hamada, D., Suzuki, K. N., Sakata, I. and Yanagihara, I. (2008). Molecular basis of actin reorganization promoted by binding of enterohaemorrhagic *Escherichia coli* EspB to alpha-catenin. *FEBS J* **275**, 6260-7.
Hartland, E. L., Batchelor, M., Delahay, R. M., Hale, C., Matthews, S., Dougan, G., Knutton, S., Connerton, I. and Frankel, G. (1999). Binding of intimin from enteropathogenic *Escherichia coli* to Tir and to host cells. *Mol Microbiol* **32**, 151-8.
Hartland, E. L., Daniell, S. J., Delahay, R. M., Neves, B. C., Wallis, T., Shaw, R. K., Hale, C., Knutton, S. and Frankel, G. (2000). The type III protein translocation system of enteropathogenic *Escherichia coli* involves EspA-EspB protein interactions. *Mol Microbiol* **35**, 1483-92.
Hartley, J. L., Temple, G. F. and Brasch, M. A. (2000). DNA cloning using in vitro site-specific recombination. *Genome Res* **10**, 1788-95.
Hauser, R., Blasche, S., Dokland, T., Haggard-Ljungquist, E., von Brunn, A., Salas, M., Casjens, S., Molineux, I. and Uetz, P. (2012). Bacteriophage protein-protein interactions. *Adv Virus Res* **83**, 219-98.
Hauser, R., Sabri, M., Moineau, S. and Uetz, P. (2011). The proteome and interactome of Streptococcus pneumoniae phage Cp-1. *J Bacteriol* **193**, 3135-8.
Hay, S. and Kannourakis, G. (2002). A time to kill: viral manipulation of the cell death program. *J Gen Virol* **83**, 1547-64.
Heczko, U., Carthy, C. M., O'Brien, B. A. and Finlay, B. B. (2001). Decreased apoptosis in the ileum and ileal Peyer's patches: a feature after infection with rabbit enteropathogenic *Escherichia coli* O103. *Infect Immun* **69**, 4580-9.
Hemrajani, C., Berger, C. N., Robinson, K. S., Marches, O., Mousnier, A. and Frankel, G. (2010). NleH effectors interact with Bax inhibitor-1 to block apoptosis during enteropathogenic *Escherichia coli* infection. *Proc Natl Acad Sci U S A* **107**, 3129-34.
Hendrix, R. W. and Duda, R. L. (1992). Bacteriophage lambda PaPa: not the mother of all lambda phages. *Science* **258**, 1145-8.
Hendrix, R. W., Smith, M. C., Burns, R. N., Ford, M. E. and Hatfull, G. F. (1999). Evolutionary relationships among diverse bacteriophages and prophages: all the world's a phage. *Proc Natl Acad Sci U S A* **96**, 2192-7.
Herman, C., Thevenet, D., D'Ari, R. and Bouloc, P. (1997). The HflB protease of *Escherichia coli* degrades its inhibitor lambda cIII. *J Bacteriol* **179**, 358-63.
Herold, S., Siebert, J., Huber, A. and Schmidt, H. (2005). Global expression of prophage genes in *Escherichia coli* O157:H7 strain EDL933 in response to norfloxacin. *Antimicrob Agents Chemother* **49**, 931-44.
Hitomi, J., Katayama, T., Eguchi, Y., Kudo, T., Taniguchi, M., Koyama, Y., Manabe, T., Yamagishi, S., Bando, Y., Imaizumi, K. et al. (2004). Involvement of caspase-4 in endoplasmic reticulum stress-induced apoptosis and Abeta-induced cell death. *J Cell Biol* **165**, 347-56.
Hornung, V., Ablasser, A., Charrel-Dennis, M., Bauernfeind, F., Horvath, G., Caffrey, D. R., Latz, E. and Fitzgerald, K. A. (2009). AIM2 recognizes cytosolic dsDNA and forms a caspase-1-activating inflammasome with ASC. *Nature* **458**, 514-8.
Hu, C. D., Chinenov, Y. and Kerppola, T. K. (2002). Visualization of interactions among bZIP and Rel family proteins in living cells using bimolecular fluorescence complementation. *Mol Cell* **9**, 789-98.
Huang, Z., Sutton, S. E., Wallenfang, A. J., Orchard, R. C., Wu, X., Feng, Y., Chai, J. and Alto, N. M. (2009). Structural insights into host GTPase isoform selection by a family of bacterial GEF mimics. *Nat Struct Mol Biol* **16**, 853-60.
Huber, F. and Erni, B. (1996). Membrane topology of the mannose transporter of *Escherichia coli* K12. *Eur J Biochem* **239**, 810-7.
Hurt, J. A., Thibodeau, S. A., Hirsh, A. S., Pabo, C. O. and Joung, J. K. (2003). Highly specific zinc finger proteins obtained by directed domain shuffling and cell-based selection. *Proc Natl Acad Sci U S A* **100**, 12271-6.
Ide, T., Laarmann, S., Greune, L., Schillers, H., Oberleithner, H. and Schmidt, M. A. (2001). Characterization of translocation pores inserted into plasma membranes by type III-secreted Esp proteins of enteropathogenic *Escherichia coli*. *Cell Microbiol* **3**, 669-79.

Johnstone, R. W., Frew, A. J. and Smyth, M. J. (2008). The TRAIL apoptotic pathway in cancer onset, progression and therapy. *Nat Rev Cancer* **8**, 782-98.
Jones, J. W., Kayagaki, N., Broz, P., Henry, T., Newton, K., O'Rourke, K., Chan, S., Dong, J., Qu, Y., Roose-Girma, M. et al. (2010). Absent in melanoma 2 is required for innate immune recognition of Francisella tularensis. *Proc Natl Acad Sci U S A* **107**, 9771-6.
Jost, P. J., Grabow, S., Gray, D., McKenzie, M. D., Nachbur, U., Huang, D. C., Bouillet, P., Thomas, H. E., Borner, C., Silke, J. et al. (2009). XIAP discriminates between type I and type II FAS-induced apoptosis. *Nature* **460**, 1035-9.
Joung, J. K., Ramm, E. I. and Pabo, C. O. (2000). A bacterial two-hybrid selection system for studying protein-DNA and protein-protein interactions. *Proc Natl Acad Sci U S A* **97**, 7382-7.
Kanneganti, T. D., Body-Malapel, M., Amer, A., Park, J. H., Whitfield, J., Franchi, L., Taraporewala, Z. F., Miller, D., Patton, J. T., Inohara, N. et al. (2006). Critical role for Cryopyrin/Nalp3 in activation of caspase-1 in response to viral infection and double-stranded RNA. *J Biol Chem* **281**, 36560-8.
Kanneganti, T. D., Lamkanfi, M. and Nunez, G. (2007). Intracellular NOD-like receptors in host defense and disease. *Immunity* **27**, 549-59.
Kantari, C. and Walczak, H. (2011). Caspase-8 and bid: caught in the act between death receptors and mitochondria. *Biochim Biophys Acta* **1813**, 558-63.
Kaper, J. B., Nataro, J. P. and Mobley, H. L. (2004). Pathogenic *Escherichia coli*. *Nat Rev Microbiol* **2**, 123-40.
Kawai, T. and Akira, S. (2006). TLR signaling. *Cell Death Differ* **13**, 816-25.
Kedzierska, B., Lee, D. J., Wegrzyn, G., Busby, S. J. and Thomas, M. S. (2004). Role of the RNA polymerase alpha subunits in CII-dependent activation of the bacteriophage lambda pE promoter: identification of important residues and positioning of the alpha C-terminal domains. *Nucleic Acids Res* **32**, 834-41.
Kedzierska, B., Szambowska, A., Herman-Antosiewicz, A., Lee, D. J., Busby, S. J., Wegrzyn, G. and Thomas, M. S. (2007). The C-terminal domain of the *Escherichia coli* RNA polymerase alpha subunit plays a role in the CI-dependent activation of the bacteriophage lambda pM promoter. *Nucleic Acids Res* **35**, 2311-20.
Kenny, B. (1999). Phosphorylation of tyrosine 474 of the enteropathogenic *Escherichia coli* (EPEC) Tir receptor molecule is essential for actin nucleating activity and is preceded by additional host modifications. *Mol Microbiol* **31**, 1229-41.
Kenny, B. (2001). The enterohaemorrhagic *Escherichia coli* (serotype O157:H7) Tir molecule is not functionally interchangeable for its enteropathogenic *E. coli* (serotype O127:H6) homologue. *Cell Microbiol* **3**, 499-510.
Kenny, B. and Jepson, M. (2000). Targeting of an enteropathogenic *Escherichia coli* (EPEC) effector protein to host mitochondria. *Cell Microbiol* **2**, 579-90.
Kihara, A., Akiyama, Y. and Ito, K. (2001). Revisiting the lysogenization control of bacteriophage lambda. Identification and characterization of a new host component, HflD. *J Biol Chem* **276**, 13695-700.
Knodler, L. A., Finlay, B. B. and Steele-Mortimer, O. (2005). The Salmonella effector protein SopB protects epithelial cells from apoptosis by sustained activation of Akt. *J Biol Chem* **280**, 9058-64.
Knutton, S., Rosenshine, I., Pallen, M. J., Nisan, I., Neves, B. C., Bain, C., Wolff, C., Dougan, G. and Frankel, G. (1998). A novel EspA-associated surface organelle of enteropathogenic *Escherichia coli* involved in protein translocation into epithelial cells. *EMBO J* **17**, 2166-76.
Kobayashi, S. D., Braughton, K. R., Whitney, A. R., Voyich, J. M., Schwan, T. G., Musser, J. M. and DeLeo, F. R. (2003). Bacterial pathogens modulate an apoptosis differentiation program in human neutrophils. *Proc Natl Acad Sci U S A* **100**, 10948-53.
Kobiler, O., Oppenheim, A. B. and Herman, C. (2004). Recruitment of host ATP-dependent proteases by bacteriophage lambda. *J Struct Biol* **146**, 72-8.
Kobiler, O., Rokney, A. and Oppenheim, A. B. (2007). Phage lambda CIII: a protease inhibitor regulating the lysis-lysogeny decision. *PLoS One* **2**, e363.

Koegl, M. and Uetz, P. (2007). Improving yeast two-hybrid screening systems. *Brief Funct Genomic Proteomic* **6**, 302-12.
Kornitzer, D., Altuvia, S. and Oppenheim, A. B. (1991). The activity of the CIII regulator of lambdoid bacteriophages resides within a 24-amino acid protein domain. *Proc Natl Acad Sci U S A* **88**, 5217-21.
Kulkarni, S. K. and Stahl, F. W. (1989). Interaction between the sbcC gene of *Escherichia coli* and the gam gene of phage lambda. *Genetics* **123**, 249-53.
Lamesch, P., Li, N., Milstein, S., Fan, C., Hao, T., Szabo, G., Hu, Z., Venkatesan, K., Bethel, G., Martin, P. et al. (2007). hORFeome v3.1: a resource of human open reading frames representing over 10,000 human genes. *Genomics* **89**, 307-15.
Lamkanfi, M. and Dixit, V. M. (2009). Inflammasomes: guardians of cytosolic sanctity. *Immunol Rev* **227**, 95-105.
Lamkanfi, M. and Dixit, V. M. (2010). Manipulation of host cell death pathways during microbial infections. *Cell Host Microbe* **8**, 44-54.
LeBowitz, J. H. and McMacken, R. (1986). The *Escherichia coli* dnaB replication protein is a DNA helicase. *J Biol Chem* **261**, 4738-48.
Lederberg, E. (1951). Lysogenicity of *Escherichia coli* strain K-12. *Microbial Genetics Bulletin*.
Lee, H. C. and Goodman, J. L. (2006). Anaplasma phagocytophilum causes global induction of antiapoptosis in human neutrophils. *Genomics* **88**, 496-503.
Leffers, G. G., Jr. and Gottesman, S. (1998). Lambda Xis degradation in vivo by Lon and FtsH. *J Bacteriol* **180**, 1573-7.
Li, M., Moyle, H. and Susskind, M. M. (1994). Target of the transcriptional activation function of phage lambda cI protein. *Science* **263**, 75-7.
Liberek, K., Georgopoulos, C. and Zylicz, M. (1988). Role of the *Escherichia coli* DnaK and DnaJ heat shock proteins in the initiation of bacteriophage lambda DNA replication. *Proc Natl Acad Sci U S A* **85**, 6632-6.
Linding, R., Russell, R. B., Neduva, V. and Gibson, T. J. (2003). GlobPlot: Exploring protein sequences for globularity and disorder. *Nucleic Acids Res* **31**, 3701-8.
Lukyanenko, V., Malyukova, I., Hubbard, A., Delannoy, M., Boedeker, E., Zhu, C., Cebotaru, L. and Kovbasnjuk, O. (2011). Enterohemorrhagic *Escherichia coli* infection stimulates Shiga toxin 1 macropinocytosis and transcytosis across intestinal epithelial cells. *Am J Physiol Cell Physiol* **301**, C1140-9.
Ma, C., Wickham, M. E., Guttman, J. A., Deng, W., Walker, J., Madsen, K. L., Jacobson, K., Vogl, W. A., Finlay, B. B. and Vallance, B. A. (2006). Citrobacter rodentium infection causes both mitochondrial dysfunction and intestinal epithelial barrier disruption in vivo: role of mitochondrial associated protein (Map). *Cell Microbiol* **8**, 1669-86.
Magalhaes, A. C., Dunn, H. and Ferguson, S. S. (2012). Regulation of GPCR activity, trafficking and localization by GPCR-interacting proteins. *Br J Pharmacol* **165**, 1717-36.
Mallory, J. B., Alfano, C. and McMacken, R. (1990). Host virus interactions in the initiation of bacteriophage lambda DNA replication. Recruitment of *Escherichia coli* DnaB helicase by lambda P replication protein. *J Biol Chem* **265**, 13297-307.
Marches, O., Batchelor, M., Shaw, R. K., Patel, A., Cummings, N., Nagai, T., Sasakawa, C., Carlsson, S. R., Lundmark, R., Cougoule, C. et al. (2006). EspF of enteropathogenic *Escherichia coli* binds sorting nexin 9. *J Bacteriol* **188**, 3110-5.
Mariathasan, S., Newton, K., Monack, D. M., Vucic, D., French, D. M., Lee, W. P., Roose-Girma, M., Erickson, S. and Dixit, V. M. (2004). Differential activation of the inflammasome by caspase-1 adaptors ASC and Ipaf. *Nature* **430**, 213-8.
Mariathasan, S., Weiss, D. S., Newton, K., McBride, J., O'Rourke, K., Roose-Girma, M., Lee, W. P., Weinrauch, Y., Monack, D. M. and Dixit, V. M. (2006). Cryopyrin activates the inflammasome in response to toxins and ATP. *Nature* **440**, 228-32.
Marr, M. T., Datwyler, S. A., Meares, C. F. and Roberts, J. W. (2001). Restructuring of an RNA polymerase holoenzyme elongation complex by lambdoid phage Q proteins. *Proc Natl Acad Sci U S A* **98**, 8972-8.
Marr, M. T., Roberts, J. W., Brown, S. E., Klee, M. and Gussin, G. N. (2004). Interactions among CII protein, RNA polymerase and the lambda PRE promoter: contacts between RNA

polymerase and the -35 region of PRE are identical in the presence and absence of CII protein. *Nucleic Acids Res* **32**, 1083-90.
Marsic, N., Roje, S., Stojiljkovic, I., Salaj-Smic, E. and Trgovcevic, Z. (1993). In vivo studies on the interaction of RecBCD enzyme and lambda Gam protein. *J Bacteriol* **175**, 4738-43.
Martinez, E., Schroeder, G. N., Berger, C. N., Lee, S. F., Robinson, K. S., Badea, L., Simpson, N., Hall, R. A., Hartland, E. L., Crepin, V. F. et al. (2010). Binding to Na(+) /H(+) exchanger regulatory factor 2 (NHERF2) affects trafficking and function of the enteropathogenic *Escherichia coli* type III secretion system effectors Map, EspI and NleH. *Cell Microbiol* **12**, 1718-31.
Martinon, F., Burns, K. and Tschopp, J. (2002). The inflammasome: a molecular platform triggering activation of inflammatory caspases and processing of proIL-beta. *Mol Cell* **10**, 417-26.
Martinon, F. and Tschopp, J. (2007). Inflammatory caspases and inflammasomes: master switches of inflammation. *Cell Death Differ* **14**, 10-22.
Mason, S. W. and Greenblatt, J. (1991). Assembly of transcription elongation complexes containing the N protein of phage lambda and the *Escherichia coli* elongation factors NusA, NusB, NusG, and S10. *Genes Dev* **5**, 1504-12.
Massari, P., Ho, Y. and Wetzler, L. M. (2000). Neisseria meningitidis porin PorB interacts with mitochondria and protects cells from apoptosis. *Proc Natl Acad Sci U S A* **97**, 9070-5.
Massari, P., King, C. A., Ho, A. Y. and Wetzler, L. M. (2003). Neisserial PorB is translocated to the mitochondria of HeLa cells infected with Neisseria meningitidis and protects cells from apoptosis. *Cell Microbiol* **5**, 99-109.
Maxwell, K. L., Reed, P., Zhang, R. G., Beasley, S., Walmsley, A. R., Curtis, F. A., Joachimiak, A., Edwards, A. M. and Sharples, G. J. (2005). Functional similarities between phage lambda Orf and *Escherichia coli* RecFOR in initiation of genetic exchange. *Proc Natl Acad Sci U S A* **102**, 11260-5.
Mensa-Wilmot, K., Seaby, R., Alfano, C., Wold, M. C., Gomes, B. and McMacken, R. (1989). Reconstitution of a nine-protein system that initiates bacteriophage lambda DNA replication. *J Biol Chem* **264**, 2853-61.
Miao, E. A., Alpuche-Aranda, C. M., Dors, M., Clark, A. E., Bader, M. W., Miller, S. I. and Aderem, A. (2006). Cytoplasmic flagellin activates caspase-1 and secretion of interleukin 1beta via Ipaf. *Nat Immunol* **7**, 569-75.
Min, J. and Defea, K. (2011). beta-arrestin-dependent actin reorganization: bringing the right players together at the leading edge. *Mol Pharmacol* **80**, 760-8.
Miyamoto, H., Nakai, W., Yajima, N., Fujibayashi, A., Higuchi, T., Sato, K. and Matsushiro, A. (1999). Sequence analysis of Stx2-converting phage VT2-Sa shows a great divergence in early regulation and replication regions. *DNA Res* **6**, 235-40.
Mohr, K. and Koegl, M. (2012). High-throughput yeast two-hybrid screening of complex cDNA libraries. *Methods Mol Biol* **812**, 89-102.
Mount, D. W., Harris, A. W., Fuerst, C. R. and Siminovitch, L. (1968). Mutations in bacteriophage lambda affecting particle morphogenesis. *Virology* **35**, 134-49.
Muniyappa, K. and Mythili, E. (1993). Phage lambda beta protein, a component of general recombination, is associated with host ribosomal S1 protein. *Biochem Mol Biol Int* **31**, 1-11.
Munoz-Pinedo, C. (2012). Signaling pathways that regulate life and cell death: evolution of apoptosis in the context of self-defense. *Adv Exp Med Biol* **738**, 124-43.
Murialdo, H. (1979). Early intermediates in bacteriophage lambda prohead assembly. *Virology* **96**, 341-67.
Newton, H. J., Pearson, J. S., Badea, L., Kelly, M., Lucas, M., Holloway, G., Wagstaff, K. M., Dunstone, M. A., Sloan, J., Whisstock, J. C. et al. (2010). The type III effectors NleE and NleB from enteropathogenic *E. coli* and OspZ from *Shigella* block nuclear translocation of NF-kappaB p65. *PLoS Pathog* **6**, e1000898.
Nickels, B. E., Roberts, C. W., Sun, H., Roberts, J. W. and Hochschild, A. (2002). The sigma(70) subunit of RNA polymerase is contacted by the (lambda)Q antiterminator during early elongation. *Mol Cell* **10**, 611-22.

Nickles, D., Falschlehner, C., Metzig, M. and Boutros, M. (2012). A genome-wide RNA interference screen identifies caspase 4 as a factor required for tumor necrosis factor alpha signaling. *Mol Cell Biol* **32**, 3372-81.
Nougayrede, J. P. and Donnenberg, M. S. (2004). Enteropathogenic *Escherichia coli* EspF is targeted to mitochondria and is required to initiate the mitochondrial death pathway. *Cell Microbiol* **6**, 1097-111.
Nougayrede, J. P., Foster, G. H. and Donnenberg, M. S. (2007). Enteropathogenic *Escherichia coli* effector EspF interacts with host protein Abcf2. *Cell Microbiol* **9**, 680-93.
Obeng, E. A. and Boise, L. H. (2005). Caspase-12 and caspase-4 are not required for caspase-dependent endoplasmic reticulum stress-induced apoptosis. *J Biol Chem* **280**, 29578-87.
Orchard, R. C. and Alto, N. M. (2012). Mimicking GEFs: a common theme for bacterial pathogens. *Cell Microbiol* **14**, 10-8.
Papatheodorou, P., Domanska, G., Oxle, M., Mathieu, J., Selchow, O., Kenny, B. and Rassow, J. (2006). The enteropathogenic *Escherichia coli* (EPEC) Map effector is imported into the mitochondrial matrix by the TOM/Hsp70 system and alters organelle morphology. *Cell Microbiol* **8**, 677-89.
Parsot, C., Hamiaux, C. and Page, A. L. (2003). The various and varying roles of specific chaperones in type III secretion systems. *Curr Opin Microbiol* **6**, 7-14.
Parua, P. K., Mondal, A. and Parrack, P. (2010). HflD, an *Escherichia coli* protein involved in the lambda lysis-lysogeny switch, impairs transcription activation by lambdaCII. *Arch Biochem Biophys* **493**, 175-83.
Pelletier, N., Casamayor-Palleja, M., De Luca, K., Mondiere, P., Saltel, F., Jurdic, P., Bella, C., Genestier, L. and Defrance, T. (2006). The endoplasmic reticulum is a key component of the plasma cell death pathway. *J Immunol* **176**, 1340-7.
Pfefferle, S., Schopf, J., Kogl, M., Friedel, C. C., Muller, M. A., Carbajo-Lozoya, J., Stellberger, T., von Dall'Armi, E., Herzog, P., Kallies, S. et al. (2011). The SARS-coronavirus-host interactome: identification of cyclophilins as target for pan-coronavirus inhibitors. *PLoS Pathog* **7**, e1002331.
Phillips, N., Hayward, R. D. and Koronakis, V. (2004). Phosphorylation of the enteropathogenic *E. coli* receptor by the Src-family kinase c-Fyn triggers actin pedestal formation. *Nat Cell Biol* **6**, 618-25.
Pirbhai, M., Dong, F., Zhong, Y., Pan, K. Z. and Zhong, G. (2006). The secreted protease factor CPAF is responsible for degrading pro-apoptotic BH3-only proteins in Chlamydia trachomatis-infected cells. *J Biol Chem* **281**, 31495-501.
Ptashne, M. (2006). A Genetic Switch. Phage Lambda Revisited. Cold Spring Harbor, NY: Cold Spring Harbor Laboratory Press.
Quevillon, E., Silventoinen, V., Pillai, S., Harte, N., Mulder, N., Apweiler, R. and Lopez, R. (2005). InterProScan: protein domains identifier. *Nucleic Acids Res* **33**, W116-20.
Rajagopala, S. V., Casjens, S. and Uetz, P. (2011). The protein interaction map of bacteriophage lambda. *BMC Microbiol* **11**, 213.
Rajagopala, S. V., Hughes, K. T. and Uetz, P. (2009). Benchmarking yeast two-hybrid systems using the interactions of bacterial motility proteins. *Proteomics* **9**, 5296-302.
Rajagopala, S. V., Yamamoto, N., Zweifel, A. E., Nakamichi, T., Huang, H. K., Mendez-Rios, J. D., Franca-Koh, J., Boorgula, M. P., Fujita, K., Suzuki, K. et al. (2010). The *Escherichia coli* K-12 ORFeome: a resource for comparative molecular microbiology. *BMC Genomics* **11**, 470.
Rathinam, V. A., Jiang, Z., Waggoner, S. N., Sharma, S., Cole, L. E., Waggoner, L., Vanaja, S. K., Monks, B. G., Ganesan, S., Latz, E. et al. (2010). The AIM2 inflammasome is essential for host defense against cytosolic bacteria and DNA viruses. *Nat Immunol* **11**, 395-402.
Richard, A. and Tulasne, D. (2012). Caspase cleavage of viral proteins, another way for viruses to make the best of apoptosis. *Cell Death Dis* **3**, e277.
Roberts, C. W. and Roberts, J. W. (1996). Base-specific recognition of the nontemplate strand of promoter DNA by *E. coli* RNA polymerase. *Cell* **86**, 495-501.

Roberts, J. W., Yarnell, W., Bartlett, E., Guo, J., Marr, M., Ko, D. C., Sun, H. and Roberts, C. W. (1998). Antitermination by bacteriophage lambda Q protein. *Cold Spring Harb Symp Quant Biol* **63**, 319-25.
Roessner, C. A., Struck, D. K. and Ihler, G. M. (1983). Injection of DNA into liposomes by bacteriophage lambda. *J Biol Chem* **258**, 643-8.
Ruchaud-Sparagano, M. H., Muhlen, S., Dean, P. and Kenny, B. (2011). The enteropathogenic *E. coli* (EPEC) Tir effector inhibits NF-kappaB activity by targeting TNFalpha receptor-associated factors. *PLoS Pathog* **7**, e1002414.
Sabri, M., Hauser, R., Ouellette, M., Liu, J., Dehbi, M., Moeck, G., Garcia, E., Titz, B., Uetz, P. and Moineau, S. (2011). Genome annotation and intraviral interactome for the Streptococcus pneumoniae virulent phage Dp-1. *J Bacteriol* **193**, 551-62.
Saelens, X., Festjens, N., Vande Walle, L., van Gurp, M., van Loo, G. and Vandenabeele, P. (2004). Toxic proteins released from mitochondria in cell death. *Oncogene* **23**, 2861-74.
Sandvig, K., Bergan, J., Dyve, A. B., Skotland, T. and Torgersen, M. L. (2010). Endocytosis and retrograde transport of Shiga toxin. *Toxicon* **56**, 1181-5.
Sarkar, A., Hellberg, L., Bhattacharyya, A., Behnen, M., Wang, K., Lord, J. M., Moller, S., Kohler, M., Solbach, W. and Laskay, T. (2012). Infection with Anaplasma phagocytophilum activates the phosphatidylinositol 3-Kinase/Akt and NF-kappaB survival pathways in neutrophil granulocytes. *Infect Immun* **80**, 1615-23.
Sauer, J. D., Witte, C. E., Zemansky, J., Hanson, B., Lauer, P. and Portnoy, D. A. (2010). Listeria monocytogenes triggers AIM2-mediated pyroptosis upon infrequent bacteriolysis in the macrophage cytosol. *Cell Host Microbe* **7**, 412-9.
Serebriiskii, I. G. and Golemis, E. A. (2001). Two-hybrid system and false positives. Approaches to detection and elimination. *Methods Mol Biol* **177**, 123-34.
Shames, S. R., Deng, W., Guttman, J. A., de Hoog, C. L., Li, Y., Hardwidge, P. R., Sham, H. P., Vallance, B. A., Foster, L. J. and Finlay, B. B. (2010). The pathogenic *E. coli* type III effector EspZ interacts with host CD98 and facilitates host cell prosurvival signalling. *Cell Microbiol* **12**, 1322-39.
Shannon, P., Markiel, A., Ozier, O., Baliga, N. S., Wang, J. T., Ramage, D., Amin, N., Schwikowski, B. and Ideker, T. (2003). Cytoscape: a software environment for integrated models of biomolecular interaction networks. *Genome Res* **13**, 2498-504.
Shaw, R. K., Cleary, J., Murphy, M. S., Frankel, G. and Knutton, S. (2005). Interaction of enteropathogenic *Escherichia coli* with human intestinal mucosa: role of effector proteins in brush border remodeling and formation of attaching and effacing lesions. *Infect Immun* **73**, 1243-51.
Shawgo, M. E., Shelton, S. N. and Robertson, J. D. (2009). Caspase-9 activation by the apoptosome is not required for fas-mediated apoptosis in type II Jurkat cells. *J Biol Chem* **284**, 33447-55.
Shin, S., Sung, B. J., Cho, Y. S., Kim, H. J., Ha, N. C., Hwang, J. I., Chung, C. W., Jung, Y. K. and Oh, B. H. (2001). An anti-apoptotic protein human survivin is a direct inhibitor of caspase-3 and -7. *Biochemistry* **40**, 1117-23.
Shotland, Y., Shifrin, A., Ziv, T., Teff, D., Koby, S., Kobiler, O. and Oppenheim, A. B. (2000). Proteolysis of bacteriophage lambda CII by *Escherichia coli* FtsH (HflB). *J Bacteriol* **182**, 3111-6.
Sollberger, G., Strittmatter, G. E., Kistowska, M., French, L. E. and Beer, H. D. (2012). Caspase-4 is required for activation of inflammasomes. *J Immunol* **188**, 1992-2000.
Song, J. J. and Lee, Y. J. (2008). Differential cleavage of Mst1 by caspase-7/-3 is responsible for TRAIL-induced activation of the MAPK superfamily. *Cell Signal* **20**, 892-906.
Spears, K. J., Roe, A. J. and Gally, D. L. (2006). A comparison of enteropathogenic and enterohaemorrhagic *Escherichia coli* pathogenesis. *FEMS Microbiol Lett* **255**, 187-202.
Stark, C., Breitkreutz, B. J., Chatr-Aryamontri, A., Boucher, L., Oughtred, R., Livstone, M. S., Nixon, J., Van Auken, K., Wang, X., Shi, X. et al. (2011). The BioGRID Interaction Database: 2011 update. *Nucleic Acids Res* **39**, D698-704.
Stebbins, C. E. and Galan, J. E. (2003). Priming virulence factors for delivery into the host. *Nat Rev Mol Cell Biol* **4**, 738-43.

Stellberger, T., Hauser, R., Baiker, A., Pothineni, V. R., Haas, J. and Uetz, P. (2010). Improving the yeast two-hybrid system with permutated fusions proteins: the Varicella Zoster Virus interactome. *Proteome Sci* **8**, 8.
Stennicke, H. R. and Salvesen, G. S. (1999). Caspases: preparation and characterization. *Methods* **17**, 313-9.
Strasser, A., Jost, P. J. and Nagata, S. (2009). The many roles of FAS receptor signaling in the immune system. *Immunity* **30**, 180-92.
Strasser, A., O'Connor, L. and Dixit, V. M. (2000). Apoptosis signaling. *Annu Rev Biochem* **69**, 217-45.
Sutterwala, F. S., Ogura, Y., Szczepanik, M., Lara-Tejero, M., Lichtenberger, G. S., Grant, E. P., Bertin, J., Coyle, A. J., Galan, J. E., Askenase, P. W. et al. (2006). Critical role for NALP3/CIAS1/Cryopyrin in innate and adaptive immunity through its regulation of caspase-1. *Immunity* **24**, 317-27.
Swimm, A., Bommarius, B., Li, Y., Cheng, D., Reeves, P., Sherman, M., Veach, D., Bornmann, W. and Kalman, D. (2004). Enteropathogenic *Escherichia coli* use redundant tyrosine kinases to form actin pedestals. *Mol Biol Cell* **15**, 3520-9.
Szambowska, A., Pierechod, M., Wegrzyn, G. and Glinkowska, M. (2011). Coupling of transcription and replication machineries in {lambda} DNA replication initiation: evidence for direct interaction of *Escherichia coli* RNA polymerase and the {lambda}O protein. *Nucleic Acids Res* **39**, 168-77.
Tahoun, A., Siszler, G., Spears, K., McTeer, S., Tree, J., Paxton, E., Gillespie, T. L., Martinez-Argudo, I., Jepson, M. A., Shaw, D. J. et al. (2011). Comparative Analysis of EspF Variants in the Inhibition of *E. coli* Phagocytosis by Macrophages and the Inhibition of *E. coli* Translocation Through Human- and Bovine-Derived M-cells. *Infect Immun*.
Tang, E. D., Wang, C. Y., Xiong, Y. and Guan, K. L. (2003). A role for NF-kappaB essential modifier/IkappaB kinase-gamma (NEMO/IKKgamma) ubiquitination in the activation of the IkappaB kinase complex by tumor necrosis factor-alpha. *J Biol Chem* **278**, 37297-305.
Taylor, R. C., Cullen, S. P. and Martin, S. J. (2008). Apoptosis: controlled demolition at the cellular level. *Nat Rev Mol Cell Biol* **9**, 231-41.
Temple, G. Gerhard, D. S. Rasooly, R. Feingold, E. A. Good, P. J. Robinson, C. Mandich, A. Derge, J. G. Lewis, J. Shoaf, D. et al. (2009). The completion of the Mammalian Gene Collection (MGC). *Genome Res* **19**, 2324-33.
Teodoro, J. G. and Branton, P. E. (1997). Regulation of apoptosis by viral gene products. *J Virol* **71**, 1739-46.
Timmer, J. C. and Salvesen, G. S. (2007). Caspase substrates. *Cell Death Differ* **14**, 66-72.
Tinsley, C. R., Bille, E. and Nassif, X. (2006). Bacteriophages and pathogenicity: more than just providing a toxin? *Microbes Infect* **8**, 1365-71.
Titz, B., Rajagopala, S. V., Goll, J., Hauser, R., McKevitt, M. T., Palzkill, T. and Uetz, P. (2008). The binary protein interactome of Treponema pallidum--the syphilis spirochete. *PLoS One* **3**, e2292.
Tobe, T., Beatson, S. A., Taniguchi, H., Abe, H., Bailey, C. M., Fivian, A., Younis, R., Matthews, S., Marches, O., Frankel, G. et al. (2006). An extensive repertoire of type III secretion effectors in *Escherichia coli* O157 and the role of lambdoid phages in their dissemination. *Proc Natl Acad Sci U S A* **103**, 14941-6.
Tournier, C., Hess, P., Yang, D. D., Xu, J., Turner, T. K., Nimnual, A., Bar-Sagi, D., Jones, S. N., Flavell, R. A. and Davis, R. J. (2000). Requirement of JNK for stress-induced activation of the cytochrome c-mediated death pathway. *Science* **288**, 870-4.
Uetz, P., Dong, Y. A., Zeretzke, C., Atzler, C., Baiker, A., Berger, B., Rajagopala, S. V., Roupelieva, M., Rose, D., Fossum, E. et al. (2006). Herpesviral protein networks and their interaction with the human proteome. *Science* **311**, 239-42.
Uetz, P., Giot, L., Cagney, G., Mansfield, T. A., Judson, R. S., Knight, J. R., Lockshon, D., Narayan, V., Srinivasan, M., Pochart, P. et al. (2000). A comprehensive analysis of protein-protein interactions in Saccharomyces cerevisiae. *Nature* **403**, 623-7.
Vanlangenakker, N., Vanden Berghe, T., Krysko, D. V., Festjens, N. and Vandenabeele, P. (2008). Molecular mechanisms and pathophysiology of necrotic cell death. *Curr Mol Med* **8**, 207-20.

Vingadassalom, D., Kazlauskas, A., Skehan, B., Cheng, H. C., Magoun, L., Robbins, D., Rosen, M. K., Saksela, K. and Leong, J. M. (2009). Insulin receptor tyrosine kinase substrate links the *E. coli* O157:H7 actin assembly effectors Tir and EspF(U) during pedestal formation. *Proc Natl Acad Sci U S A* **106**, 6754-9.

Wachter, C., Beinke, C., Mattes, M. and Schmidt, M. A. (1999). Insertion of EspD into epithelial target cell membranes by infecting enteropathogenic *Escherichia coli*. *Mol Microbiol* **31**, 1695-707.

Waldor, M. K. and Mekalanos, J. J. (1996). Lysogenic conversion by a filamentous phage encoding cholera toxin. *Science* **272**, 1910-4.

Wang, J., Hofnung, M. and Charbit, A. (2000). The C-terminal portion of the tail fiber protein of bacteriophage lambda is responsible for binding to LamB, its receptor at the surface of *Escherichia coli* K-12. *J Bacteriol* **182**, 508-12.

Wang, K., Yin, X. M., Chao, D. T., Milliman, C. L. and Korsmeyer, S. J. (1996). BID: a novel BH3 domain-only death agonist. *Genes Dev* **10**, 2859-69.

Wegrzyn, G., Licznerska, K. and Wegrzyn, A. (2012). Phage lambda--new insights into regulatory circuits. *Adv Virus Res* **82**, 155-78.

Weiss, S. M., Ladwein, M., Schmidt, D., Ehinger, J., Lommel, S., Stading, K., Beutling, U., Disanza, A., Frank, R., Jansch, L. et al. (2009). IRSp53 links the enterohemorrhagic *E. coli* effectors Tir and EspFU for actin pedestal formation. *Cell Host Microbe* **5**, 244-58.

Wendel, A. M., Johnson, D. H., Sharapov, U., Grant, J., Archer, J. R., Monson, T., Koschmann, C. and Davis, J. P. (2009). Multistate outbreak of *Escherichia coli* O157:H7 infection associated with consumption of packaged spinach, August-September 2006: the Wisconsin investigation. *Clin Infect Dis* **48**, 1079-86.

Werts, C., Michel, V., Hofnung, M. and Charbit, A. (1994). Adsorption of bacteriophage lambda on the LamB protein of *Escherichia coli* K-12: point mutations in gene J of lambda responsible for extended host range. *J Bacteriol* **176**, 941-7.

Wienken, C. J., Baaske, P., Rothbauer, U., Braun, D. and Duhr, S. (2010). Protein-binding assays in biological liquids using microscale thermophoresis. *Nat Commun* **1**, 100.

Williams, N., Fox, D. K., Shea, C. and Roseman, S. (1986). Pel, the protein that permits lambda DNA penetration of *Escherichia coli*, is encoded by a gene in ptsM and is required for mannose utilization by the phosphotransferase system. *Proc Natl Acad Sci U S A* **83**, 8934-8.

Wommack, K. E. and Colwell, R. R. (2000). Virioplankton: viruses in aquatic ecosystems. *Microbiol Mol Biol Rev* **64**, 69-114.

Wong, A. R., Pearson, J. S., Bright, M. D., Munera, D., Robinson, K. S., Lee, S. F., Frankel, G. and Hartland, E. L. (2011). Enteropathogenic and enterohaemorrhagic *Escherichia coli*: even more subversive elements. *Mol Microbiol* **80**, 1420-38.

Xiao, Y., Zhong, Y., Greene, W., Dong, F. and Zhong, G. (2004). Chlamydia trachomatis infection inhibits both Bax and Bak activation induced by staurosporine. *Infect Immun* **72**, 5470-4.

Yamamuro, A., Kishino, T., Ohshima, Y., Yoshioka, Y., Kimura, T., Kasai, A. and Maeda, S. (2011). Caspase-4 directly activates caspase-9 in endoplasmic reticulum stress-induced apoptosis in SH-SY5Y cells. *J Pharmacol Sci* **115**, 239-43.

Yazdi, A. S., Guarda, G., D'Ombrain, M. C. and Drexler, S. K. (2010). Inflammatory caspases in innate immunity and inflammation. *J Innate Immun* **2**, 228-37.

Yin, X. M., Wang, K., Gross, A., Zhao, Y., Zinkel, S., Klocke, B., Roth, K. A. and Korsmeyer, S. J. (1999). Bid-deficient mice are resistant to Fas-induced hepatocellular apoptosis. *Nature* **400**, 886-91.

Yokoyama, K., Makino, K., Kubota, Y., Watanabe, M., Kimura, S., Yutsudo, C. H., Kurokawa, K., Ishii, K., Hattori, M., Tatsuno, I. et al. (2000). Complete nucleotide sequence of the prophage VT1-Sakai carrying the Shiga toxin 1 genes of the enterohemorrhagic *Escherichia coli* O157:H7 strain derived from the Sakai outbreak. *Gene* **258**, 127-39.

Yu, H., Braun, P., Yildirim, M. A., Lemmens, I., Venkatesan, K., Sahalie, J., Hirozane-Kishikawa, T., Gebreab, F., Li, N., Simonis, N. et al. (2008). High-quality binary protein interaction map of the yeast interactome network. *Science* **322**, 104-10.

Zhong, Y., Weininger, M., Pirbhai, M., Dong, F. and Zhong, G. (2006). Inhibition of staurosporine-induced activation of the proapoptotic multidomain Bcl-2 proteins Bax and Bak by three invasive chlamydial species. *J Infect* **53**, 408-14.
Zozulya, S. and Stryer, L. (1992). Calcium-myristoyl protein switch. *Proc Natl Acad Sci U S A* **89**, 11569-73.
Zylicz, M., Ang, D., Liberek, K. and Georgopoulos, C. (1989). Initiation of lambda DNA replication with purified host- and bacteriophage-encoded proteins: the role of the dnaK, dnaJ and grpE heat shock proteins. *EMBO J* **8**, 1601-8.

PUBLICATIONS

Hauser, R., Blasche, S., Dokland, T., Haggard-Ljungquist, E., von Brunn, A., Salas, M., Casjens, S., Molineux, I. and Uetz, P. (2012). Bacteriophage protein-protein interactions. *Adv Virus Res* **83**, 219-98.

Blasche, S., Mörtl, M., Steuber, H., Siszler, G., Nisa, S., Schwarz, F., Lavrik, I., Gronewold, T. M. A., Maskos, K., Donnenberg, M. S., Ullmann, D., Uetz, P. and Koegl, M. The *E. coli* effector protein NleF is a caspase inhibitor **(submitted)**.

Blasche, S, Siszler, G., Schwarz, F., Uetz, P. and Koegl, M. The EHEC-host interactome **(in preparation)**.

6 Appendix

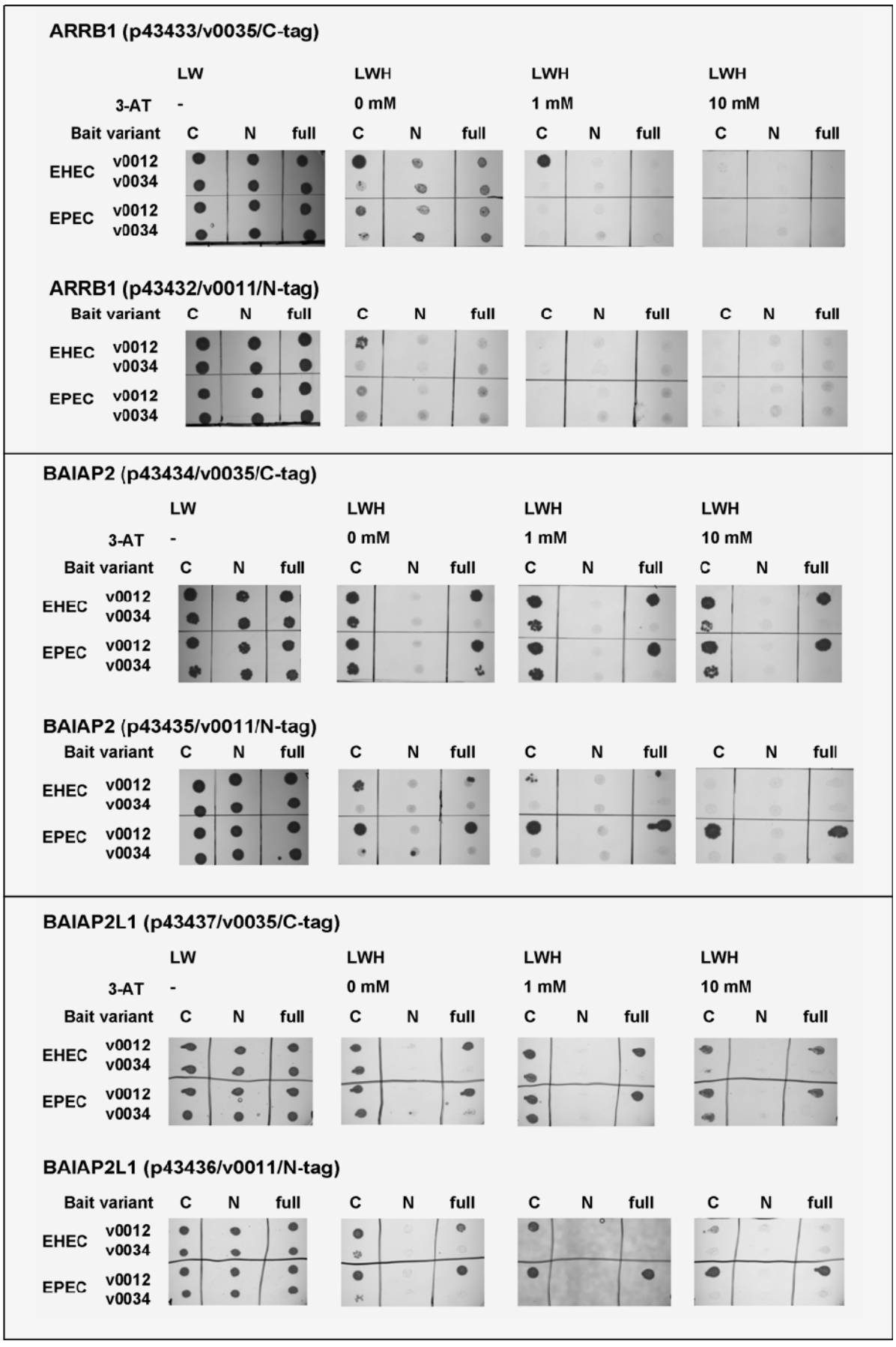
ARRB1 (p43433/v0035/C-tag)
LW
LWH
LWH
LWH
3-AT
-
0 mM
1 mM
10 mM
Bait variant
C
N
full
EHEC
v0012
v0034
EPEC
v0012
v0034
ARRB1 (p43432/v0011/N-tag)
BAIAP2 (p43434/v0035/C-tag)
BAIAP2 (p43435/v0011/N-tag)
BAIAP2L1 (p43437/v0035/C-tag)
BAIAP2L1 (p43436/v0011/N-tag)

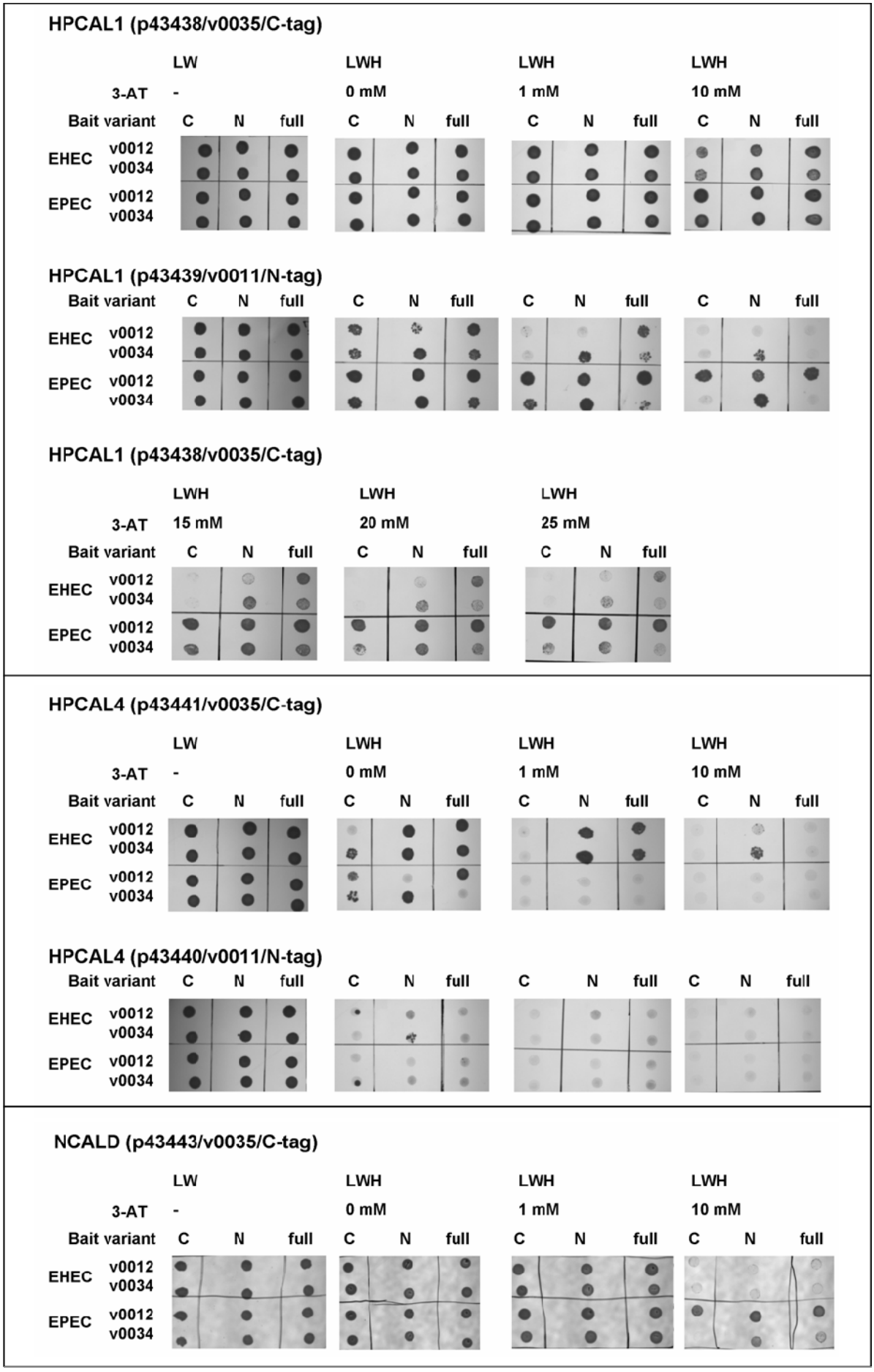
HPCAL1 (p43438/v0035/C-tag)
LW
LWH
LWH
LWH
3-AT
-
0 mM
1 mM
10 mM
Bait variant
C N full C N full C N full C N full
EHEC v0012
v0034
EPEC v0012
v0034
HPCAL1 (p43439/v0011/N-tag)
Bait variant
C N full C N full C N full C N full
EHEC v0012
v0034
EPEC v0012
v0034
HPCAL1 (p43438/v0035/C-tag)
LWH
LWH
LWH
3-AT
15 mM
20 mM
25 mM
Bait variant
C N full C N full C N full
EHEC v0012
v0034
EPEC v0012
v0034
HPCAL4 (p43441/v0035/C-tag)
LW
LWH
LWH
LWH
3-AT
-
0 mM
1 mM
10 mM
Bait variant
C N full C N full C N full C N full
EHEC v0012
v0034
EPEC v0012
v0034
HPCAL4 (p43440/v0011/N-tag)
Bait variant
C N full C N full C N full C N full
EHEC v0012
v0034
EPEC v0012
v0034
NCALD (p43443/v0035/C-tag)
LW
LWH
LWH
LWH
3-AT
-
0 mM
1 mM
10 mM
Bait variant
C N full C N full C N full C N full
EHEC v0012
v0034
EPEC v0012
v0034

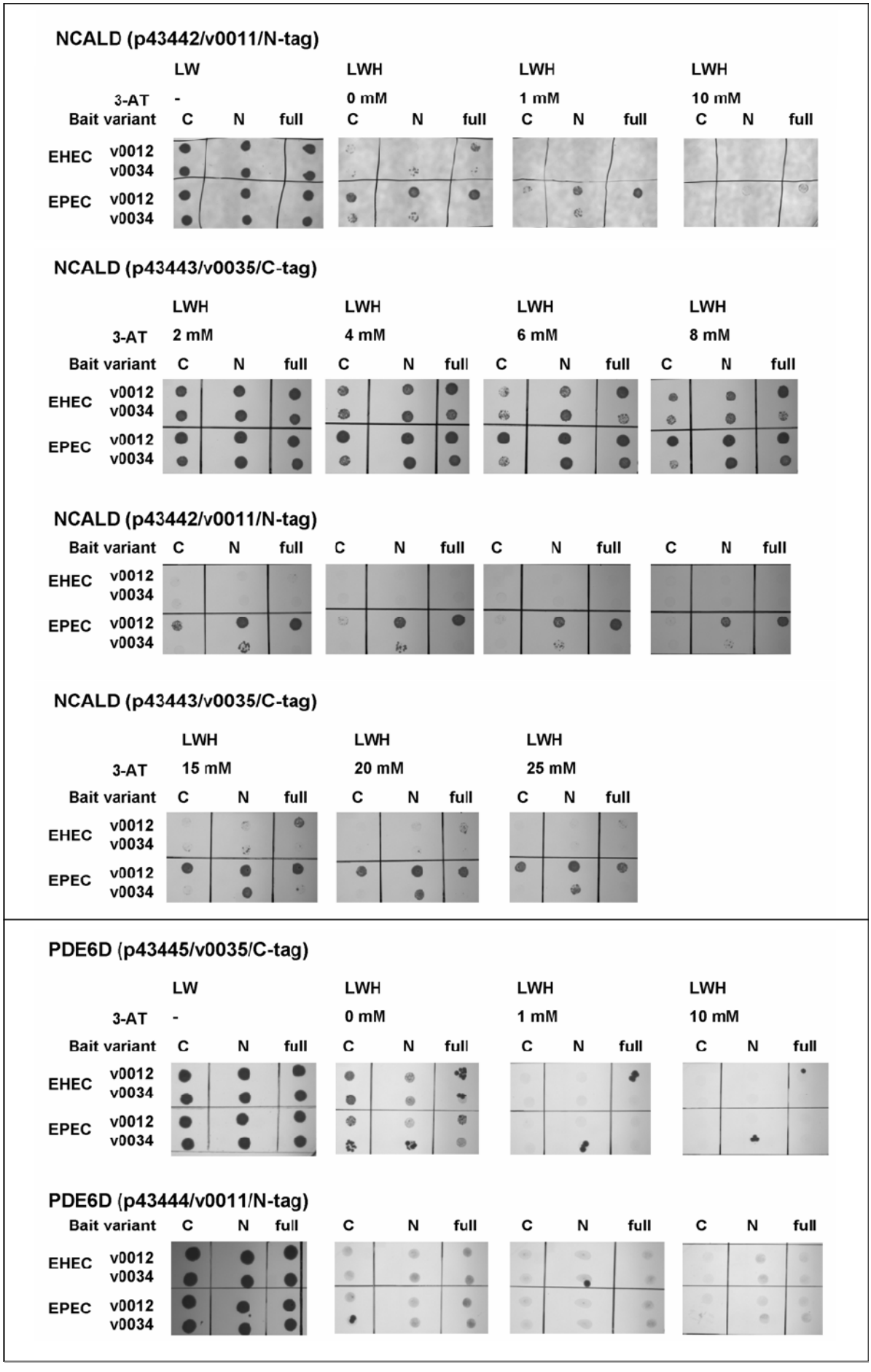
NCALD (p43442/v0011/N-tag)
LW
LWH
LWH
LWH
3-AT
-
0 mM
1 mM
10 mM
Bait variant
C
N
full
EHEC
v0012
v0034
EPEC
v0012
v0034
NCALD (p43443/v0035/C-tag)
LWH
LWH
LWH
LWH
3-AT
2 mM
4 mM
6 mM
8 mM
NCALD (p43442/v0011/N-tag)
NCALD (p43443/v0035/C-tag)
LWH
LWH
LWH
3-AT
15 mM
20 mM
25 mM
PDE6D (p43445/v0035/C-tag)
LW
LWH
LWH
LWH
3-AT
-
0 mM
1 mM
10 mM
PDE6D (p43444/v0011/N-tag)

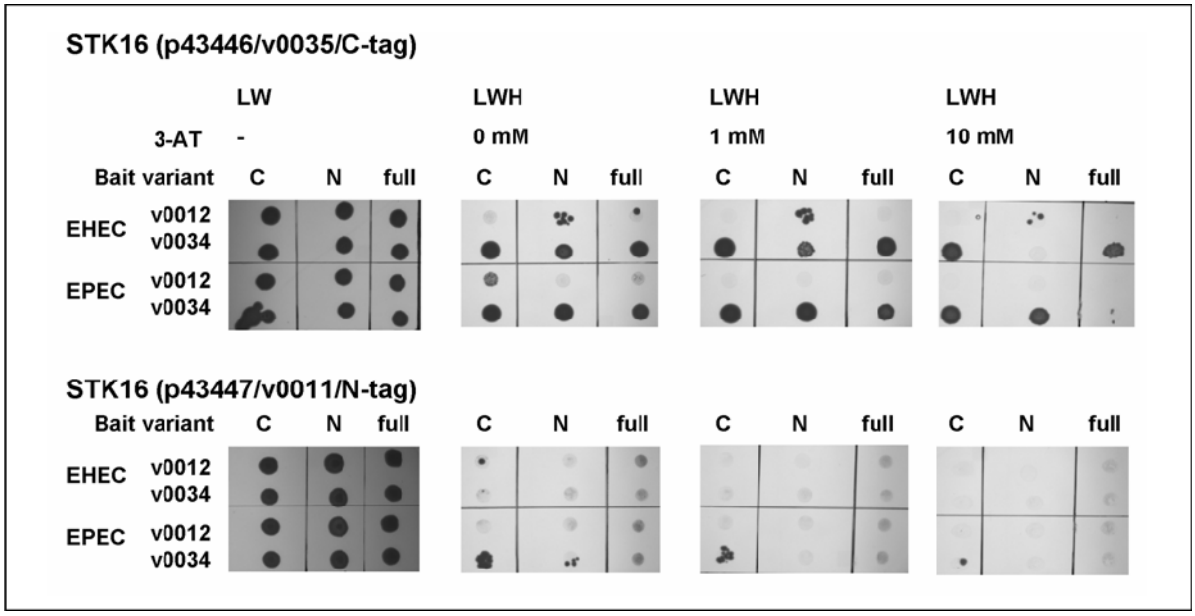

Supplementary figure 1. Binary yeast two hybrid tests of EHEC and EPEC TIR against the human proteins ARRB1, BAIAP2, BAIAP2L1, HPCAL1, HPCAL4, NCALD, PDE6D and STK16 at different 3-AT concentrations. N – amino-terminal TIR fragment; C – carboxy-terminal TIR fragemnt; full – full length TIR; v0011 – pGAD424; v0012 – pGBT9; v0034 – pGBKCg; v0035 – pGADCg.

Supplementary table 1. Complete list of detected EHEC/host interactions. 3'UTR – hit was in the 3'UTR and did not contain coding sequence; Prey prom – prey promiscuity assessed as total number of different baits the respective prey was found to interact with (raw counts), if the number is 6 or above, the prey is tagged as promiscuous.

Bait ID	EHEC bait	Prey gene symbol	Prey count	3'UTR	Prey prom	Description	GeneID
ECs0061	EspY1	CDKN2AIPNL	51	0	2	CDKN2A interacting protein N-terminal like	91368
ECs0061	EspY1	RING1	19	0	11	ring finger protein 1	6015
ECs0061	EspY1	PIH1D1	6	0	2	PIH1 domain containing 1	55011
ECs0061	EspY1	PSMC1	5	0	4	proteasome (prosome, macropain) 26S subunit, ATPase, 1	5700
ECs0061	EspY1	CAPN3	3	0	3	calpain 3, (p94)	825
ECs0061	EspY1	PCID2	3	0	4	PCI domain-containing protein 2 (CSN12-like protein).	55795
ECs0061	EspY1	DNAJC14	2	0	3	DnaJ (Hsp40) homologue, subfamily C, member 14	85406
ECs0061	EspY1	ZNHIT1	2	0	5	zinc finger, HIT type 1	10467
ECs0061	EspY1	CLK1	1	0	3	CDC-like kinase 1	1195
ECs0847	NleC	C8orf71	3	0	1	chromosome 8 open reading frame 71	26138
ECs0847	NleC	CTDSPL2	3	0	1	CTD (carboxy-terminal domain, RNA polymerase II, polypeptide A) small phosphatase like 2	51496
ECs0847	NleC	CREM	1	0	1	cAMP responsive element modulator	1390
ECs0847	NleC	CBWD1	1	0	1	COBW domain containing 1	55871
ECs0847	NleC	LCP2	1	0	1	lymphocyte cytosolic protein 2 (SH2 domain containing leukocyte protein of 76kDa)	3937
ECs0847	NleC	MCART1	1	0	1	mitochondrial carrier triple repeat 1	92014
ECs0847	NleC	ZC3H14	1	0	2	zinc finger CCCH-type containing 14	79882
ECs0847	NleC	HEPH	1	0	2	hephaestin	9843
ECs0847	NleC	FKBP3	1	0	3	FK506 binding protein 3, 25kDa	2287
ECs0847	NleC	YLPM1	1	0	4	YLP motif containing 1	56252
ECs0847	NleC	ADRBK2	1	1	1	adrenergic, beta, receptor kinase 2	157
ECs0847	NleC	NEBL	1	1	1	nebulette	10529
ECs0847	NleC	PPP3R2	1	1	1	protein phosphatase 3 (formerly 2B), regulatory subunit B, beta isoform	5535
ECs0847	NleC	RIN2	1	1	1	Ras and Rab interactor 2	54453
ECs0847	NleC	ZFYVE16	1	1	1	zinc finger, FYVE domain containing 16	9765
ECs0847	NleC	SLC31A2	1	1	2	solute carrier family 31 (copper transporters), member 2	1318
ECs0847	NleC	ZRANB2	1	1	2	zinc finger, RAN-binding domain containing 2	9406
ECs0847	NleC	CYB5B	1	1	3	cytochrome b5 type B (outer mitochondrial membrane)	80777
ECs0847	NleC	NOMO1	1	1	4	NODAL modulator 1	23420
ECs0847	NleC	PTPN6	1	0	6	protein tyrosine phosphatase	5777

ECs0847	NleC	DNAJC7	1	0	9	DnaJ (Hsp40) homolog, subfamily C, member 7	7266
ECs0847	NleC	RPL21	1	0	11	ribosomal protein L21	6144
ECs0847	NleC	BHMT	1	1	8	betaine-homocysteine methyltransferase	635
ECs0847	NleC	EIF4B	1	1	10	eukaryotic translation initiation factor 4B	1975
ECs0848	NleH1-1	ENSG00000206444	1	0	1	CDNA FLJ46428 fis, clone THYMU3014173, moderately similar to HLA class I histocompatibility antigen, alpha chain E*0101/E*0102.	
ECs0848	NleH1-1	ENSG00000206507	1	0	1	CDNA FLJ46428 fis, clone THYMU3014173, moderately similar to HLA class I histocompatibility antigen, alpha chain E*0101/E*0102.	
ECs0848	NleH1-1	TYRO3	1	0	1	TYRO3 protein tyrosine kinase	7301
ECs0848	NleH1-1	ACP5	1	0	1	acId phosphatase 5, tartrate resistant	54
ECs0848	NleH1-1	ATP6V1D	1	0	1	ATPase, H+ transporting, lysosomal 34kDa, V1 subunit D	51382
ECs0848	NleH1-1	C12orf72	1	0	1	chromosome 12 open reading frame 72	254013
ECs0848	NleH1-1	C20orf196	1	0	1	chromosome 20 open reading frame 196	149840
ECs0848	NleH1-1	C3orf38	1	0	1	chromosome 3 open reading frame 38	285237
ECs0848	NleH1-1	CADM3	1	0	1	cell adhesion molecule 3	57863
ECs0848	NleH1-1	CALML4	1	0	1	calmodulin-like 4	91860
ECs0848	NleH1-1	CCDC102A	1	0	1	coiled-coil domain containing 102A	92922
ECs0848	NleH1-1	CYB561D2	1	0	1	cytochrome b-561 domain containing 2	11068
ECs0848	NleH1-1	DNAJC24	1	0	1	DnaJ (Hsp40) homolog, subfamily C, member 24	120526
ECs0848	NleH1-1	DNAJC3	1	0	1	DnaJ (Hsp40) homolog, subfamily C, member 3	5611
ECs0848	NleH1-1	ERGIC2	1	0	1	ERGIC and golgi 2	51290
ECs0848	NleH1-1	FGL2	1	0	1	fibrinogen-like 2	10875
ECs0848	NleH1-1	FXC1	1	0	1	fracture callus 1 homolog (rat)	26515
ECs0848	NleH1-1	GZMB	1	0	1	granzyme B (granzyme 2, cytotoxic T-lymphocyte-associated serine esterase 1)	3002
ECs0848	NleH1-1	ICT1	1	0	1	immature colon carcInoma transcript 1	3396
ECs0848	NleH1-1	LOC100294459	1	0	1	similar to immunoglobulin lambda-like polypeptide 1	100294459
ECs0848	NleH1-1	LOC643406	1	0	1	hypothetical protein LOC643406	643406
ECs0848	NleH1-1	LYSMD3	1	0	1	LysM, putative peptidoglycan-binding, domain containing 3	116068
ECs0848	NleH1-1	NDUFAF4	1	0	1	NADH dehydrogenase 1 alpha subcomplex, assembly factor 4	29078
ECs0848	NleH1-1	OR2L13	1	0	1	olfactory receptor, family 2, subfamily L, member 13	284521

ECs0848	NleH1-1	PDHB	1	0	1	pyruvate dehydrogenase (lipoamide) beta	5162
ECs0848	NleH1-1	PEX16	1	0	1	peroxisomal biogenesis factor 16	9409
ECs0848	NleH1-1	PLA2G16	1	0	1	phospholipase A2, group XVI	11145
ECs0848	NleH1-1	PODXL2	1	0	1	podocalyxin-like 2	50512
ECs0848	NleH1-1	PRSS35	1	0	1	protease, serine, 35	167681
ECs0848	NleH1-1	RPL13AP17	1	0	1	ribosomal protein L13a pseudogene 17	399670
ECs0848	NleH1-1	SCGB2A1	1	0	1	secretoglobin, family 2A, member 1	4246
ECs0848	NleH1-1	SPATA1	1	0	1	spermatogenesis associated 1	64173
ECs0848	NleH1-1	SPATA3	1	0	1	spermatogenesis associated 3	130560
ECs0848	NleH1-1	SPINLW1	1	0	1	serine peptidase inhibitor-like, with Kunitz and WAP domains 1 (eppin)	57119
ECs0848	NleH1-1	TM4SF18	1	0	1	transmembrane 4 L six family member 18	116441
ECs0848	NleH1-1	TMEM180	1	0	1	transmembrane protein 180	79847
ECs0848	NleH1-1	TMEM184B	1	0	1	transmembrane protein 184B	25829
ECs0848	NleH1-1	TYMP	1	0	1	thymidine phosphorylase	1890
ECs0848	NleH1-1	UBE2D1	1	0	1	ubiquitin-conjugating enzyme E2D 1 (UBC4/5 homolog, yeast)	7321
ECs0848	NleH1-1	ZNF385C	1	0	1	zinc finger protein 385C	201181
ECs0848	NleH1-1	AATF	1	0	2	apoptosis antagonizing transcription factor	26574
ECs0848	NleH1-1	ASCC3	1	0	2	activating signal cointegrator 1 complex subunit 3	10973
ECs0848	NleH1-1	COX7B2	1	0	2	cytochrome c oxidase subunit VIIb2	170712
ECs0848	NleH1-1	DCUN1D1	1	0	2	DCN1, defective in cullin neddylation 1, domain containing 1 (S. cerevisiae)	54165
ECs0848	NleH1-1	DDX54	1	0	2	DEAD (Asp-Glu-Ala-Asp) box polypeptide 54	79039
ECs0848	NleH1-1	HSBP1	1	0	2	heat shock factor binding protein 1	3281
ECs0848	NleH1-1	IL24	1	0	2	interleukin 24	11009
ECs0848	NleH1-1	LRTM1	1	0	2	leuclne-rich repeats and transmembrane domains 1	57408
ECs0848	NleH1-1	PARL	1	0	2	presenilin associated, rhomboid-like	55486
ECs0848	NleH1-1	RNASE6	1	0	2	ribonuclease, RNase A family, k6	6039
ECs0848	NleH1-1	SYNJ2BP	1	0	2	synaptojanin 2 binding protein	55333
ECs0848	NleH1-1	IFI27	1	0	3	interferon, alpha-inducIble protein 27	3429
ECs0848	NleH1-1	NDUFV3	1	0	6	NADH dehydrogenase (ubiquinone) flavoprotein 3, 10kDa	4731
ECs0848	NleH1-1	NEK2	1	0	6	NIMA (never in mitosis gene a)-related kinase 2	4751
ECs0848	NleH1-1	HBA1	1	0	7	hemoglobin, alpha 1	3039
ECs0848	NleH1-1	SEP15	1	0	7	15 kDa selenoprotein	9403

ECs0848	NleH1-1	HBA2	1	0	13	hemoglobin, alpha 2	3040
ECs0848	NleH1-1	LOC100170939	1	0	3	glucuronidase, beta pseudogene	100170939
ECs0848	NleH1-1	LOC653391	1	0	3	glucuronidase, beta pseudogene	653391
ECs0848	NleH1-1	RBMS2	1	0	3	RNA binding motif, single stranded interacting protein 2	5939
ECs0848	NleH1-1	RPL14	1	0	3	ribosomal protein L14	9045
ECs0848	NleH1-1	PSMB2	1	0	4	proteasome (prosome, macropain) subunit, beta type, 2	5690
ECs0848	NleH1-1	RPL37A	1	0	5	ribosomal protein L37a	6168
ECs0848	NleH1-1	DUSP13	1	1	1	dual specIficIty phosphatase 13	51207
ECs0848	NleH1-1	FOXN3	1	1	2	forkhead box N3	1112
ECs0848	NleH1-1	PRKCH	1	1	2	protein kinase C, eta	5583
ECs0848	NleH1-1	STK10	1	1	5	serine/threonine kinase 10	6793
ECs0850	NleD	METTL2A	6	0	1	methyltransferase like 2A	339175
ECs0850	NleD	OTX2	3	0	55	orthodenticle homeobox 2	5015
ECs0850	NleD	MEOX2	3	0	87	mesenchyme homeobox 2	4223
ECs0850	NleD	CRX	3	0	138	cone-rod homeobox	1406
ECs0850	NleD	ATP5G1	1	0	2	ATP synthase, H+ transporting, mitochondrial F0 complex, subunit C1 (subunit 9)	516
ECs0850	NleD	XRCC6	1	0	9	X-ray repair complementing defective repair in Chinese hamster cells 6 (Ku autoantigen, 70kDa)	2547
ECs1567	EspO1-1	FEM1B	2	0	4	fem-1 homolog b (C. elegans)	10116
ECs1567	EspO1-1	Hs.722170	1	0	1		
ECs1567	EspO1-1	SSFA2	1	0	5	sperm specIfic antigen 2	6744
ECs1567	EspO1-1	CCDC117	1	1	1	coiled-coil domain containing 117	150275
ECs1567	EspO1-1	IPO7	1	1	1	importin 7	10527
ECs1567	EspO1-1	ZFPM2	1	1	1	zinc finger protein, multitype 2	23414
ECs1567	EspO1-1	DNAJB9	1	1	2	DnaJ (Hsp40) homolog, subfamily B, member 9	4189
ECs1567	EspO1-1	SFRS6	1	1	2	splicIng factor, arginine/serine-rich 6	6431
ECs1567	EspO1-1	CALU	1	1	3	calumenin	813
ECs1567	EspO1-1	COL5A2	1	1	3	collagen, type V, alpha 2	1290
ECs1568	EspK	GAS1	1	1	5	growth arrest-specIfic 1	2619
ECs1812	NleA	CDCA4	10	0	9	cell division cycle associated 4	55038
ECs1812	NleA	DSCR4	2	0	2	Down syndrome critical region gene 4	10281
ECs1812	NleA	FRMD3	1	0	1	FERM domain containing 3	257019
ECs1812	NleA	PENK	1	0	2	proenkephalin	5179
ECs1812	NleA	PTP4A1	1	0	2	protein tyrosine phosphatase type IVA, member 1	7803
ECs1812	NleA	SDHD	1	0	6	succInate dehydrogenase complex, subunit D	6392
ECs1814	NleH1-2	UFC1	2	0	2	ubiquitin-fold modifier	51506

						conjugating enzyme 1	
ECs1814	NleH1-2	DNAJC12	1	0	1	DnaJ (Hsp40) homolog, subfamily C, member 12	56521
ECs1814	NleH1-2	EIF1AY	1	0	1	eukaryotic translation initiation factor 1A, Y-linked	9086
ECs1814	NleH1-2	MITD1	1	0	1	MIT, microtubule interacting and transport, domain containing 1	129531
ECs1814	NleH1-2	RNF181	1	0	1	ring finger protein 181	51255
ECs1814	NleH1-2	HS3ST5	1	0	1	Heparan sulfate glucosamine 3-O-sulfotransferase	222537
ECs1814	NleH1-2	MTHFD2L	1	0	1	methylenetetrahydrofolate dehydrogenase (NADP+ dependent) 2-like	441024
ECs1814	NleH1-2	Hs.677634	1	0	1		
ECs1814	NleH1-2	AGXT2	1	0	1	alanine-glyoxylate aminotransferase 2	64902
ECs1814	NleH1-2	CDK13	1	0	1	CDK13 cyclin-dependent kinase 13 [	8621
ECs1814	NleH1-2	PLEKHA9	1	0	1	pleckstrin homology domain containing, family A (phosphoinositide binding specIfic) member 9	51054
ECs1814	NleH1-2	PWP1	1	0	1	PWP1 homolog (S. cerevisiae)	11137
ECs1814	NleH1-2	RBM5	1	0	1	RNA binding motif protein 5	10181
ECs1814	NleH1-2	ZNF287	1	0	1	zinc finger protein 287	57336
ECs1814	NleH1-2	COPS2	1	0	2	COP9 constitutive photomorphogenic homolog subunit 2 (Arabidopsis)	9318
ECs1814	NleH1-2	HEPH	1	0	2	hephaestin	9843
ECs1814	NleH1-2	PSMA4	1	0	3	proteasome (prosome, macropain) subunit, alpha type, 4	5685
ECs1814	NleH1-2	ATP2C1	1	1	1	ATPase, Ca++ transporting, type 2C, member 1	27032
ECs1814	NleH1-2	BBS10	1	1	1	Bardet-Biedl syndrome 10	79738
ECs1814	NleH1-2	CCDC50	1	1	1	coiled-coil domain containing 50	152137
ECs1814	NleH1-2	CDK17	1	1	1	CDK17 cyclin-dependent kinase 17	5128
ECs1814	NleH1-2	L3MBTL4	1	1	1	l(3)mbt-like 4 (Drosophila)	91133
ECs1814	NleH1-2	MAML3	1	1	1	mastermind-like 3	55534
ECs1814	NleH1-2	VPS13D	1	1	1	vacuolar protein sorting 13 homolog D	55187
ECs1814	NleH1-2	BAG5	1	1	2	BCL2-assoclated athanogene 5	9529
ECs1814	NleH1-2	C6orf62	1	1	2	chromosome 6 open reading frame 62	81688
ECs1814	NleH1-2	PPP1CC	1	1	2	protein phosphatase 1, catalytic subunit, gamma isoform	5501
ECs1814	NleH1-2	RAB31	1	1	2	RAB31, member RAS oncogene family	11031
ECs1814	NleH1-2	UBE2E2	1	1	2	ubiquitin-conjugating enzyme E2E 2 (UBC4/5 homolog, yeast)	7325

ECs1814	NleH1-2	HSP90AA1	1	1	3	heat shock protein 90kDa alpha (cytosolic), class A member 1	3320
ECs1814	NleH1-2	PCSK6	1	1	3	proprotein convertase subtilisin/kexin type 6	5046
ECs1814	NleH1-2	VAMP2	1	1	3	vesicle-associated membrane protein 2 (synaptobrevin 2)	6844
ECs1814	NleH1-2	ZBTB44	1	1	3	zinc finger and BTB domain containing 44	29068
ECs1814	NleH1-2	GMFB	1	1	5	glia maturation factor, beta	2764
ECs1814	NleH1-2	SFRS3	1	1	6	splicIng factor, arginine/serine-rich 3	6428
ECs1814	NleH1-2	CTDSP2	1	1	15	CTD (carboxy-terminal domain, RNA polymerase II, polypeptide A) small phosphatase 2	10106
ECs1815	NleF	CASP9	49	0	1	caspase 9, apoptosis-related cysteine peptidase	842
ECs1815	NleF	DHFR	21	0	1	dihydrofolate reductase	1719
ECs1815	NleF	BEND7	4	0	32	BEN domain containing 7	222389
ECs1815	NleF	FAM13A	1	0	1	family with sequence similarity 13, member A	10144
ECs1815	NleF	FAM181B	1	0	1	family with sequence similarity 181, member B	220382
ECs1815	NleF	WFDC2	1	0	1	WAP four-disulfide core domain 2	10406
ECs1815	NleF	ERI3	1	0	2	ERI3 exoribonuclease 3 [Homo sapiens]	79033
ECs1815	NleF	GUSBL1	1	0	2	glucuronidase, beta-like 1	387036
ECs1815	NleF	HMGN2	1	0	2	high-mobility group nucleosomal binding domain 2	3151
ECs1815	NleF	LMO4	1	0	2	LIM domain only 4	8543
ECs1815	NleF	LOC100170939	1	0	3	glucuronidase, beta pseudogene	100170939
ECs1815	NleF	LOC653391	1	0	3	glucuronidase, beta pseudogene	653391
ECs1815	NleF	TRNT1	1	0	3	tRNA nucleotidyl transferase, CCA-adding, 1	51095
ECs1815	NleF	TIMM8A	1	0	6	translocase of inner mitochondrial membrane 8 homolog A (yeast)	1678
ECs1815	NleF	CDCA4	1	0	9	cell division cycle associated 4	55038
ECs1815	NleF	TIGD1	1	0	15	tigger transposable element derived 1	200765
ECs1824	NleG	ZNF343	15	0	8	zinc finger protein 343	79175
ECs1824	NleG	OTX2	7	0	55	orthodenticle homeobox 2	5015
ECs1824	NleG	CRX	5	0	138	cone-rod homeobox	1406
ECs1824	NleG	ALX1	4	0	15	ALX homeobox 1	8092
ECs1824	NleG	MEOX2	2	0	87	mesenchyme homeobox 2	4223
ECs1824	NleG	PILRB	1	0	1	paired immunoglobin-like type 2 receptor beta	29990
ECs1824	NleG	METTL8	1	0	1	methyltransferase like 8	79828
ECs1824	NleG	CNN3	1	0	1	calponin 3, acIdic	1266
ECs1824	NleG	CXCL10	1	0	1	chemokine (C-X-C motif) ligand 10	3627
ECs1824	NleG	CYFIP2	1	0	1	cytoplasmic FMR1 interacting protein 2	26999

ECs1824	NleG	DKC1	1	0	1	dyskeratosis congenita 1, dyskerin	1736
ECs1824	NleG	ENOSF1	1	0	1	enolase superfamily member 1	55556
ECs1824	NleG	GGCT	1	0	1	gamma-glutamyl cyclotransferase	79017
ECs1824	NleG	MMP28	1	0	1	matrix metallopeptidase 28	79148
ECs1824	NleG	MPPED2	1	0	1	metallophosphoesterase domain containing 2	744
ECs1824	NleG	RASGEF1C	1	0	1	RasGEF domain family, member 1C	255426
ECs1824	NleG	RMI1	1	0	1	RMI1, RecQ mediated genome instability 1, homolog (S. cerevisiae)	80010
ECs1824	NleG	RUVBL2	1	0	1	RuvB-like 2 (*E. coli*)	10856
ECs1824	NleG	SNX31	1	0	1	sorting nexin 31	169166
ECs1824	NleG	TFB1M	1	0	1	transcription factor B1, mitochondrial	51106
ECs1824	NleG	WIPI1	1	0	1	WD repeat domain, phosphoinositide interacting 1	55062
ECs1824	NleG	ZNF37A	1	0	1	zinc finger protein 37A	7587
ECs1824	NleG	TOMM7	1	0	2	translocase of outer mitochondrial membrane 7 homolog (yeast)	54543
ECs1824	NleG	LOC284912	1	0	2	hypothetical gene supported by BC001801	284912
ECs1824	NleG	DDX54	1	0	2	DEAD (Asp-Glu-Ala-Asp) box polypeptide 54	79039
ECs1824	NleG	SLC4A2	1	0	2	solute carrier family 4, anion exchanger, member 2 (erythrocyte membrane protein band 3-like 1)	6522
ECs1824	NleG	SNRNP25	1	0	2	SNRNP25 small nuclear ribonucleoprotein 25kDa (U11/U12)	79622
ECs1824	NleG	TBXAS1	1	0	2	thromboxane A synthase 1 (platelet, cytochrome P450, family 5, subfamily A)	6916
ECs1824	NleG	DEXI	1	0	3	dexamethasone-induced transcript	28955
ECs1824	NleG	HLA-DPB1	1	0	3	major histocompatibility complex, class II, DP beta 1	3115
ECs1824	NleG	SPINK2	1	0	3	serine peptidase inhibitor, Kazal type 2 (acrosin-trypsin inhibitor)	6691
ECs1824	NleG	TALDO1	1	0	3	transaldolase 1	6888
ECs1824	NleG	FBXO8	1	0	4	F-box protein 8	26269
ECs1824	NleG	OLA1	1	0	4	Obg-like ATPase 1	29789
ECs1824	NleG	PSMC1	1	0	4	proteasome (prosome, macropain) 26S subunit, ATPase, 1	5700
ECs1824	NleG	PARP14	1	1	2	poly (ADP-ribose) polymerase family, member 14	54625
ECs1824	NleG	CBX4	1	0	6	chromobox homolog 4 (Pc class homolog, Drosophila)	8535
ECs1824	NleG	SDHD	1	0	6	succInate dehydrogenase complex, subunit D	6392

ECs1824	NleG	TIMM8A	1	0	6	translocase of inner mitochondrial membrane 8 homolog A (yeast)	1678
ECs1994	NleG2-2	Hs.575672	1	0	1		
ECs1994	NleG2-2	Hs.722049	1	0	1		
ECs1994	NleG2-2	ALDH7A1	1	0	1	aldehyde dehydrogenase 7 family, member A1	501
ECs1994	NleG2-2	FLJ43950	1	0	1	FLJ43950 protein	347127
ECs1994	NleG2-2	KIF2B	1	0	1	kinesin family member 2B	84643
ECs1994	NleG2-2	OR7E156P	1	0	1	olfactory receptor, family 7, subfamily E, member 156 pseudogene	283491
ECs1994	NleG2-2	RBM6	1	0	1	RNA binding motif protein 6	10180
ECs1994	NleG2-2	SERPINI1	1	0	1	serpin peptidase inhibitor, clade I (neuroserpin), member 1	5274
ECs1994	NleG2-2	THAP10	1	0	1	THAP domain containing 10	56906
ECs1994	NleG2-2	GHITM	1	0	2	growth hormone inducIble transmembrane protein	27069
ECs1994	NleG2-2	ANK3	1	0	4	ankyrin 3, node of Ranvier (ankyrin G)	288
ECs1994	NleG2-2	ARAP3	1	1	1	ARAP3 ArfGAP with RhoGAP domain, ankyrin repeat and PH domain 3	64411
ECs1994	NleG2-2	RRAS2	1	1	1	related RAS viral (r-ras) oncogene homolog 2	22800
ECs1994	NleG2-2	RYK	1	1	2	RYK receptor-like tyrosine kinase	6259
ECs1994	NleG2-2	STX7	1	1	2	syntaxin 7	8417
ECs1994	NleG2-2	GAS1	1	1	5	growth arrest-speclfic 1	2619
ECs1994	NleG2-2	MTMR9	1	1	7	myotubularin related protein 9	66036
ECs2714	EspJ	IFT20	20	0	2	intraflagellar transport 20 homolog (Chlamydomonas)	90410
ECs2714	EspJ	RIC8A	15	0	5	resistance to inhibitors of cholinesterase 8 homolog A (C. elegans)	60626
ECs2714	EspJ	CENPH	13	0	1	centromere protein H	64946
ECs2714	EspJ	CETN1	1	0	1	centrin, EF-hand protein, 1	1068
ECs2714	EspJ	MRFAP1L1	1	0	2	Morf4 family assoclated protein 1-like 1	114932
ECs2715	TccP	ZNF626	2	0	2	zinc finger protein 626	199777
ECs2715	TccP	Hs.595320	1	0	1		
ECs2715	TccP	Hs.686358	1	0	1		
ECs2715	TccP	CCDC45	1	0	1	coiled-coil domain containing 45	90799
ECs2715	TccP	CES1	1	0	1	carboxylesterase 1 (monocyte/macrophage serine esterase 1)	1066
ECs2715	TccP	MIOS	1	0	1	MIOS missing oocyte, meiosis regulator, homolog (Drosophila)	54468
ECs2715	TccP	MYO5B	1	0	1	myosin VB	4645
ECs2715	TccP	SNHG10	1	0	1	small nucleolar RNA host gene 10 (non-protein coding)	283596
ECs2715	TccP	DBNDD2	1	0	2	dysbindin (dystrobrevin binding protein 1) domain containing 2	55861

ECs2715	TccP	ATP5B	1	0	2	ATP synthase, H+ transporting, mitochondrial F1 complex, beta polypeptide	506
ECs2715	TccP	KIAA2026	1	0	2	KIAA2026	158358
ECs2715	TccP	OGT	1	0	2	O-linked N-acetylglucosamine (GlcNAc) transferase (UDP-N-acetylglucosamine:polypeptide-N-acetylglucosaminyl transferase)	8473
ECs2715	TccP	SH3GLB1	1	0	2	SH3-domain GRB2-like endophilin B1	51100
ECs2715	TccP	SH3BGRL	1	0	3	SH3 domain binding glutamic acId-rich protein like	6451
ECs2715	TccP	CCDC80	1	0	3	coiled-coil domain containing 80	151887
ECs2715	TccP	RNF6	1	0	3	ring finger protein (C3H2C3 type) 6	6049
ECs2715	TccP	TTC29	1	0	3	tetratricopeptide repeat domain 29	83894
ECs2715	TccP	IMMT	1	0	5	inner membrane protein, mitochondrial (mitofilin)	10989
ECs2715	TccP	RAB11A	1	0	5	RAB11A, member RAS oncogene family	8766
ECs2715	TccP	ANKIB1	1	1	1	ankyrin repeat and IBR domain containing 1	54467
ECs2715	TccP	FGF13	1	1	1	fibroblast growth factor 13	2258
ECs2715	TccP	IFT80	1	1	1	intraflagellar transport 80 homolog (Chlamydomonas)	57560
ECs2715	TccP	KTELC1	1	1	1	KTEL (Lys-Tyr-Glu-Leu) containing 1	56983
ECs2715	TccP	SLC35E2	1	1	1	solute carrier family 35, member E2	9906
ECs2715	TccP	UBQLN2	1	1	1	ubiquilin 2	29978
ECs2715	TccP	SGCB	1	1	2	sarcoglycan, beta (43kDa dystrophin-assoclated glycoprotein)	6443
ECs2715	TccP	LAMP2	1	1	4	lysosomal-assoclated membrane protein 2	3920
ECs2715	TccP	MPV17	1	0	6	MpV17 mitochondrial inner membrane protein	4358
ECs2715	TccP	PALLD	1	1	12	palladin, cytoskeletal assoclated protein	23022
ECs3857	NleB1	ZNF343	98	0	8	zinc finger protein 343	79175
ECs3857	NleB1	XRCC6	7	0	9	X-ray repair complementing defective repair in Chinese hamster cells 6 (Ku autoantigen, 70kDa)	2547
ECs3857	NleB1	LRRC18	7	0	2	leuclne rich repeat containing 18	474354
ECs3857	NleB1	DRG2	5	0	4	developmentally regulated GTP binding protein 2	1819
ECs3857	NleB1	POLR2E	3	0	1	polymerase (RNA) II (DNA directed) polypeptide E, 25kDa	5434
ECs3857	NleB1	CDRT4	1	0	1	CMT1A duplicated region transcript 4	284040
ECs3857	NleB1	GUSBP3	1	0	1	GUSBP3 glucuronidase, beta pseudogene 3	653188

ECs3857	NleB1	LOC100287046	1	0	1	glucuronidase, beta pseudogene	100287046
ECs3857	NleB1	LOC100287078	1	0	1		
ECs3857	NleB1	PCGF1	1	0	1	polycomb group ring finger 1	84759
ECs3857	NleB1	SLC6A13	1	0	1	solute carrier family 6 (neurotransmitter transporter, GABA), member 13	6540
ECs3857	NleB1	YPEL3	1	0	2	yippee-like 3 (Drosophila)	83719
ECs3857	NleB1	MGC4294	1	0	2	hypothetical protein MGC4294	79160
ECs3857	NleB1	GOSR2	1	0	3	golgi SNAP receptor complex member 2	9570
ECs3857	NleB1	LOC100170939	1	0	3	glucuronidase, beta pseudogene	100170939
ECs3857	NleB1	LOC653391	1	0	3	glucuronidase, beta pseudogene	653391
ECs3857	NleB1	TTC29	1	0	3	tetratricopeptide repeat domain 29	83894
ECs3857	NleB1	PCID2	1	0	4	PCI domain-containing protein 2 (CSN12-like protein).	55795
ECs3857	NleB1	TTC19	1	0	4	tetratricopeptide repeat domain 19	54902
ECs3857	NleB1	TIGD1	1	0	15	tigger transposable element derived 1	200765
ECs3857	NleB1	BEND7	1	0	32	BEN domain containing 7	222389
ECs3858	NleE	ZNF343	11	0	8	zinc finger protein 343	79175
ECs3858	NleE	ADIG	1	0	1	adipogenin	149685
ECs3858	NleE	LRRC18	1	0	2	leucIne rich repeat containing 18	474354
ECs4550	EspF1	SNX33	16	0	1	sorting nexin 33	257364
ECs4550	EspF1	SNX9	2	0	1	sorting nexin 9	51429
ECs4550	EspF1	MAD2L2	1	0	2	MAD2 mitotic arrest deficIent-like 2 (yeast)	10459
ECs4554	EspB	RBCK1	78	0	5	RanBP-type and C3HC4-type zinc finger containing 1	10616
ECs4554	EspB	STK16	48	0	3	serine/threonine kinase 16	8576
ECs4554	EspB	VEGFB	9	0	8	vascular endothelial growth factor B	7423
ECs4554	EspB	SNX3	3	0	12	sorting nexin 3	8724
ECs4554	EspB	SNAPC5	1	0	1	small nuclear RNA activating complex, polypeptide 5, 19kDa	10302
ECs4554	EspB	PCID2	1	0	4	PCI domain-containing protein 2 (CSN12-like protein).	55795
ECs4554	EspB	URM1	1	0	7	ubiquitin related modifier 1 homolog (S. cerevisiae)	81605
ECs4561	TIR	HPCAL1	56	0	4	hippocalcIn-like 1	3241
ECs4561	TIR	MCRS1	33	0	6	microspherule protein 1	10445
ECs4561	TIR	STK16	11	0	3	serine/threonine kinase 16	8576
ECs4561	TIR	NCALD	7	0	1	neurocalcIn delta	83988
ECs4561	TIR	TIGD1	6	0	16	tigger transposable element derived 1	200765
ECs4561	TIR	BAIAP2L1	5	0	1	BAI1-assoclated protein 2-like 1	55971
ECs4561	TIR	TTC1	3	0	6	tetratricopeptide repeat domain 1	7265

ECs4561	TIR	ARRB1	2	0	2	arrestin, beta 1	408
ECs4561	TIR	BAIAP2	2	0	3	BAI1-assoclated protein 2	10458
ECs4561	TIR	HPCAL4	1	0	1	hippocalcln like 4	51440
ECs4561	TIR	RPAP3	1	1	1	RNA polymerase II assoclated protein 3	79657
ECs4561	TIR	PDE6D	1	0	3	phosphodiesterase 6D, cGMP-speclfic, rod, delta	5147
ECs4562	Map	PNMA1	22	0	7	paraneoplastic antigen MA1	9240
ECs4562	Map	RING1	15	0	11	ring finger protein 1	6015
ECs4562	Map	SLC9A3R2	13	0	2	solute carrier family 9 (sodium/hydrogen exchanger), member 3 regulator 2	9351
ECs4562	Map	RHPN1	3	0	2	rhophilin, Rho GTPase binding protein 1	114822
ECs4562	Map	BEND7	1	0	32	BEN domain containing 7	222389
ECs4562	Map	CLK1	1	0	3	CDC-like kinase 1	1195
ECs4562	Map	DSCR4	1	0	2	Down syndrome critical region gene 4	10281
ECs4562	Map	GALNT10	1	0	1	UDP-N-acetyl-alpha-D-galactosamine:polypeptide N-acetylgalactosaminyltransferase 10 (GalNAc-T10)	55568
ECs4562	Map	SDHD	1	0	6	succlnate dehydrogenase complex, subunit D, integral membrane protein	6392
ECs4562	Map	TIGD1	1	0	15	tigger transposable element derived 1	200765
ECs4564	EspH	ABCG2	1	0	2	ATP-binding cassette, sub-family G (WHITE), member 2	9429
ECs4564	EspH	COPS5	1	0	110	COP9 constitutive photomorphogenic homolog subunit 5 (Arabidopsis) [Homo sapiens]	10987
ECs4590	EspG	Hs.658052	3	0	1		100589704
ECs4590	EspG	NMI	1	0	1	N-myc (and STAT) interactor	9111
ECs4590	EspG	NCOA3	1	0	2	nuclear receptor coactivator 3	8202
ECs4590	EspG	C5orf15	1	1	1	chromosome 5 open reading frame 15	56951
ECs4590	EspG	COL5A2	1	1	3	collagen, type V, alpha 2	1290

Supplementary table 2. Published intraspecies interactions of the human interaction partners of EHEC effectors. The column 'Direct' contains the human interactors of EHEC effector proteins, whereas the column 'Indirect' contains published intraspecies interactions of these proteins.

No.	Direct	Description	Indirect	Description
1	ARRB1	arrestin, beta 1	ADRB1	adrenergic, beta-1-, receptor
2	ARRB1	arrestin, beta 1	AP3B1	adaptor-related protein complex 3, beta 1 subunit
3	ARRB1	arrestin, beta 1	ARF6	ADP-ribosylation factor 6
4	ARRB1	arrestin, beta 1	ARR3	arrestin 3, retinal (X-arrestin)
5	ARRB1	arrestin, beta 1	ARRB2	arrestin, beta 2
6	ARRB1	arrestin, beta 1	BOP1	block of proliferation 1
7	ARRB1	arrestin, beta 1	CCL14	chemokine (C-C motif) ligand 14
8	ARRB1	arrestin, beta 1	CCR5	chemokine (C-C motif) receptor 5
9	ARRB1	arrestin, beta 1	CDC42	cell division cycle 42 (GTP binding protein, 25kDa)
10	ARRB1	arrestin, beta 1	CHD1	chromodomain helicase DNA binding protein 1
11	ARRB1	arrestin, beta 1	CMBL	carboxymethylenebutenolidase homolog (Pseudomonas)
12	ARRB1	arrestin, beta 1	CSK	c-src tyrosine kinase
13	ARRB1	arrestin, beta 1	CSNK2A1	casein kinase 2, alpha 1 polypeptide
14	ARRB1	arrestin, beta 1	CXCR2	chemokine (C-X-C motif) receptor 2
15	ARRB1	arrestin, beta 1	CYTH2	cytohesin 2
16	ARRB1	arrestin, beta 1	DDX27	DEAD (Asp-Glu-Ala-Asp) box polypeptide 27
17	ARRB1	arrestin, beta 1	DVL1	dishevelled, dsh homolog 1 (Drosophila)
18	ARRB1	arrestin, beta 1	DVL2	dishevelled, dsh homolog 2 (Drosophila)
19	ARRB1	arrestin, beta 1	GNMT	glycine N-methyltransferase
20	ARRB1	arrestin, beta 1	HDGFRP2	hepatoma-derived growth factor-related protein 2
21	ARRB1	arrestin, beta 1	ITCH	itchy E3 ubiquitin protein ligase homolog (mouse)
22	ARRB1	arrestin, beta 1	JAK1	Janus kinase 1 (a protein tyrosine kinase)
23	ARRB1	arrestin, beta 1	JUN	jun oncogene
24	ARRB1	arrestin, beta 1	KHK	ketohexokinase (fructokinase)
25	ARRB1	arrestin, beta 1	KPNA3	karyopherin alpha 3 (importin alpha 4)
26	ARRB1	arrestin, beta 1	MAPK10	mitogen-activated protein kinase 10
27	ARRB1	arrestin, beta 1	MDM2	Mdm2 p53 binding protein homolog (mouse)
28	ARRB1	arrestin, beta 1	NEDD4	neural precursor cell expressed, developmentally down-regulated 4
29	ARRB1	arrestin, beta 1	NOLC1	nucleolar and coiled-body phosphoprotein 1
30	ARRB1	arrestin, beta 1	NSF	N-ethylmaleimide-sensitive factor
31	ARRB1	arrestin, beta 1	OPRD1	opioid receptor, delta 1
32	ARRB1	arrestin, beta 1	PES1	pescadillo homolog 1, containing BRCT domain (zebrafish)
33	ARRB1	arrestin, beta 1	PTHLH	parathyroid hormone-like hormone
34	ARRB1	arrestin, beta 1	RALGDS	ral guanine nucleotide dissociation stimulator
35	ARRB1	arrestin, beta 1	RPL7L1	ribosomal protein L7-like 1
36	ARRB1	arrestin, beta 1	RTF1	Rtf1, Paf1/RNA polymerase II complex component, homolog (S. cerevisiae)

37	ARRB1	arrestin, beta 1	SREBF2	sterol regulatory element binding transcription factor 2
38	ARRB1	arrestin, beta 1	TCOF1	Treacher Collins-Franceschetti syndrome 1
39	ARRB1	arrestin, beta 1	ZBTB43	zinc finger and BTB domain containing 43
40	ARRB1	arrestin, beta 1	ZRANB2	zinc finger, RAN-binding domain containing 2
41	BAIAP2	BAI1-associated protein 2	ATN1	atrophin 1
42	BAIAP2	BAI1-associated protein 2	C14orf1	chromosome 14 open reading frame 1
43	BAIAP2	BAI1-associated protein 2	CDC42	cell division cycle 42 (GTP binding protein, 25kDa)
44	BAIAP2	BAI1-associated protein 2	ENAH	enabled homolog (Drosophila)
45	BAIAP2	BAI1-associated protein 2	EPS8	epidermal growth factor receptor pathway substrate 8
46	BAIAP2	BAI1-associated protein 2	NCKIPSD	NCK interacting protein with SH3 domain
47	BAIAP2	BAI1-associated protein 2	PAK1	p21 protein (Cdc42/Rac)-activated kinase 1
48	BAIAP2	BAI1-associated protein 2	RAC1	ras-related C3 botulinum toxin substrate 1 (rho family, small GTP binding protein Rac1)
49	BAIAP2	BAI1-associated protein 2	SHANK1	SH3 and multiple ankyrin repeat domains 1
50	BAIAP2	BAI1-associated protein 2	WASF1	WAS protein family, member 1
51	BAIAP2	BAI1-associated protein 2	WASF2	WAS protein family, member 2
52	BAIAP2	BAI1-associated protein 2	YWHAG	tyrosine 3-monooxygenase/tryptophan 5-monooxygenase activation protein, gamma polypeptide
53	BAIAP2L1	BAI1-associated protein 2-like 1	PRKAA2	protein kinase, AMP-activated, alpha 2 catalytic subunit
54	BAIAP2L1	BAI1-associated protein 2-like 1	PRKAB2	protein kinase, AMP-activated, beta 2 non-catalytic subunit
55	BAIAP2L1	BAI1-associated protein 2-like 1	TERF1	telomeric repeat binding factor (NIMA-interacting) 1
56	BAIAP2L1	BAI1-associated protein 2-like 1	TERF2	telomeric repeat binding factor 2
57	CAPN3	calpain 3, (p94)	FLNC	filamin C, gamma (actin binding protein 280)
58	CAPN3	calpain 3, (p94)	NECAB2	N-terminal EF-hand calcium binding protein 2
59	CAPN3	calpain 3, (p94)	TTN	titin
60	CASP9	caspase 9, apoptosis-related cysteine peptidase	APAF1	apoptotic peptidase activating factor 1
61	CASP9	caspase 9, apoptosis-related cysteine peptidase	BCL2L1	BCL2-like 1
62	CASP9	caspase 9, apoptosis-related cysteine peptidase	BIRC2	baculoviral IAP repeat-containing 2
63	CASP9	caspase 9, apoptosis-related cysteine peptidase	BIRC3	baculoviral IAP repeat-containing 3
64	CASP9	caspase 9, apoptosis-related cysteine peptidase	BIRC5	baculoviral IAP repeat-containing 5
65	CASP9	caspase 9, apoptosis-related cysteine peptidase	BIRC6	baculoviral IAP repeat-containing 6
66	CASP9	caspase 9, apoptosis-related cysteine peptidase	BIRC7	baculoviral IAP repeat-containing 7
67	CASP9	caspase 9, apoptosis-related cysteine peptidase	BIRC8	baculoviral IAP repeat-containing 8

68	CASP9	caspase 9, apoptosis-related cysteine peptidase	CASP10	caspase 10, apoptosis-related cysteine peptidase
69	CASP9	caspase 9, apoptosis-related cysteine peptidase	CASP2	caspase 2, apoptosis-related cysteine peptidase
70	CASP9	caspase 9, apoptosis-related cysteine peptidase	CASP8	caspase 8, apoptosis-related cysteine peptidase
71	CASP9	caspase 9, apoptosis-related cysteine peptidase	DCC	deleted in colorectal carcinoma
72	CASP9	caspase 9, apoptosis-related cysteine peptidase	MAPK1	mitogen-activated protein kinase 1
73	CASP9	caspase 9, apoptosis-related cysteine peptidase	NAIP	NLR family, apoptosis inhibitory protein
74	CASP9	caspase 9, apoptosis-related cysteine peptidase	NLRP1	NLR family, pyrin domain containing 1
75	CASP9	caspase 9, apoptosis-related cysteine peptidase	NOD1	nucleotide-binding oligomerization domain containing 1
76	CASP9	caspase 9, apoptosis-related cysteine peptidase	RNF2	ring finger protein 2
77	CASP9	caspase 9, apoptosis-related cysteine peptidase	UBC	ubiquitin C
78	CASP9	caspase 9, apoptosis-related cysteine peptidase	XIAP	X-linked inhibitor of apoptosis
79	CENPH	centromere protein H	CENPA	centromere protein A
80	CENPH	centromere protein H	CENPH	centromere protein H
81	CENPH	centromere protein H	KIF2C	kinesin family member 2C
82	CENPH	centromere protein H	PMVK	phosphomevalonate kinase
83	DHFR	dihydrofolate reductase	FKBP1A	FK506 binding protein 1A, 12kDa
84	DHFR	dihydrofolate reductase	HSPD1	heat shock 60kDa protein 1 (chaperonin)
85	DHFR	dihydrofolate reductase	MDM2	Mdm2 p53 binding protein homolog (mouse)
86	DHFR	dihydrofolate reductase	THBS1	thrombospondin 1
87	DHFR	dihydrofolate reductase	TP53	tumor protein p53
88	DHFR	dihydrofolate reductase	SUMO2	SMT3 suppressor of mif two 3 homolog 2 (S. cerevisiae)
89	DHFR	dihydrofolate reductase	UBC	ubiquitin C
90	DNAJC14	DnaJ (Hsp40) homolog, subfamily C, member 14	DRD1	dopamine receptor D1
91	DNAJC14	DnaJ (Hsp40) homolog, subfamily C, member 14	LYST	lysosomal trafficking regulator
92	DRG2	developmentally regulated GTP binding protein 2	RWDD1	RWD domain containing 1
93	FEM1B	fem-1 homolog b (C. elegans)	COPS6	COP9 constitutive photomorphogenic homolog subunit 6 (Arabidopsis)
94	HPCAL1	hippocalcin-like 1	DTX2	deltex homolog 2 (Drosophila)
95	HPCAL1	hippocalcin-like 1	HMG20A	high-mobility group 20A
96	HPCAL1	hippocalcin-like 1	IKBKG	inhibitor of kappa light polypeptide gene enhancer in B-cells, kinase gamma
97	IFT20	intraflagellar transport 20 homolog (Chlamydomonas)	ABI2	abl interactor 2
98	IFT20	intraflagellar transport 20 homolog (Chlamydomonas)	C19orf50	chromosome 19 open reading frame 50
99	IFT20	intraflagellar transport 20 homolog (Chlamydomonas)	EXOC7	exocyst complex component 7
100	IFT20	intraflagellar transport 20 homolog (Chlamydomonas)	FBF1	Fas (TNFRSF6) binding factor 1
101	IFT20	intraflagellar transport 20 homolog (Chlamydomonas)	TREX1	three prime repair exonuclease 1

102	LRRC18	leucine rich repeat containing 18	KCTD17	potassium channel tetramerisation domain containing 17
103	NCALD	neurocalcin delta	ACTB	actin, beta
104	NCALD	neurocalcin delta	DTX2	deltex homolog 2 (Drosophila)
105	PCID2	PCI domain containing 2	NEK6	NIMA (never in mitosis gene a)-related kinase 6
106	PCID2	PCI domain containing 2	SHFM1	split hand/foot malformation (ectrodactyly) type 1
107	PIH1D1	PIH1 domain containing 1	C8orf41	chromosome 8 open reading frame 41
108	PIH1D1	PIH1 domain containing 1	FBL	fibrillarin
109	PIH1D1	PIH1 domain containing 1	GPN1	GPN-loop GTPase 1
110	PIH1D1	PIH1 domain containing 1	RPAP2	RNA polymerase II associated protein 2
111	PIH1D1	PIH1 domain containing 1	RPAP3	RNA polymerase II associated protein 3
112	PIH1D1	PIH1 domain containing 1	RUVBL1	RuvB-like 1 (*E. coli*)
113	PIH1D1	PIH1 domain containing 1	RUVBL2	RuvB-like 2 (*E. coli*)
114	PIH1D1	PIH1 domain containing 1	TSC22D4	TSC22 domain family, member 4
115	PIH1D1	PIH1 domain containing 1	TTI1	TELO2 interacting protein 1
116	POLR2E	polymerase (RNA) II (DNA directed) polypeptide E, 25kDa	C19orf2	chromosome 19 open reading frame 2
117	POLR2E	polymerase (RNA) II (DNA directed) polypeptide E, 25kDa	GTF2F2	general transcription factor IIF, polypeptide 2, 30kDa
118	POLR2E	polymerase (RNA) II (DNA directed) polypeptide E, 25kDa	IKBKG	inhibitor of kappa light polypeptide gene enhancer in B-cells, kinase gamma
119	POLR2E	polymerase (RNA) II (DNA directed) polypeptide E, 25kDa	INTS3	integrator complex subunit 3
120	POLR2E	polymerase (RNA) II (DNA directed) polypeptide E, 25kDa	INTS5	integrator complex subunit 5
121	POLR2E	polymerase (RNA) II (DNA directed) polypeptide E, 25kDa	INTS6	integrator complex subunit 6
122	POLR2E	polymerase (RNA) II (DNA directed) polypeptide E, 25kDa	ITCH	itchy E3 ubiquitin protein ligase homolog (mouse)
123	POLR2E	polymerase (RNA) II (DNA directed) polypeptide E, 25kDa	LZTR1	leucine-zipper-like transcription regulator 1
124	POLR2E	polymerase (RNA) II (DNA directed) polypeptide E, 25kDa	MED1	mediator complex subunit 1
125	POLR2E	polymerase (RNA) II (DNA directed) polypeptide E, 25kDa	MED10	mediator complex subunit 10
126	POLR2E	polymerase (RNA) II (DNA directed) polypeptide E, 25kDa	MED12	mediator complex subunit 12
127	POLR2E	polymerase (RNA) II (DNA directed) polypeptide E, 25kDa	MED19	mediator complex subunit 19
128	POLR2E	polymerase (RNA) II (DNA directed) polypeptide E, 25kDa	MED26	mediator complex subunit 26
129	POLR2E	polymerase (RNA) II (DNA directed) polypeptide E, 25kDa	MED28	mediator complex subunit 28
130	POLR2E	polymerase (RNA) II (DNA directed) polypeptide E, 25kDa	MED29	mediator complex subunit 29
131	POLR2E	polymerase (RNA) II (DNA directed) polypeptide E, 25kDa	MED9	mediator complex subunit 9
132	POLR2E	polymerase (RNA) II (DNA directed) polypeptide E, 25kDa	NEDD4	neural precursor cell expressed, developmentally down-regulated 4
133	POLR2E	polymerase (RNA) II (DNA directed) polypeptide E, 25kDa	PML	promyelocytic leukemia
134	POLR2E	polymerase (RNA) II (DNA directed) polypeptide E, 25kDa	POLR1A	polymerase (RNA) I polypeptide A, 194kDa
135	POLR2E	polymerase (RNA) II (DNA directed) polypeptide E, 25kDa	POLR2A	polymerase (RNA) II (DNA directed) polypeptide A, 220kDa

136	POLR2E	polymerase (RNA) II (DNA directed) polypeptide E, 25kDa	POLR2B	polymerase (RNA) II (DNA directed) polypeptide B, 140kDa
137	POLR2E	polymerase (RNA) II (DNA directed) polypeptide E, 25kDa	POLR2C	polymerase (RNA) II (DNA directed) polypeptide C, 33kDa
138	POLR2E	polymerase (RNA) II (DNA directed) polypeptide E, 25kDa	POLR2E	polymerase (RNA) II (DNA directed) polypeptide E, 25kDa
139	POLR2E	polymerase (RNA) II (DNA directed) polypeptide E, 25kDa	POLR2F	polymerase (RNA) II (DNA directed) polypeptide F
140	POLR2E	polymerase (RNA) II (DNA directed) polypeptide E, 25kDa	POLR2G	polymerase (RNA) II (DNA directed) polypeptide G
141	POLR2E	polymerase (RNA) II (DNA directed) polypeptide E, 25kDa	POLR2H	polymerase (RNA) II (DNA directed) polypeptide H
142	POLR2E	polymerase (RNA) II (DNA directed) polypeptide E, 25kDa	POLR2J	polymerase (RNA) II (DNA directed) polypeptide J, 13.3kDa
143	POLR2E	polymerase (RNA) II (DNA directed) polypeptide E, 25kDa	POLR2K	polymerase (RNA) II (DNA directed) polypeptide K, 7.0kDa
144	POLR2E	polymerase (RNA) II (DNA directed) polypeptide E, 25kDa	POLR2L	polymerase (RNA) II (DNA directed) polypeptide L, 7.6kDa
145	POLR2E	polymerase (RNA) II (DNA directed) polypeptide E, 25kDa	POLR3D	polymerase (RNA) III (DNA directed) polypeptide D, 44kDa
146	POLR2E	polymerase (RNA) II (DNA directed) polypeptide E, 25kDa	RPAP3	RNA polymerase II associated protein 3
147	POLR2E	polymerase (RNA) II (DNA directed) polypeptide E, 25kDa	RUVBL2	RuvB-like 2 (*E. coli*)
148	POLR2E	polymerase (RNA) II (DNA directed) polypeptide E, 25kDa	STAP1	signal transducing adaptor family member 1
149	POLR2E	polymerase (RNA) II (DNA directed) polypeptide E, 25kDa	TAF10	TAF10 RNA polymerase II, TATA box binding protein (TBP)-associated factor, 30kDa
150	POLR2E	polymerase (RNA) II (DNA directed) polypeptide E, 25kDa	TAF15	TAF15 RNA polymerase II, TATA box binding protein (TBP)-associated factor, 68kDa
151	POLR2E	polymerase (RNA) II (DNA directed) polypeptide E, 25kDa	TRIM29	tripartite motif-containing 29
152	POLR2E	polymerase (RNA) II (DNA directed) polypeptide E, 25kDa	USP11	ubiquitin specific peptidase 11
153	POLR2E	polymerase (RNA) II (DNA directed) polypeptide E, 25kDa	XRCC5	X-ray repair complementing defective repair in Chinese hamster cells 5 (double-strand-break rejoining)
154	POLR2E	polymerase (RNA) II (DNA directed) polypeptide E, 25kDa	ZSCAN1	zinc finger and SCAN domain containing 1
155	PSMC1	proteasome (prosome, macropain) 26S subunit, ATPase, 1	ATG4C	ATG4 autophagy related 4 homolog C (S. cerevisiae)
156	PSMC1	proteasome (prosome, macropain) 26S subunit, ATPase, 1	ATXN7	ataxin 7
157	PSMC1	proteasome (prosome, macropain) 26S subunit, ATPase, 1	CCDC85B	coiled-coil domain containing 85B
158	PSMC1	proteasome (prosome, macropain) 26S subunit, ATPase, 1	PAAF1	proteasomal ATPase-associated factor 1
159	PSMC1	proteasome (prosome, macropain) 26S subunit, ATPase, 1	PMS1	PMS1 postmeiotic segregation increased 1 (S. cerevisiae)
160	PSMC1	proteasome (prosome, macropain) 26S subunit, ATPase, 1	PMS2	PMS2 postmeiotic segregation increased 2 (S. cerevisiae)
161	PSMC1	proteasome (prosome, macropain) 26S subunit, ATPase, 1	PSMC2	proteasome (prosome, macropain) 26S subunit, ATPase, 2
162	PSMC1	proteasome (prosome, macropain) 26S subunit, ATPase, 1	PSMC4	proteasome (prosome, macropain) 26S subunit, ATPase, 4

163	PSMC1	proteasome (prosome, macropain) 26S subunit, ATPase, 1	PSMC5	proteasome (prosome, macropain) 26S subunit, ATPase, 5
164	PSMC1	proteasome (prosome, macropain) 26S subunit, ATPase, 1	PSMD10	proteasome (prosome, macropain) 26S subunit, non-ATPase, 10
165	PSMC1	proteasome (prosome, macropain) 26S subunit, ATPase, 1	PSMD13	proteasome (prosome, macropain) 26S subunit, non-ATPase, 13
166	PSMC1	proteasome (prosome, macropain) 26S subunit, ATPase, 1	PSMD14	proteasome (prosome, macropain) 26S subunit, non-ATPase, 14
167	PSMC1	proteasome (prosome, macropain) 26S subunit, ATPase, 1	PSMD2	proteasome (prosome, macropain) 26S subunit, non-ATPase, 2
168	PSMC1	proteasome (prosome, macropain) 26S subunit, ATPase, 1	PSMD5	proteasome (prosome, macropain) 26S subunit, non-ATPase, 5
169	PSMC1	proteasome (prosome, macropain) 26S subunit, ATPase, 1	PSMD6	proteasome (prosome, macropain) 26S subunit, non-ATPase, 6
170	PSMC1	proteasome (prosome, macropain) 26S subunit, ATPase, 1	PSMD7	proteasome (prosome, macropain) 26S subunit, non-ATPase, 7
171	PSMC1	proteasome (prosome, macropain) 26S subunit, ATPase, 1	SRRM2	serine/arginine repetitive matrix 2
172	PSMC1	proteasome (prosome, macropain) 26S subunit, ATPase, 1	TRAF6	TNF receptor-associated factor 6
173	PSMC1	proteasome (prosome, macropain) 26S subunit, ATPase, 1	UBC	ubiquitin C
174	PSMC1	proteasome (prosome, macropain) 26S subunit, ATPase, 1	UCHL5	ubiquitin carboxyl-terminal hydrolase L5
175	PSMC1	proteasome (prosome, macropain) 26S subunit, ATPase, 1	USP14	ubiquitin specific peptidase 14 (tRNA-guanine transglycosylase)
176	PSMC1	proteasome (prosome, macropain) 26S subunit, ATPase, 1	VCP	valosin-containing protein
177	RBCK1	RanBP-type and C3HC4-type zinc finger containing 1	BACH1	BTB and CNC homology 1, basic leucine zipper transcription factor 1
178	RBCK1	RanBP-type and C3HC4-type zinc finger containing 1	IKBKG	inhibitor of kappa light polypeptide gene enhancer in B-cells, kinase gamma
179	RBCK1	RanBP-type and C3HC4-type zinc finger containing 1	IREB2	iron-responsive element binding protein 2
180	RBCK1	RanBP-type and C3HC4-type zinc finger containing 1	PRKCB	protein kinase C, beta
181	RBCK1	RanBP-type and C3HC4-type zinc finger containing 1	RBCK1	RanBP-type and C3HC4-type zinc finger containing 1
182	RBCK1	RanBP-type and C3HC4-type zinc finger containing 1	RNF31	ring finger protein 31
183	RBCK1	RanBP-type and C3HC4-type zinc finger containing 1	TNF	tumor necrosis factor (TNF superfamily, member 2)
184	RBCK1	RanBP-type and C3HC4-type zinc finger containing 1	UBA1	ubiquitin-like modifier activating enzyme 1
185	RBCK1	RanBP-type and C3HC4-type zinc finger containing 1	UBC	ubiquitin C
186	RBCK1	RanBP-type and C3HC4-type zinc finger containing 1	UBE2D3	ubiquitin-conjugating enzyme E2D 3 (UBC4/5 homolog, yeast)
187	RBCK1	RanBP-type and C3HC4-type zinc finger containing 1	UBE2D4	ubiquitin-conjugating enzyme E2D 4 (putative)
188	RBCK1	RanBP-type and C3HC4-type zinc finger containing 1	UBE2G1	ubiquitin-conjugating enzyme E2G 1 (UBC7 homolog, yeast)
189	RBCK1	RanBP-type and C3HC4-type zinc finger containing 1	UBE2K	ubiquitin-conjugating enzyme E2K (UBC1 homolog, yeast)
190	RBCK1	RanBP-type and C3HC4-type zinc finger containing 1	UBE2L3	ubiquitin-conjugating enzyme E2L 3

191	RBCK1	RanBP-type and C3HC4-type zinc finger containing 1	UBE2L6	ubiquitin-conjugating enzyme E2L 6
192	RBCK1	RanBP-type and C3HC4-type zinc finger containing 1	UBE2N	ubiquitin-conjugating enzyme E2N (UBC13 homolog, yeast)
193	RBCK1	RanBP-type and C3HC4-type zinc finger containing 1	UBE2S	ubiquitin-conjugating enzyme E2S
194	RBCK1	RanBP-type and C3HC4-type zinc finger containing 1	UBE2U	ubiquitin-conjugating enzyme E2U (putative)
195	RHPN1	rhophilin, Rho GTPase binding protein 1	CALCOCO2	calcium binding and coiled-coil domain 2
196	RHPN1	rhophilin, Rho GTPase binding protein 1	EFEMP2	EGF-containing fibulin-like extracellular matrix protein 2
197	RHPN1	rhophilin, Rho GTPase binding protein 1	KRT15	keratin 15
198	RHPN1	rhophilin, Rho GTPase binding protein 1	TRIM37	tripartite motif-containing 37
199	RIC8A	resistance to inhibitors of cholinesterase 8 homolog A (C. elegans)	GNA13	guanine nucleotide binding protein (G protein), alpha 13
200	RIC8A	resistance to inhibitors of cholinesterase 8 homolog A (C. elegans)	GNAI1	guanine nucleotide binding protein (G protein), alpha inhibiting activity polypeptide 1
201	RIC8A	resistance to inhibitors of cholinesterase 8 homolog A (C. elegans)	GNAI2	guanine nucleotide binding protein (G protein), alpha inhibiting activity polypeptide 2
202	RIC8A	resistance to inhibitors of cholinesterase 8 homolog A (C. elegans)	GNAI3	guanine nucleotide binding protein (G protein), alpha inhibiting activity polypeptide 3
203	RIC8A	resistance to inhibitors of cholinesterase 8 homolog A (C. elegans)	GNAO1	guanine nucleotide binding protein (G protein), alpha activating activity polypeptide O
204	RIC8A	resistance to inhibitors of cholinesterase 8 homolog A (C. elegans)	GNAQ	guanine nucleotide binding protein (G protein), q polypeptide
205	RIC8A	resistance to inhibitors of cholinesterase 8 homolog A (C. elegans)	GNAS	GNAS complex locus
206	RIC8A	resistance to inhibitors of cholinesterase 8 homolog A (C. elegans)	MAPK8IP3	mitogen-activated protein kinase 8 interacting protein 3
207	RIC8A	resistance to inhibitors of cholinesterase 8 homolog A (C. elegans)	TERF1	telomeric repeat binding factor (NIMA-interacting) 1
208	RIC8A	resistance to inhibitors of cholinesterase 8 homolog A (C. elegans)	TUBB2A	tubulin, beta 2A
209	RIC8A	resistance to inhibitors of cholinesterase 8 homolog A (C. elegans)	UBQLN1	ubiquilin 1
210	RIC8A	resistance to inhibitors of cholinesterase 8 homolog A (C. elegans)	ZNF585B	zinc finger protein 585B
211	SLC9A3R2	solute carrier family 9 (sodium/hydrogen exchanger), member 3 regulator 2	ACTN4	actinin, alpha 4
212	SLC9A3R2	solute carrier family 9 (sodium/hydrogen exchanger), member 3 regulator 2	ADORA2B	adenosine A2b receptor

213	SLC9A3R2	solute carrier family 9 (sodium/hydrogen exchanger), member 3 regulator 2	ADRB2	adrenergic, beta-2-, receptor, surface
214	SLC9A3R2	solute carrier family 9 (sodium/hydrogen exchanger), member 3 regulator 2	CFTR	cystic fibrosis transmembrane conductance regulator (ATP-binding cassette sub-family C, member 7)
215	SLC9A3R2	solute carrier family 9 (sodium/hydrogen exchanger), member 3 regulator 2	EZR	ezrin
216	SLC9A3R2	solute carrier family 9 (sodium/hydrogen exchanger), member 3 regulator 2	KCNJ1	potassium inwardly-rectifying channel, subfamily J, member 1
217	SLC9A3R2	solute carrier family 9 (sodium/hydrogen exchanger), member 3 regulator 2	LPAR2	lysophosphatidic acid receptor 2
218	SLC9A3R2	solute carrier family 9 (sodium/hydrogen exchanger), member 3 regulator 2	OTUD7B	OTU domain containing 7B
219	SLC9A3R2	solute carrier family 9 (sodium/hydrogen exchanger), member 3 regulator 2	PDPK1	3-phosphoinositide dependent protein kinase-1
220	SLC9A3R2	solute carrier family 9 (sodium/hydrogen exchanger), member 3 regulator 2	PDZK1	PDZ domain containing 1
221	SLC9A3R2	solute carrier family 9 (sodium/hydrogen exchanger), member 3 regulator 2	PHLPP1	PH domain and leucine rich repeat protein phosphatase 1
222	SLC9A3R2	solute carrier family 9 (sodium/hydrogen exchanger), member 3 regulator 2	PHLPP2	PH domain and leucine rich repeat protein phosphatase 2
223	SLC9A3R2	solute carrier family 9 (sodium/hydrogen exchanger), member 3 regulator 2	PIK3CA	phosphoinositide-3-kinase, catalytic, alpha polypeptide
224	SLC9A3R2	solute carrier family 9 (sodium/hydrogen exchanger), member 3 regulator 2	PLCB3	phospholipase C, beta 3 (phosphatidylinositol-specific)
225	SLC9A3R2	solute carrier family 9 (sodium/hydrogen exchanger), member 3 regulator 2	PODXL	podocalyxin-like
226	SLC9A3R2	solute carrier family 9 (sodium/hydrogen exchanger), member 3 regulator 2	PTH1R	parathyroid hormone 1 receptor
227	SLC9A3R2	solute carrier family 9 (sodium/hydrogen exchanger), member 3 regulator 2	SGK1	serum/glucocorticoid regulated kinase 1
228	SLC9A3R2	solute carrier family 9 (sodium/hydrogen exchanger), member 3 regulator 2	SLC26A3	solute carrier family 26, member 3
229	SLC9A3R2	solute carrier family 9 (sodium/hydrogen exchanger), member 3 regulator 2	SLC9A3	solute carrier family 9 (sodium/hydrogen exchanger), member 3
230	SLC9A3R2	solute carrier family 9 (sodium/hydrogen exchanger), member 3 regulator 2	TRIP6	thyroid hormone receptor interactor 6
231	SLC9A3R2	solute carrier family 9 (sodium/hydrogen exchanger), member 3 regulator 2	WWTR1	WW domain containing transcription regulator 1
232	SNX9	sorting nexin 9	ADAM15	ADAM metallopeptidase domain 15

233	SNX9	sorting nexin 9	ADAM9	ADAM metallopeptidase domain 9 (meltrin gamma)
234	SNX9	sorting nexin 9	CLTC	clathrin, heavy chain (Hc)
235	SNX9	sorting nexin 9	DNM2	dynamin 2
236	SNX9	sorting nexin 9	MPP6	membrane protein, palmitoylated 6 (MAGUK p55 subfamily member 6)
237	STK16	serine/threonine kinase 16	ADAMTSL4	ADAMTS-like 4
238	STK16	serine/threonine kinase 16	CNTF	ciliary neurotrophic factor
239	STK16	serine/threonine kinase 16	EBLN2	endogenous Bornavirus-like nucleoprotein 2
240	STK16	serine/threonine kinase 16	ELK1	ELK1, member of ETS oncogene family
241	STK16	serine/threonine kinase 16	EXT2	exostoses (multiple) 2
242	STK16	serine/threonine kinase 16	HNF4A	hepatocyte nuclear factor 4, alpha
243	STK16	serine/threonine kinase 16	ICA1	islet cell autoantigen 1, 69kDa
244	STK16	serine/threonine kinase 16	KCTD17	potassium channel tetramerisation domain containing 17
245	STK16	serine/threonine kinase 16	MKKS	McKusick-Kaufman syndrome
246	STK16	serine/threonine kinase 16	NAGK	N-acetylglucosamine kinase
247	STK16	serine/threonine kinase 16	PASK	PAS domain containing serine/threonine kinase
248	STK16	serine/threonine kinase 16	ROCK2	Rho-associated, coiled-coil containing protein kinase 2
249	STK16	serine/threonine kinase 16	RPIA	ribose 5-phosphate isomerase A
250	STK16	serine/threonine kinase 16	SNRK	SNF related kinase
251	STK16	serine/threonine kinase 16	STK16	serine/threonine kinase 16
252	STK16	serine/threonine kinase 16	TGIF1	TGFB-induced factor homeobox 1
253	STK16	serine/threonine kinase 16	VHL	von Hippel-Lindau tumor suppressor
254	Ufc1	ubiquitin-fold modifier conjugating enzyme 1	CDK5RAP3	CDK5 regulatory subunit associated protein 3
255	Ufc1	ubiquitin-fold modifier conjugating enzyme 1	UBA5	ubiquitin-like modifier activating enzyme 5
256	Ufc1	ubiquitin-fold modifier conjugating enzyme 1	Ufm1	ubiquitin-fold modifier 1
257	ZNHIT1	zinc finger, HIT type 1	TP53	tumor protein p53
258	ZNHIT1	zinc finger, HIT type 1	MAPK14	mitogen-activated protein kinase 14
259	ZNHIT1	zinc finger, HIT type 1	UBC	ubiquitin C
260	ZNHIT1	zinc finger, HIT type 1	H2AFZ	H2A histone family, member Z
261	ZNHIT1	zinc finger, HIT type 1	ACTR6	ARP6 actin-related protein 6 homolog (yeast)

Supplementary table 3. Complete list of detected phage lambda/*E. coli* interactions.

Bait locus tag	Lambda bait	*E. coli* prey	Prey count	ECK ID	JW ID	b ID	Annotation
lambdap01	nu1	dcrB	2	ECK3456	JW5682	b3472	protein DcrB
lambdap01	nu1	yajI	2	ECK0406	JW5056	b0412	YajI
lambdap01	nu1	mltB	2	ECK2696	JW2671	b2701	lytic murein transglycosylase B
lambdap01	nu1	yfiO	1	ECK2593	JW2577	b2595	lipoprotein YfiO
lambdap01	nu1	yohN	1	ECK2100	JW5346	b2107	conserved hypothetical protein
lambdap01	nu1	ycfM	1	ECK1091	JW5157	b1105	lipoprotein, putative
lambdap01	nu1	nohA	1	ECK1541	JW1541	b1548	bacteriophage DNA packaging protein
lambdap01	nu1	yraP	1	ECK3138	JW3119	b3150	conserved exported protein
lambdap01	nu1	ynjB	1	ECK1752	JW5284	b1754	conserved hypothetical protein
lambdap02	A	nohA	9	ECK1541	JW1541	b1548	bacteriophage DNA packaging protein
lambdap02	A	nohB	4	ECK0552	JW0549	b0560	bacteriophage DNA packaging protein
lambdap02	A	leuB	1	ECK0075	JW5807	b0073	3-isopropylmalate dehydrogenase
lambdap03	W	flxA	5	ECK1560	JW1558	b1566	protein FlxA
lambdap03	W	yfaE	1	ECK2228	JW2230	b2236	adrenodoxin family ferredoxin
lambdap06	nu3	flxA	4	ECK1560	JW1558	b1566	protein FlxA
lambdap07	D	flxA	4	ECK1560	JW1558	b1566	protein FlxA
lambdap09	Fi	dicB	48	ECK1569	JW1566	b1575	conserved domain protein
lambdap09	Fi	mltB	11	ECK2696	JW2671	b2701	lytic murein transglycosylase B
lambdap09	Fi	flxA	6	ECK1560	JW1558	b1566	protein FlxA
lambdap09	Fi	metN	6	ECK0199	JW0195	b0199	D-methionine ABC transporter, ATP-binding protein
lambdap09	Fi	phnG	6	ECK4094	JW4062	b4101	protein PhnG
lambdap09	Fi	ydgH	4	ECK1599	JW1596	b1604	protein YdgH
lambdap09	Fi	fixB	3	ECK0043	JW0041	b0042	protein FixB
lambdap09	Fi	ygiT	3	ECK3012	JW2989	b3021	transcriptional regulator, XRE family
lambdap09	Fi	minE	2	ECK1162	JW1163	b1174	cell division topological specificity factor MinE
lambdap09	Fi	smpA	2	ECK2613	JW2598	b2617	small protein A
lambdap09	Fi	proQ	1	ECK1830	JW5300	b1831	ProP effector
lambdap09	Fi	cchB	1	ECK2451	JW2440	b2456	ethanolamine utilization protein EutN
lambdap09	Fi	dcrB	1	ECK3456	JW5682	b3472	protein DcrB
lambdap09	Fi	yeeD	1	ECK2006	JW1994	b2012	conserved domain protein
lambdap09	Fi	ycfL	1	ECK1090	JW1090	b1104	conserved hypothetical protein
lambdap09	Fi	ydcE	1	ECK1455	JW1456	b1461	conserved domain protein
lambdap09	Fi	fixX	1	ECK0045	JW0043	b0044	conserved hypothetical protein
lambdap09	Fi	fimG	1	ECK4310	JW4282	b4319	protein FimG
lambdap11	Z	ynfN	1	ECK1545	JW5254	b1551	hypothetical protein
lambdap12	U	ydaW	1	ECK1359	JW5211	b1361	conserved hypothetical protein
lambdap13	V	ydaL	1	ECK1337	JW1334	b1340	Smr protein/MutS2
lambdap13	V	yheL	1	ECK3330	JW3305	b3343	sulfur relay protein TusD/DsrH

lambdap13	V	artI	1	ECK0854	JW0847	b0863	arginine-binding periplasmic protein 1
lambdap13	V	panF	1	ECK3245	JW3226	b3258	sodium/pantothenate symporter
lambdap13	V	sfmC	1	ECK0524	JW0520	b0531	chaperone protein FimC
lambdap13	V	ydeQ	1	ECK1495	JW1496	b1502	protein FimH
lambdap14	G	dicB	84	ECK1569	JW1566	b1575	conserved domain protein
lambdap14	G	ycgE	48	ECK1149	JW1149	b1162	HTH-type transcriptional regulator MlrA
lambdap14	G	clpP	43	ECK0431	JW0427	b0437	ATP-dependent Clp protease, proteolytic subunit ClpP
lambdap14	G	fhuF	21	ECK4357	JW4331	b4367	ferric iron reductase protein FhuF
lambdap14	G	flxA	18	ECK1560	JW1558	b1566	protein FlxA
lambdap14	G	fdoH	8	ECK3886	JW3864	b3893	formate dehydrogenase, beta subunit
lambdap14	G	yohN	5	ECK2100	JW5346	b2107	conserved hypothetical protein
lambdap14	G	chaC	4	ECK1212	JW1209	b1218	cation transport protein ChaC
lambdap14	G	ycbQ	4	ECK0929	JW5122	b0938	fimbrial subunit
lambdap14	G	metN	4	ECK0199	JW0195	b0199	D-methionine ABC transporter, ATP-binding protein
lambdap14	G	proQ	3	ECK1830	JW5300	b1831	ProP effector
lambdap14	G	yliL	3	ECK0805	JW5969	b0816	b0816 hypothetical protein (yliL)
lambdap14	G	yceK	2	ECK1036	JW5151	b1050	lipoprotein, putative
lambdap14	G	ykgL	2	ECK0294	JW5033	b0295	hypothetical protein (ykgL)
lambdap14	G	ydaL	2	ECK1337	JW1334	b1340	Smr protein/MutS2
lambdap14	G	iscR	1	ECK2528	JW2515	b2531	iron-sulfur cluster assembly transcription factor IscR
lambdap14	G	fabI	1	ECK1283	JW1281	b1288	b1288 enoyl-[acyl-carrier-protein] reductase, NADH-dependent (fabI)
lambdap14	G	hypA	1	ECK2721	JW2696	b2726	hydrogenase nickel insertion protein HypA
lambdap14	G	yeaE	1	ECK1779	JW1770	b1781	oxidoreductase, aldo/keto reductase family
lambdap14	G	yliI	1	ECK0827	JW0821	b0837	hydrophobic compound transport factor
lambdap14	G	ynjE	1	ECK1755	JW5287	b1757	putative thiosulfate sulfur transferase
lambdap14	G	yqeG	1	ECK2843	JW2813	b2845	serine transporter
lambdap16	H	dicB	84	ECK1569	JW1566	b1575	conserved domain protein
lambdap16	H	flxA	10	ECK1560	JW1558	b1566	protein FlxA
lambdap16	H	yliL	10	ECK0805	JW5969	b0816	b0816 hypothetical protein (yliL)
lambdap16	H	fixX	7	ECK0045	JW0043	b0044	conserved hypothetical protein
lambdap16	H	acpS	5	ECK2561	JW2547	b2563	holo-(acyl-carrier-protein) synthase
lambdap16	H	yeiW	4	ECK2164	JW5361	b4502	proteinase inhibitor
lambdap16	H	ymjB	4	ECK1314	JW5203	b4524	putative ATP-binding component of a transport system
lambdap16	H	ybgD	4	ECK0708	JW0709	b0719	fimbrial protein

lambdap16	H	ycbQ	4	ECK0929	JW5122	b0938	fimbrial subunit
lambdap16	H	yfcQ	4	ECK2328	JW2331	b2334	conserved hypothetical protein
lambdap16	H	yohH	4	ECK2132	JW5358	b2139	YohH
lambdap16	H	phnG	4	ECK4094	JW4062	b4101	protein PhnG
lambdap16	H	dnaN	3	ECK3693	JW3678	b3701	DNA polymerase III, beta subunit
lambdap16	H	ECK1157	3	ECK1157	JW5901+ JW5176	b44	putative ATP-binding component of a transport system
lambdap16	H	hyfG	3	ECK2483	JW2472	b2487	hydrogenase-4 component G
lambdap16	H	sfmF	3	ECK0527	JW5072	b0534	major fimbrial subunit
lambdap16	H	ynfC	3	ECK1580	JW5258	b1585	lipoprotein YnfC
lambdap16	H	yehD	3	ECK2104	JW2098	b2111	fimbrial protein
lambdap16	H	yraH	3	ECK3130	JW3111	b3142	fimbrial protein
lambdap16	H	ydaW	3	ECK1359	JW5211	b1361	conserved hypothetical protein
lambdap16	H	metN	3	ECK0199	JW0195	b0199	D-methionine ABC transporter, ATP-binding protein
lambdap16	H	sfmA	2	ECK0523	JW0519	b0530	type-1 fimbrial protein, A chain
lambdap16	H	cspF	2	ECK1552	JW1550	b1558	conserved domain protein
lambdap16	H	ydiT	2	ECK1698	JW1690	b1700	conserved hypothetical protein
lambdap16	H	ynjB	1	ECK1752	JW5284	b1754	conserved hypothetical protein
lambdap16	H	mltB	1	ECK2696	JW2671	b2701	lytic murein transglycosylase B
lambdap16	H	ECK3207	1	ECK3207	JW3187	b4549	conserved hypothetical protein
lambdap16	H	fimG	1	ECK4310	JW4282	b4319	protein FimG
lambdap16	H	yraK	1	ECK3133	JW3114	b3145	lipoprotein, putative
lambdap16	H	yadM	1	ECK0137	JW0134	b0138	conserved hypothetical protein
lambdap16	H	yodA	1	ECK1969	JW1956	b1973	zinc-binding lipoprotein AdcA
lambdap16	H	yeeD	1	ECK2006	JW1994	b2012	conserved domain protein
lambdap16	H	ycbU	1	ECK0933	JW0925	b0942	fimbrial subunit
lambdap16	H	ygiL	1	ECK3034	JW3011	b3043	fimbrial protein
lambdap16	H	rpmA	1	ECK3174	JW3152	b3185	ribosomal protein L27
lambdap19	K	insN	2	ECK0257	JW5024	b0255	transposase InsN for insertion sequence element A
lambdap19	K	ynjB	2	ECK1752	JW5284	b1754	conserved hypothetical protein
lambdap19	K	fliA	2	ECK1921	JW1907	b1922	RNA polymerase sigma factor for flagellar operon
lambdap19	K	ydaL	1	ECK1337	JW1334	b1340	Smr protein/MutS2
lambdap20	I	torI	1	ECK2359	JW5387	b4501	conserved domain protein
lambdap20	I	ydcM	1	ECK1426	JW5228	b1432	ISAfe8, transposase
lambdap20	I	yegR	1	ECK2081	JW5837	b2085	
lambdap26	lom	ydaL	1	ECK1337	JW1334	b1340	Smr protein/MutS2
lambdap27	orf-401	stfR	89	ECK1367	JW1366	b1372	putative membrane protein
lambdap27	orf-401	dicB	4	ECK1569	JW1566	b1575	conserved domain protein
lambdap27	orf-401	fucU	1	ECK2799	JW2775	b2804	fucose operon FucU protein
lambdap27	orf-401	yeeD	1	ECK2006	JW1994	b2012	conserved domain protein

lambdap28	orf-314	tfaR	152	ECK1368	JW1367	b1373	tail fiber assembly protein
lambdap28	orf-314	clpP	7	ECK0431	JW0427	b0437	ATP-dependent Clp protease, proteolytic subunit ClpP
lambdap28	orf-314	ycgE	4	ECK1149	JW1149	b1162	HTH-type transcriptional regulator MlrA
lambdap28	orf-314	tfaQ	2	ECK1539	JW1539	b1546	tail fiber assembly protein
lambdap28	orf-314	ycfZ	1	ECK1107	JW1107	b1121	inner membrane protein YcfZ
lambdap28	orf-314	yicI	1	ECK3646	JW3631	b3656	alpha-glucosidase
lambdap33	int	fliA	17	ECK1921	JW1907	b1922	RNA polymerase sigma factor for flagellar operon
lambdap33	int	nohB	7	ECK0552	JW0549	b0560	bacteriophage DNA packaging protein
lambdap33	int	nlpI	6	ECK3151	JW3132	b3163	lipoprotein NlpI
lambdap33	int	paaC	6	ECK1387	JW1385	b1390	phenylacetate-CoA oxygenase, PaaI subunit
lambdap33	int	ynjB	5	ECK1752	JW5284	b1754	conserved hypothetical protein
lambdap33	int	spr	2	ECK2169	JW2163	b2175	lipoprotein spr
lambdap33	int	tbpA	2	ECK0069	JW0067	b0068	thiamin/thiamin pyrophosphate ABC transporter, thiamin/thiamin pyrophospate-binding protein
lambdap33	int	mltB	2	ECK2696	JW2671	b2701	lytic murein transglycosylase B
lambdap33	int	ynfO	1	ECK1542	JW5251	b4533	conserved hypothetical protein
lambdap33	int	stfR	1	ECK1367	JW1366	b1372	putative membrane protein
lambdap33	int	frvR	1	ECK3890	JW3868	b3897	putative frv operon regulatory protein
lambdap33	int	fliM	1	ECK1943	JW1929	b1945	flagellar motor switch protein FliM
lambdap33	int	ansB	1	ECK2952	JW2924	b2957	L-asparaginase II
lambdap33	int	nohA	1	ECK1541	JW1541	b1548	bacteriophage DNA packaging protein
lambdap36	ea8.5	dicB	45	ECK1569	JW1566	b1575	conserved domain protein
lambdap36	ea8.5	phnG	36	ECK4094	JW4062	b4101	protein PhnG
lambdap36	ea8.5	flxA	17	ECK1560	JW1558	b1566	protein FlxA
lambdap36	ea8.5	spr	7	ECK2169	JW2163	b2175	lipoprotein spr
lambdap36	ea8.5	mltB	7	ECK2696	JW2671	b2701	lytic murein transglycosylase B
lambdap36	ea8.5	yjhV	4	ECK4276	JW4246	b4286	conserved hypothetical protein
lambdap36	ea8.5	fixX	4	ECK0045	JW0043	b0044	conserved hypothetical protein
lambdap36	ea8.5	ydaW	4	ECK1359	JW5211	b1361	conserved hypothetical protein
lambdap36	ea8.5	metN	4	ECK0199	JW0195	b0199	D-methionine ABC transporter, ATP-binding protein
lambdap36	ea8.5	yjdI	3	ECK4119	JW4087	b4126	conserved hypothetical protein
lambdap36	ea8.5	yohH	3	ECK2132	JW5358	b2139	YohH
lambdap36	ea8.5	minE	2	ECK1162	JW1163	b1174	cell division topological specificity factor MinE
lambdap36	ea8.5	yraP	2	ECK3138	JW3119	b3150	conserved exported protein
lambdap36	ea8.5	yeiW	2	ECK2164	JW5361	b4502	proteinase inhibitor

lambdap36	ea8.5	ymdE	2	ECK1016	JW5145	b1028	hypothetical protein
lambdap36	ea8.5	smpA	2	ECK2613	JW2598	b2617	small protein A
lambdap36	ea8.5	ubiF	2	ECK0654	JW0659	b0662	2-octaprenyl-3-methyl-6-methoxy-1,4-benzoquinol hydroxylase
lambdap36	ea8.5	ynfO	2	ECK1542	JW5251	b4533	conserved hypothetical protein
lambdap36	ea8.5	ydcE	2	ECK1455	JW1456	b1461	conserved domain protein
lambdap36	ea8.5	wza	2	ECK2056	JW2047	b2062	membrane protein
lambdap36	ea8.5	yajI	1	ECK0406	JW5056	b0412	YajI
lambdap36	ea8.5	ynjB	1	ECK1752	JW5284	b1754	conserved hypothetical protein
lambdap36	ea8.5	yjgZ	1	ECK4267	JW4236	b4277	
lambdap36	ea8.5	ynfC	1	ECK1580	JW5258	b1585	lipoprotein YnfC
lambdap36	ea8.5	sfmF	1	ECK0527	JW5072	b0534	major fimbrial subunit
lambdap36	ea8.5	ECK2994	1	ECK2994	JW5496	b3000	carboxymethylenebutenol idase
lambdap36	ea8.5	mltC	1	ECK2958	JW5481	b2963	membrane-bound lytic murein transglycosylase C
lambdap36	ea8.5	ybhC	1	ECK0761	JW0755	b0772	acyl-CoA thioester hydrolase YbgC
lambdap36	ea8.5	yaiV	1	ECK0370	JW0366	b0375	conserved hypothetical protein
lambdap36	ea8.5	ECK0356	1	ECK0356	JW0350	b0359	putative transferase
lambdap36	ea8.5	csgC	1	ECK1029	JW1026	b1043	putative curli production protein CsgC
lambdap36	ea8.5	fimG	1	ECK4310	JW4282	b4319	protein FimG
lambdap37	orf61	mltB	4	ECK2696	JW2671	b2701	lytic murein transglycosylase B
lambdap37	orf61	yqhC	3	ECK3002	JW5849	b3010	putative HTH-type transcriptional regulator YqhC
lambdap37	orf61	spr	3	ECK2169	JW2163	b2175	lipoprotein spr
lambdap37	orf61	yiaF	3	ECK3541	JW5655	b3554	lipoprotein, putative
lambdap37	orf61	yjdI	2	ECK4119	JW4087	b4126	conserved hypothetical protein
lambdap37	orf61	yheL	2	ECK3330	JW3305	b3343	sulfur relay protein TusD/DsrH
lambdap37	orf61	flxA	2	ECK1560	JW1558	b1566	protein FlxA
lambdap37	orf61	wza	2	ECK2056	JW2047	b2062	membrane protein
lambdap37	orf61	phnG	2	ECK4094	JW4062	b4101	protein PhnG
lambdap37	orf61	yihD	1	ECK3850	JW3830	b3858	protein YihD
lambdap37	orf61	dicB	1	ECK1569	JW1566	b1575	conserved domain protein
lambdap37	orf61	yjhV	1	ECK4276	JW4246	b4286	conserved hypothetical protein
lambdap37	orf61	ynjB	1	ECK1752	JW5284	b1754	conserved hypothetical protein
lambdap37	orf61	ubiF	1	ECK0654	JW0659	b0662	2-octaprenyl-3-methyl-6-methoxy-1,4-benzoquinol hydroxylase
lambdap37	orf61	yccT	1	ECK0955	JW0947	b0964	protein YccT
lambdap37	orf61	rseB	1	ECK2569	JW2555	b2571	sigma-E factor regulatory protein RseB
lambdap37	orf61	cysH	1	ECK2757	JW2732	b2762	phosphoadenosine phosphosulfate reductase
lambdap37	orf61	ECK1962	1	ECK1962	JW1949	b1966	outer membrane protein N
lambdap37	orf61	nfsA	1	ECK0842	JW0835	b0851	oxygen-insensitive NADPH nitroreductase
lambdap37	orf61	yohN	1	ECK2100	JW5346	b2107	conserved hypothetical protein

lambdap37	orf61	yhdW	1	ECK3255	JW3236	b3268	general L-amino acid-binding periplasmic protein AapJ
lambdap37	orf61	yeiW	1	ECK2164	JW5361	b4502	proteinase inhibitor
lambdap37	orf61	sgcE	1	ECK4290	JW4263	b4301	protein SgcE
lambdap37	orf61	yhfG	1	ECK3350	JW3325	b3362	conserved hypothetical protein
lambdap37	orf61	flgJ	1	ECK1066	JW1068	b1081	flagellar rod assembly protein/muramidase FlgJ
lambdap38	orf63	yqhC	4	ECK3002	JW5849	b3010	putative HTH-type transcriptional regulator YqhC
lambdap39	orf60a	tbpA	1	ECK0069	JW0067	b0068	thiamin/thiamin pyrophosphate ABC transporter, thiamin/thiamin pyrophospate-binding protein
lambdap41	exo	ynjB	9	ECK1752	JW5284	b1754	conserved hypothetical protein
lambdap41	exo	spr	2	ECK2169	JW2163	b2175	lipoprotein spr
lambdap41	exo	tbpA	2	ECK0069	JW0067	b0068	thiamin/thiamin pyrophosphate ABC transporter, thiamin/thiamin pyrophospate-binding protein
lambdap41	exo	yiaF	1	ECK3541	JW5655	b3554	lipoprotein, putative
lambdap42	Gam	ynjB	9	ECK1752	JW5284	b1754	conserved hypothetical protein
lambdap42	Gam	spr	7	ECK2169	JW2163	b2175	lipoprotein spr
lambdap42	Gam	yiaF	5	ECK3541	JW5655	b3554	lipoprotein, putative
lambdap42	Gam	ynfO	4	ECK1542	JW5251	b4533	conserved hypothetical protein
lambdap42	Gam	mltB	1	ECK2696	JW2671	b2701	lytic murein transglycosylase B
lambdap42	Gam	yncM	1	ECK1453	JW5237	b1459	hypothetical protein (yncM)
lambdap42	Gam	yhfG	1	ECK3350	JW3325	b3362	conserved hypothetical protein
lambdap42	Gam	yqhC	1	ECK3002	JW5849	b3010	putative HTH-type transcriptional regulator YqhC
lambdap45	ea10	yqjI	63	ECK3061	JW3042	b3071	transcriptional regulator, PadR family protein
lambdap45	ea10	frvA	43	ECK3893	JW3871	b3900	phosphoenolpyruvate-dependent sugar phosphotransferase system, eiia 2, putative
lambdap45	ea10	ynfO	33	ECK1542	JW5251	b4533	conserved hypothetical protein
lambdap45	ea10	rmf	17	ECK0944	JW0936	b0953	ribosome modulation factor (rmf)
lambdap45	ea10	dicB	8	ECK1569	JW1566	b1575	conserved domain protein
lambdap45	ea10	rpmA	8	ECK3174	JW3152	b3185	ribosomal protein L27
lambdap45	ea10	yliL	8	ECK0805	JW5969	b0816	hypothetical protein (yliL)
lambdap45	ea10	rpsG	7	ECK3328	JW3303	b3341	ribosomal protein S7
lambdap45	ea10	flxA	6	ECK1560	JW1558	b1566	protein FlxA
lambdap45	ea10	cedA	5	ECK1729	JW1720	b1731	conserved hypothetical protein
lambdap45	ea10	yjiR	5	ECK4331	JW4303	b4340	aminotransferase, classes I and II superfamily

lambdap45	ea10	mltB	4	ECK2696	JW2671	b2701	lytic murein transglycosylase B
lambdap45	ea10	priC	4	ECK0461	JW0456	b0467	primosomal replication protein N
lambdap45	ea10	rpsS	4	ECK3303	JW3278	b3316	30S ribosomal protein S19
lambdap45	ea10	ypjJ	4	ECK2641	JW5421	b4548	hypothetical protein (ypjJ)
lambdap45	ea10	cobB	3	ECK1106	JW1106	b1120	NAD-dependent deacetylase
lambdap45	ea10	soxS	3	ECK4054	JW4023	b4062	regulatory protein SoxS
lambdap45	ea10	ykiA	3	ECK0387	JW0383	b0392	conserved hypothetical protein
lambdap45	ea10	yncM	3	ECK1453	JW5237	b1459	hypothetical protein (yncM)
lambdap45	ea10	ycbG	3	ECK0947	JW0939	b0956	protein YcbG
lambdap45	ea10	glcC	3	ECK2975	JW2947	b2980	Glc operon transcriptional activator
lambdap45	ea10	phnG	3	ECK4094	JW4062	b4101	protein PhnG
lambdap45	ea10	spr	3	ECK2169	JW2163	b2175	lipoprotein spr
lambdap45	ea10	ydaL	3	ECK1337	JW1334	b1340	Smr protein/MutS2
lambdap45	ea10	hupA	2	ECK3992	JW3964	b4000	DNA-binding protein HU-alpha
lambdap45	ea10	rplC	2	ECK3307	JW3282	b3320	ribosomal protein L3
lambdap45	ea10	ECK0356	2	ECK0356	JW0350	b0359	b0359 predicted acyl transferase
lambdap45	ea10	chaA	2	ECK1210	JW1207	b1216	calcium/proton antiporter
lambdap45	ea10	cspH	2	ECK0979	JW5134	b0989	conserved domain protein
lambdap45	ea10	prfH	2	ECK0237	JW0226	b0236	putative peptide chain release factor H
lambdap45	ea10	rrmJ	2	ECK3168	JW3146	b3179	ribosomal RNA large subunit methyltransferase J
lambdap45	ea10	soxR	2	ECK4055	JW4024	b4063	redox-sensitive transcriptional activator SoxR
lambdap45	ea10	yaiV	2	ECK0370	JW0366	b0375	conserved hypothetical protein
lambdap45	ea10	ybjP	2	ECK0856	JW0849	b0865	YbjP
lambdap45	ea10	ycaL	2	ECK0900	JW0892	b0909	peptidase M48, Ste24p
lambdap45	ea10	ycdC	2	ECK1004	JW0998	b1013	HTH-type transcriptional regulator RutR
lambdap45	ea10	ydcI	2	ECK1416	JW5226	b1422	putative HTH-type transcriptional regulator YdcI
lambdap45	ea10	yeaM	2	ECK1788	JW1779	b1790	putative HTH-type transcriptional regulator YeaM
lambdap45	ea10	ykgM	2	ECK0295	JW5034	b4506	ribosomal protein L36
lambdap45	ea10	ykfI	2	ECK0246	JW0234	b0245	YeeV protein
lambdap45	ea10	ymfC	2	ECK1121	JW1121	b1135	RNA pseudouridylate synthase family protein
lambdap45	ea10	wza	2	ECK2056	JW2047	b2062	membrane protein
lambdap45	ea10	yjgZ	2	ECK4267	JW4236	b4277	
lambdap45	ea10	yjhV	2	ECK4276	JW4246	b4286	conserved hypothetical protein
lambdap45	ea10	metN	1	ECK0199	JW0195	b0199	D-methionine ABC transporter, ATP-binding protein
lambdap45	ea10	ydaW	1	ECK1359	JW5211	b1361	conserved hypothetical protein
lambdap45	ea10	ydcE	1	ECK1455	JW1456	b1461	conserved domain protein

lambdap45	ea10	ygiT	1	ECK3012	JW2989	b3021	transcriptional regulator, XRE family
lambdap45	ea10	yhiK	1	ECK3474	JW5674	b3489	hypothetical protein
lambdap45	ea10	cdaR	1	ECK0161	JW5013	b0162	carbohydrate diacid regulator
lambdap45	ea10	cobC	1	ECK0631	JW0633	b0638	alpha-ribazole phosphatase
lambdap45	ea10	ECK3633	1	ECK3633	JW3618	b3643	defective ribonuclease PH
lambdap45	ea10	ECK4273	1	ECK4273	JW5772	b4561	transposase
lambdap45	ea10	glcD	1	ECK2974	JW2946	b2979	glycolate oxidase, subunit GlcD
lambdap45	ea10	hcaB	1	ECK2538	JW2525	b2541	2,3-dihydroxy-2,3-dihydro-phenylpropionate dehydrogenase
lambdap45	ea10	melR	1	ECK4111	JW4079	b4118	melibiose operon regulatory protein
lambdap45	ea10	mltC	1	ECK2958	JW5481	b2963	membrane-bound lytic murein transglycosylase C
lambdap45	ea10	mrdA	1	ECK0628	JW0630	b0635	penicillin-binding protein 2
lambdap45	ea10	nuoA	1	ECK2282	JW2283	b2288	NADH-quinone oxidoreductase chain a
lambdap45	ea10	wbbJ	1	ECK2027	JW2018	b2033	b2033 predicted acyl transferase (wbbJ)
lambdap45	ea10	wzb	1	ECK2055	JW2046	b2061	Low molecular weight protein-tyrosine-phosphatase wzb
lambdap45	ea10	ycjD	1	ECK1284	JW1282	b1289	14kDa protein
lambdap45	ea10	ydgH	1	ECK1599	JW1596	b1604	protein YdgH
lambdap45	ea10	ydiB	1	ECK1690	JW1682	b1692	quinate/shikimate dehydrogenase
lambdap45	ea10	yeeS	1	ECK1995	JW1984	b2002	Z1217 protein
lambdap45	ea10	yfdY	1	ECK2373	JW2374	b2377	conserved hypothetical protein
lambdap45	ea10	yfjG	1	ECK2615	JW2600	b2619	oligoketide cyclase/lipid transport protein
lambdap45	ea10	ygcR	1	ECK2765	JW5441	b2770	putative transport protein
lambdap45	ea10	ygeP	1	ECK2858	JW2831	b2862	hypothetical protein (ygeP)
lambdap45	ea10	ygiU	1	ECK3013	JW2990	b3022	b3022 predicted cyanide hydratase (ygiU)
lambdap45	ea10	yigI	1	ECK3814	JW5588	b3820	f161
lambdap45	ea10	yjdI	1	ECK4119	JW4087	b4126	conserved hypothetical protein
lambdap45	ea10	ymdB	1	ECK1031	JW1032	b1045	protein YmdB
lambdap45	ea10	ymfO	1	ECK1137	JW1137	b1151	portal protein
lambdap45	ea10	yohH	1	ECK2132	JW5358	b2139	YohH
lambdap45	ea10	yqhC	1	ECK3002	JW5849	b3010	putative HTH-type transcriptional regulator YqhC
lambdap48		pntA	1	ECK1598	JW1595	b1603	NAD(P) transhydrogenase, alpha subunit
lambdap48		ydcH	1	ECK1419	JW5823	b1426	conserved domain protein
lambdap49	N	mltB	7	ECK2696	JW2671	b2701	lytic murein transglycosylase B
lambdap49	N	ynjB	6	ECK1752	JW5284	b1754	conserved hypothetical protein
lambdap49	N	ynfO	5	ECK1542	JW5251	b4533	conserved hypothetical protein

lambdap49	N	yihD	4	ECK3850	JW3830	b3858	protein YihD
lambdap49	N	yicI	4	ECK3646	JW3631	b3656	alpha-glucosidase
lambdap49	N	hcr	3	ECK0863	JW5117	b0872	NADH oxidoreductase hcr
lambdap49	N	ydcE	3	ECK1455	JW1456	b1461	conserved domain protein
lambdap49	N	ygiT	3	ECK3012	JW2989	b3021	transcriptional regulator, XRE family
lambdap49	N	yiaF	3	ECK3541	JW5655	b3554	lipoprotein, putative
lambdap49	N	secB	3	ECK3599	JW3584	b3609	protein-export chaperone SecB
lambdap49	N	ego	2	ECK1506	JW1506	b1513	putative ABC transporter ATP-binding protein ego
lambdap49	N	ppc	2	ECK3947	JW3928	b3956	phosphoenolpyruvate carboxylase
lambdap49	N	nohA	2	ECK1541	JW1541	b1548	bacteriophage DNA packaging protein
lambdap49	N	nuoG	2	ECK2277	JW2278	b2283	NADH-quinone oxidoreductase, chain g
lambdap49	N	yebR	2	ECK1831	JW1821	b1832	protein YebR
lambdap49	N	yjeP	2	ECK4155	JW4120	b4159	BspA protein
lambdap49	N	fliA	1	ECK1921	JW1907	b1922	RNA polymerase sigma factor for flagellar operon
lambdap49	N	insN	1	ECK0257	JW5024	b0255	transposase InsN for insertion sequence element A
lambdap49	N	spr	1	ECK2169	JW2163	b2175	lipoprotein spr
lambdap49	N	tbpA	1	ECK0069	JW0067	b0068	thiamin/thiamin pyrophosphate ABC transporter, thiamin/thiamin pyrophospate-binding protein
lambdap49	N	ydaW	1	ECK1359	JW5211	b1361	conserved hypothetical protein
lambdap49	N	yjgZ	1	ECK4267	JW4236	b4277	
lambdap49	N	ybeB	1	ECK0630	JW5090	b0637	iojap-like ribosome-associated protein
lambdap49	N	nusA	1	ECK3158	JW3138	b3169	transcription elongation protein NusA
lambdap49	N	rpoS	1	ECK2736	JW5437	b2741	RNA polymerase sigma factor RpoS
lambdap49	N	yccT	1	ECK0955	JW0947	b0964	protein YccT
lambdap49	N	caiD	1	ECK0037	JW0035	b0036	carnitinyl-CoA dehydratase
lambdap49	N	ccmD	1	ECK2190	JW2186	b2198	conserved domain protein
lambdap49	N	ccmH	1	ECK2186	JW2182	b2194	cytoChrome c-type biogenesis protein CcmH
lambdap49	N	cysB	1	ECK1269	JW1267	b1275	HTH-type transcriptional regulator CysB
lambdap49	N	envR	1	ECK3251	JW3232	b3264	probable acrEF/envCD operon repressor
lambdap49	N	glpK	1	ECK3918	JW3897	b3926	glycerol kinase
lambdap49	N	minC	1	ECK1164	JW1165	b1176	septum site-determining protein MinC
lambdap49	N	nrfB	1	ECK4064	JW4032	b4071	cytochrome c nitrite reductase, pentaheme subunit
lambdap49	N	ogrK	1	ECK2079	JW2067	b2082	Ogr
lambdap49	N	phoB	1	ECK0393	JW0389	b0399	phosphate regulon transcriptional regulatory protein PhoB
lambdap49	N	slp	1	ECK3490	JW3474	b3506	outer membrane protein slp

lambdap49	N	yagT	1	ECK0285	JW0280	b0286	ferredoxin
lambdap49	N	ybjP	1	ECK0856	JW0849	b0865	YbjP
lambdap49	N	ycbG	1	ECK0947	JW0939	b0956	protein YcbG
lambdap49	N	ycgB	1	ECK1176	JW1177	b1188	unidentified protein
lambdap49	N	ycgE	1	ECK1149	JW1149	b1162	HTH-type transcriptional regulator MlrA
lambdap49	N	ydhL	1	ECK1644	JW5827	b1648	conserved hypothetical protein (ydhL)
lambdap49	N	ydiT	1	ECK1698	JW1690	b1700	conserved hypothetical protein
lambdap49	N	ydjA	1	ECK1763	JW1754	b1765	protein YdjA
lambdap49	N	yeeW	1	ECK1999	JW1988	b2006	YeeW protein
lambdap49	N	yfdL	1	ECK2349	JW5384	b2355	conserved hypothetical protein
lambdap49	N	yfdM	1	ECK2350	JW2352	b2356	DNA N-6-adenine-methyltransferase (Dam) superfamily
lambdap49	N	yfhL	1	ECK2560	JW2546	b2562	iron-sulfur cluster-binding protein
lambdap49	N	yqhC	1	ECK3002	JW5849	b3010	putative HTH-type transcriptional regulator YqhC
lambdap49	N	yhdW	1	ECK3255	JW3236	b3268	general L-amino acid-binding periplasmic protein AapJ
lambdap49	N	yibA	1	ECK3583	JW3568	b3594	protein YibA
lambdap49	N	yiiF	1	ECK3883	JW5563	b3890	conserved hypothetical protein
lambdap49	N	yjfN	1	ECK4184	JW5742	b4188	conserved hypothetical protein
lambdap53	rexb	yiaF	1	ECK3541	JW5655	b3554	lipoprotein, putative
lambdap59	cII	yiaF	1	ECK3541	JW5655	b3554	lipoprotein, putative
lambdap59	cII	yjbE	1	ECK4018	JW3986	b4026	putative outer membrane protein
lambdap59	cII	ylcG	1	ECK0542	JW5076	b4509	conserved hypothetical protein
lambdap61	P	fliA	14	ECK1921	JW1907	b1922	RNA polymerase sigma factor for flagellar operon
lambdap61	P	ynfO	7	ECK1542	JW5251	b4533	conserved hypothetical protein
lambdap61	P	ygiT	5	ECK3012	JW2989	b3021	transcriptional regulator, XRE family
lambdap61	P	atpC	3	ECK3724	JW3709	b3731	ATP synthase F1, epsilon subunit
lambdap61	P	ycbG	2	ECK0947	JW0939	b0956	protein YcbG
lambdap61	P	eutC	2	ECK2435	JW2433	b2440	ethanolamine ammonia-lyase, light chain
lambdap61	P	ydaG	2	ECK1353	JW5210	b1355	conserved hypothetical protein
lambdap61	P	fliM	2	ECK1943	JW1929	b1945	flagellar motor switch protein FliM
lambdap61	P	yqhC	2	ECK3002	JW5849	b3010	putative HTH-type transcriptional regulator YqhC
lambdap61	P	ydcE	2	ECK1455	JW1456	b1461	conserved domain protein
lambdap61	P	yjhV	2	ECK4276	JW4246	b4286	conserved hypothetical protein
lambdap61	P	yiaF	1	ECK3541	JW5655	b3554	lipoprotein, putative
lambdap61	P	insN	1	ECK0257	JW5024	b0255	transposase InsN for insertion sequence element A
lambdap61	P	yihD	1	ECK3850	JW3830	b3858	protein YihD

lambdap61	P	acrE	1	ECK3252	JW3233	b3265	acriflavine resistance protein E
lambdap61	P	ycdC	1	ECK1004	JW0998	b1013	HTH-type transcriptional regulator RutR
lambdap61	P	slp	1	ECK3490	JW3474	b3506	outer membrane protein slp
lambdap61	P	glyQ	1	ECK3548	JW3531	b3560	glycyl-tRNA synthetase, alpha subunit
lambdap61	P	ycfL	1	ECK1090	JW1090	b1104	conserved hypothetical protein
lambdap61	P	holA	1	ECK0633	JW0635	b0640	DNA polymerase III, delta subunit
lambdap61	P	rpoE	1	ECK2571	JW2557	b2573	RNA polymerase sigma factor RpoE
lambdap61	P	ansB	1	ECK2952	JW2924	b2957	L-asparaginase II
lambdap61	P	dinJ	1	ECK0227	JW0216	b0226	DNA-damage-inducible protein J
lambdap61	P	paaC	1	ECK1387	JW1385	b1390	phenylacetate-CoA oxygenase, PaaI subunit
lambdap61	P	phoB	1	ECK0393	JW0389	b0399	phosphate regulon transcriptional regulatory protein PhoB
lambdap62	ren	ynjB	8	ECK1752	JW5284	b1754	conserved hypothetical protein
lambdap62	ren	yiaF	4	ECK3541	JW5655	b3554	lipoprotein, putative
lambdap63	NinB	flxA	8	ECK1560	JW1558	b1566	protein FlxA
lambdap63	NinB	yqjI	6	ECK3061	JW3042	b3071	transcriptional regulator, PadR family protein
lambdap63	NinB	ynjB	5	ECK1752	JW5284	b1754	conserved hypothetical protein
lambdap63	NinB	fliA	4	ECK1921	JW1907	b1922	RNA polymerase sigma factor for flagellar operon
lambdap63	NinB	dicB	3	ECK1569	JW1566	b1575	conserved domain protein
lambdap63	NinB	metN	3	ECK0199	JW0195	b0199	D-methionine ABC transporter, ATP-binding protein
lambdap63	NinB	phnG	3	ECK4094	JW4062	b4101	protein PhnG
lambdap63	NinB	yiaF	3	ECK3541	JW5655	b3554	lipoprotein, putative
lambdap63	NinB	ynfO	3	ECK1542	JW5251	b4533	conserved hypothetical protein
lambdap63	NinB	rpsE	2	ECK3290	JW3265	b3303	ribosomal protein S5
lambdap63	NinB	yajI	2	ECK0406	JW5056	b0412	YajI
lambdap63	NinB	insN	1	ECK0257	JW5024	b0255	transposase InsN for insertion sequence element A
lambdap63	NinB	ydaW	1	ECK1359	JW5211	b1361	conserved hypothetical protein
lambdap63	NinB	ygiT	1	ECK3012	JW2989	b3021	transcriptional regulator, XRE family
lambdap63	NinB	yihD	1	ECK3850	JW3830	b3858	protein YihD
lambdap63	NinB	ydcA	1	ECK1411	JW1416	b1419	conserved hypothetical protein
lambdap63	NinB	yjiT	1	ECK4333	JW5787	b4342	conserved hypothetical protein
lambdap64	NinC	spr	5	ECK2169	JW2163	b2175	lipoprotein spr
lambdap64	NinC	yiaF	2	ECK3541	JW5655	b3554	lipoprotein, putative
lambdap64	NinC	mltB	1	ECK2696	JW2671	b2701	lytic murein transglycosylase B
lambdap64	NinC	fliA	1	ECK1921	JW1907	b1922	RNA polymerase sigma factor for flagellar operon
lambdap64	NinC	flxA	1	ECK1560	JW1558	b1566	protein FlxA

lambdap65	NinD	dicB	15	ECK1569	JW1566	b1575	conserved domain protein
lambdap65	NinD	phnG	13	ECK4094	JW4062	b4101	protein PhnG
lambdap65	NinD	yjhV	13	ECK4276	JW4246	b4286	conserved hypothetical protein
lambdap65	NinD	yjgZ	7	ECK4267	JW4236	b4277	
lambdap65	NinD	ydiT	6	ECK1698	JW1690	b1700	conserved hypothetical protein
lambdap65	NinD	ydaW	5	ECK1359	JW5211	b1361	conserved hypothetical protein
lambdap65	NinD	pyrF	5	ECK1276	JW1273	b1281	orotidine 5'-phosphate decarboxylase
lambdap65	NinD	yfiM	5	ECK2584	JW2570	b2586	conserved hypothetical protein
lambdap65	NinD	yhdW	5	ECK3255	JW3236	b3268	general L-amino acid-binding periplasmic protein AapJ
lambdap65	NinD	minE	4	ECK1162	JW1163	b1174	cell division topological specificity factor MinE
lambdap65	NinD	yjdI	4	ECK4119	JW4087	b4126	conserved hypothetical protein
lambdap65	NinD	smpA	4	ECK2613	JW2598	b2617	small protein A
lambdap65	NinD	slp	4	ECK3490	JW3474	b3506	outer membrane protein slp
lambdap65	NinD	yajI	3	ECK0406	JW5056	b0412	YajI
lambdap65	NinD	csrA	3	ECK2691	JW2666	b2696	carbon storage regulator
lambdap65	NinD	HycG	3	ECK2714	JW2689	b2719	hydrogenase-4 component I
lambdap65	NinD	sdiA	3	ECK1915	JW1901	b1916	regulatory protein SdiA
lambdap65	NinD	soxS	3	ECK4054	JW4023	b4062	regulatory protein SoxS
lambdap65	NinD	yebR	3	ECK1831	JW1821	b1832	protein YebR
lambdap65	NinD	yeeW	3	ECK1999	JW1988	b2006	YeeW protein
lambdap65	NinD	yohH	3	ECK2132	JW5358	b2139	YohH
lambdap65	NinD	ECK2994	2	ECK2994	JW5496	b3000	carboxymethylenebutenolidase
lambdap65	NinD	yeiW	2	ECK2164	JW5361	b4502	proteinase inhibitor
lambdap65	NinD	yheL	2	ECK3330	JW3305	b3343	sulfur relay protein TusD/DsrH
lambdap65	NinD	fhuF	2	ECK4357	JW4331	b4367	ferric iron reductase protein FhuF
lambdap65	NinD	mltC	2	ECK2958	JW5481	b2963	membrane-bound lytic murein transglycosylase C
lambdap65	NinD	feaB	2	ECK1382	JW1380	b1385	phenylacetaldehyde dehydrogenase
lambdap65	NinD	ykfI	2	ECK0246	JW0234	b0245	YeeV protein
lambdap65	NinD	ydcE	2	ECK1455	JW1456	b1461	conserved domain protein
lambdap65	NinD	fixX	2	ECK0045	JW0043	b0044	conserved hypothetical protein
lambdap65	NinD	insN	2	ECK0257	JW5024	b0255	transposase InsN for insertion sequence element A
lambdap65	NinD	ynfO	2	ECK1542	JW5251	b4533	conserved hypothetical protein
lambdap65	NinD	spr	2	ECK2169	JW2163	b2175	lipoprotein spr
lambdap65	NinD	metN	1	ECK0199	JW0195	b0199	D-methionine ABC transporter, ATP-binding protein
lambdap65	NinD	flxA	1	ECK1560	JW1558	b1566	protein FlxA
lambdap65	NinD	yccT	1	ECK0955	JW0947	b0964	protein YccT
lambdap65	NinD	ygbT	1	ECK2750	JW2725	b2755	crispr-associated protein Cas1

lambdap65	NinD	yfaE	1	ECK2228	JW2230	b2236	adrenodoxin family ferredoxin
lambdap65	NinD	hydN	1	ECK2708	JW2683	b2713	protein AegA
lambdap65	NinD	ECK2645	1	ECK2645	JW5423	b2648	putative DNA-invertase from prophage CP4-44
lambdap65	NinD	yajO	1	ECK0413	JW0409	b0419	aldo/keto reductase
lambdap65	NinD	ssuB	1	ECK0924	JW0916	b0933	putative aliphatic sulfonates transport ATP-binding protein SsuB
lambdap65	NinD	oppF	1	ECK1241	JW1239	b1247	oligopeptide transport ATP-binding protein OppF
lambdap65	NinD	hyfH	1	ECK2484	JW2473	b2488	hydrogenase-4 component H
lambdap65	NinD	flhC	1	ECK1892	JW1880	b1891	flagellar transcriptional activator FlhC
lambdap65	NinD	eutC	1	ECK2435	JW2433	b2440	ethanolamine ammonia-lyase, light chain
lambdap65	NinD	ymjB	1	ECK1314	JW5203	b4524	putative ATP-binding component of a transport system
lambdap65	NinD	yjiT	1	ECK4333	JW5787	b4342	conserved hypothetical protein
lambdap65	NinD	ygcQ	1	ECK2764	JW5440	b2769	putative electron transfer flavoprotein subunit YgcQ
lambdap65	NinD	purR	1	ECK1654	JW1650	b1658	transcriptional repressor for pur regulon, GlyA, glnB, prsA, speA
lambdap65	NinD	holD	1	ECK4363	JW4334	b4372	DNA polymerase III, psi subunit
lambdap65	NinD	glcD	1	ECK2974	JW2946	b2979	glycolate oxidase, subunit GlcD
lambdap65	NinD	hyfI	1	ECK2485	JW5805	b2489	hydrogenase-4 component I
lambdap65	NinD	paaC	1	ECK1387	JW1385	b1390	phenylacetate-CoA oxygenase, PaaI subunit
lambdap65	NinD	xdhC	1	ECK2864	JW2836	b2868	[2Fe-2S] binding domain protein
lambdap65	NinD	ycbQ	1	ECK0929	JW5122	b0938	fimbrial subunit
lambdap65	NinD	yhjG	1	ECK3509	JW3492	b3524	b3524 predicted outer membrane biogenesis protein (yhjG) {Esc
lambdap65	NinD	yhiJ	1	ECK3473	JW3455	b3488	conserved hypothetical protein
lambdap65	NinD	ykgM	1	ECK0295	JW5034	b4506	ribosomal protein L36
lambdap65	NinD	yicI	1	ECK3646	JW3631	b3656	alpha-glucosidase
lambdap65	NinD	ilvM	1	ECK3761	JW3742	b3769	acetolactate synthase isozyme II small subunit
lambdap65	NinD	ymdE	1	ECK1016	JW5145	b1028	conserved hypothetical protein
lambdap65	NinD	rseB	1	ECK2569	JW2555	b2571	sigma-E factor regulatory protein RseB
lambdap65	NinD	rarA	1	ECK1000	JW0994	b1009	protein RutD
lambdap65	NinD	csgE	1	ECK1025	JW1022	b1039	curli production assembly/transport component CsgE
lambdap65	NinD	ykgJ	1	ECK0287	JW0282	b0288	predicted ferredoxin (ykgJ)
lambdap65	NinD	ygiL	1	ECK3034	JW3011	b3043	fimbrial protein
lambdap65	NinD	minC	1	ECK1164	JW1165	b1176	septum site-determining protein MinC
lambdap65	NinD	fixB	1	ECK0043	JW0041	b0042	protein FixB

lambdap65	NinD	ECK0356	1	ECK0356	JW0350	b0359	putative transferase
lambdap65	NinD	flgA	1	ECK1057	JW1059	b1072	flagella basal body P-ring formation protein FlgA
lambdap65	NinD	yoaF	1	ECK1791	JW1782	b1793	lipoprotein, putative
lambdap65	NinD	flhE	1	ECK1879	JW1867	b1878	flagellar protein FlhE
lambdap65	NinD	ypfN	1	ECK2468	JW2457	b4547	conserved hypothetical protein
lambdap66	NinE	ynjB	4	ECK1752	JW5284	b1754	conserved hypothetical protein
lambdap66	NinE	nlpI	3	ECK3151	JW3132	b3163	lipoprotein NlpI
lambdap66	NinE	fliA	2	ECK1921	JW1907	b1922	RNA polymerase sigma factor for flagellar operon
lambdap66	NinE	spr	1	ECK2169	JW2163	b2175	lipoprotein spr
lambdap66	NinE	yiaF	1	ECK3541	JW5655	b3554	lipoprotein, putative
lambdap66	NinE	tbpA	1	ECK0069	JW0067	b0068	thiamin/thiamin pyrophosphate ABC transporter, thiamin/thiamin pyrophospate-binding protein
lambdap66	NinE	phoB	1	ECK0393	JW0389	b0399	phosphate regulon transcriptional regulatory protein PhoB
lambdap71	Q	ynfO	6	ECK1542	JW5251	b4533	conserved hypothetical protein
lambdap71	Q	fliA	4	ECK1921	JW1907	b1922	RNA polymerase sigma factor for flagellar operon
lambdap71	Q	yihD	4	ECK3850	JW3830	b3858	protein YihD
lambdap71	Q	nlpI	4	ECK3151	JW3132	b3163	lipoprotein NlpI
lambdap71	Q	ynjB	3	ECK1752	JW5284	b1754	conserved hypothetical protein
lambdap71	Q	yibA	2	ECK3583	JW3568	b3594	protein YibA
lambdap71	Q	glyQ	2	ECK3548	JW3531	b3560	glycyl-tRNA synthetase, alpha subunit
lambdap71	Q	yqhC	2	ECK3002	JW5849	b3010	putative HTH-type transcriptional regulator YqhC
lambdap71	Q	yajI	1	ECK0406	JW5056	b0412	YajI
lambdap71	Q	yiaF	1	ECK3541	JW5655	b3554	lipoprotein, putative
lambdap71	Q	ybeB	1	ECK0630	JW5090	b0637	iojap-like ribosome-associated protein
lambdap71	Q	rfaD	1	ECK3609	JW3594	b3619	ADP-L-glycero-D-manno-heptose-6-epimerase
lambdap71	Q	rpoE	1	ECK2571	JW2557	b2573	RNA polymerase sigma factor RpoE
lambdap71	Q	yjeB	1	ECK4174	JW4136	b4178	protein YjeB
lambdap71	Q	ycfM	1	ECK1091	JW5157	b1105	lipoprotein, putative
lambdap71	Q	fhuF	1	ECK4357	JW4331	b4367	ferric iron reductase protein FhuF
lambdap71	Q	yfcC	1	ECK2292	JW2295	b2298	short-chain fatty acids transporter
lambdap71	Q	yodC	1	ECK1955	JW1940	b1957	conserved hypothetical protein
lambdap71	Q	paaC	1	ECK1387	JW1385	b1390	phenylacetate-CoA oxygenase, PaaI subunit
lambdap73	orf-64	spr	2	ECK2169	JW2163	b2175	lipoprotein spr
lambdap73	orf-64	ynjB	1	ECK1752	JW5284	b1754	conserved hypothetical protein
lambdap73	orf-64	yiaF	1	ECK3541	JW5655	b3554	lipoprotein, putative
lambdap73	orf-64	ygiT	1	ECK3012	JW2989	b3021	transcriptional regulator, XRE family

lambdap73	orf-64	rpoE	1	ECK2571	JW2557	b2573	RNA polymerase sigma factor RpoE
lambdap73	orf-64	caiD	1	ECK0037	JW0035	b0036	carnitinyl-CoA dehydratase
lambdap74	S	ynjB	3	ECK1752	JW5284	b1754	conserved hypothetical protein
lambdap74	S	yiaF	1	ECK3541	JW5655	b3554	lipoprotein, putative
lambdap75	R	dicB	10	ECK1569	JW1566	b1575	conserved domain protein
lambdap75	R	fhuF	10	ECK4357	JW4331	b4367	ferric iron reductase protein FhuF
lambdap75	R	flxA	5	ECK1560	JW1558	b1566	protein FlxA
lambdap75	R	metN	3	ECK0199	JW0195	b0199	D-methionine ABC transporter, ATP-binding protein
lambdap75	R	caiF	3	ECK0035	JW0033	b0034	transcriptional activatory protein CaiF
lambdap75	R	ynjB	2	ECK1752	JW5284	b1754	conserved hypothetical protein
lambdap75	R	ydaW	1	ECK1359	JW5211	b1361	conserved hypothetical protein
lambdap75	R	yfcQ	1	ECK2328	JW2331	b2334	conserved hypothetical protein
lambdap75	R	ydcK	1	ECK1421	JW1424	b1428	conserved hypothetical protein
lambdap75	R	ynbE	1	ECK1379	JW1377	b1382	conserved domain protein
lambdap76	Rz	mltB	22	ECK2696	JW2671	b2701	lytic murein transglycosylase B
lambdap76	Rz	ynjB	4	ECK1752	JW5284	b1754	conserved hypothetical protein
lambdap76	Rz	yiaF	2	ECK3541	JW5655	b3554	lipoprotein, putative
lambdap76	Rz	spr	2	ECK2169	JW2163	b2175	lipoprotein spr
lambdap77	Bor	ynjB	2	ECK1752	JW5284	b1754	conserved hypothetical protein
lambdap78	orf_78	ispB	4	ECK3176	JW3154	b3187	octaprenyl-diphosphate synthase
lambdap78	0	ynjB	1	ECK1752	JW5284	b1754	conserved hypothetical protein
lambdap78	0	ydaW	1	ECK1359	JW5211	b1361	conserved hypothetical protein
lambdap78	0	insN	1	ECK0257	JW5024	b0255	transposase InsN for insertion sequence element A
lambdap78	lambdap78	phoB	1	ECK0393	JW0389	b0399	phosphate regulon transcriptional regulatory protein PhoB
lambdap79	orf_79	ybcW	1	ECK0551	JW0548	b0559	conserved hypothetical protein
lambdap79	orf_79	tfaR	1	ECK1368	JW1367	b1373	tail fiber assembly protein
lambdap80	ea47	yihD	10	ECK3850	JW3830	b3858	protein YihD
lambdap80	ea47	ynfO	10	ECK1542	JW5251	b4533	conserved hypothetical protein
lambdap80	ea47	ynjB	8	ECK1752	JW5284	b1754	conserved hypothetical protein
lambdap80	ea47	spr	7	ECK2169	JW2163	b2175	lipoprotein spr
lambdap80	ea47	ubiF	5	ECK0654	JW0659	b0662	2-octaprenyl-3-methyl-6-methoxy-1,4-benzoquinol hydroxylase
lambdap80	ea47	yiaF	4	ECK3541	JW5655	b3554	lipoprotein, putative
lambdap80	ea47	yjiT	4	ECK4333	JW5787	b4342	conserved hypothetical protein
lambdap80	ea47	flxA	3	ECK1560	JW1558	b1566	protein FlxA
lambdap80	ea47	sucC	2	ECK0716	JW0717	b0728	succinyl-CoA synthetase beta chain

lambdap80	ea47	ubiH	2	ECK2902	JW2875	b2907	2-polyprenyl-6-methoxyphenol 4-hydroxylase
lambdap80	ea47	fliA	2	ECK1921	JW1907	b1922	RNA polymerase sigma factor for flagellar operon
lambdap80	ea47	metN	1	ECK0199	JW0195	b0199	D-methionine ABC transporter, ATP-binding protein
lambdap80	ea47	mltB	1	ECK2696	JW2671	b2701	lytic murein transglycosylase B
lambdap80	ea47	ydaW	1	ECK1359	JW5211	b1361	conserved hypothetical protein
lambdap80	ea47	ygiT	1	ECK3012	JW2989	b3021	transcriptional regulator, XRE family
lambdap80	ea47	hybO	1	ECK2991	JW2965	b2997	[Ni/Fe] hydrogenase, small subunit
lambdap80	ea47	modC	1	ECK0754	JW0748	b0765	molybdate ABC transporter, ATP-binding protein
lambdap80	ea47	rng	1	ECK3235	JW3216	b3247	ribonuclease, Rne/Rng family
lambdap80	ea47	thiF	1	ECK3984	JW3956	b3992	thiazole biosynthesis adenylyltransferase ThiF
lambdap80	ea47	wbbK	1	ECK2026	JW2017	b2032	glycosyl transferase, group 1 family protein
lambdap80	ea47	ycdC	1	ECK1004	JW0998	b1013	HTH-type transcriptional regulator RutR
lambdap80	ea47	yqhC	1	ECK3002	JW5849	b3010	putative HTH-type transcriptional regulator YqhC
lambdap80	ea47	yhiJ	1	ECK3473	JW3455	b3488	conserved hypothetical protein
lambdap81	ea31	yiaF	1	ECK3541	JW5655	b3554	lipoprotein, putative
lambdap83	ea22	dicB	42	ECK1569	JW1566	b1575	conserved domain protein
lambdap83	ea22	norR	26	ECK2704	JW5843	b2709	anaerobic nitric oxide reductase transcription regulator NorR
lambdap83	ea22	phnG	11	ECK4094	JW4062	b4101	protein PhnG
lambdap83	ea22	glcC	7	ECK2975	JW2947	b2980	Glc operon transcriptional activator
lambdap83	ea22	mltB	5	ECK2696	JW2671	b2701	lytic murein transglycosylase B
lambdap83	ea22	spr	4	ECK2169	JW2163	b2175	lipoprotein spr
lambdap83	ea22	ydaW	4	ECK1359	JW5211	b1361	conserved hypothetical protein
lambdap83	ea22	yliL	4	ECK0805	JW5969	b0816	hypothetical protein (yliL)
lambdap83	ea22	metN	3	ECK0199	JW0195	b0199	D-methionine ABC transporter, ATP-binding protein
lambdap83	ea22	soxS	3	ECK4054	JW4023	b4062	regulatory protein SoxS
lambdap83	ea22	ybiS	2	ECK0809	JW0803	b0819	protein YbiS
lambdap83	ea22	ymcD	2	ECK0978	JW5133	b0987	hypothetical protein
lambdap83	ea22	fixX	2	ECK0045	JW0043	b0044	conserved hypothetical protein
lambdap83	ea22	fliA	1	ECK1921	JW1907	b1922	RNA polymerase sigma factor for flagellar operon
lambdap83	ea22	flxA	1	ECK1560	JW1558	b1566	protein FlxA
lambdap83	ea22	tbpA	1	ECK0069	JW0067	b0068	thiamin/thiamin pyrophosphate ABC transporter, thiamin/thiamin pyrophospate-binding protein

lambdap83	ea22	wza	1	ECK2056	JW2047	b2062	membrane protein
lambdap83	ea22	yajI	1	ECK0406	JW5056	b0412	YajI
lambdap83	ea22	ydcE	1	ECK1455	JW1456	b1461	conserved domain protein
lambdap83	ea22	yjgZ	1	ECK4267	JW4236	b4277	
lambdap83	ea22	yjhV	1	ECK4276	JW4246	b4286	conserved hypothetical protein
lambdap83	ea22	ynfO	1	ECK1542	JW5251	b4533	conserved hypothetical protein
lambdap83	ea22	ynjB	1	ECK1752	JW5284	b1754	conserved hypothetical protein
lambdap83	ea22	rpsJ	1	ECK3308	JW3283	b3321	ribosomal protein S10
lambdap83	ea22	ansB	1	ECK2952	JW2924	b2957	L-asparaginase II
lambdap83	ea22	eutC	1	ECK2435	JW2433	b2440	ethanolamine ammonia-lyase, light chain
lambdap83	ea22	fimG	1	ECK4310	JW4282	b4319	protein FimG
lambdap83	ea22	minE	1	ECK1162	JW1163	b1174	cell division topological specificity factor MinE
lambdap83	ea22	proQ	1	ECK1830	JW5300	b1831	ProP effector
lambdap83	ea22	recG	1	ECK3642	JW3627	b3652	ATP-dependent DNA helicase RecG
lambdap83	ea22	rseB	1	ECK2569	JW2555	b2571	sigma-E factor regulatory protein RseB
lambdap83	ea22	sfmA	1	ECK0523	JW0519	b0530	type-1 fimbrial protein, A chain
lambdap83	ea22	tolB	1	ECK0729	JW5100	b0740	Tol-Pal system beta propeller repeat protein TolB
lambdap83	ea22	ybgD	1	ECK0708	JW0709	b0719	fimbrial protein
lambdap83	ea22	ybjP	1	ECK0856	JW0849	b0865	YbjP
lambdap83	ea22	ycfL	1	ECK1090	JW1090	b1104	conserved hypothetical protein
lambdap83	ea22	yfcQ	1	ECK2328	JW2331	b2334	conserved hypothetical protein
lambdap83	ea22	ygeK	1	ECK2853	JW5458	b2855	hypothetical protein
lambdap83	ea22	ykiA	1	ECK0387	JW0383	b0392	conserved hypothetical protein
lambdap83	ea22	ylcG	1	ECK0542	JW5076	b4509	conserved hypothetical protein
lambdap83	ea22	ymcC	1	ECK0977	JW0969	b0986	YmcC
lambdap83	ea22	ymfT	1	ECK1132	JW5169	b1146	conserved hypothetical protein
lambdap83	ea22	yncH	1	ECK1449	JW5235	b1455	conserved hypothetical protein
lambdap83	ea22	yoaH	1	ECK1809	JW1800	b1811	conserved domain protein
lambdap88	cI	yiaF	3	ECK3541	JW5655	b3554	lipoprotein, putative
lambdap88	cI	pldB	3	ECK3819	JW5584	b3825	lysophospholipase L2
lambdap88	cI	eutC	2	ECK2435	JW2433	b2440	ethanolamine ammonia-lyase, light chain
lambdap88	cI	fliM	2	ECK1943	JW1929	b1945	flagellar motor switch protein FliM
lambdap88	cI	mdtE	2	ECK3497	JW3481	b3513	multidrug resistance protein MdtE
lambdap88	cI	rseB	2	ECK2569	JW2555	b2571	sigma-E factor regulatory protein RseB
lambdap88	cI	smpA	2	ECK2613	JW2598	b2617	small protein A
lambdap88	cI	ydiT	2	ECK1698	JW1690	b1700	conserved hypothetical protein
lambdap88	cI	flxA	2	ECK1560	JW1558	b1566	protein FlxA
lambdap88	cI	phnG	2	ECK4094	JW4062	b4101	protein PhnG
lambdap88	cI	ydaW	2	ECK1359	JW5211	b1361	conserved hypothetical protein

lambdap88	cI	mltB	1	ECK2696	JW2671	b2701	lytic murein transglycosylase B
lambdap88	cI	wza	1	ECK2056	JW2047	b2062	membrane protein
lambdap88	cI	yihD	1	ECK3850	JW3830	b3858	protein YihD
lambdap88	cI	yjgZ	1	ECK4267	JW4236	b4277	
lambdap88	cI	ECK0356	1	ECK0356	JW0350	b0359	putative transferase
lambdap88	cI	ECK3769	1	ECK3769	JW3750	b3777	conserved hypothetical protein
lambdap88	cI	lacA	1	ECK0339	JW0333	b0342	galactoside O-acetyltransferase
lambdap88	cI	lpxL	1	ECK1039	JW1041	b1054	lipid A biosynthesis lauroyl acyltransferase
lambdap88	cI	napB	1	ECK2195	JW5367	b2203	periplasmiC nitrate reductase, diheme cytochrome c subunit
lambdap88	cI	nuoC	1	ECK2280	JW5375	b2286	NADH-quinone oxidoreductase chain c/d
lambdap88	cI	slp	1	ECK3490	JW3474	b3506	outer membrane protein slp
lambdap88	cI	xdhC	1	ECK2864	JW2836	b2868	[2Fe-2S] binding domain protein
lambdap88	cI	ybcY	1	ECK0554	JW0551	b0562	b0562DLP12 predicted SAM-dependent methyltransferase (ybcY)
lambdap88	cI	ybgD	1	ECK0708	JW0709	b0719	fimbrial protein
lambdap88	cI	ycjR	1	ECK1309	JW5202	b1314	AP endonuclease, family 2
lambdap88	cI	yfdX	1	ECK2371	JW2372	b2375	protein YfdX
lambdap88	cI	yhdW	1	ECK3255	JW3236	b3268	general L-amino acid-binding periplasmic protein AapJ
lambdap88	cI	yjdI	1	ECK4119	JW4087	b4126	conserved hypothetical protein
lambdap88	cI	ykgJ	1	ECK0287	JW0282	b0288	predicted ferredoxin (ykgJ)
lambdap88	cI	yqhC	1	ECK3002	JW5849	b3010	putative HTH-type transcriptional regulator YqhC
lambdap88	cI	ubiF	1	ECK0654	JW0659	b0662	2-octaprenyl-3-methyl-6-methoxy-1,4-benzoquinol hydroxylase
lambdap89	O	ppk	15	ECK2497	JW2486	b2501	polyphosphate kinase
lambdap89	O	yjhP	15	ECK4296	JW4268	b4306	conserved hypothetical protein
lambdap89	O	tfaQ	3	ECK1539	JW1539	b1546	tail fiber assembly protein
lambdap89	O	mviM	2	ECK1053	JW1055	b1068	putative Virulence factor MviM homolog
lambdap89	O	clpP	1	ECK0431	JW0427	b0437	ATP-dependent Clp protease, proteolytic subunit ClpP
lambdap89	O	dsdX	1	ECK2361	JW2362	b2365	DsdX permease
lambdap89	O	yaaW	1	ECK0011	JW0010	b0011	positive regulator for sigma H
lambdap90	orf206b	prfH	3	ECK0237	JW0226	b0236	putative peptide chain release factor H
lambdap90	orf206b	yjbF	2	ECK4019	JW5711	b4027	YmcC
lambdap90	orf206b	ypfJ	2	ECK2471	JW2460	b2475	neutral zinc metallopeptidase family
lambdap90	orf206b	yajI	1	ECK0406	JW5056	b0412	YajI
lambdap90	orf206b	clpP	1	ECK0431	JW0427	b0437	ATP-dependent Clp protease, proteolytic subunit ClpP

lambdap90	orf206b	hokD	1	ECK1556	JW1554	b1562	b1562 small toxic polypeptide (hokD)
lambdap90	orf206b	yjdP	1	ECK4084	JW5890	b4487	conserved hypothetical protein